UNIVERSITÉ DE NANTES

UFR SCIENCES ET TECHNIQUES DES ACTIVITES PHYSIQUES ET SPORTIVES

Habilitation à Diriger des Recherches

ANALYSE ELECTROMYOGRAPHIQUE DES COORDINATIONS MUSCULAIRES ET DES CONTRAINTES IMPOSEES AU SYSTEME NEUROMUSCULAIRE

Présentée le 17 novembre 2009

FRANÇOIS HUG
Maître de conférences

LABORATOIRE « MOTRICITE, INTERACTIONS, PERFORMANCE »
EQUIPE D'ACCUEIL 4334

ECOLE DOCTORALE « COGNITION, EDUCATION, INTERACTIONS» (ED 504)
SPECIALITE « SCIENCES ET TECHNIQUES DES ACTIVITES PHYSIQUES ET SPORTIVES » (SECTION CNU N°74)

Jury :

Martin BILODEAU (Professeur, Université d'Ottawa, Canada)	Rapporteur
Laurent GRÉLOT (PU, Université d'Aix-Marseille II, France)	
Arnaud GUÉVEL (PU, Université de Nantes, France)	
Guillaume MILLET (PU, Université de Saint-Étienne, France)	Rapporteur
Stéphane PERREY (MCU-HDR, Université de Montpellier I, France)	Rapporteur
Thomas SIMILOWSKI (PU-PH, Université de Paris VI, France)	

Année 2009

Avant-propos

J'adresse mes très sincères et respectueux remerciements aux membres du jury, messieurs les Professeurs Martin BILODEAU, Laurent GRÉLOT, Arnaud GUÉVEL, Guillaume MILLET, Stéphane PERREY et Thomas SIMILOWSKI, qui me font l'honneur d'évaluer ce travail.

Mes remerciements s'adressent également à l'ensemble de ceux qui, de près ou de loin, ont contribué à l'aboutissement de ces travaux, et tout particulièrement :

Au Pr Yves JAMMES et au Dr Patrick DECHERCHI. Vous avez activement participé à ma formation doctorale, il y a de cela déjà 6 ans …. Recevez ici tous mes remerciements,

Au Pr Laurent GRÉLOT. Merci pour tout ce que j'ai appris à tes cotés ! Merci pour ton amitié,

Au Pr Thomas SIMILOWSKI qui a accepté de m'accueillir au sein de son équipe pour un stage post-doctoral. Cette période reste pour moi un excellent souvenir, j'ai tellement appris. J'espère que je saurai donner autant à mes étudiants que ce que vous donnez aux vôtres. Un grand Merci!

À mes fidèles co-auteurs et amis, les Drs Tanguy MARQUESTE, David LAPLAUD, Antoine COUTURIER, Sylvain DOREL, Antoine NORDEZ. C'est aussi votre HDR, Merci pour tout et vivement les prochains projets (et/ou les prochaines escapades vélocipédiques nocturnes vers les hangars de Nantes…)

À tous ceux avec qui j'ai pris un grand plaisir à collaborer, les Drs Marie-Noelle FIAMMA, Mathieu RAUX, Capucine MORELOT-PANZINI, Thomas GALLOT, Stefan CATHELINE, David BENDAHAN, Marion FAUCHER et Mathieu COULANGE,

Aux membres du laboratoire « Motricité, Interactions, Performance » qui m'ont accueilli il y a de cela 3 ans. Un merci tout particulier au Pr Arnaud GUÉVEL pour ses encouragements et ses précieux conseils.

Aux étudiants que j'ai eu le plaisir d'encadrer, avec une mention très spéciale pour Gaël GUILHEM qui est malheureusement passé trop vite entre mes mains… Mais rendez-vous aux hangars (cf. ci-avant… je ne t'avais pas oublié…).

Aux sujets des différentes manips sans qui rien n'aurait été possible,

Enfin, je remercie l'ensemble des personnes avec qui je n'ai peut-être pas activement collaboré mais que j'ai pris un grand plaisir à côtoyer. De peur d'oublier quelqu'un, je vous laisse le soin de rajouter votre nom à cette liste…

Sans oublier ceux qui, autour de moi au sein de l'UFR STAPS, assument de lourdes responsabilités adminsitratives/pédagogiques et qui me permettent en quelque sorte de continuer plus sereinement mon activité de recherche,

Et bien évidemment à Émilie, Adèle et Mathieu, avec une mention spéciale pour Adèle et Mathieu qui se sont relayés pour me permettre de travailler de très bonne heure le matin, week-ends et vacances compris, et une mention très spéciale pour Émilie … zut, plus de place…. pour …..TOUT.

Sommaire

Présentation du document

Ce mémoire d'Habilitation à Diriger des Recherches est articulé en quatre grandes parties. La **première partie** présente mon parcours de formation, mon activité scientifique ainsi que mes expériences d'encadrement de la recherche. Après une formation doctorale en « Sciences du mouvement humain », encadrée par le Pr Yves JAMMES et le Dr Patrick DECHERCHI (Université de Aix-Marseille II – thèse soutenue en décembre 2003), j'ai réalisé un stage post-doctoral d'un an sous la supervision du Pr Thomas SIMILOWSKI (Laboratoire EA 2397 – Université de Paris VI). J'ai ensuite occupé un poste d'enseignant-chercheur à l'Institut National du Sport et de l'Education Physique (INSEP, Paris) avant d'être recruté comme maître de conférences à l'Université de Nantes (septembre 2006). L'activité de recherche menée au sein de ces différentes structures m'a amené à publier 32 articles dans des revues indexées ISI. En plus de l'encadrement des étudiants de Licence et Master 1ère année, j'ai (co-)encadré un étudiant en master 2, une étudiante en thèse de spécialité médicale et je co-encadre actuellement un étudiant en thèse. La **deuxième partie** de ce mémoire présente succinctement la technique d'électromyographie. Elle a pour vocation de permettre au lecteur d'appréhender le cadre méthodologique dans lequel s'insèrent nos travaux. **La troisième partie** résume mes activités de recherche. Dans un soucis d'homogénéité, seuls 13 des 22 articles publiés depuis la fin de la thèse sont présentés. Ces travaux sont regroupés en 4 axes de recherches : « électromyographie et analyse des coordinations musculaires », « détection électromyographique d'une charge imposée au système respiratoire », « évaluation électromyographique de la fatigue neuromusculaire » et « caractérisation du délai électromécanique ». Dans une **quatrième partie** j'expose les projets de recherches qui me paraissent les plus pertinents à mener à court ou moyen terme. Certains s'inscrivent dans la continuité de travaux déjà réalisés, i.e., «électromyographie et analyse des coordinations musculaires » et « évaluation électromyographique de la fatigue neuromusculaire ». Nous verrons que ces projets soulèvent des questions auxquelles je me propose d'essayer de répondre en développant nouvel axe de recherche intitulé « estimation de la force musculaire et étude de sa transmission ».
Des annexes sont associées à ce document. Elles regroupent les publications scientifiques présentées dans la deuxième partie et permettront au lecteur de trouver le détail de certaines informations présentées que très succinctement dans ce mémoire.

Chapitre 1 - Titres et travaux

1.1. Curriculum Vitae

François HUG
Né le 20 juillet 1978 à Clamart (92)
Nationalité française
PACSE, 2 enfants

Coordonnées professionnelles :
UFR STAPS
25 bis boulevard Guy Mollet
BP 72206
44322 Nantes cedex 3
Tel : 02 51 83 72 24
E-mail : francois.hug@univ-nantes.fr

Coordonnées personnelles :
5 rue Diane
44300 Nantes
Tel : 06 12 43 85 59

Statut actuel

2006-présent Maître de conférences (74ème section), UFR STAPS, Université de Nantes.

Formation universitaire

2001-2003 Doctorat, Spécialité *Sciences du Mouvement Humain*, Université d'Aix-Marseille II
Mention Très Honorable
Titre du mémoire : « *Evolution des variables respiratoires et électromyographiques au cours de l'exercice : étude chez des sujets sédentaires, des cyclistes amateurs et professionnels* »
Sous la direction du Pr Yves JAMMES (PU-PH) et du Dr Patrick DECHERCHI (MCU)

2000-2001 DEA, Spécialité *Sciences du Mouvement Humain,* Université d'Aix-Marseille II
Option *Physiologie*
Mention Bien
Titre du mémoire: « *Etude chez des cyclistes entraînés et des sujets sédentaires des corrélations entre les variables électromyographiques et respiratoires lors d'épreuves d'effort de type triangulaire et rectangulaire* »
Sous la direction du Pr Yves JAMMES (PU-PH) et du Dr Patrick DECHERCHI (MCU)

1999-2000 Maîtrise STAPS, Université d'Aix-Marseille II
Option *Recherche*
Mention Bien
Titre du mémoire : « *Effet de l'électromyostimulation chronique sur la régénération des afférences métabosensibles chez le rat* »
Sous la direction du Dr Patrick DECHERCHI (MCU)

Obtention de l'AQA « entraînement des activités du cyclisme » (équivalence BEESAC)

1998-1999 Licence STAPS, Université de Paris XI
Option *Entraînement sportif*
Mention Assez-Bien

1996-1998 DEUG STAPS, Université de Paris XI

Expérience professionnelle

2005-2006 **Enseignant-Chercheur**, Institut National du Sport (INSEP, Paris)
Laboratoire de biomécanique et physiologie

2004-2005 **Stage de recherche post-doctoral**, Université Pierre et Marie Curie (Paris VI)
Sujet de recherche : « Substrats neurophysiologiques de la dyspnée : Modalités de recrutement des muscles ventilatoires en réponse aux charges métaboliques et mécaniques chez l'Homme et corrélation avec les sensations respiratoires »
Sous la supervision du Pr Thomas SIMILOWSKI (PU-PH)
Financement : fédération ANTADIR

2003-2004 **Allocataire de recherche**, Assistance Publique des Hôpitaux de Marseille

2002-2003 **Enseignant vacataire**, UFR STAPS, Université d'Aix-Marseille II

2001-2002 **Enseignant vacataire**, UFR STAPS, Université d'Aix-Marseille II

2000-2004 **Agent de développement/entraîneur (emploi jeune)**, Vélo Club Aubagnais (13)

Responsabilités administratives

2008-présent **Responsable pédagogique de la Licence 3 « entraînement sportif »**, UFR STAPS, Université de Nantes

2008-présent **Membre élu du conseil scientifique**, UFR STAPS, Université de Nantes

2006-présent **Participation aux jurys** de Licence STAPS 2ème et 3ème années, Université de Nantes

2006-présent **Responsable disciplinaire «physiologie»**, UFR STAPS, Université de Nantes

2009 **Membre du comité de sélection** du poste MCF n°1569

2006-2007 **Membre élu du conseil pédagogique**, UFR STAPS, Université de Nantes

Activité d'enseignement

2008-2009 **Maître de conférences** , UFR STAPS, Université de Nantes
69h CM, 82h TD, 18h TP (soit 197 h eq TD)

2007-2008 **Maître de conférences** , UFR STAPS, Université de Nantes
77h CM, 58h TD, 40h TP (soit 200 h eq TD)

2006-2007 Maître de conférences , UFR STAPS, Université de Nantes
85h CM, 52h TD, 48h TP (soit 211 h eq TD)

2005-2006 Enseignant-chercheur, Institut National du Sport (INSEP, Paris)
9h CM, 4h TP (soit 16 h eq TD)

2002-2003 Enseignant vacataire TD, UFR STAPS, Université d'Aix-Marseille II
60h TD (soit 60 h eq TD)

2001-2002 Enseignant vacataire TP/TD, UFR STAPS, Université d'Aix-Marseille II
50h TD et 48 h TP (soit 107 h eq TD)

Collaborations scientifiques

Collaborations en cours :

- Laboratoire de géophysique interne et tectonophysique (LGIT - UMR CNRS), Université de Grenoble. (collaboration avec le Dr Stefan CATHELINE)

- Laboratoire de Biomécanique et Physiologie, Institut National du Sport et de l'Education Physique (INSEP). (collaboration avec les Dr Sylvain DOREL et Antoine COUTURIER)

- Groupe VélUS, Département de génie mécanique, Université de Sherbrooke, Canada. (collaboration avec le Pr Yvan CHAMPOUX et le Dr Jean-Marc DROUET)

Collaborations passées :

- Centre de Résonance Magnétique Biologique et Médicale (CRMBM – UMR CNRS 6612), Faculté de médecine de Marseille, Université d'Aix-Marseille II. (collaboration avec le Dr David BENDAHAN)

- Service de Cardiologie. CHU de la Timone, Marseille. (collaboration avec le Dr Bernard SAVIN)

- Exercise Physiology Laboratory. Université européenne de Madrid, Espagne. (Collaboration avec le Pr Alejandro LUCIA)

- IMNSSA (Institut de Médecine Navale). Toulon. (Collaboration avec le Dr François GALLAND)

Expertise scientifique

Editorial board :

- Membre de l'editorial board de *Journal of Electromyography and Kinesiology* (depuis février 2009)

Expertise d'articles :
(nombre d'expertises entre parenthèses)

- *Applied Physiology, Nutrition and Metabolism* (1)
- *Biomedical Signal Processing & Control* (1)
- *Brain* (1)
- *British Journal of Sports Medicine* (1)
- *Canadian Journal of Physiology and Pharmacology* (1)
- *Clinical Neurophysiology* (1)

- *European Journal of Applied Physiology* (8)
- *International Journal of Sports Medicine* (2)
- *Journal of Electromyography and Kinesiology* (13)
- *Journal of Magnetic Resonance Imaging* (1)
- *Medicine & Science in Sports & Exercise* (3)
- *Sports Medicine* (1)

Expertise de projets scientifiques :
(nombre d'expertises entre parenthèses)

- Ministère de la santé et des sports (2)

Jury de thèse :

- Examinateur de la thèse soutenue par Sebastien BOYAS
Titre de la thèse : « analyse des évolutions du signal électromyographique en vue de la prédiction de l'endurance limite lors de tâches mono- et multi-segmentaires »
Soutenue le 4 octobre 2007
Jury : Patrick LEGROS (rapporteur), Guillaume MILLET (rapporteur), Pierre PORTERO (Président du jury), François HUG (examinateur) et Arnaud GUÉVEL (directeur de thèse)

Sociétés savantes, réseaux

- Membre de l'American Physiological Society (APS)
- Membre de l'International Society of Electrophysiology and Kinesiology (ISEK)
- Membre de la Société de Biomécanique (SB)

- Membre du réseau Recherche et Sport en Pays de la Loire (RSPDL)

1.2. Publications scientifiques, congrès et contrats de recherche

Articles publiés dans des revues indexées (ISI)

Pour chaque publication, l'impact factor (IF 2008) de la revue et son classement AERES (section STAPS – mars 2009) figurent entre parenthèses.
**, articles utilisés dans le cadre de ce mémoire d'Habilitation à Diriger des Recherches.*

Année 2009

(A32*) Hug, F., Nordez, A., Guével, A.
Can the electromyographic fatigue threshold be determined from superficial elbow flexor muscles during an isometric single-joint task? *European Journal of Applied Physiology.* 2009. 107 :193-201. (IF = 1,9 ; A+)

(A31*) Nordez, A., Gallot, T., Catheline, S., Guevel, A., Cornu, C., Hug, F.
Electromechanical delay revisited using very high frame rate ultrasound. *Journal of Applied Physiology*. 2009. 106(6) : 1970-1975. (IF=3,6 ; A+)

(A30*) Dorel, S., Drouet, JM., Champoux, Y., Couturier, A., Hug, F.
Changes of pedaling technique and muscle coordination during an exhaustive exercise. *Medecine & Science in Sports & Exercise.* 2009. 41(6) : 1277-1286. (IF=3,4; A+)

(A29*) Nordez, A., Catheline, S., Hug, F.
A novel method for measuring electromechanical delay on the vastus medialis obliquus and vastus lateralis. *Ultrasound in Medicine and Biology*. 2009. 35(5) : 172 – lettre à l'éditeur. (IF=2,4; NC)

(A28*) Dorel, S., Couturier, A., Hug, F.
Influence of different racing positions on mechanical and electromyographic patterns during pedaling. *Scandinavian Journal of Medicine & Science in Sports*. 2009. 19 : 44-54. (IF =2,3 ; A)

(A27) Guilhem, G., Dorel, S., Hug, F.
Effects of a prior short exercise on the subsequent ventilatory thresholds occurence. *Journal of Science and Medicine in Sports.* 2009. 12(2) : 273-279. (IF = 1,9 ; A)

(A26*) Hug, F., Dorel, S.
Electromyographic analysis of pedaling: a review. *Journal Electromyography and Kinesiology*. 2009. 19(2) : 182-198. (IF = 1,9 ; A)

Année 2008

(A25*) Chiti, L., Biondi, G., Morélot-Panzini, C., Raux, M., Similowski, T., Hug, F.
Scalene muscle activity during progressive inspiratory loading under pressure support ventilation on normal humans. *Respiratory Physiology and Neurobiology*. 2008. 164(3) : 440-447. (IF = 2,0 ; A+)

(A24*) Hug, F., Drouet, JM., Champoux, Y., Couturier, A., Dorel, S.
Inter-individual variability of EMG patterns and pedal force profiles in trained cyclists. *European Journal of Applied Physiology* 2008. 104(4) : 667-678. (IF = 1,9 ; A+)

(A23) Coulange, M., Barthelemy, A., Hug, F., Thierry, AL., De Haro.
Reliability of new pulse CO-oximeter in victims of carbon monoxyde poisoning. *Undersea and Hyperbaric Medicine*. 2008. 35(2) : 107-111. (IF = 0,9 ; NC)

(A22) Slawinski J, Dorel S, Hug F, Couturier A, Fournel V, Morin JB, Hanon, C.
Incline versus level maximal sprint running in elite athletes. *Medecine & Science in Sports & Exercise*. 2008. 40(6) : 1155-1162. (IF=3,4; A+)

(A21*) Dorel, S., Couturier, A., Hug, F.
Intra-session repeatability of lower limb muscles activation pattern during pedaling. *Journal of Electromyography and Kinesiology*. 2008. 18(5) : 857-865. (IF=1,9 ; A)

Année 2007

(A20) Raux, M., Straus, C., Redolfi, C., Morelot-Panzini, C., Couturier, A., Hug, F., Similowski, T.
Electroencephalographic evidence for premotor cortex activation during inspiratory loading in humans. *Journal of Physiology (London).* 2007. 578 : 569-578. (IF = 4,6 ; A+)

Année 2006

(A19) Argentin, S., Levêque, JM., Bieuzen, F., Hug, F., Brisswalter, J., Hausswirth, C.
Choix et évolution de la cadence de pédalage au cours d'un test progressif maximal continu : influence de l'expertise. *Science & Sports*. 2006. 21(5) : 273-279. (0,1 ; NC)

(A18) Hug, F., Grélot, L., Le Fur, Y., Cozzone, P., Bendahan, D.
Exercise-induced metabolic changes and corresponding recovery during successive bouts of exercise in professional road cyclists: a ^{31}P-MRS study. *Medicine and Science in Sports and Exercise*. 2006. 38(12) :2151-2158. (IF=3,4; A+)

(A17) Coulange, M., Hug, F., Kipson, N., Robinet, C., Desruelle, AM., Melin, B., Gimenez, C., Galland, F., Jammes, Y.
Consequences of prolonged total body immersion in cold water on muscle performance and EMG activity. *Pflugers Arch.* 2006. 19:1-11. (3,5 ; A+)

(A16*) Laplaud, D., Hug, F., Grélot, L.
Reproducibility of eight lower limb muscles activity level in the course of an incremental pedalling exercise. *Journal of Electromyography and Kinesiology*. 2006. 16(2):158-166. (IF=1,9 ; A)

(A15) Hug, F., Marqueste, T., Le Fur, Y., Cozzone, P., Grélot, L., Bendahan, D.
Selective training-induced muscles hypertrophy in professional road cyclists. *European Journal of Applied Physiology*. 97(5):591-597. (IF = 1,9 ; A+)

(A14*) Hug, F., Laplaud, D., Lucia, A., Grélot, L.
Comparison of visual and mathematical detection of the EMG threshold during incremental pedalling exercise. *Journal of Strength and Conditionning Research*. 2006. 20(3):704-708. (IF = 0,8; A)

(A13*) Hug, F., Laplaud, D., Lucia, A., Grélot, L.
EMG threshold determination in 8 lower limb muscles during cycling exercise: a pilot study. I*nternational Journal of Sports Medicine*. 2006. 27(6):456-462. (1,6 ; A+)

(A12*) Hug, F., Raux, M., Prella, M., Morelot-Panzini, C., Straus, C., Similowski T.
Optimized analysis of surface electromyograms of the scalenes during quiet breathing in humans. *Respiratory Physiology and Neurobiology*. 2006. 25;150(1):75-81. (IF = 2,0 ; A+)

Année 2005

(A11) Hug, F., Bendahan, D., Le Fur, Y., Cozzone, P., Grélot, L.
Metabolic recovery associated with aerobic training. A ^{31}P-MRS study in professional road cyclists. *Médicine and Science in Sports and Exercise*. 2005. 37(5):846-52. (IF=3,4; A+)

Année 2004

(A10) Faucher, M., Steinberg, JG., Barbier, D., Hug, F., Jammes, Y.
Influence of chronic hypoxemia on peripheral muscle function and oxidative stress in humans. *Clinical Physiology and Functional Imaging*. 2004. 24(2): 75-84. (IF = 1,2 ; NC)

(A9) Laplaud, D., Hug, F., Menier, R.
Training-induced changes in aerobic aptitudes of professional basketball players. *International Journal of sports medicine*. 2004. 25, 103-108. (1,6 ; A+)

(A8) Hug, F., Bendahan, D., Le Fur, Y., Cozzone, P., Grélot, L.
Heterogeneity of muscle recruitment pattern during pedaling in professional road cyclists. A MRI and EMG study. European Journal of Applied Physiology. 2004. 92(3): 334-342. (IF = 1,9 ; A+)

(A7) Hug, F., Faucher, M., Marqueste, T., Guillot, C., Kipson, N., Jammes, Y.
EMG signs of neuromuscular fatigue are concomitant with further increase in ventilation during static handgrip. *Clinical Physiology and Functional Imaging*. 2004. 24(1), 25-32. (IF = 1,2 ; NC)

(A6) Hug, F., Decherchi, P., Marqueste, T., Jammes, Y.
EMG versus oxygen uptake during cycling exercise in trained and untrained subjects. *Journal of Electromyography and Kinesiology*. 2004. 14(2), 187-195. (IF=1,9 ; A)

Année 2003

(A5) Decherchi, P., Dousset, E., Marqueste, T., Berthelin, F., Hug, F., Grélot, L., Jammes, Y.
Electromyostimulation et récupération fonctionnelle d'un muscle dénérvé. *Science & Sports*. 2003. 18(5), 253-263. (0,1 ; NC)

(A4) Marqueste, T., Hug, F., Decherchi, P., Jammes, Y.
Changes in neuromuscular function after training by functional electrical stimulation. *Muscle and Nerve*. 2003. 28, 181-188. (2,6 ; A+)

(A3) Hug, F., Bendahan, D., Savin, B., Cozzone, P., Grélot, L.
Caractéristiques physiques et physiologiques de cyclistes professionnels. *Science & Sports*. 2003. 18(4), 212-215. (0,1 ; NC)

(A2) Hug, F., Faucher, M., Kipson, N., Jammes, Y.
EMG signs of neuromuscular fatigue related to the ventilatory threshold during cycling exercise. *Clinical Physiology and Functional Imaging*. 2003. 23, 208-214. (IF = 1,2 ; NC)

(A1) Hug, F., Laplaud, D., Savin, B., Grélot, L.
Occurrence of electromyographic and ventilatory thresholds in professional road cyclists. *European Journal of Applied Physiology*. 2003. 90, 643-646. (IF = 1,9 ; A+)

Articles soumis ou en révision dans des revues indexées (ISI)

(AS1) Hug, F., Turpin, N., Guével, A., Dorel, S.
Is interindividual variability of EMG patterns in trained cyclists related to different muscle synergies? *Journal of Neurophysiology*. En révision majeure – août 2009. (IF = 3,6 ; A+)

(AS2) Nordez, A., Hug, F.
Muscle shear elastic modulus measured using supersonic shear imaging is highly related to muscle activity level: preliminary results. *Journal of Biomechanics*. Soumis – août 2009. (IF = 2,8, A+)

(AS3) Guével, A., Boyas, S., Guihard, V., Cornu, C., Hug, F., Nordez, A.
Thigh muscle activities during codified training sequences of on-water rowing. *European Journal of Applied Physiology*. Soumis – juillet 2009. (IF = 1,9 ; A+)

(AS4) Dorel, S., Couturier, A., Lacour, JR., Vandewalle, H., Hautier, D., Hug, F.
Force-velocity relationship in cycling revisited: benefit of 2D pedal forces analysis. *Medicine and Science in Sports and Exercise*. En révision mineure – septembre 2009. (IF=3,4; A+)

Articles publiés dans des revues non indexées

(1) Decherchi, P., Marqueste, T., Dousset, E., Berthelin, F., Hug, F., Gounard, F., Grélot, L., Jammes, Y. Electrothérapie et régénération nerveuse sensitive. *Les Annales de Kinésithérapie*. 2003. 11-12, 28-40.

Chapitres d'ouvrages, ouvrages

Chapitres d'ouvrages

(3) Marqueste, T., Hug, F.
Neurophysiologie du mouvement. In F. Hug (Ed), *Le mouvement*. Paris : Editions revue EPS. À paraître (octobre 2009).

(2) Hanon, C., Dorel, S., Hug, F.
Analyse du mouvement et performance de haut niveau. In F. Hug (Ed), *Le mouvement*. Paris : Editions revue EPS. À paraître (octobre 2009).

(1) Hug, F., Coulange, M., Jammes, Y.
Travail musculaire en hyperbarie. in JL. Méliet, F. Brousolle, M. Coulange (Eds), Physiologie et Médecine de la Plongée (2ème édition). Editions Ellipses. 2006.

Ouvrage

(1) F. Hug (Ed), Le mouvement. Paris : Editions revue EPS. À paraître (octobre 2009).

Communications orales ou affichées avec publication de résumé

(C12) Morelot-Panzini, C., Mayaux, J., Hug, F., Willer, JC., Similowski, T.
Analgesia-inducing properties of dyspnea: a comparison of 'air hunger' with 'excessive respiratory effort'. *Fundamental & Clinical Pharmacology*. 2008. 22 Supplement 1:7.

(C11) Dorel, S., Drouet, JM., Hug, F., Lepretre, P.M. Champoux. Y.
New instrumented pedals to quantify 2D forces at the shoe-pedal interface in ecological conditions: preliminary study in elite track cyclists. *Computer Methods in Biomechanics and Biomedical Engineering*. 2008. 11, 89-90.

(C10) Coulange, M., De Haro, L., Barthélémy, A., Thierry, AL., Hug, F., Arditti, J., Sainty, JM.
Mesure non invasive de carboxyhémoglobine par CO-oxymètre de pouls chez l'intoxiqué au monoxyde de carbone. *Journal Européen des Urgences*. 2007. 20, 103.

(C9) Tremoureux, L., Raux, M., Couturier, A., Hug, F., Similowski, T.
Effet de la restriction de la bande passante et de l'utilisation d'une référence auriculaire unique sur la détection des potentiels prémoteurs inspiratoires. *Revue des maladies respiratoires.* 2006. 23, 587.

(C8) Raux, M., Straus. C., Redolfi, S., Morelot-Panzini, C., Couturier, A., Hug, F., Zelter, M., Derenne, JP., Similowski,T.
Activation du cortex prémoteur en réponse à l'application d'une charge inspiratoire chez l'homme. *Revue des maladies respiratoires.* 2006. 23, 580.

(C7) Hug, F., Raux, M., Morélot-Panzini, C., Similowski, T. Quantification non invasive de l'activité d'un muscle dilatateur des voies aériennes (Alae nasi) en ventilation spontanée avec aide inspiratoire. *Réanimation.* 2007. 15 (Suppl. 1), S347.

(C6) Chiti, L., Hug, F., Biondi, G., Morelot-Panzini, C., Raux, M., Similowski, T.
Apport de l'EMG de surface du scalène dans la détection d'une dysharmonie patient-ventilateur. *Réanimation.* 2006. 15 (Suppl. 1), S149.

(C5) Raux, M., Hug, F., Prella, M., Ray, P., Derenne, JP., Zelter, M., Straus, S., Similowski, T.
Optimisation de la détection électromyographique de surface de l'activité inspiratoire du scalène. *Revue des Maladies Respiratoires*. 2005. 22, 1S62.

(C4) Raux, M., Hug, F., Prella, M., Duguet, A.,Ray, P., Derenne, JP., Zelter, M., Straus, S., Similowski, T.
Quantification de l'activité des muscles inspiratoires du cou en ventilation spontanée avec aide inspiratoire. *Réanimation.* 2005. 14 (Suppl. 1), S174.

(C3) Bendahan, D., Hug, F., Le Fur, Y., Grélot, L., Cozzone, P.J.
Heterogeneity of muscle recruitment pattern during pedaling in professional road cyclists: a combined MRI-EMG study. MAGMA. 2004. 17, suppl 1, S60.

(C2) Hug, F., Bendahan, D., Savin, B., Cozzone, PJ., Grélot, L.
Détermination par IRM et EMG des muscles impliqués dans le pédalage chez des cyclistes professionnels. *Les cahiers de l'INSEP : expertise et sport de haut niveau. 2003. 34 :397*.

(C1) Hug, F., Decherchi, P., Grélot, L., Jammes, Y.
Correlation between EMG and metabolic data during cycling exercises. MAGMA. 2002. 14, 61-212.

Symposium invités

(2) Hug, F., Dorel, S.
L'analyse du cycle de pédalage à travers l'étude des paramètres mécaniques et électromyographiques. Les entretiens de l'INSEP. Avril 2006. INSEP, Paris, France.

(1) Hug, F., Bendahan, D., Le Fur, Y., Cozzone, PJ., Grélot, L.
Détermination par l'IRM et l'EMG des muscles impliqués dans le pédalage chez des cyclistes professionnels. *Xèmes congrès international de l'association des chercheurs en activités physiques et sportives*. *Symposium « cyclisme et performance ».* 30-1 novembre 2003, Toulouse, France.

Participation à des contrats de recherche

2009-présent Association Française contre les Myopathies (AFM – contrat n° 14084)
Titre du projet : « Characterization of the electromechanical delay by using ultrafast echographic imaging of in vivo muscle-tendon unit »
Financement de 12 340 euros
Porteur du projet : François HUG
Article publié n°A31

2008-présent Région pays de la Loire (Projet OPERF2A)
Titre du projet : « Optimisation de la performance et interactions homme-machine en sport automobile et en aviron »
Financement de 300 000 euros (dont 2 allocations de thèse et 2 post-doctorants)
Porteur du projet : Arnaud GUÉVEL
(Responsable de deux axes d'étude)

2007-présent Ministère de la jeunesse, des sports et de la vie associative (contrat n°07-006)
Titre du projet : « effets de la cryothérapie sur la récupération musculaire subséquente à un exercice excentrique fatigant »
Financement de 55 000 euros
Porteurs du projet : Sylvain DOREL et Antoine COUTURIER

2007-2008 Entreprise CP Technology (Saint-Herblain, France)
Titre du projet : «Impact de l'utilisation des outils de vissage sur les contraintes musculaires imposées à l'opérateur »
Financement de 7600 euros
Responsable du projet : Arnaud GUÉVEL

2006-2007 Ministère de la jeunesse, des sports et de la vie associative (contrat n°06-029)
Titre du projet : « Analyse comparée des contraintes énergétiques et musculaires d'un effort maximal réalisé sur le plat et en côtes »
Financement de 10 000 euros
Porteurs du projet : Christine HANON et Jean SLAWINSKI
Article publié n°A22.

2006-2007 Ministère de la jeunesse, des sports et de la vie associative (contrat n° 06-046)
Titre du projet : « Evolution des paramètres électromyographiques et mécaniques au cours d'une épreuve rectangulaire de pédalage menée jusqu'à épuisement »
Financement de 11 800 euros
Porteurs du projet : Sylvain DOREL et François HUG
Articles publiés n°A21, A24, A26, A28 et A30

2004-2005 Fédération ANTADIR
Titre du projet : «Substrats neurophysiologiques de la dyspnée »
Financement de 15 000 euros (bourse de recherche post-doctorale)
Porteurs du projet : François HUG et Thomas SIMILOWSKI
Articles publiés n°A12 et A25 ; communications n°C4, C5, C6 et C7

2003-2004 Assistance Publique des hôpitaux de Marseille (AP-HM)
Titre du projet : « BPCO et stress oxydatif »
Financement de 5000 euros (allocation de recherche)
Porteur du projet : Yves JAMMES

2001-2003 Amaury Sport Organisation (Société du Tour de France)
Titre du projet : « Physiologie et physiopathologie d'une population de cyclistes professionnels »
Financement de 75 000 euros
Porteur du projet : Laurent GRÉLOT
Articles publiés n°A1, A3, A8, A11, A13, A15 et A18 ; communications n°C2 et C3

Évaluation de l'impact des articles publiés ou « sous presse »

n°	Revue	Année de publication	Facteur d'impact de la revue (ISI 2008)	Nombre de citations (au 05/09/2009) *source scopus*
A32	*European Journal of Applied Physiology*	2009	1,9	-
A31	*Journal of Applied Physiology*	2009	3,6	-
A30	*Medecine & Science in Sports & Exercise*	2009	3,4	-
A29	*Ultrasound in Medicine and Biology*	2009	2,4	1
A28	*Scandinavian Journal of Medicine & Science in Sports*	2009	2,3	1
A27	*Journal of Science and Medicine in Sports*	2009	1,9	-
A26	*Journal of Electromyography and Kinesiology*	2009	1,9	2
A25	*Respiratory Physiology and Neurobiology*	2008	2,0	2
A24	*European Journal of Applied Physiology*	2008	1,9	2
A23	*Undersea and Hyperbaric Medicine*	2008	0,8	1
A22	*Medecine & Science in Sports & Exercise*	2008	3,4	1
A21	*Journal of electromyography and Kinesiology*	2008	1,9	2
A20	*Journal of Physiology (London)*	2007	4,6	12
A19	*Science & Sport*	2006	0,1	-
A18	*Medecine & Science in Sports & Exercise*	2006	3,4	7
A17	*Pflügers Archiv*	2006	3,5	3
A16	*Journal of Electromyography and Kinesiology*	2006	1,9	12
A15	*European Journal of Applied Physiology*	2006	1,9	3
A14	*Journal of Strength and Conditionning Research*	2006	0,8	-
A13	*International Journal of Sports Medicine*	2006	1,6	5
A12	*Respiratory Physiology and Neurobiology*	2006	2,0	5
A11	*Medecine & Science in Sports & Exercise*	2005	3,4	13
A10	*Clinical Physiology and Functional Imaging*	2004	1,2	9
A9	*International Journal of Sports Medicine*	2004	1,6	7
A8	*European Journal of Applied Physiology*	2004	1,9	17
A7	*Clinical Physiology and Functional Imaging*	2004	1,2	8
A6	*Journal of Electromyography and Kinesiology*	2004	1,9	13
A5	*Science & Sport*	2003	0,1	-
A4	*Muscle and Nerve*	2003	2,6	13
A3	*Science & Sport*	2003	0,1	-
A2	*Clinical Physiology and Functional Imaging*	2003	1,2	13
A1	*European Journal of Applied Physiology*	2003	1,9	9

1.3. Encadrements et co-encadrements de travaux de recherche

Thèse de doctorat

2008-présent **Co-encadrement de la thèse** de Mr Nicolas TURPIN
Titre de la thèse : « Etude des coordinations musculaires et de la fatigue neuromusculaire chez des rameurs de haut niveau »
Financement : Région Pays de la Loire (projet OPERF2A)
Directeur de thèse : Pr Arnaud GUÉVEL

Thèse de spécialité médicale

2004-2005 **Co-encadrement de la thèse de spécialité médicale** de Mlle Linda CHITI (Florence, Italie)
Titre de la thèse : « Apport de l'EMG des muscles du cou dans l'étude de la dysharmonie patient-ventilateur »
Directeur de thèse : Pr Thomas SIMILOWSKI
Article publié n°A25

Master 2ème année

2009-2010 **Co-direction** de Mr Killian BOUILLARD (Master 2 STAPS EPI, Université de Nantes)
Titre du mémoire : « Étude du seuil EMG de la fatigue et de la prédiction de l'endurance limite lors d'une tâche d'adduction de l'index »
Co-directeur : Pr Arnaud GUÉVEL

2005-2006 **Co-direction** de Mr Gaël GUILHEM (Master 2 STAPS, Paris V – major de promotion)
Titre du mémoire : « Effets d'un exercice préalable sur l'apparition des seuils ventilatoires »
Co-directeur : Dr Sylvain DOREL
Article publié n°A27

Master 1ère année

2008-2009 **Encadrement** de Mr Killian BOUILLARD (Master STAPS EPI, Université de Nantes)
Titre du mémoire : « Pistes de réflexion pour la conception d'un protocole expérimental permettant une prédiction de l'endurance-limite »

2007-2008 **Encadrement** de Mlle Christelle BERLANGER (Master STAPS AMES, Université de Nantes)
Titre du mémoire : « Mesure des contraintes cardiorespiratoires au cours d'un cross chez le cavalier complet de haut niveau »

2006-2007 **Encadrement** de Mr Johann GENTY (Master STAPS AMES, Université de Nantes)
Titre du mémoire : « Etude des sollicitations musculaires de l'activité de pilotage en karting et conception d'un ergomètre spécifique »

2005-2006 **Encadrement** de Mr Olivier NICOLLE (Master STAPS, Université de Paris XII)
Titre du mémoire : « Influence d'une position de contre la montre sur les patrons d'activité musculai

Chapitre 2 – Présentation de la technique d'électromyographie

Le point commun de la plupart des travaux présentés dans ce mémoire d'habilitation à diriger des recherches est l'exploration de la fonction neuromusculaire par la technique d'électromyographie (EMG). Il nous paraît donc important de présenter cette technique à travers le recueil du signal, la signification physiologique des résultats obtenus, les limites méthodologiques et les méthodes de traitement utilisées dans les études présentées dans ce mémoire. À dessein, cette partie n'a pas vocation à présenter la technique d'électromyographie de manière exhaustive, mais doit seulement permettre au lecteur d'appréhender le cadre méthodologique dans lequel s'insèrent nos travaux.

Il est difficile de parler d'électromyographie sans évoquer les travaux princeps de Luigi Galvani[1]. Ses recherches consacrées aux effets de l'électricité sur des préparations nerf-muscle de grenouille ont été les premières à mettre en évidence « une électricité animale » responsable de la contraction musculaire (Figure 1). Même si l'origine de cette « électricité animale » n'était pas encore connue, ces résultats ont participé à la création d'une nouvelle discipline : la neurophysiologie. Au XX^{ème} siècle, de nombreuses études ont contribué à la compréhension de la contraction musculaire à travers l'étude des phénomènes électriques concomitants. Ainsi, H. Piper a été le premier, en 1912, à mesurer l'activité électromyographique au cours d'une contraction musculaire.

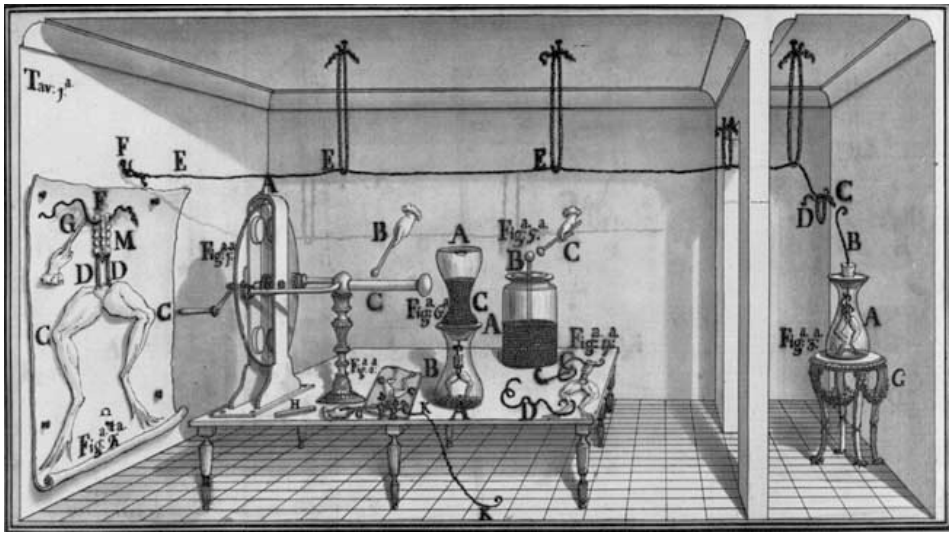

Figure 1. Illustration des travaux de Galvani portant sur les effets de l'électricité sur le muscle de grenouille.

L'électromyographie peut être définie comme l'étude fonctionnelle du muscle à travers le recueil et l'analyse du signal électrique généré au niveau des muscles en contraction (Basmajian et De Luca, 1985). Cette activité électrique peut être mesurée de manière invasive par une électrode-aiguille (ou filaire) insérée dans le muscle ou de manière non invasive en utilisant des électrodes posées à la surface de la peau. L'utilisation des électrodes-aiguilles (i.e., EMG intramusculaire ou élémentaire) présente l'avantage de fournir une mesure de l'activité électrique d'un nombre restreint d'unités motrices, offrant la possibilité de calculer directement leur fréquence de décharge. Néanmoins, cette sélectivité peut aussi constituer un inconvénient majeur puisque l'activité mesurée

[1] Physicien et médecin italien (1737-1798). Ses travaux sur « l'électricité animale » ont largement influencé Allessandro Volta (1745-1827), inventeur de la pile électrique.

par ces électrodes n'est représentative que d'une petite partie du muscle considéré. De plus, le caractère invasif de cette technique la rend difficilement applicable aux études portant sur l'analyse du mouvement. À l'inverse, l'utilisation d'électrodes de surface (i.e., EMG de surface ou global) permet de mesurer une activité EMG représentative d'un volume musculaire plus conséquent et est donc davantage reliée aux caractéristiques mécaniques du mouvement [force développée, vitesse de déplacement, type de contraction etc., Bouisset et Maton (1995)]. De ce fait, ce type de mesure est généralement préféré bien que présentant certaines limites que nous détaillerons ci-après.

Depuis les premiers enregistrements réalisés par H. Piper, les appareils de mesure ont beaucoup évolué. Récemment, la technique Wi-Fi[2] a été utilisée pour remplacer les câbles habituellement utilisés pour les relier les électrodes EMG à la chaîne d'acquisition. Cette technique devrait permettre de simplifier la mise en place des électrodes, et rendre possible l'enregistrement d'un nombre plus important de muscles. L'apparition récente d'amplificateurs EMG multicanaux (jusqu'à 128 voies) permet d'outrepasser certaines limites inhérentes à l'utilisation de l'EMG de surface classique (i.e., deux électrodes en mode de détection bipolaire ou monopolaire) et d'envisager de nouvelles applications (cf. partie 4 de ce mémoire « projets de recherche ») (Figure 2).

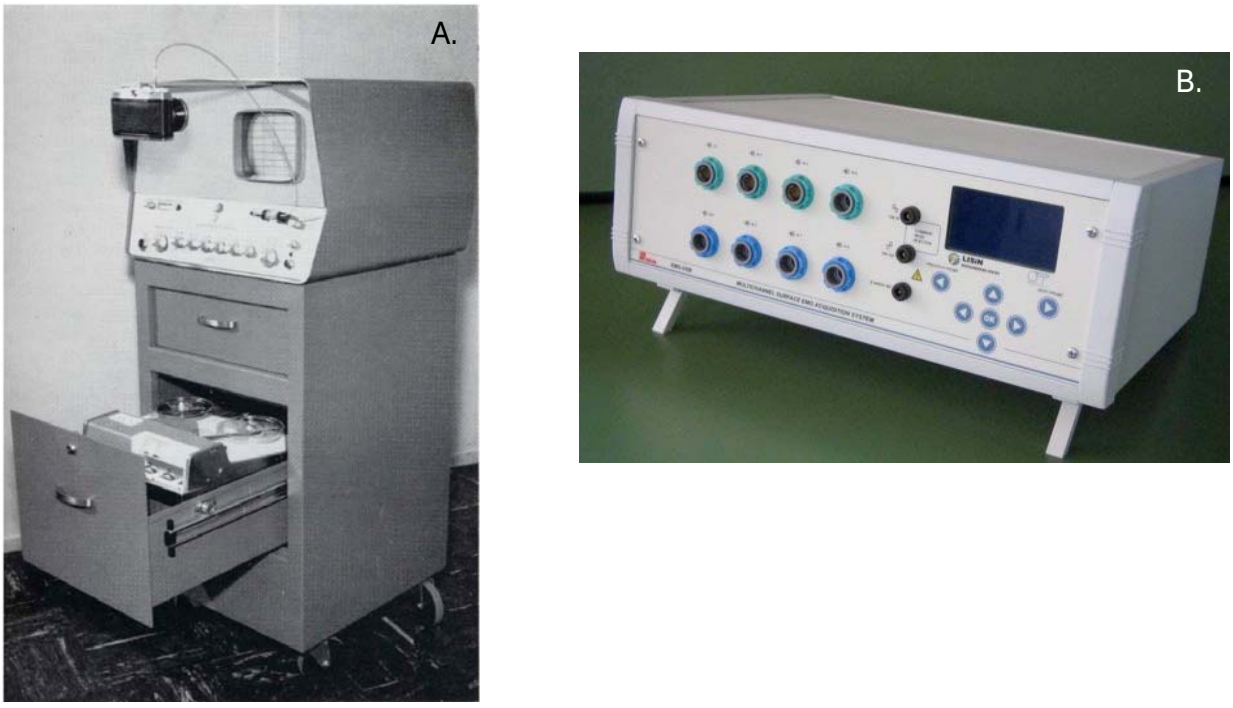

Figure 2. Deux chaînes d'acquisition du signal électromyographique séparées par 45 ans de développement technologique. A, électromyographe datant des années 1955-1960 (201 A-1, Meditron) utilisé pour l'évaluation clinique et ne permettant d'enregistrer qu'une seule voie EMG. B, chaîne d'acquisition multicanaux (EMG-128, LISin – OT Biolettronica) permettant d'enregistrer jusqu'à 128 voies simultanément *via* des matrices ou vecteurs d'électrodes.

Le signal EMG est généré par l'activité électrique des fibres musculaires activées pendant la contraction. Il résulte de la sommation algébrique des potentiels d'action des fibres musculaires activées (Figure 3).

[2] Wireless Fidelity

Considérant une fibre musculaire donnée, le potentiel d'action prend naissance au niveau de la jonction neuromusculaire et se propage de part et d'autre de celle-ci vers les deux extrémités tendineuses dans lesquelles il s'éteint. Ainsi, le signal EMG de surface est principalement lié au nombre d'unités motrices (UMs) recrutées (recrutement spatial) et à leur fréquence de décharge (recrutement temporel). Néanmoins, de nombreux autres facteurs, physiologiques et non-physiologiques, sont susceptibles de modifier le signal (pour revue, voir (Farina *et al*., 2004). Parmi les facteurs « physiologiques », on distingue les variables anatomiques (e.g., diamètre des fibres musculaires, répartition spatiale des unités motrices dans le muscle, épaisseur des couches de tissu sous-cutané) et fonctionnelles (e.g., vitesse de conduction des potentiels d'action musculaires, forme des potentiels d'action musculaires, synchronisation des unités motrices).

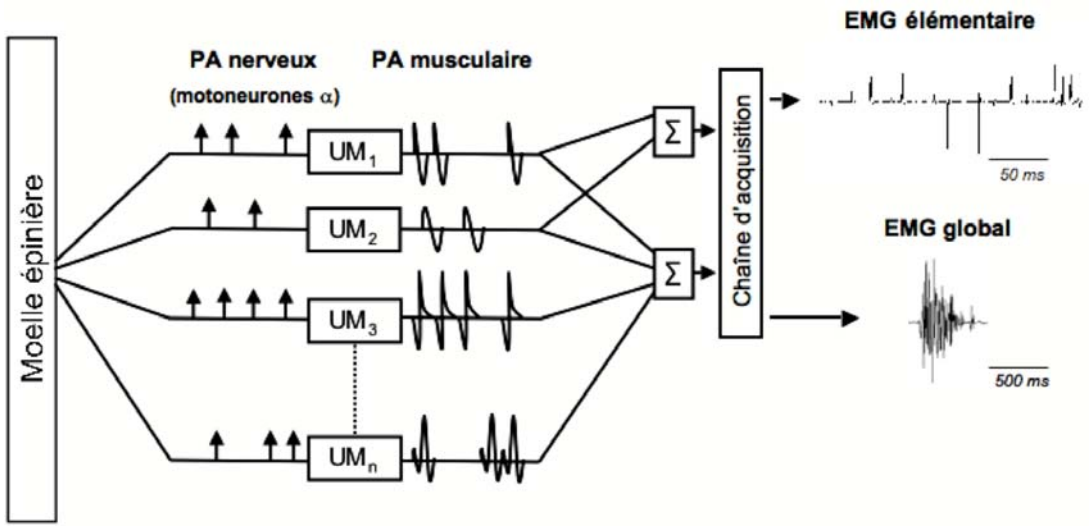

Figure 3. Modélisation du signal EMG à partir de potentiels d'unités motrices (UMs). La séquence de décharge des motoneurones α détermine celle du train de potentiels des UMs. La sommation de l'ensemble des UMs (situées dans le champ de détection des électrodes de surface) donne naissance à un signal EMG global. La sommation de quelques UMs (au regard de l'électrode aiguille) donne naissance à un signal EMG élémentaire. Adapté de De Luca (1979).

Les facteurs « non-physiologiques » sont principalement liés au système de recueil du signal (e.g., taille et forme des électrodes, placement des électrodes). Parmis ces facteurs « non-physiologiques » deux phénomènes sont connus pour influencer de manière non négligeable le signal EMG : le « crosstalk » et le « signal cancellation ». Le « crosstalk » désigne une partie du signal ne provenant pas du muscle visé par le système de détection, mais de muscles adjacents comme nous l'avons mis en évidence lors d'enregistrements EMG de surface du scalène (Chiti *et al*., 2008). À ce jour, il n'existe pas de méthode fiable pour quantifier simplement ce phénomène de « crosstalk » sur des enregistrements EMG de surface (Farina *et al*., 2004). Le phénomène de « signal cancellation » désigne quant à lui la perte d'une partie du signal EMG liée à une superposition de phases positives et négatives de potentiels d'action qui s'annulent. Ce phénomène serait majoré lorsque la vitesse de conduction des potentiels d'action musculaires diminue (Keenan *et al.*, 2005). Pour réduire l'influence de ces

phénomènes sur le signal EMG, il est recommandé de suivre les préconisations de l'International Society of Electrophysiology and Kinesiology (https://www.isek-online.org/standards_emg.asp) ou de SENIAM « Surface Electromyography for the Non-Invasive Assessment of Muscles » (http://www.seniam.org/) en matière d'enregistrement du signal électromyographique.

Dans ce paragraphe, nous n'aborderons que les méthodes de traitement utilisées dans les études présentées dans ce mémoire. Nous privilégierons donc les paramètres temporels de l'EMG permettant de quantifier le niveau d'activité myoélectrique. Les paramètres fréquentiels, caractérisant le contenu fréquentiel du signal et dont l'interprétation est beaucoup plus sujette à caution, ne seront donc pas présentés dans ce mémoire.

Le Root Mean Square (ou valeur efficace) est une variable classiquement calculée pour quantifier le niveau d'activité EMG. Le calcul de cette variable ne nécessite pas de redresser le signal et se fait selon la formule :

$$x_{\mathrm{RMS}} = \sqrt{\frac{1}{N}\sum_{i=1}^{N} x_i^2} = \sqrt{\frac{x_1^2 + x_2^2 + \cdots + x_N^2}{N}}\ .$$

Le recueil des données EMG peut permettre de caractériser le patron d'activité musculaire au cours de mouvements très variés (e.g., gestes sportifs, mouvements de la vie quotidienne, etc…). Nous nous focaliserons ci-après sur l'ultilisation de l'EMG pour l'analyse d'activités cycliques. Le niveau d'activité EMG est classiquement quantifié par la valeur RMS (Root Mean Square ; (Duc et al., 2006; Laplaud *et al*., 2006) et/ou par l'intégrale du signal EMG (EMGi ; (Ericson, 1986; Jorge et Hull, 1986). Ce calcul peut être effectué sur le cycle complet ou uniquement sur la « bouffée d'activité ». Les caractéristiques de la séquence d'activité sont le plus souvent identifiées par les temps (en % du cycle complet ou en degrés de rotation de la manivelle lors du pédalage) correspondant au début (on) et à la fin (off) de la bouffée d'activité du muscle considéré et par la durée de celle-ci (Jorge et Hull, 1986; Li et Caldwell, 1998). La Figure 4 résume de façon simplifiée les procédures de calcul de ces variables.

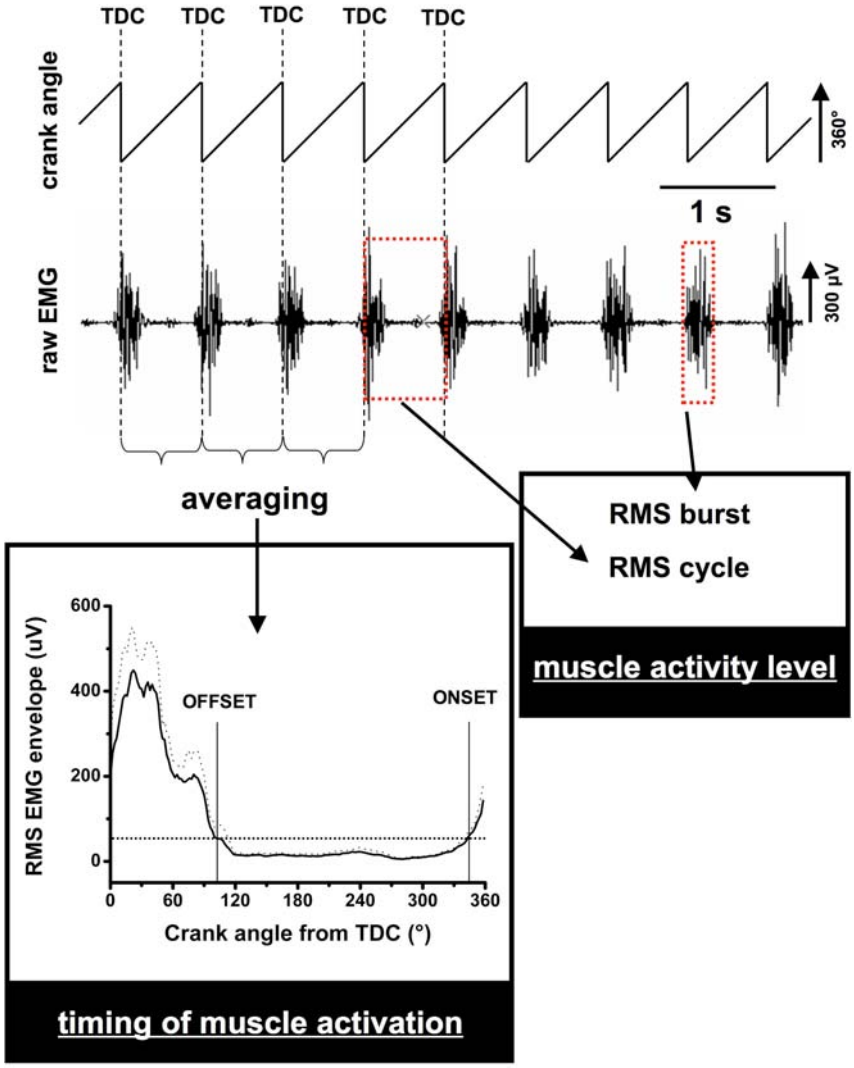

Figure 4. Exemple de procédure de traitement d'un signal EMG de surface pour calculer : i) le niveau d'activité EMG RMS sur le cycle entier (i.e., 360°, RMS_{cycle}) et/ou la bouffée d'activité (RMS_{burst}) ainsi que ii) les valeurs de début et de fin de bouffée (onset et offset) à partir de l'enveloppe EMG RMS moyenne (obtenue en moyennant plusieurs cycles consécutifs) et l'utilisation d'un seuil (i.e., ici 20% de la valeur pic, trait en pointillé). TDC (point mort haut), 0°. D'après Hug et Dorel (2009).

En utilisant ces différents indicateurs, de nombreuses études ont décrit les patrons d'activité musculaire au cours d'activités cycliques (e.g., pédalage, course à pied) (Houtz et Fischer, 1959; Ericson, 1986; Jorge et Hull, 1986; Lucia *et al.*, 2004; Duc *et al.*, 2006; Hettinga *et al.*, 2006). Récemment, la technique de cross-corrélation a été proposée afin de déterminer de façon plus objective l'évolution des caractéristiques temporelles des patrons d'activité EMG. Jusqu'alors elle avait été très peu utilisée dans ce contexte (Li et Caldwell, 1999; Wren *et al.*, 2006). Cette méthodologie, basée sur la corrélation de deux signaux possède l'avantage de prendre en compte l'ensemble des valeurs caractérisant le patron d'activité sur le cycle complet (Figure 5). Par conséquent, le coefficient de cross-corrélation et la valeur k de décalage temporel entre les deux signaux considérés qui en résultent reflètent des modifications à la fois de la séquence d'activité mais également du profil général (la forme) de l'enveloppe EMG.

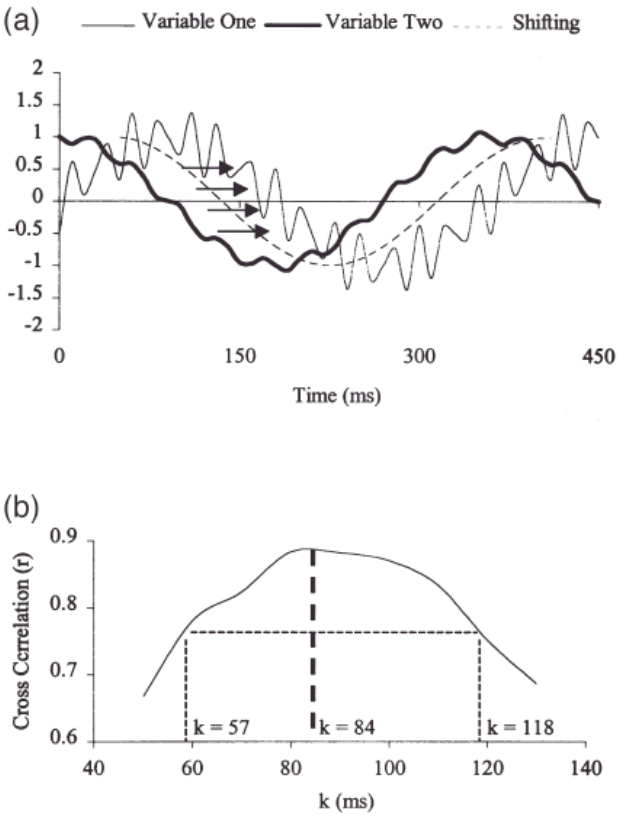

Figure 5. Illustration de 2 signaux déphasés (a). Le coefficient de cross-corrélation entre les 2 pour ces données originales est r(0)=-0,015. En décalant dans le temps un signal par rapport à l'autre par des incréments successifs k, r(k) peut être calculé pour l'ensemble des valeurs k (b). r(84 ms)=0.883 est le coefficient de corrélation maximal qui peut être obtenu par la procédure de décalage. 84 ms peut être considéré comme le déphasage temporel entre les 2 signaux. k=57 et k=118 représentent l'intervalle de confiance à 95% signifiant dans ce cas que cette valeur de k=84ms est significative. D'après Li et Caldwell (1999).

Chapitre 3 – Synthèse de l'activité de recherche

Cette formation à la recherche s'inscrit dans le cadre général de la physiologie neuromusculaire et comprend quatre axes principaux.

Le premier axe intitulé « électromyographie et analyse des coordinations musculaires» concerne l'analyse électromyographique du mouvement, et plus particulièrement du mouvement de pédalage. Il s'inscrit dans la suite de certains travaux menés lors de ma thèse. Ces études ont été réalisées au sein du laboratoire de biomécanique et physiologie de l'Institut National du Sport et de l'Education Physique (INSEP, Paris), en collaboration avec les Dr Sylvain DOREL et Antoine COUTURIER. Les ressources humaines et matérielles mises à notre disposition (e.g., pédale instrumentée, dans le cadre d'une collaboration avec le groupe VéLUS de l'Université de Sherbrooke, Canada) nous ont permis d'appréhender le mouvement de pédalage de manière beaucoup plus complète que ce qui avait pu être fait lors de ma thèse. Cet axe de recherche continue d'être développé, en particulier *via* le co-encadrement de la thèse de Mr Nicolas TURPIN intitulée «étude des coordinations musculaires et de la fatigue neuromusculaire chez des rameurs de haut niveau» (financement de la région des Pays de la Loire, Projet OPERF2A).

Le deuxième axe porte sur la détection électromyographique d'une charge mécanique imposée au système respiratoire et a été développé au cours de mon année de stage post-doctoral réalisée au sein du Laboratoire de Physiopathologie Respiratoire (EA 2397, université Pierre et Marie Curie, Paris VI), sous la supervision du Pr Thomas SIMILOWSKI. Cette année a été l'occasion de me former à de nouvelles techniques d'exploration de la fonction neuromusculaire (e.g., électromyographie *via* des électrodes intramusculaires et oesophagiennes, stimulation magnétique transcranienne, électroencéphalographie). Une partie des travaux présentés dans ce mémoire d'Habilitation à Diriger des Recherches a été mené en collaboration avec une étudiante italienne (Mlle Linda CHITI, université de Florence, Italie) dont j'ai co-encadré la thèse de spécialité médicale. Un article est actuellement en cours de rédaction.

Le troisième axe porte sur l'évaluation électromyographique de la fatigue neuromusculaire. Une partie des travaux présentés a été réalisée dans l'année qui a suivi ma soutenance de thèse, dans le cadre d'une collaboration avec le Pr Alenjandro LUCIA (université européenne de Madrid, Espagne), et visait à compléter les travaux déjà réalisés. Cet axe de travail est actuellement poursuivi au sein du laboratoire « Motricité, Interactions, Performance » (EA 4334, université de Nantes).

Le dernier axe de recherche présenté dans ce mémoire concerne la caractérisation du délai électromécanique au moyen d'une technique d'échographie ultrarapide. Le développement de cette thématique au sein du laboratoire « Motricité, Interactions, Performance » est très récent (juillet 2008). Il a été rendu possible par une collaboration avec le Dr Antoine NORDEZ (laboratoire « Motricité, Interactions, Performance ») et le Dr Stefan CATHELINE (laboratoire de Géophysique Interne et Tectonophysique, université de Grenoble). Un contrat de recherche obtenu récemment (Association Française contre les Myopathies - AFM, contrat n° 14084) nous permet de continuer à développer activement cet axe.

3.1. Électromyographie et analyse des coordinations musculaires

3.1.1. État de la question.

Hug, F., Dorel, S. Electromyographic analysis of pedaling: a review. *Journal of electromyography and kinesiology*. 2009. 19(2) : 182-198 (revue de littérature).

Lors de l'activité de pédalage, la force totale appliquée sur les pédales résulte essentiellement de l'action des muscles des membres inférieurs (*Gluteus maximus, Rectus femoris, Vastus lateralis, Vastus medialis, Biceps femoris, Semi-membranosus, Gastrocnemius medialis* et *lateralis, Soleus* et *Tibialis anterior* ; Figure 6). De nombreux auteurs ont démontré que les contraintes mécaniques liées au trajet circulaire de la pédale induisent une séquence temporelle spécifique d'activité des principaux muscles impliqués dans le mouvement (Figure 7) [pour revue, voir (Hug et Dorel, 2009)]. Cette séquence semble répondre à un souci d'optimisation du transfert des forces produites essentiellement par les muscles mono-articulaires en mode concentrique (e.g., Gluteus maximus, Vastus lateralis et Vastus medialis) depuis les articulations proximales vers les articulations distales. Le rôle des muscles bi-articulaires (e.g., chef long du *Biceps femoris* et *Gastrocnemius*) est primordial dans ce transfert car ils permettent la redistribution des moments articulaires afin d'optimiser l'orientation de la force résultante sur la pédale (Gregor *et al*., 1985; van Ingen Schenau *et al*., 1992). Le patron d'activité des principaux muscles du membre inférieur répond donc, non seulement à une contrainte de production de force, mais aussi de transfert et d'optimisation de son orientation au niveau de la pédale.

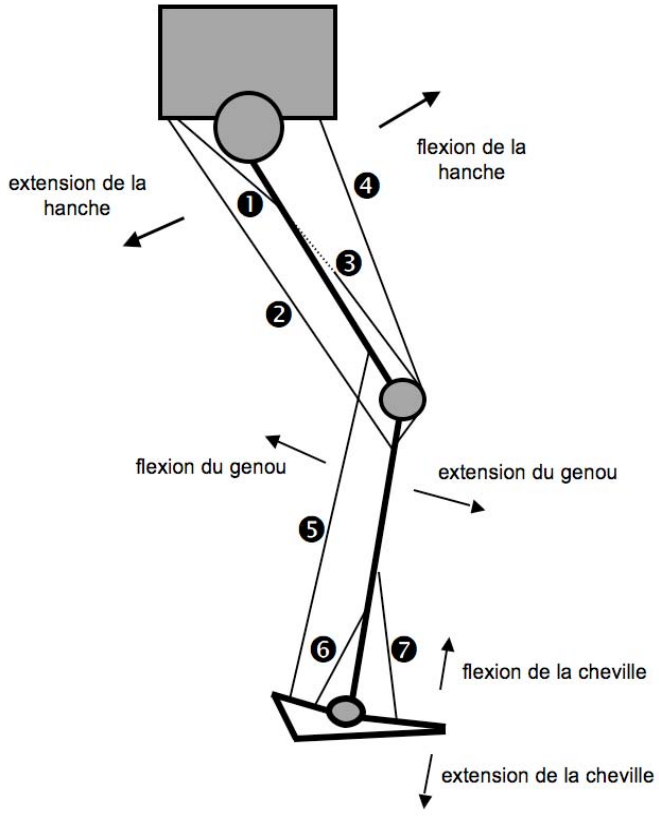

Figure 6. Représentation schématique des principaux muscles impliqués dans le mouvement de pédalage. (1) Gluteus maximus (extenseur de la hanche) ; (2) Semimembranosus et Biceps femoris (chef long) (extenseurs de la hanche, fléchisseurs du genou) ; (3) Vastus medialis et Vastus lateralis (extenseurs du genou) ; (4) Rectus femoris (extenseur du genou, fléchisseur de la hanche) ; (5) Gastrocnemius lateralis et medialis (fléchisseurs du genou, extenseurs de la cheville) ; (6) Soleus (extenseur de la cheville) et (7) Tibialis anterior (fléchisseur de la cheville). D'après Hug et Dorel (2009).

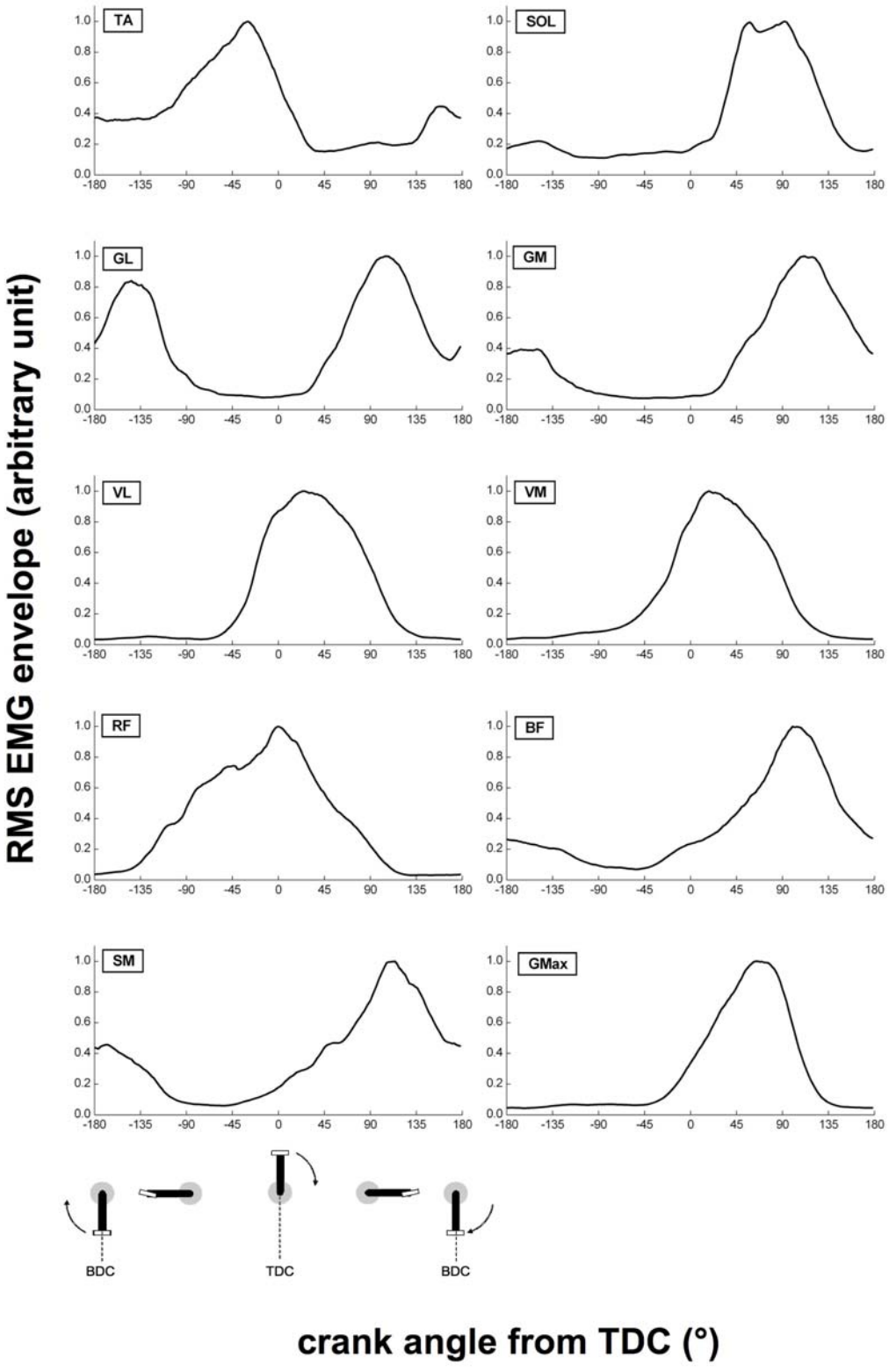

Figure 7. Enveloppes EMG RMS de 10 muscles du membre inférieur. Les enveloppes ont été moyennées sur 45 cycles consécutifs, chez 12 triathlètes pédalant à la puissance associée au 1er seuil ventilatoire (238 ± 23 W). Pour chaque sujet, le niveau d'activité EMG a été normalisé par rapport à l'activité maximale enregistrée au cours du cycle. TDC, point haut (0°); BDC, point bas (180°) ; GMax, *Gluteus maximus* ; SM, *Semimembranosus* ; BF, *Biceps femoris* (chef long) ; VM, *Vastus medialis* ; VL, *Vastus lateralis* ; GM, *Gastrocnemius medialis* ; GL, *Gastrocnemius lateralis* ; SOL, *Soleus* ; TA, *Tibialis anterior*. D'après Hug et Dorel (2009).

Sur le plan biomécanique, la force totale appliquée sur la pédale résultant de l'action de ces différents muscles varie en intensité et en direction en fonction de la position de la manivelle. Comme l'illustre la Figure 8, le moment résultant au niveau de l'axe du pédalier dépend de la valeur de cette force et de la capacité à orienter efficacement cette dernière (Ericson, 1986). La phase motrice principale, c'est-à-dire celle pour laquelle le moment résultant est positif, se situe lors de la phase descendante de la pédale (entre 20° et 160°, positions de 1 à 8 sur la Figure 8) avec une valeur maximale aux alentours de 90°. Le moment est beaucoup plus faible entre les positions 8 et 12 pour devenir ensuite nul ou négatif lors de la phase ascendante de la pédale (positions de 12 à 18) puis lors du passage au point mort haut (position 20).

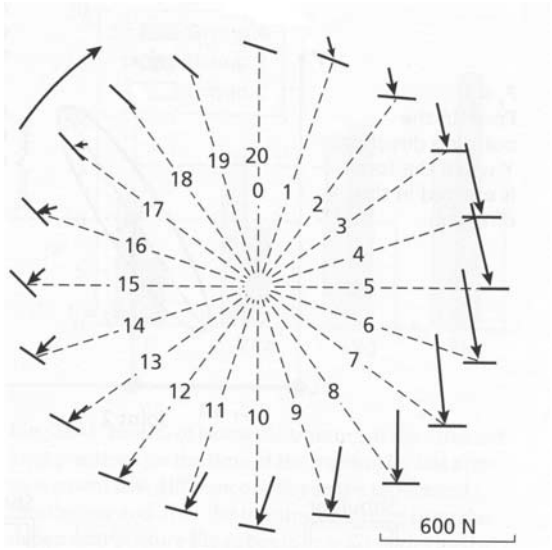

Figure 8. Force totale appliquée sur la pédale au cours du mouvement de pédalage. Valeurs moyennes pour 20 positions de la pédale pour un cycliste élite pédalant à une puissance de 400 W et une cadence de 100 rpm. D'après Cavanagh *et al.* (1986).

Ainsi, pour un niveau de puissance et de cadence de pédalage donné, le profil de la force efficace (ou du moment) en fonction de la position de la manivelle apparaît comme relativement stéréotypé (Sanderson, 1991; van Ingen Schenau *et al*., 1992). Néanmoins, il a été suggéré que certaines différences sur le plan technique pouvaient apparaître dans la production de cette force efficace (Gregor *et al*., 1991). Par conséquent, pour caractériser mécaniquement la production de la force, il est important de considérer que la force efficace (F_{eff}, qui agit perpendiculairement à la manivelle et produit le mouvement circulaire de la pédale) ne constitue qu'une des deux composantes de la force résultante produite à l'interface pied-pédale dans le plan sagittal. Une seconde composante dite inefficace (F_{Ineff}) agit dans l'axe de la manivelle, ne participant donc pas à la production de travail mécanique (Hull et Butler, 1981) (Figure 10). Depuis les années 80, plusieurs systèmes de pédales instrumentées ont été développés (Hull et Jorge, 1985) offrant la possibilité de quantifier ces deux composantes de force. Ainsi, on peut calculer un indice d'efficacité mécanique (IE) défini comme le rapport entre la force efficace et la force totale exercée par le pied sur la pédale (LaFortune et Cavanagh, 1983) et tentant de rendre compte de la capacité du sujet à orienter efficacement la force sur la pédale. Néanmoins, la nature de la relation entre cette efficacité mécanique et la performance n'est pas établie. En effet, de récentes études ont montré que l'amélioration de l'efficacité mécanique entraîne une diminution du rendement énergétique (Korff *et al*., 2007;

Mornieux *et al*., 2008). En d'autres termes les sujets sont plus efficaces d'un point de vue mécanique mais utilisent plus d'énergie pour produire le même travail.

3.1.2. Répétabilité[3] et reproductibilité[4] des paramètres électromyographiques.

Laplaud, D., Hug, F., Grélot, L. Reproducibility of eight lower limb muscles activity level in the course of an incremental pedalling exercise. *Journal of Electromyography and Kinesiology*. 2006. 16(2):158-166.

Dorel, S., Couturier, A., Hug, F. Intra-session repeatability of lower limb muscles activation pattern during pedaling. *Journal of Electromyography and Kinesiology*. 2008. 18(5) : 857-865.

La reproductibilité de certains paramètres EMG (e.g., EMG integré, RMS) a été largement démontrée au cours d'exercices impliquant des contractions isométriques (Rainoldi *et al*., 1999; Dedering *et al*., 2000; Falla *et al*., 2002; Lariviere *et al*., 2002) ou isocinétiques en concentrique (Larsson *et al*., 1999; Larsson *et al*., 2003). Pourtant, il est surprenant de constater qu'au cours de l'exercice de pédalage, la reproductibilité des enregistrements EMG n'a pas été étudiée. Dans une première étude, nous avons montré une bonne reproductibilité du niveau d'activité EMG pour 8 muscles (i.e., valeurs RMS calculées sur 5 cycles consécutifs, sur toute la durée de l'exercice) durant une épreuve triangulaire de pédalage menée jusqu'à épuisement (Laplaud *et al*., 2006). La principale limite de cette étude réside dans le fait qu'elle n'explore pas la reproductibilité des patrons d'activité musculaire (évolution de l'activité EMG au cours du cycle de pédalage) et ne rapporte aucun résultat sur la séquence d'activité (début et fin de l'activité EMG). De surcroît, même si la reproductibilité d'une séance à l'autre suggère une bonne répétabilité intra-session, elle n'a jamais été clairement établie. Pourtant, une bonne répétabilité des patrons d'activité EMG est une condition préalable à remplir pour les études visant à mettre en évidence des évolutions au cours du temps. En effet, bien que les problèmes méthodologiques liés au replacement des électrodes soient absents lors de la comparaison de signaux enregistrés au cours d'une même session, la question de l'adoption et du maintien stable des patrons d'activité musculaire, propres à un sujet, du début à la fin de la session reste posée. Y répondre semblait donc être un préambule nécessaire afin de garantir la robustesse des résultats obtenus dans le cadre de protocoles que nous comptions mener sur les effets de différents facteurs d'influence (e.g., position, fatigue) sur les patrons d'activité EMG. Dans ce contexte, nous avons mis en place un protocole permettant d'étudier la répétabilité intra-session des patrons d'activité EMG au cours d'un exercice sous-maximal réalisé à puissance constante (Dorel *et al*., 2008). Le patron d'activité EMG de 10 muscles a été enregistré avant et après une session d'entraînement simulé (durée = 53 minutes). Nous avons testé la répétabilité du patron d'activité musculaire (i.e., forme du signal), du niveau d'activité et de la séquence d'activité (i.e., début et fin de l'activité EMG). Les résultats de cette étude ont mis en évidence une bonne répétabilité du patron d'activité musculaire pour l'ensemble des muscles étudiés. Ils ont également mis en avant

[3] La répétabilité représente l'étroitesse de l'accord entre les résultats des mesures successives de la même grandeur effectuées dans les conditions suivantes : même méthode de mesure, même observateur, même instrument de mesure, même lieu, mêmes conditions d'utilisation, répétition sur une courte durée.

[4] La reproductibilité représente l'étroitesse de l'accord entre les résultats des mesures successives lorsqu'une ou plusieurs conditions de la mesure de répétabilité ne sont pas réunies. Par exemple, il est possible de déterminer la reproductibilité en changeant d'expérimentateur et/ou en réalisant des expérimentations sur deux jours différents.

les limites des méthodes classiques de détection du début et de la fin de l'activité EMG (i.e., choix d'un seuil *a priori*, puis ajustement après inspection visuelle des bouffées d'activité EMG). Ces limites sont plus largement discutées dans l'article issu de ce travail (Dorel *et al*., 2008) et la revue de littérature (Hug et Dorel, 2009) (cf. annexes de ce mémoire). Au final, ces résultats ont permis de justifier l'utilisation de la cross-corrélation comme méthode complémentaire plus objective d'estimation de la similitude des patrons d'activité EMG. En effet, en utilisant cette technique, nous observons une répétabilité forte pour l'ensemble des muscles considérés même s'il est intéressant de constater que les plus faibles corrélations sont obtenues pour les muscles présentant les répétabilités les plus faibles des valeurs de début et/ou de fin d'activité (i.e., *Rectus femoris*, *Tibialis anterior* et *Soleus*). Pour ces raisons, dans les études qui ont suivi, nous avons fait le choix d'utiliser la méthode de cross-corrélation pour comparer les patrons d'activité EMG (début et fin d'activité, forme).

Ces résultats, qu'ils concernent le niveau ou le patron d'activité EMG, doivent être discutés en prenant en considération la complexité du concept de coordination musculaire lors de ce type de mouvement poly-articulaires (van Soest *et al.*, 1993; Li et Caldwell, 1998). Les stratégies de coordination musculaire permettant de produire le mouvement de pédalage sont en théorie très nombreuses. Ainsi, une partie de la variabilité des patrons d'activité EMG pourraient être en rapport avec une variation naturelle dans le temps de ces stratégies. La Figure 9 basée sur des résultats issus de cette étude (exemple individuel), illustre les compensations intermusculaires qui peuvent apparaître (notamment entre *Gastrocnemius lateralis* et *Soleus* dans ce cas) au cours du protocole. Ce phénomène conduit à une très bonne répétabilité du patron d'activité du groupe musculaire (*Triceps sural*) responsable de l'extension de la cheville (Ankle-Ext, représentant la somme des activités EMG du *Soleus*, *Gastrocnemius lateralis* et *Gastrocnelius medialis*), confirmant ainsi la grande stabilité du rôle fonctionnel de ces différents muscles malgré une variabilité non négligeable lorsqu'ils sont considérés individuellement (*Soleus* essentiellement).

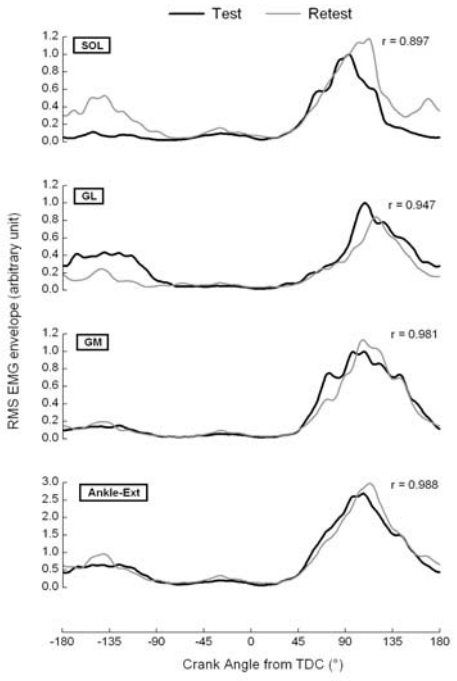

Figure 9. Patrons d'activité EMG obtenus chez un sujet pour chaque muscle extenseur de la cheville (*Soleus*, *Gastrocnemius lateralis, Gastrocnelius medialis*) au début (noir) et à la fin (gris) d'une session simulée d'entraînement. Le dernier graphique représente la somme des trois patrons précédénts (Ankle-Ext). Toutes les courbes sont normalisées par rapport à la valeur EMG maximale obtenue pendant le premier test. Cette figure met en évidence les phénomènes de compensation relative entre le *Soleus* et le *Gastrocnemius lateralis* pendant la phase de poussée (45 à 180°) ainsi que pendant la première partie de la phase de tirage (-180 à -90°), conduisant à une activité globale des muscles extenseurs de la cheville (Ankle-Ext) très similaire entre le début et la fin. r, coefficient de cross-corrélation entre les deux patrons d'activité EMG. D'après Dorel *et al*. (2008).

Bien que ce phénomène de compensation n'ait été observé que chez un seul sujet, ce résultat nous amènent à réaffirmer le fait que l'enregistrement de l'ensemble des principaux muscles du membre inférieur impliqués dans le mouvement de pédalage (et pas seulement d'une paire agoniste-antagoniste par articulation) est une recommandation importante à suivre dans les futures études ; ceci afin de garantir une certaine pertinence au regard des modifications potentielles observées au niveau des coordination musculaires.

3.1.3. Variabilité interindividuelle des patrons d'activité EMG.

Hug, F., Drouet, JM., Champoux, Y., Couturier, A., Dorel, S. Inter-individual variability of EMG patterns and pedal force profiles in trained cyclists. *European Journal of Applied Physiology* 2008. 104(4) : 667-678.

Comme souligné précédemment, les solutions motrices possibles pour parvenir au même résultat (i.e., au niveau de la cinématique et de la dynamique du mouvement) sont nombreuses et toujours plus importantes que les solutions utilisées (Bernstein, 1967). Cette redondance motrice traduit l'idée qu'un même résultat peut être obtenu par plusieurs coordinations musculaires (et donc par des patrons d'activité EMG différents) (van Bolhuis et Gielen, 1999). Par exemple, dans le cadre de travaux menés lors de ma thèse, nous avons rapporté une hétérogénéité du niveau d'activité EMG des muscles des membres inférieurs chez une population de cyclistes professionnels par ailleurs homogène en termes d'aptitudes physiques et physiologiques (Hug *et al.*, 2004a). Toutefois, nous ne nous sommes intéressés dans cette étude qu'au niveau d'activité EMG (valeur RMS calculée sur 7 cycles consécutifs) ne fournissant donc pas d'information sur la variabilité des patrons d'activité EMG (évolution de l'activité EMG au cours du cycle ; i.e., forme du signal). Cette information est nécessaire dans la mesure où un même niveau d'activité peut être obtenu avec des patrons d'activité différents. En d'autres termes, l'hétérogénéité mise en évidence dans cette étude (Hug *et al.*, 2004a) a pu être sous-estimée du fait du traitement utilisé pour les signaux EMG. De plus, la relation entre ces différences de niveaux d'activité EMG et les patrons d'application des forces sur les pédales n'a pas été explorée. Il semble important de déterminer si l'hétérogénéité des patrons d'activités EMG implique une hétérogénéité similaire des patrons d'application des forces sur les pédales (et donc de l'efficacité mécanique du pédalage) ou s'il s'agit « uniquement » d'une illustration supplémentaire du concept de « redondance motrice ».

Une collaboration avec le Pr Yvan Champoux et le Dr Jean-Marc Drouet (Groupe VelUS, Université de Sherbrooke, Canada) nous a permis de disposer d'une pédale instrumentée [Figure 10, A ; pour plus d'information sur cette pédale instrumentée voir Drouet *et al*. (2008)]. Il s'agit d'une paire de pédales équipées chacune de huit jauges de contraintes permettant la mesure des forces en deux dimensions sur chaque pédale (i.e., dans le plan sagittal). La mesure des composantes tangentielle et normale à la surface de la pédale ainsi que la mesure par un potentiomètre de l'angle manivelle-pédale permet de calculer par trigonométrie la force totale résultante (i.e., force appliquée par le cycliste sur la pédale) (Figure 10, B). Celle-ci peut alors être décomposée en deux autres composantes : une perpendiculaire à l'axe longitudinal de la manivelle (F_{eff}, force efficace) et l'autre selon l'axe longitudinal de celle-ci (F_{ineff}, force inefficace). La force efficace est celle qui permet

à la manivelle de tourner (et donc au cycliste d'avancer) alors que la force inefficace est une force que l'on peut considérer comme « inutile » pour la propulsion du cycliste. Un index d'efficacité mécanique (IE) peut ensuite être calculé : $IE=F_{eff}\times100/F_{tot}$. Il ressort de cette équation que l'efficacité mécanique maximale (i.e., 100%) est obtenue lorsque la force totale est égale à la force efficace (i.e., le cycliste applique, à un moment donné du cycle de pédalage, une force totale perpendiculaire à l'axe longitudinal de la manivelle dans la direction du mouvement). En conséquence, l'index d'efficacité mécanique reflète la capacité à orienter efficacement la force sur la pédale. Bien évidemment, cette configuration n'est pas possible durant tout le cycle de pédalage.

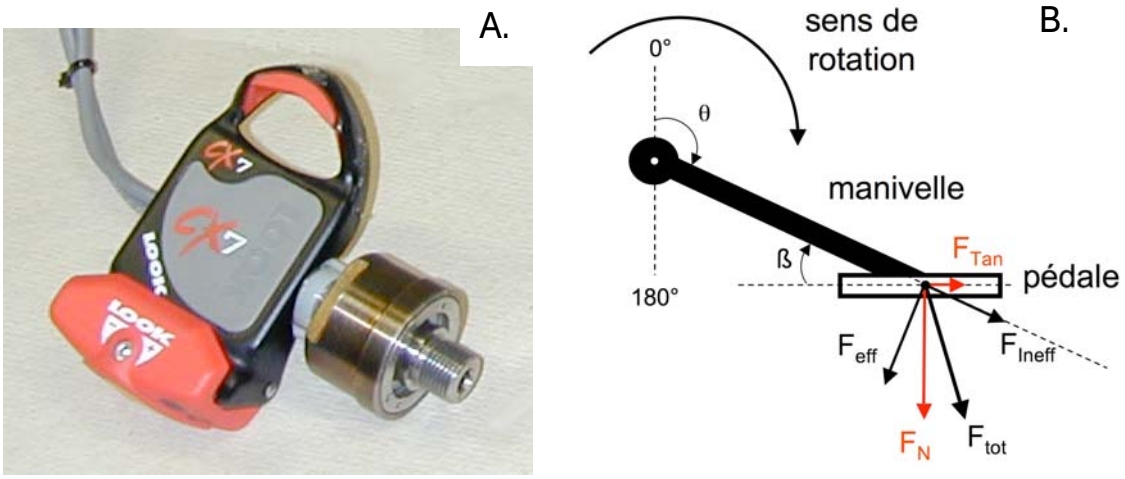

Figure 10. Pédale instrumentée développée par le groupe VelUS et utilisée dans le cadre de plusieurs études présentées dans ce mémoire (A). Représentation des forces appliquées sur la pédale dans le plan sagittal (B). Les données mesurées par la pédale sont : la force tangentielle (F_{Tan}), la force normale (F_N) et l'angle entre la pédale et la manivelle (β). *Les données calculées sont : la force efficace (F_{eff}), la force inefficace (F_{Ineff}) et la force résultante totale (F_{tot}).*

En utilisant cette pédale instrumentée, nous avons mis en place un protocole expérimental permettant : i) de caractériser la variabilité interindividuelle des patrons d'activité musculaire lors d'un exercice de pédalage chez une population de cyclistes entraînés (niveau national) et ii) de déterminer si cette variabilité interindividuelle est liée à une même variabilité du patron d'application des forces sur les pédales (et donc de l'efficacité mécanique du pédalage). L'activité EMG de 10 muscles du membre inférieur droit a été enregistrée au cours de deux exercices sous-maximaux (i.e., 150 et 250 Watts ; cadence de pédalage = 95 rev/min) et synchronisée avec les données mécaniques mesurées par la pédale instrumentée. La variabilité interindividuelle des patrons d'activité EMG et des patrons d'application des forces sur les pédales a été évaluée par l'intermédiaire de paramètres « classiques » tels que l'écart-type et l'erreur-type de mesure mais aussi par un paramètre moins utilisé dans ce contexte : le coefficient de cross-corrélation. Les résultats ont montré une variabilité interindividuelle importante des patrons d'activité EMG pour tous les muscles et plus spécialement pour un muscle mono-articulaire, i.e., *Tibialis anterior* et deux muscles bi-articulaires, i.e., *Gastrocnemius lateralis* et *Rectus femoris* (Figure 11, A). Il est intéressant de noter qu'il se dégage deux patrons distincts d'activité pour le muscle *Tibialis anterior*. Alors que ce muscle est activé qu'aux alentours du point mort haut pour certains sujets, il est également activé lors du

passage au niveau du point mort bas pour d'autres. Puisque la variabilité interindividuelle mise en évidence dans cette étude dépasse très largement la variabilité intraindividuelle mesurée avant et après une session d'entraînement simulée (Dorel *et al*., 2008 ; cf. partie 3.1.2.), nous pouvons supposer que malgré un patron d'activité musculaire stable au cours du temps, chaque sujet adopte une stratégie de coordination musculaire qui lui est propre. Il est intéressant de noter qu'en dépit d'une faible variabilité des patrons mécaniques au cours de la phase de remontée de la pédale et du point haut, la forte hétérogénéité mise en évidence sur les patrons EMG n'est pas retrouvée sur les patrons d'application des forces sur les pédales (Figure 11, B). Ce résultat illustre, une fois de plus, la redondance du système musculo-articulaire.

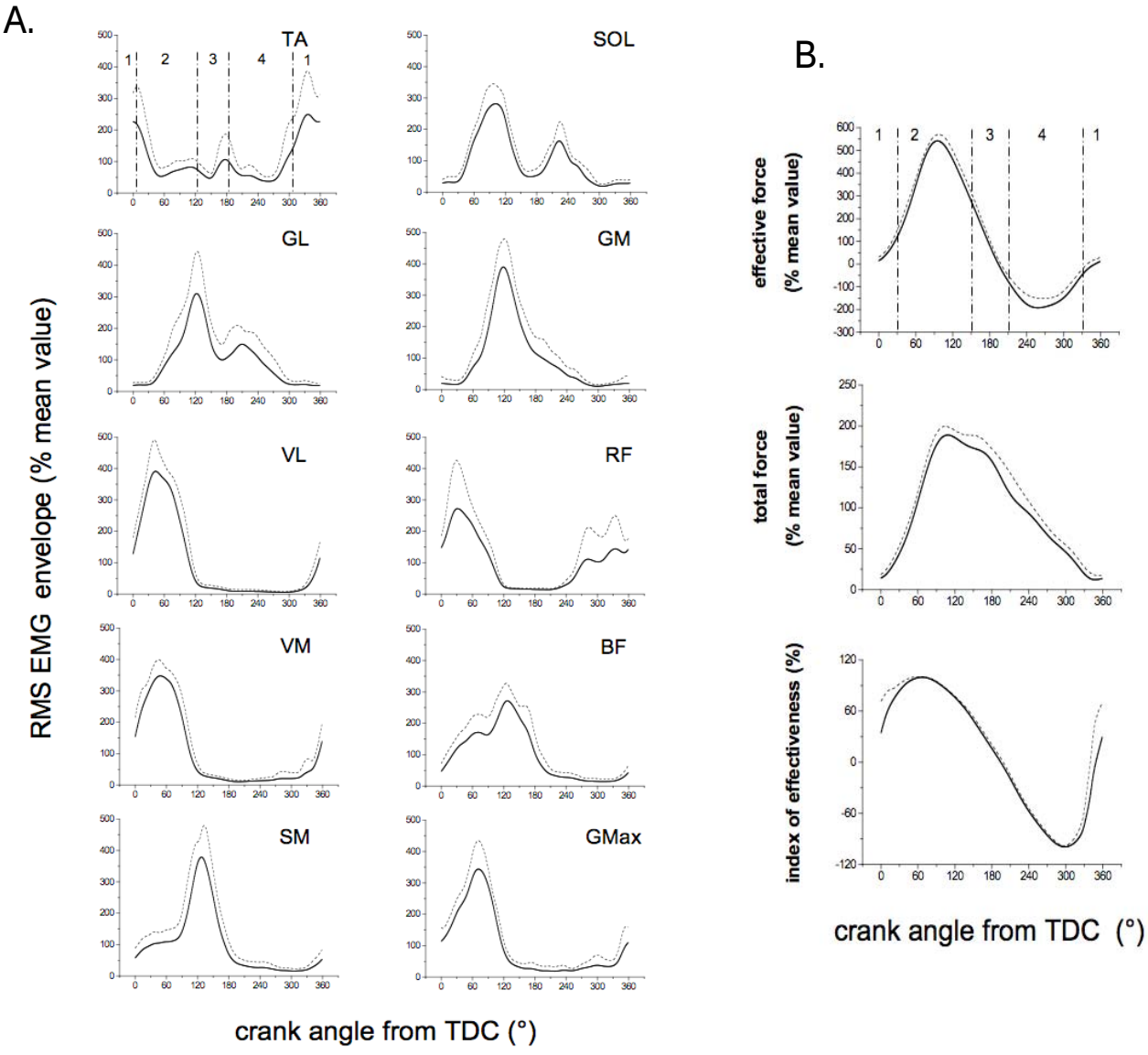

Figure 11. Patrons d'activité EMG (A) et patrons d'application des forces sur les pédales (B) obtenus durant un exercice de pédalage réalisé à 150 Watts. Les patrons d'activité EMG et ceux correspondant à la force efficace et la force totale sont normalisés par rapport à la valeur moyenne mesurée sur le cycle. Chaque graphique correspond à la moyenne (en noir) ± l'écart-type (en pointillés) d'une population de 11 cyclistes. GMax, *Gluteus maximus* ; SM, *Semimembranosus* ; BF, *Biceps femoris* (chef long) ; VM, *Vastus medialis* ; VL, *Vastus lateralis* ; GM, *Gastrocnemius medialis ;* GL, *Gastrocnemius lateralis* ; SOL, *Soleus* ; TA, *Tibialis anterior*. Les lignes verticales correspondent à différents secteurs. Secteur 1 (de 330° à 30°), secteur 2 (de 30° à 150°), secteur 3 (de 150° à 210°) et secteur 4 (de 210° à 330°). D'après Hug *et al.* (2008).

3.1.4. Patrons d'activité EMG et facteurs d'influence.

Dorel, S., Drouet, JM., Champoux, Y., Couturier, A., Hug, F. Changes of pedaling technique and muscle coordination during an exhaustive exercise. *Medecine & Science in Sports & Exercise.* 2009. 41(6) : 1277-1286.

Dorel, S., Couturier, A., Hug, F. Influence of different racing positions on mechanical and electromyographic patterns during pedaling. *Scandinavian Journal of Medicine & Science in Sports.* 2009. 19 : 44-54.

Le patron d'activité EMG des muscles des membres inférieurs peut être modifié en réponse aux modifications de certaines variables physiologiques, mécaniques ou contraintes externes. Parmi les principaux facteurs d'influence on trouve la cadence de pédalage (Ericson, 1986), la puissance (Neptune *et al*., 1997) et le type de pédales utilisées (Ericson, 1986). Dans le cadre d'un contrat de recherche associant l'INSEP et le ministère de la santé et des sports (contrat n°06-046), nous avons étudié : i) l'évolution des paramètres EMG et mécaniques au cours d'une épreuve rectangulaire de pédalage menée jusqu'à épuisement et ii) les effets d'une position de « contre la montre » sur les paramètres EMG et mécaniques.

a) Influence de la fatigue. L'objectif de cette étude était de décrire les effets de la fatigue sur les patrons d'activité musculaire et les paramètres mécaniques associés à la production de la force sur les pédales. Nous nous sommes donc intéressés aux évolutions simultanées des paramètres mécaniques et électromyographiques au cours d'une épreuve rectangulaire de pédalage menée jusqu'à épuisement (Dorel *et al*., 2009). Nous avons testé l'hypothèse selon laquelle les modifications de la biomécanique du pédalage (se traduisant par une altération de l'efficacité mécanique du mouvement) observées au cours d'un exercice épuisant (Sanderson et Black, 2003), sont liées à des adaptations du patron d'activité EMG des muscles du membre inférieur (i.e., niveau et séquence d'activité EMG). Dans cette optique, 10 cyclistes de niveau « national » ont réalisé un exercice de temps limite à 80% de la puissance maximale tolérée[5]. Les différentes composantes de la force exercée sur la pédale (utilisation de la pédale instrumentée préalablement présentée, cf. paragraphe 3.1.3.) ainsi que l'activité EMG de 10 muscles du membre inférieur ont été enregistrés en continu. Les résultats ont confirmé les modifications de la technique de pédalage rapportées par Sanderson et Black (2003) au cours d'un protocole de fatigue similaire. Plus précisément, nous avons observé à la fin de l'exercice, une augmentation de la force efficace produite durant la phase de poussée (de 30 à 150°) et une diminution concomitante de l'efficacité mécanique de pédalage et de la force produite au cours du passage au point haut de la pédale (de 330 à 30°). L'apparition de la fatigue induit un certain nombre d'ajustements des patrons d'activité EMG (Figure 12) pouvant expliquer, en partie, ces modifications de la biomécanique du pédalage. Tandis que la baisse du niveau d'activité du *Gastrocnemius medialis* ne semble pas avoir une influence majeure sur le patron d'application de la force efficace, la baisse du niveau d'activité du *Tibialis anterior* et du *Rectus femoris* (en tant que fléchisseur de la hanche) constitue un élément explicatif de la diminution de l'efficacité mécanique au niveau du point haut. L'augmentation importante de l'activité du *Gluteus maximus* et du chef long *Biceps femoris* est plus délicate à interpréter. En effet, l'augmentation du niveau d'activité EMG au cours d'un exercice fatigant réalisé à intensité constante peut être

[5] La puissance maximale tolérée est définie ici comme le dernier palier réalisé entièrement au cours d'une épreuve triangulaire de pédalage menée jusqu'à épuisement. Elle se distingue de la puissance maximale aérobie définie comme étant la première puissance correspondante à l'atteinte de VO_2max.

attribuée au recrutement progressif d'unités motrices supplémentaires dans le but de contrecarrer la diminution de la force produite par la contraction des fibres musculaires fatiguées (Gandevia, 2001). Ainsi, plusieurs études ont mis en évidence une augmentation progressive du niveau d'activité EMG des muscles du quadriceps au cours d'un exercice rectangulaire de pédalage (Petrofsky, 1979; Ryan et Gregor, 1992; Housh *et al.*, 2000), i.e., une augmentation du rapport entre le niveau d'activité EMG et la force produite. Dans la présente étude, nous n'avons observé aucune augmentation du niveau d'activité EMG pour les muscles *Vastus lateralis* et *Vastus medialis*. Néanmoins, cette absence de modification de la réponse EMG, également observée par d'autres auteurs (Lucia *et al.*, 2000), n'implique pas nécessairement une absence de fatigue musculaire et donc une stabilité de la force produite par ces muscles. En effet, en accord avec une augmentation du rapport EMG/force au cours d'un exercice fatigant, nous pourrions supposer que, pour un même niveau d'activité, la force produite par ces muscles a diminué au cours du test de temps limite. Lepers *et al.* (2001) ont mis en évidence une baisse de l'amplitude de la secousse musculaire (i.e., baisse de force produite par une stimulation électrique supramaximale du nerf moteur) pour le groupe musculaire quadriceps après 30 min d'exercice réalisé à 80% de la puissance maximale aérobie (protocole de fatigue similaire à celui réalisé dans notre étude). En se basant sur ces résultats, nous pouvons alors raisonnablement penser qu'une telle altération de la fonction contractile (i.e., fatigue) est intervenue sur les muscles du quadriceps (*Vastus lateralis* et *Vastus medialis*) au cours de notre exercice. Néanmoins, la puissance d'exercice étant maintenue constante, cette chute de force supposée au niveau des extenseurs du genou a du être compensée par une augmentation de l'activité d'autres muscles producteurs de puissance. L'augmentation significative du niveau d'activité du *Gluteus maximus* (+ 29%) et *Biceps femoris* (+15%) semble corroborer en partie cette hypothèse. Cette augmentation pourrait donc être liée à : i) un changement des stratégies de coordination (pour compenser la baisse de force supposée du *Vastus lateralis* et *Vastus medialis* ; ii) un recrutement d'unités motrices additionnelles pour compenser l'altération de la fonction contractile intevenant sur ces muscles (i.e.,fatigue) ou iii) une combinaison des deux. Pour autant, le *Gluteus maximus* est un muscle activé à un niveau bien moindre que les *vastii*, e.g., 40% vs. 80% du niveau d'activité maximal lors d'un exercice à 240 W (Ericson, 1986). De surcroît, une augmentation du moment maximal d'extension de la hanche a déjà été rapportée au cours d'un exercice similaire (Sanderson et Black, 2003). Par conséquent, nous pouvons penser que l'augmentation du niveau d'activité du *Gluteus maximus* et du *Biceps femoris* au cours de l'épreuve de temps limite, plutôt qu'être vu comme une manifestation d'une fatigue de ces muscles, pourrait être considérée comme une stratégie de compensation permettant de contrecarrer la baisse de force produite par les *vastii*. Cette étude souligne les limites de l'interprétation des signaux EMG lorsqu'il s'agit de relier le niveau d'activité à un niveau de force produit (cf. chapitre 4 de ce mémoire « projets de recherche »).

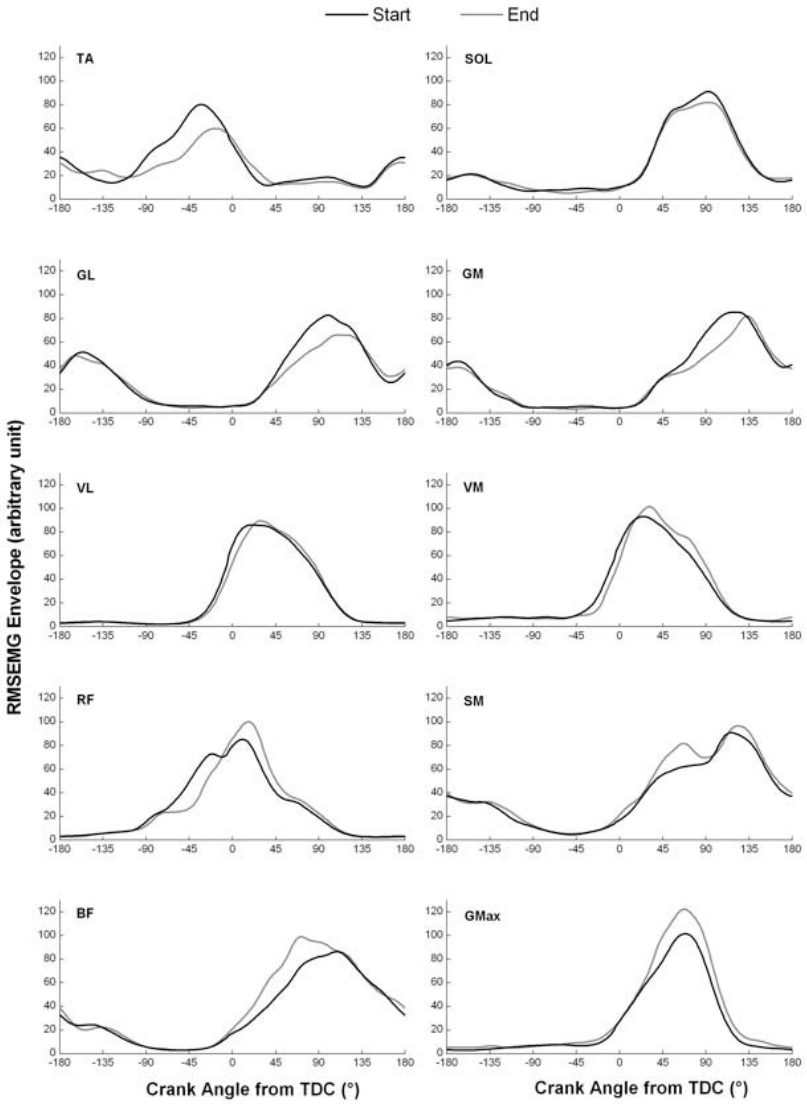

Figure 12. Enveloppes EMG RMS de 10 muscles du membre inférieur obtenues au début (en noir) et à la fin (en gris) d'un exercice de pédalage réalisé à 80% de la puissance maximale tolérée et mené jusqu'à épuisement. Chaque profil correspond à la moyenne des 10 sujets. Les valeurs sont normalisées par rapport à la valeur RMS moyenne calculée sur le cycle complet correspondant au début de l'exercice. GMax, Gluteus maximus ; SM, Semimembranosus ; BF, Biceps femoris (chef long) ; VM, Vastus medialis ; VL, Vastus lateralis ; GM, Gastrocnemius medialis ; GL, Gastrocnemius lateralis ; SOL, Soleus ; TA, Tibialis anterior. D'après Dorel *et al.* (2009).

b) Influence de la position. Dans un souci de réduire au maximum l'effet de la résistance de l'air, l'optimisation de la position du haut du corps des cyclistes a suscité un intérêt particulier depuis ces vingt dernières années. Le bénéfice aérodynamique lié à l'adoption de la position dite de « contre la montre » par rapport à une position plus classique redressée avec les mains en haut du guidon (UP), ou avec les mais posées dans le creux du guidon (DP) est maintenant bien établi (Capelli *et al.*, 1993). Concernant les conséquences sur la réponse cardio-ventilatoire, certains auteurs n'ont observé aucune différence significative entre ces positions (Origenes *et al.*, 1993) tandis que d'autres ont rapporté une augmentation du coût métabolique en position de « contre la montre » (Gnehm *et al.*, 1997). Bien que déjà mis en évidence pour l'adoption de la position « en danseuse » (Li et Caldwell, 1998), l'effet de l'adoption d'une position de contre la montre sur les patrons d'activité EMG des muscles des membres inférieurs et sur la production de force n'a jamais été rapporté. Nous avons donc voulu étudier, à partir des paramètres EMG (10 muscles) et mécaniques, si la position de « contre la montre », en comparaison avec deux positions standards (i.e., DP et UP ; Figure 13), induit des changements au niveau des patrons d'activité musculaire et d'application de la force sur la pédale. La pédale instrumentée présentée ci-avant

n'a pas pu être utilisée pour cette étude. De ce fait, seule la force efficace a été mesurée par des jauges de contraintes disposées dans les manivelles du cycloergomètre (Excalibur sport, Lode, Pays-Bas). Les résultats ont montré que la position de contre la montre induit une diminution significative de la capacité à produire de la force efficace au cours de la phase de remontée de la pédale et du passage du point haut (i.e., 0°). Parallèlement, la force requise dans la phase propulsive et le passage du point bas est augmentée d'environ 5,4%. Même si les patrons d'activité EMG sont très similaires entre les positions, les différences de niveau d'activité observées sont en adéquation avec les données mécaniques: i.e. diminution significative de l'activité d'un fléchisseur de la hanche (*Rectus femoris*) et augmentation significative d'un extenseur de la hanche (*Gluteus maximus*) et d'un extenseur du genoux (*Vastus medialis*) dans la position de contre la montre comparativement à une position plus classique (i.e., UP). Ces résultats conduisent à s'interroger sur les effets de ces modifications au cours d'un exercice fatigant et sur la nécessité de s'entraîner spécifiquement dans ce type de position.

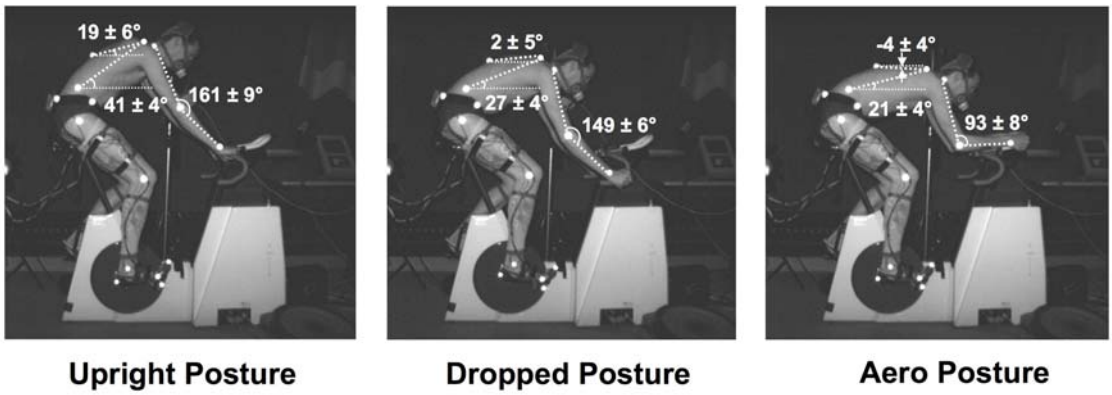

Figure 13. Illustration des trois positions testées. D'après Dorel *et al.* (2009).

3.1.5. Transfert de connaissances vers le milieu de l'entraînement.

Outre l'aspect méthodologique de certains des travaux présentés dans cette partie (e.g., étude de la reproductibilité et répétabilité), les études menées ici ont pour vocation, *in fine*, l'optimisation de la performance sportive. Par exemple, une meilleure connaissance des modifications des sollicitations musculaires induites par un exercice fatigant ou le changement de position peut permettre à l'entraîneur d'orienter plus efficacement le travail de renforcement musculaire. Ces résultats permettent également d'expliquer certaines attitudes adoptées spontanément par les cyclistes. En effet, au cours d'une course de contre la montre, les résultats que nous rapportons (Dorel *et al.*, 2009) pourraient expliquer que lorsque la vitesse diminue (et donc que la résistance aérodynamique diminue), en côte par exemple, les cyclistes quittent spontanément la position de contre la montre pour une position de type « UP », ce qui leur permettrait d'augmenter la force efficace au cours de la phase de remontée de la pédale et du passage du point haut et de diminuer le niveau d'activité des extenseurs de la hanche et du genou. Enfin, la méthodologie développée dans ces études permet d'envisager des partenariats avec des industriels pour tester de nouveaux matériels et plus précisément leurs effets sur la performance (e.g., efficacité mécanique du pédalage, coordinations musculaires, etc.).

Électromyographie et analyse des coordinations musculaires

Résumé : Après avoir mis en évidence la bonne répétabilité et reproductibilité des coordinations musculaires au cours d'un exercice de pédalage, cette partie s'intéresse à la variabilité interindividuelle des patrons d'activité musculaire et à l'effet de certains facteurs d'influence (i.e., fatigue et position). La plupart de ces travaux couplent l'enregistrement de paramètres mécaniques (*via* une pédale instrumentée) et électromyographiques (10 muscles du membre inférieur droit).

Nous avons mis en évidence des différences interindividuelles concernant les patrons d'activité musculaire chez une population de cyclistes entraînés par ailleurs homogène en termes d'aptitudes physiques. Cette variabilité, davantage marquée sur les muscles biarticulaires, est beaucoup moins présente sur les patrons d'application des forces sur les pédales illustrant ainsi la notion de redondance motrice.

Une autre étude suggère des compensations musculaires au cours d'un exercice fatigant, notamment par une implication croissante des muscles extenseurs de la hanche (*Gluteus maximus* et chef long du *Biceps femoris*) pour compenser la baisse de la force produite par les muscles extenseurs du genou (*vastii*).

Enfin, dans une dernière étude, nous avons mis en évidence des modifications mineures des coordinations musculaires entre trois positions classiquement utilisées par les cyclistes (mains en haut du guidon, mains dans le creux du guidon et position de contre la montre). Il en ressort notamment une diminution de l'activité des muscles fléchisseurs de la hanche compensée par une augmentation du niveau d'activité des muscles extenseurs de la hanche et du genou dans la position de contre la montre comparativement aux deux autres positions.

Publications : 6 articles publiés dans des revues indexées ISI

Contrats de recherche : 2 contrats (ministère de la jeunesse, des sports et de la vie associative – n°06-046, Amaury Sport Organisation – Société du Tour de France)

Encadrement : 1 étudiant de Master 1ère année

3.2. Électromyographie et détection d'une charge mécanique imposée au système respiratoire

3.2.1. État de la question.

La ventilation est le résultat de l'activation phasique des différents muscles respiratoires et relève de deux types de contrôle. Le premier, automatique, dépend de structures neuronales spécifiques situées dans le tronc cérébral (*i.e.* centres respiratoires), et est responsable de la production du rythme ventilatoire et de l'adaptation de la ventilation aux demandes métaboliques. Le second, "supra-pontin", détermine les aspects comportementaux de la ventilation (cortex limbique) et son contrôle volontaire (néo-cortex).

Chez l'Homme sain, en condition de repos, l'inspiration repose pour l'essentiel sur le travail du diaphragme mais implique également d'autres muscles tels que les intercostaux parasternaux et les scalènes (Beau et Maissiat, 1843; Raper *et al.*, 1966; De Troyer et Estenne, 1984) (Figure 14). On distingue également d'autres muscles inspiratoires, les muscles « dilatateurs » des voies aériennes supérieures (e.g., alae nasi, génioglosse), dont la contraction augmente le diamètre des voies aériennes et diminue les résistances à l'écoulement de l'air.

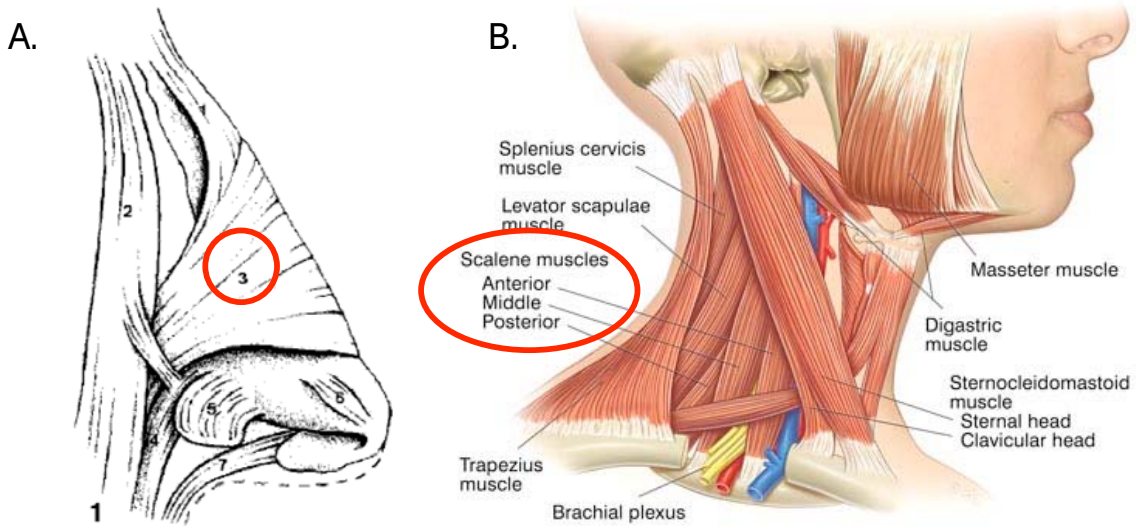

Figure 14. Planches anatomiques représentant l'alae nasi (A) et les scalènes (B)

Les scalènes sont certainement les muscles inspiratoires extradiaphragmatiques les mieux connus. Au cours d'une ventilation eupneïque, leur activité EMG phasique est détectable mais d'amplitude faible, variable entre les sujets et au cours du temps (Raper *et al.*, 1966). En revanche, si des charges sont imposées à l'appareil respiratoire, leur niveau d'activité est augmenté (Raper *et al.*, 1966). Ainsi, une activité phasique significative des scalènes est très fréquemment retrouvée chez les patients atteints de pathologies respiratoires chroniques (De Troyer *et al*., 1994). L'activation des muscles inspiratoires du cou fait partie des éléments caractéristiques de la

détresse ventilatoire aiguë. Ainsi, chez un patient placé sous assistance ventilatoire (ventilation assistée[6]), détecter la contraction du scalène par simple palpation peut être un signe de détresse respiratoire (Pardee *et al*., 1984) et peut témoigner d'une dysharmonie patient-ventilateur. En effet, le ventilateur doit délivrer son assistance en harmonie avec la commande ventilatoire du patient (et donc en phase avec l'activité des muscles inspiratoires). L'inadéquation entre l'activité des muscles respiratoires du patient et l'assistance délivrée par le ventilateur définit la dysharmonie patient-ventilateur. Le patient présente alors des difficultés à déclencher le ventilateur (et donc à déclencher l'arrivée de l'air ; i.e., l'inspiration), il semble « lutter » contre lui causant un inconfort important (i.e., dyspnée[7]) (Sassoon et Foster, 2001), une détérioration des échanges gazeux (Tobin *et al.*, 2001) et des dommages musculaires liés à l'action excentrique des muscles respiratoires (Friden *et al.*, 1991). L'évaluation de l'activité des scalènes par palpation peut donc être utile pour optimiser les réglages du ventilateur (Brochard *et al.*, 1989). Cependant le niveau d'activité musculaire perçu par palpation est influencé par de nombreux facteurs tels que l'adiposité du patient, la pression exercée par le clinicien, etc. et ne permet donc pas de quantifier précisément l'augmentation du niveau d'activité musculaire. Tous ces éléments suggèrent que l'enregistrement de l'activité EMG du scalène pourrait être particulièrement utile pour détecter une charge imposée au système respiratoire. Ainsi, minimiser son activité EMG pourrait être l'un des objectifs du clinicien visant à optimiser les réglages du ventilateur.

3.2.2. Optimisation de la détection électromyographique de l'activité inspiratoire des scalènes.

Hug, F., Raux, M., Prella, M., Morelot-Panzini, C., Straus, C., Similowski T. Optimized analysis of surface electromyograms of the scalenes during quiet breathing in humans. *Respiratory Physiology and Neurobiology*. 2006. 25;150(1):75-81.

Quantifier l'activité EMG phasique des scalènes n'est pas aisé. L'utilisation d'électrodes aiguilles (ou filaires) permet d'obtenir des signaux de bonne qualité, mais le caractère invasif de cette technique de recueil exclut son utilisation dans un contexte clinique. L'utilisation d'électrodes de surface est complexe compte tenu : i) du faible niveau d'activité de ce muscle en ventilation eupneïque et ii) de l'activité tonique liée à sa fonction posturale. De ce fait, les enregistrements de surface du scalène présentent très souvent un faible rapport signal/bruit. De surcroît, dans le cadre d'un enregistrement effectué dans un contexte clinique (e.g., unité de réanimation), des perturbations électromagnétiques liées à l'environnement peuvent détériorer davantage la qualité du signal. Dans une première étude, nous avons donc testé une technique de traitement des signaux EMG, déjà utilisée dans d'autres contextes (i.e., analyse du mouvement ; cf. partie 3.1), qui repose sur le

[6] La ventilation mécanique est utilisée dans le traitement de l'insuffisance respiratoire aiguë. On distingue la ventilation contrôlée de la ventilation assistée. La ventilation contrôlée a pour objectif d'optimiser les échanges gazeux pulmonaires chez des patients ne présentant aucune activité des muscles respiratoires. Ainsi, la totalité du travail ventilatoire est réalisée par le ventilateur. En revanche, dans le cadre de la ventilation assistée, le patient déclenche son ventilateur et contribue donc à la genèse de sa propre ventilation. La ventilation assistée offre donc un compromis entre la diminution du travail des muscles inspiratoires du patient et le maintien d'un certain niveau d'activité spontanée de ces muscles.

[7] La dyspnée est définie comme un "inconfort respiratoire survenant pour un niveau d'activité usuel, n'entraînant normalement aucune gêne" Straus C, Similowski T, Zelter M, Derenne JP. 1998. Mécanismes et diagnostic des dyspnées. In: Encyclop. Med. Chir. Paris: Elsevier. p 6-090-E-015.

moyennage d'un nombre important de cycles (ici des cycles respiratoires) (Hug *et al*., 2006c). Ce moyennage de l'activité EMG est connu pour améliorer le rapport signal/bruit (Davenport et Root, 1958). Dix sujets sains ont participé à cette étude. Le débit ventilatoire et l'activité EMG de surface du scalène antérieur (coté droit) ont été enregistrés en continu au cours d'une ventilation eupneïque. Chez quatre sujets, un enregistrement EMG intramusculaire (i.e., aiguille concentrique) a été rajouté. Le root mean square a d'abord été calculé sur la totalité du signal EMG brut (fenêtres = 2ms). Ensuite, un moyennage de 80 cycles, calé sur le début de l'inspiration (repéré grâce au signal de débit ventilatoire), a permis d'obtenir un cycle inspiratoire moyen (Figure 15).

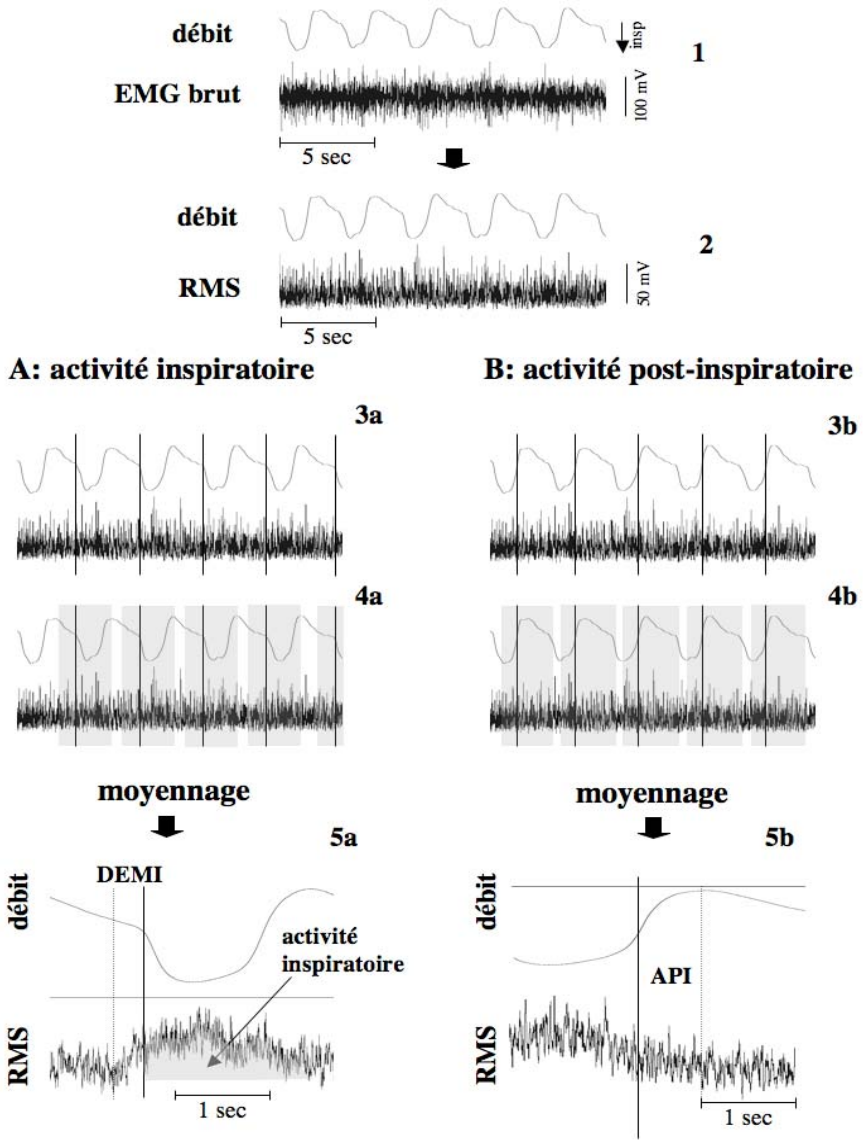

Figure 15. Représentation de la technique d'optimisation du signal EMG. 5 cycles ventilatoires consécutifs sont représentés (1). Le root mean square (RMS) est d'abord calculé à partir du signal EMG brut (2). Ensuite, le signal correspondant au débit ventilatoire est utilisé pour détecter le début (3a) et la fin (3b) de chaque phase inspiratoire. Puis, un ensemble de 80 cycles consécutifs est moyenné après avoir découpé le signal en fenêtres commençant 1 s avant le marqueur et terminant 1 s après la fin de l'inspiration (4a) ou 2 s après la fin de l'inspiration (4b). Le signal EMG moyenné permet de mettre en évidence une activité phasique inspiratoire (5a) peu visible sur le tracé brut. Ainsi il est possible de calculer le délai électromécanique inspiratoire (délai séparant le début d'activité EMG et le début de l'inspiration ; DEMI) et l'activité post-inspiratoire (activité EMG du scalene mesurée après la fin de l'inspiration ; API). Insp, inspiration. D'après Hug *et al*. (2006)

Chez 8 sujets sur 10, cette approche a permis de mettre en évidence une activité phasique inspiratoire du scalène. Les tracés obtenus donnent également accès au calcul du délai électromécanique inspiratoire et la durée de l'activité post-inspiratoire. Chez les 4 sujets testés, les enregistrements EMG de surface et intramusculaires ont conduit à des résultats comparables. Cette première étude démontre qu'il est possible de quantifier l'activité phasique du scalène, son délai électromécanique et son activité post-inspiratoire par des enregistrements de surface simples à utiliser. Cette technique devrait permettre de mieux étudier l'activité EMG des muscles inspiratoires en ventilation eupneïque et lorsqu'ils sont soumis à différentes charges mécaniques et métaboliques.

3.2.3. Détection d'une charge inspiratoire chez le sujet sain placé sous ventilation assistée.

Chiti, L., Biondi, G., Morélot-Panzini, C., Raux, M., Similowski, T., Hug, F. Scalene muscle activity during progressive inspiratory loading under pressure support ventilation on normal humans. *Respiratory Physiology and Neurobiology*. 2008. 164(3) : 440-447.

Dans un deuxième temps, nous avons appliqué cette technique de quantification de l'activité EMG des muscles inspiratoires à un modèle expérimental humain de dysharmonie patient-ventilateur en ventilation assistée (Chiti *et al*., 2008). Il s'agissait de tester la sensibilité de cette technique pour la détection d'une charge mécanique induite par l'application de triggers inspiratoires[8] fixés à différents pourcentages de la pression inspiratoire maximale (i.e., 5, 10 et 15%). Grâce à des enregistrements de surface et intramusculaires (*via* des électrodes filaires) du scalène antérieur et du sterno-cleïdo-mastoïdien (coté droit) nous avons mis en évidence : i) que l'activité EMG du scalène enregistrée avec des électrodes de surface est similaire à celle enregistrée avec des électrodes filaires (Figure 16), validant de ce fait l'utilisation des enregistrements de surface pour ce muscle et ces conditions d'enregistrement, et ii) que l'activité EMG du sterno-cleïdo-mastoïdien obtenue par des électrodes de surface n'est, dans la grande majorité des cas, qu'une contamination de l'activité EMG du scalène (Figure 16).

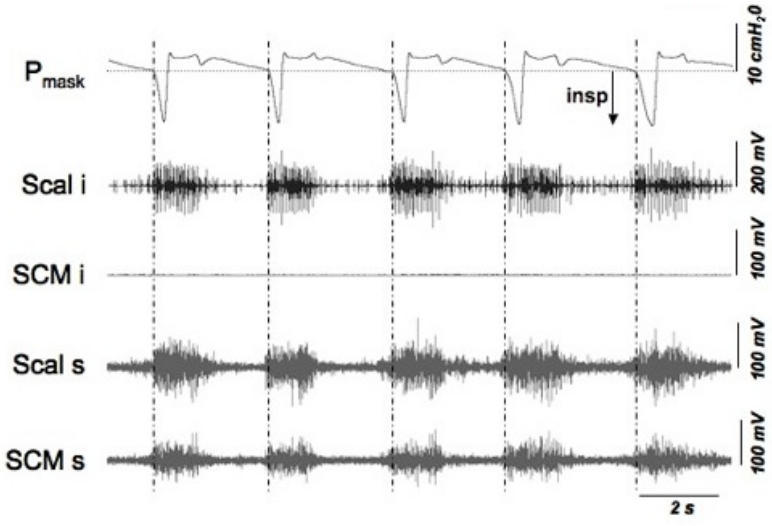

Figure 16. Exemple d'enregistrement obtenu chez un sujet pour un trigger fixé à 10 % de la pression inspiratoire maximale. Cet enregistrement démontre que l'activité EMG du sterno-cléido-mastoïdien obtenue avec des électrodes de surface (SCMs) vient de la contamination d'autres muscles (très certainement du scalène) puisque aucune activité EMG n'est visible sur l'enregistrement obtenu avec les électrodes intramusculaires (SCMi). D'après Chiti *et al.* (2008).

[8] Le modèle de charge utilisé dans cette étude est un peu particulier dans la mesure où le sujet doit, lors de la première phase de l'inspiration, développer une pression inspiratoire au moins égale à celle du trigger (effort isométrique) pour obtenir de l'air et pouvoir ensuite inspirer normalement.

La technique de moyennage a permis la description non ambiguë d'une activité EMG du scalène peu ou non visible sur le tracé brut. Cette étude a mis en évidence que l'ajout d'un trigger inspiratoire (i.e., induction d'une dysharmonie) est associé à une augmentation significative du niveau d'activité EMG pour les triggers fixés à 10 et 15 % de la pression inspiratoire maximale par rapport à la condition de base (ventilation eupneïque) (Figure 17). Cette augmentation de l'activité inspiratoire du scalène est corrélée avec l'intensité de la dyspnée.

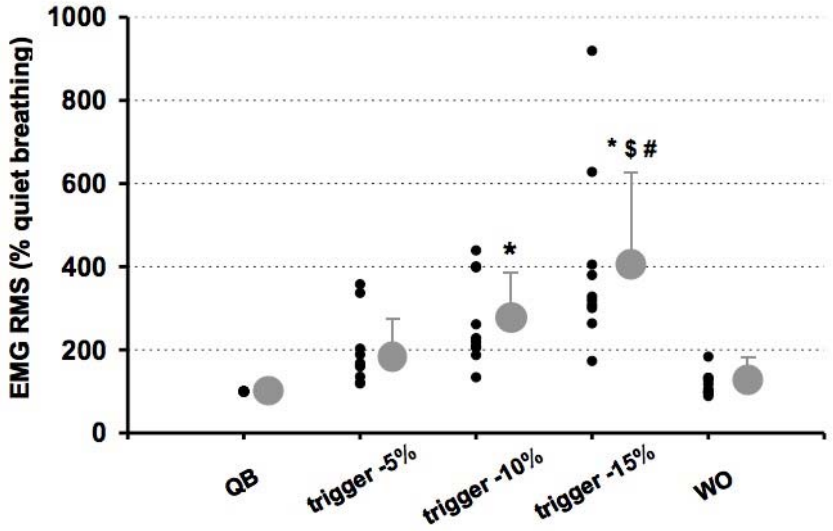

Figure 17. Niveau d'activité EMG du scalène. La valeur RMS représente la valeur moyenne sur la phase inspiratoire et est exprimée en pourcentage de la valeur mesurée au cours de la ventilation eupneïque (QB). Pour chaque valeur de trigger, les valeurs individuelles sont représentées (points noirs). Le cercle gris indique la valeur moyenne de la population ± écart-type. Les valeurs des triggers est exprimée en pourcentage de la pression inspiratoire maximale. *, différence avec la condition « QB » (ventilation eupneïque) ; $, différence avec la condition « Trigger -5% » ; #, différence avec la condition « Trigger -10% ». D'après Chiti *et al*. (2008).

Cette étude a mis en évidence la bonne sensibilité de la technique de moyennage pour détecter une faible augmentation de l'activité EMG du scalène. En effet, nous avons montré que l'amplitude de l'activité EMG augmente parallèlement à : i) l'augmentation des charges imposées à l'appareil respiratoire et ii) à l'intensité de la dyspnée. Si ces résultats se confirmaient chez des patients placés sous ventilation assistée, dans un service de réanimation, il pourrait alors être envisagé d'utiliser des enregistrements EMG du scalène en continu pour aider le clinicien à régler les paramètres du ventilateur afin d'améliorer le confort du patient et éviter qu'il ne se retrouve en condition de dysharmonie avec son ventilateur. Dans le cadre de mon stage post-doctoral, nous avons été amené à réaliser des premiers enregistrements de l'activité électromyographique du scalène chez des 26 patients recevant une assistance ventilatoire. Les premiers résultats sont encourageants et sont actuellement complétés par une étude menée au sein du Laboratoire de PhysioPathologie Respiratoire (LPPR, EA 2397).

Même si l'enregistrement de l'activité EMG du scalène semble cliniquement pertinent, la qualité du signal EMG recueilli est très dépendante de la morphologie des patients et, notamment, de l'épaisseur du tissu adipeux, et ce malgré l'application de la technique de moyennage. De surcroît, les mouvements du cou sont susceptibles d'empêcher la détection de l'activité phasique inspiratoire. Enfin, la localisation du scalène peut s'avérer compliquée et demande donc une certaine expérience du clinicien. Certains travaux menés chez

l'homme et l'animal montrent que le muscle *Alae nasi*, dilatateur des voies aériennes, est activé en situation de charge. De plus, le recueil du signal EMG du muscle *Alae nasi*, semble beaucoup plus aisé. En effet, l'absence de muscle adjacent volumineux, une faible épaisseur du tissu adipeux, un recueil non contaminé par les mouvements parasites et sa localisation facile font de l'*Alae nasi* un muscle inspiratoire potentiellement intéressant à étudier. Nous avons donc mené une étude (article en cours de rédaction) dont l'objectif était de rechercher un recrutement de l'*Alae nasi* en présence d'un trigger croissant, de le quantifier le cas échéant, et de le comparer avec celui du scalène. À quelques détails près, le protocole expérimental était similaire à celui utilisé dans le cadre de l'étude précédente, i.e., modèle expérimental humain de dysharmonie sujet-ventilateur. L'activité EMG du parasternal, du génioglosse et du diaphragme (*via* une sonde oesophagienne) a également été enregistrée. Les résultats ont montré que l'amplitude de l'activité EMG de l'*Alae nasi* augmente parallèlement à l'augmentation des charges imposées à l'appareil respiratoire. Néanmoins, contrairement au scalène, son activité est dépendante du type de ventilation (i.e., nasale vs. buccale) (Figure 18) rendant donc son enregistrement peu pertinent dans le cadre de la détection d'une dysharmonie patient-ventilateur. Dans cette situation, il est probable que le patient adopte temporairement une ventilation buccale pour diminuer les résistances des voies aériennes liées aux narines qui se collabent sous l'influence d'une pression inspiratoire importante (i.e., effort inspiratoire).

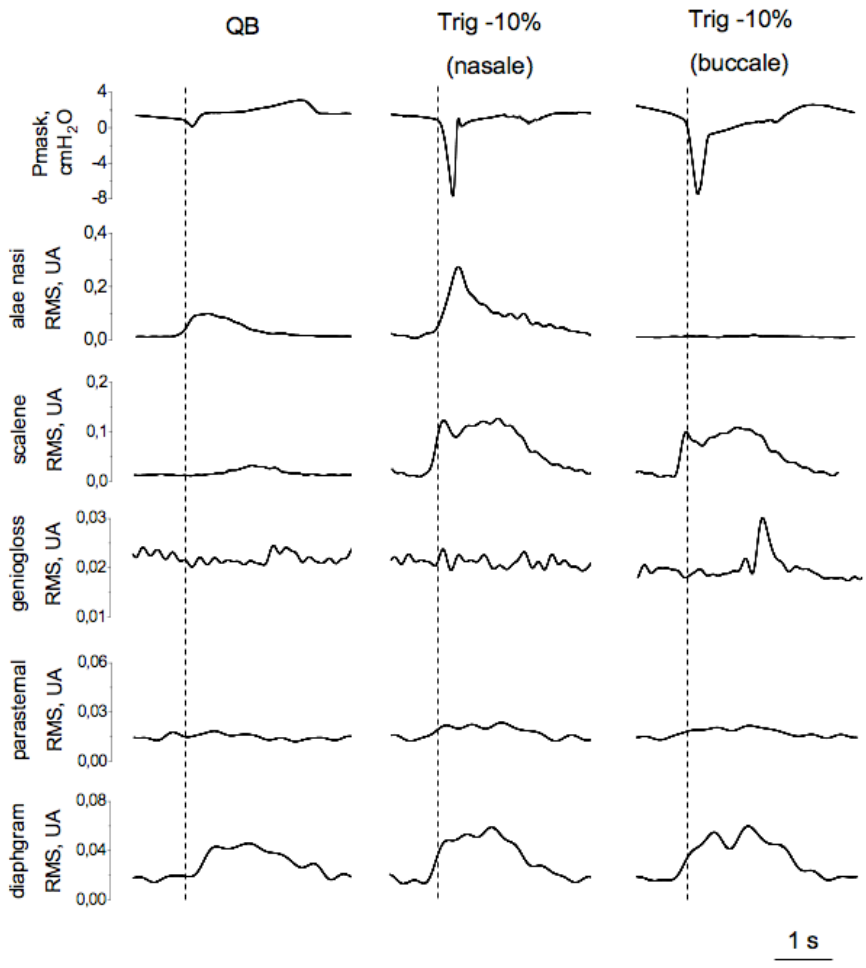

Figure 18. Exemple typique de résultats obtenus. L'activité moyenne des 5 muscles enregistrés (*Alae nasi*, scalene, genioglosse, parasternal et diaphragme) est représentée pour 3 conditions testées (ventilation spontanée (QB), trigger inspiratoire réglé à 10 % de la pression inspiratoire maximale en ventilation nasale et buccale.

Électromyographie et détection d'une charge mécanique imposée au système respiratoire

Résumé : Nous avons dans un premier temps mis au point une technique permettant de quantifier l'activité électromyographique phasique du scalène au cours de la ventilation. Cette technique repose sur le moyennage d'un nombre important de cycles ventilatoires (> 40 cycles) et permet, à partir d'un tracé électromyographique brut peu exploitable, de quantifier précisément le niveau d'activité, le délai électromécanique et la durée de l'activité post-inspiratoire. Nous avons ensuite appliqué cette technique à un modèle expérimental humain de dysharmonie patient-ventilateur en ventilation assistée. Cette étude a mis en évidence la bonne sensibilité de la technique de moyennage pour détecter une faible augmentation de l'activité électromyographique du scalène. En effet, nous avons montré que l'amplitude de l'activité EMG augmente parallèlement à : i) l'augmentation des charges imposées à l'appareil respiratoire et ii) à l'intensité de la dyspnée. L'enregistrement de l'activité électromyographique inspiratoire du scalène n'étant pas aisée (e.g., placement des électrodes, épaisseur variable du tissu adipeux, mouvements de la tête, etc.), nous avons également appliqué la technique de moyennage à un muscle dilatateur des voies aériennes, l'*Alae nasi*, bien plus facile à enregistrer. Seulement, les résultats démontrent que l'*Alae nasi* est trop sensible au type de ventilation utilisé par le sujet (i.e., nasal vs. buccal) et ne peut donc pas être utilisé pour détecter de manière fiable une augmentation de la charge imposée au système respiratoire.

Publications : 2 articles publiés dans des revues indexées ISI + 1 article en cours de préparation
Contrats de recherche : 1 contrat (Fédération ANTADIR – bourse de recherche post-doctorale)
Encadrement : 1 étudiante en thèse de spécialité médicale

3.3. Électromyographie et évaluation de la fatigue neuromusculaire

3.3.1. État de la question.

L'hypothèse selon laquelle le signal éléctromyographique constituerait un bon indicateur de la fatigue neuromusculaire repose sur les modifications du signal observées lors du maintien d'une contraction maximale isométrique. Bien que des modifications puissent affecter différents paramètres (e.g., paramètres temporels et fréquentiels), à dessein, nous focaliserons cette brève revue de littérature sur les modifications des paramètres temporels du signal EMG (i.e., amplitude). Cobb et Forbes (1923) ont sans doute été les premiers à mettre en évidence une augmentation du niveau d'activité EMG au cours d'un exercice isométrique sous-maximal réalisé à force constante. Ces résultats ont ensuite été corroborés par de nombreuses observations similaires (pour revue, voir Cifrek *et al*., 2009). Cette augmentation peut être expliquée par une augmentation du nombre d'unités motrices recrutées et/ou par une modulation de leur fréquence de décharge pour contrecarrer l'altération de la fonction contractile des fibres musculaires fatiguées (Garland *et al*., 1994; Garland *et al*., 1997; Hunter *et al*., 2004). Il est important de souligner que d'autres facteurs physiologiques (e.g., modifications de la vitesse de conduction des potentiels d'action musculaires, synchronisation des unités motrices) peuvent également modifier l'amplitude du signal EMG au cours d'un exercice fatigant (pour revue, voir Farina *et al.,* 2004). Puisque la plupart de ces phénomènes sont aussi liés, plus ou moins directement, à l'apparition de la fatigue neuromusculaire, l'origine des modifications du niveau d'activité EMG ne sera pas discutée dans les études présentées ci-après. Toutefois, cette limite méthodologique sera abordée dans la partie 4 de ce mémoire (projets de recherche).

De nombreux auteurs ont étudié l'évolution du signal EMG en fonction de la puissance d'un exercice dynamique réalisé sur un cycloergomètre ou un tapis roulant (Bigland-Ritchie et Woods, 1974; Taylor et Bronks, 1994; Gamet *et al.*, 1996; Lucia *et al.*, 1997; Hug *et al.*, 2003b). Plusieurs de ces études rapportent une relation linéaire entre l'augmentation de l'amplitude de l'EMG (EMG intégré ou RMS) et l'intensité de l'exercice (Bigland-Ritchie et Woods, 1974; Taylor et Bronks, 1994) alors que d'autres observent un une augmentation brutale de la pente au cours de l'exercice (Gamet *et al*., 1996; Lucia *et al*., 1997; Hug *et al*., 2003b). Dans ces études, cette « cassure » dans l'augmentation de l'EMG a été nommée « seuil EMG » (Figure 19) et est considéré comme étant une manifestation de l'apparition de la fatigue neuromusculaire.

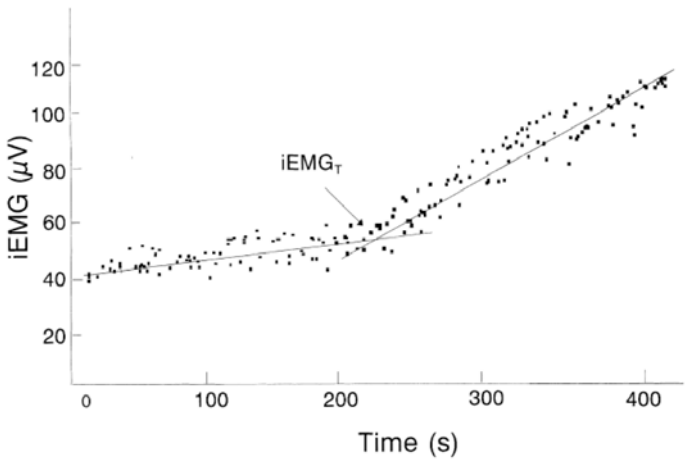

Figure 19. Exemple d'un seuil EMG déterminé *via* l'enregistrement du signal EMG du *Vastus lateralis* au cours d'une épreuve triangulaire réalisée sur cycloergomètre. D'après Lucia *et al*. (1997).

D'autres auteurs (deVries et al., 1982; Moritani et al., 1993) ont décrit une méthode différente permettant, à partir d'exercices de pédalage non fatigants, de déterminer un seuil EMG appelé « seuil EMG de la fatigue » (EMG fatigue threshold). Pour déterminer ce seuil, le sujet doit réaliser plusieurs exercices rectangulaires brefs (1 à 3 minutes) à différentes puissances. Le niveau d'activité EMG (EMG intégré ou RMS) est représenté en fonction du temps pour toutes les puissances d'exercice (Figure 20, A). Les pentes des droites de régression obtenues sont calculées et représentées graphiquement en fonction de la puissance d'exercice (Figure 20, B), permettant ainsi, par extrapolation, d'obtenir la valeur de puissance correspondante à une pente nulle (i.e., absence d'augmentation du niveau d'activité EMG). Ce seuil correspond, théoriquement, à la plus haute intensité d'exercice pouvant être maintenue sans apparition de la fatigue neuromusculaire.

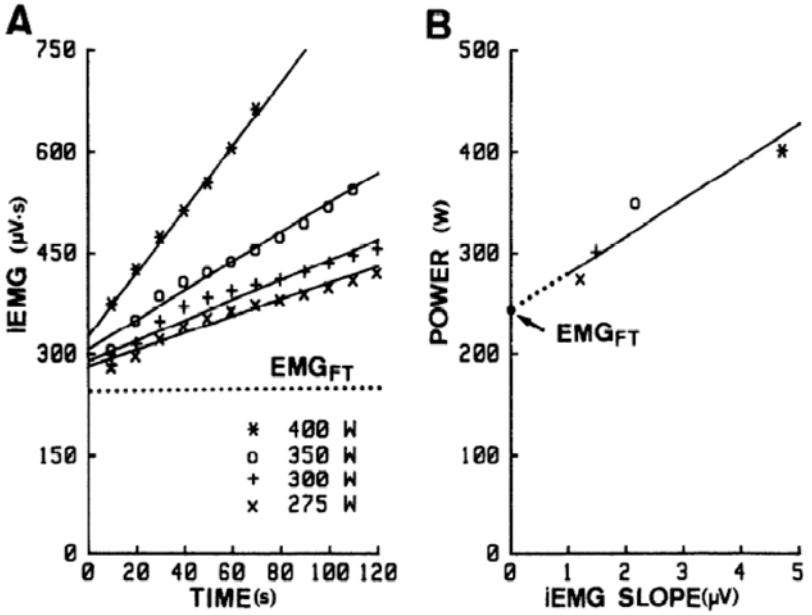

Figure 20. Méthode de détermination du seuil EMG de la fatigue. Le niveau d'activité EMG (EMG intégré) est représenté en fonction du temps pour toutes les puissances d'exercice (A). Les pentes des droites de régression obtenues sont calculées et représentées graphiquement en fonction de la puissance d'exercice (B), permettant ainsi, par extrapolation, d'obtenir la valeur de puissance correspondante à une pente nulle (i.e., le seuil EMG de la fatigue). Dans cet exemple le seuil (EMG_{FT}) est de 243 Watts. D'après Moritani *et al*. (1993).

D'après plusieurs études, ces seuils (qu'il s'agisse d'une augmentation brutale du niveau d'activité EMG au cours d'une épreuve triangulaire ou du seuil EMG de la fatigue tel que défini par De vries, 1982) peuvent être un outil intéressant pour évaluer les aptitudes physiques (deVries et al., 1982; Matsumoto et al., 1991; Moritani et al., 1993; Smith et al., 2007; Graef et al., 2008).

3.3.2. Détermination du seuil électromyographique au cours d'un exercice dynamique.

Hug, F., Laplaud, D., Lucia, A., Grélot, L. Comparison of visual and mathematical detection of the EMG threshold during incremental pedalling exercise. *Journal of Strength and Conditionning Research.* 2006. 20(3):704-708.

Hug, F., Laplaud, D., Lucia, A., Grélot, L. EMG threshold determination in 8 lower limb muscles during cycling exercise: a pilot study. *International Journal of Sports Medicine*. 2006. 27(6):456-462.

Certains travaux présentés lors de ma thèse montrent l'apparition d'une augmentation brutale de la pente de la relation entre le niveau d'activité EMG et la puissance au cours d'un exercice triangulaire de pédalage (Hug *et al*., 2003a; Hug *et al*., 2003b). Seulement, dans ces études, le seuil EMG a été déterminé

visuellement, et sa reproductibilité n'a pas été testée. Ainsi, dans l'année qui a suivi ma soutenance de thèse, et dans le cadre d'une collaboration internationale avec le Pr Alejandro LUCIA (Université Européenne de Madrid, Espagne), nous avons testé la validité de la détermination du seuil EMG, ainsi que sa reproductibilité. Une première étude (Hug *et al*., 2006a) a donc consisté à comparer la méthode de détermination visuelle du seuil EMG avec une méthode mathématique déjà utilisée dans la littérature (Lucia *et al.*, 1997)[9]. Les résultats issus de ce travail ont démontré qu'il est préférable de déterminer le seuil EMG par une technique mathématique, plus objective. Dans une deuxième étude, nous avons comparé, en utilisant cette méthode de détection, la reproductibilité du seuil EMG déterminé sur 8 muscles du membre inférieur (Hug *et al*., 2006b). Nous avons montré l'apparition d'un seuil EMG reproductible sur le *Vastus lateralis* pour tous les sujets.

3.3.3. Détermination du seuil électromyographique de la fatigue lors d'un exercice isométrique.

Hug, F., Nordez, A., Guével, A. Can the electromyographic fatigue threshold be determined from superficial elbow flexor muscles during an isometric single-joint task ? *European Journal of Applied Physiology.* 2009. 107(2) : 193-201.

Contrairement au seuil EMG décrit précédemment (i.e., augmentation brutale de la pente de la relation entre le niveau d'activité EMG et la puissance au cours d'un exercice triangulaire), le seuil EMG de la fatigue introduit par DeVries *et al.* (1982), peut être déterminé à partir d'efforts sous-maximaux ce qui représente un intérêt majeur pour les sujets qui ne peuvent pas tolérer un exercice épuisant. Seulement, jusqu'à présent, ce seuil EMG de la fatigue a essentiellement été déterminé sur un muscle du quadriceps (le plus souvent le *Vastus lateralis*), au cours d'une épreuve de pédalage, considérant que ce muscle est représentatif de tous les muscles impliqués dans ce mouvement. Or, ce n'est pas un mouvement si simple (cf. partie 3.1), d'autres muscles pourraient conduire à des seuils EMG de la fatigue différents, ce qui a d'ailleurs été mis en évidence par Housh *et al.* (1995). Dans une étude récente nous avons donc voulu appliquer la méthode de détection du seuil électromyographique de la fatigue (Moritani *et al*., 1993) à une tâche plus simple (i.e., flexion isométrique du coude). Nous avons cherché à déterminer le seuil EMG sur : i) le chef long du *Biceps brachial*, ii) le chef court du *Biceps Brachial* et ii) le *Brachioradialis* (Hug et al., 2009). La détection d'un seuil EMG valide n'a été possible que sur le chef long du *Biceps brachial* et pour seulement 3 des 8 sujets testés.

Dans une étude menée récemment, Hendrix et al. (2009b) ont réussi à déterminer un seuil EMG de la fatigue sur le *Biceps brachial* pour les 10 sujets testés lors du même type de tâche que celle réalisée dans notre étude. Cette grande divergence avec nos résultats peu s'expliquer par le fait que Hendrix et al. (2009) n'ont pas déterminé, *a priori*, de critères de validité pour leur seuil EMG. Or, puisque la détermination de ce seuil doit être utile, *in fine*, à l'évaluation de capacités physiques, il nous a semblé important de fixer des critères de validité en lien avec l'erreur de mesure. Ainsi, seuls les seuils EMG déterminés avec une erreur standard < 5% ont été retenus. L'absence de seuil EMG sur les autres muscles et chez les autres sujets a été discutée en termes de

[9] La méthode mathématique consiste à modéliser la relation EMG *vs.* intensité de l'exercice par deux régressions linéaires. On recherche alors le point délimitant deux zones qui correspond à un coût quadratique moyen minimal. Le seuil est validée si la pente de la deuxième régression linéaire est plus grande que la première.

compensations intermusculaires (cf. article joint en annexe). En effet, nous avons observé qu'en fonction de l'intensité de l'exercice (i.e., 20, 30, 40, 50 et 60 % de la contraction maximale volontaire), les muscles sollicités n'étaient pas les mêmes et qu'il existe des compensations intermusculaires, non seulement entre les muscles fléchisseurs du coude mais aussi avec des muscles sensés ne pas participer directement à la tâche (Figure 21). Ce résultat questionne donc sur la pertinence de la détermination de ce seuil EMG de la fatigue (*cf.* partie 4 « Projets de recherche »).

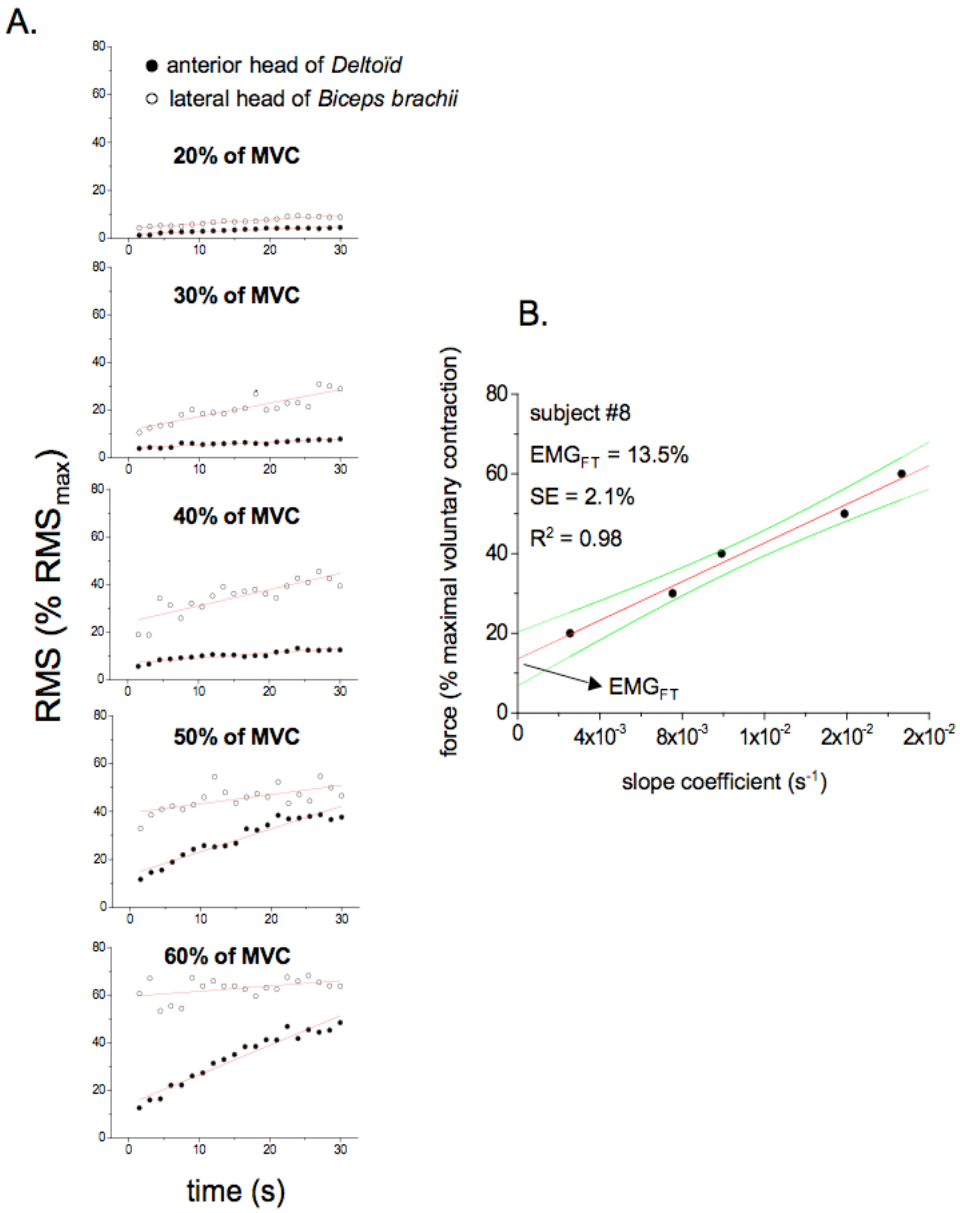

Figure 21. Illutration de possibles compensations avec le *Deltoïd anterior*. A- Le niveau d'activité EMG (RMS) du *Deltoïd anterior* et du chef long du *Biceps brachial* est représenté en fonction du temps pour les 5 exercices sous-maximaux (20, 30, 40, 50 et 60% de la contraction maximale volontaire). Alors que pour les exercices de faible intensité on observe une augmentation du niveau d'activité du chef long du *Biceps brachial*, pour les exercices d'intensités plus élevées, l'augmentation est observée sur le *Deltoïd anterior*. B- Quand la RMS (exprimé en % de RMS max) de ces deux muscles est additionnée, la détermination d'un seuil EMG de la fatigue devient possible, et ce avec une bonne précision (erreur standard = 2,1%) (B). D'après Hug *et al.* (2009).

Électromyographie et évaluation de la fatigue neuromusculaire

Résumé : Cet axe de recherche explore la notion de seuil électromyographique. Ce seuil peut être déterminé soit comme étant l'augmentation brutale de la pente de la relation linéaire entre le niveau d'activité EMG et la puissance d'exercice au cours d'une épreuve triangulaire menée sur cycloergomètre (on parle alors de seuil EMG), soit à partir d'épreuves sous-maximales selon la méthode décrite par DeVries et al. (1982) (on parle alors de seuil EMG de la fatigue).

Dans une première étude nous avons montré qu'il est préférable de détecter le seuil EMG par une technique mathématique, plus objective que la technique visuelle utilisée par certains auteurs. Dans une deuxième étude nous avons montré que le seuil EMG ne peut être déterminé de manière reproductible uniquement sur le muscle *Vastus lateralis.*

Plus récemment, nous nous sommes intéressés au seuil EMG de la fatigue qui nous paraît particulièrement intéressant puisqu'il est déterminé à partir d'exercices sous-maximaux. Toutefois, à partir d'exercices isométriques de flexions du coude, nous n'avons pu déterminer un seuil EMG de la fatigue que sur un des trois muscles investigués (i.e., chef long du *Biceps brachial*) et pour seulement trois des huit sujets testés. L'incapacité de détecter un seuil sur les autres muscles et les autres sujets a été discutée en termes de compensations intermusculaires.

Publications : 3 articles publiés dans des revues indexées ISI

Contrats de recherche : aucun

Encadrement : 2 étudiants de Licence 3ème année (stage recherche)

3.4. Caractérisation du délai électromécanique

3.4.1. État de la question.

Le délai électromécanique représente le délai entre l'activation électrique du muscle et sa production de force. Il peut être quantifié *in vivo* chez l'homme comme le délai séparant le début d'activité électromyographique du début de production de force musculaire mesurée de manière externe (Cavanagh et Komi, 1979). Ce délai est lié à de nombreux mécanismes et structures comme : i) la propagation du potentiel d'action musculaire et le couplage excitation-contraction (E-C) et ii) l'étirement des structures placées en série des structures contractiles regroupées dans la composante élastique série (CES ; fractionnée en une composante active, i.e., les myofibrilles et une composante passive i.e., principalement l'aponévrose et le tendon ; Figure 22) (Cavanagh et Komi, 1979). Le délai électromécanique est modifié à la suite de protocoles induisant une fatigue musculaire (Zhou *et al*., 1995; Paasuke *et al*., 1999; Kubo *et al*., 2001), de protocoles d'entraînements (Grosset *et al*., 2009), ou chez des sujets atteints de pathologies neuro-musculaires (Orizio *et al.*, 1997; Granata *et al.*, 2000). Cependant, la contribution relative de chacun des mécanismes et structures impliqués dans le délai électromécanique ne peut pas être déterminée *in vivo* avec les méthodes classiquement utilisées. Bien que des observations indirectes tendent à indiquer que le délai électromécanique est principalement lié à la transmission de la force musculaire (Norman et Komi, 1979; Zhou *et al.*, 1995; Muraoka *et al.*, 2004), et donc à l'étirement de la composante élastique série, cette hypothèse n'a jamais pu être vérifiée de manière directe. Pour cette raison, les différentes études s'intéressant au délai électromécanique sont limitées dans l'interprétation des résultats obtenus.

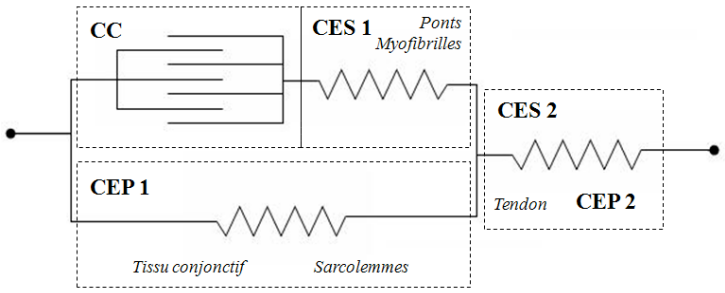

Figure 22. Modèle du complexe musculo-tendineux de Hill modifié à trois composantes. CC : composante contractile ; CES : composante élastique série composée d'une fraction passive et d'une fraction active ; CEP : composante élastique parallèle. Modifiée d'après Zajac (1989).

Une caractérisation plus complète du délai électromécanique pourrait inclure la détection du début du mouvement des fascicules musculaires et du tendon afin de dissocier leur contribution respective. Classiquement l'échographie est utilisée pour déterminer ces déplacements en temps réel (Magnusson *et al*., 2008). Cependant, la fréquence d'acquisition des échographes classiques est limitée à 50-100 Hz (résolution temporelle de 20 à 10 ms) ce qui est largement insuffisant pour étudier des phénomènes très courts comme le délai électromécanique

(compris entre 6 et 80 ms dans la littérature). Quelques études récentes ont tenté de déterminer le début de mouvement des fascicules musculaires (Pulkovski *et al*., 2008) ou du tendon (Chen *et al*., 2009) avec des échographes permettant des fréquences d'acquisition plus élevées (200-333Hz). Cependant, la résolution temporelle obtenue dans ces études reste insuffisante pour déterminer précisément des modifications du délai électromécanique. Par exemple, dans l'étude publiée récemment par Chen *et al*. (2009) la résolution temporelle est de 5 ms, soit 27% du délai électromécanique quantifié dans cette même étude. Ce point a été plus largement discuté dans une lettre à l'éditeur que nous avons récemment publié (Nordez *et al*., 2009a). La dernière génération d'échographes ultrarapides offrant la possibilité d'acquérir les signaux ultrasonores à plus de 5 kHz permettrait de s'affranchir de cette limitation méthodologique. Ainsi, Deffieux *et al*. (2006; 2008) ont montré la faisabilité de l'utilisation de cette technique pour quantifier les déplacements des fascicules musculaires *in vivo*, mais ces études ont été menées sur un nombre limité de sujets (trois au maximum) et ne se sont pas focalisées sur la détermination du début de mouvement du muscle et du tendon.

3.4.2. Caractérisation du délai électromécanique au moyen de l'échographie ultrarapide.

Nordez, A., Gallot, T., Catheline, S., Guevel, A., Cornu, C., Hug, F. Electromechanical delay revisited using very high frame rate ultrasound. *Journal of Applied Physiology*. 2009. 106(6) : 1970-1975.

Dans le cadre d'un contrat de recherche avec l'Association Française contre les Myopathies (contrat n°14084), et d'une collaboration avec le Laboratoire de Géophysique Interne et Tectonophysique (Université de Grenoble, Stefan Catheline), nous avons pu utiliser un échographe ultrarapide (fréquence d'acquisition = 4000 Hz) pour déterminer le début de mouvement des fascicules musculaires et de l'insertion myotendineuse en réponse à une stimulation électrique du *Gastrocnemius medialis* (Nordez *et al*., 2009b). Le choix de la contraction musculaire évoquée par stimulation électrique (au niveau du point moteur) se justifie par le fait que cette technique de stimulation permet à la fois d'isoler la contraction d'un seul muscle et également d'obtenir une très bonne répétabilité de la mesure du délai électromécanique. Cette expérimentation, menée chez neuf sujets, a donc permis de quantifier, *in vivo*, le délai entre i) l'artefact de stimulation et le début de mouvement des fascicules musculaires, ii) le début de mouvement des fascicules et le début de mouvement de l'insertion myotendineuse (i.e., extrémité proximale du tendon), et iii) le début de mouvement de l'insertion myotendineuse et le début de production de la force au niveau du pied (Figure 23).

Ces résultats ont été discutés en termes de contributions relatives des mécanismes et structures potentiellement impliqués dans le délai électromécanique. Ainsi, une part non négligeable (47,5 ± 6,0 %) du délai électromécanique peut être attribuée à l'étirement de la fraction passive de la CES au sein de laquelle le tendon semble représenter une part légèrement plus importante (3,22 ± 1,41 ms soit 27,6 ± 11,4% du délai électromécanique) que l'aponévrose (2,37 ± 1,30 ms soit 20,3 ± 10,7% du délai électromécanique) (Figure 23). La technique utilisée ne nous a pas permis de séparer la contribution de la transmission synaptique, du couplage excitation-contraction et de la fraction active de la CES. Néanmoins, au regard de la littérature et plus

spécifiquement des données disponibles sur le délai synaptique [1 ms selon Katz et Miledi, (1965)), le couplage excitation-contraction (2,5 ms selon Sandow, (1952)], d'une part, et la vitesse de transmission de la force dans le muscle [environ 30 $m.s^{-1}$ selon Morimoto et Takemori (2007)], d'autre part, nous suggérons que l'étirement de la composante active de la CES ne représente pas une part majeure du délai électromécanique contrairement à ce qui a été suggéré dans la littérature (Grosset *et al.*, 2009).

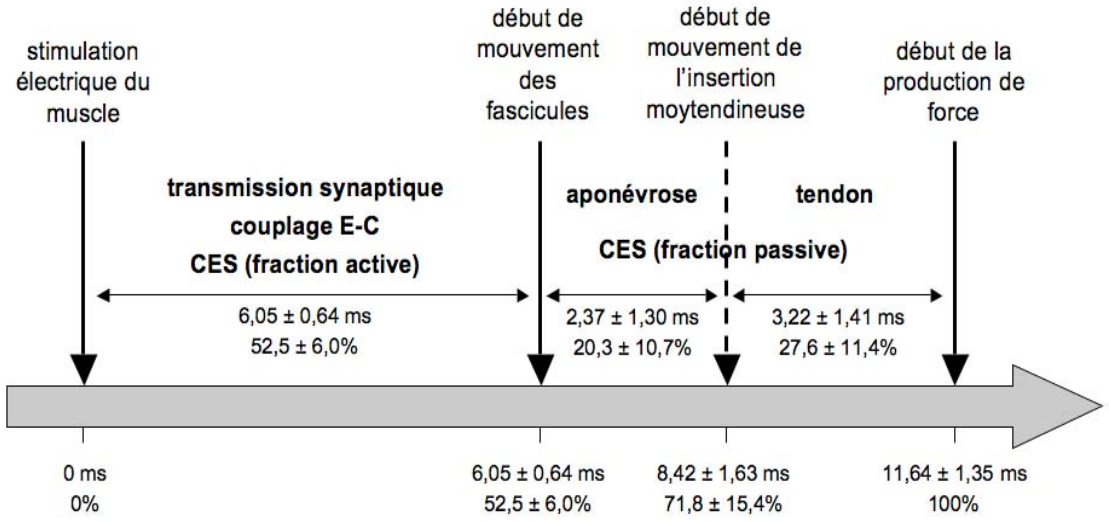

Figure 23. Représentation schématique des délais entre la stimulation musculaire (artefact de stimulation mesuré *via* les électrodes EMG) et le début de la production de force (i.e., le délai électromécanique ; ici 11,64 ±1,35 ms). Le début de mouvement des fascicules musculaires et de l'insertion myotendineuse a également été mesuré au moyen de l'échographie ultrarapide. Ces résultats permettent d'en déduire la contribution relative de la fraction passive de la CES et de chacune des deux principales structures qui la composent (i.e., aponévrose et tendon) dans le délai électromécanique. D'après *Nordez et al.* (2009).

Caractérisation du délai électromécanique

Résumé : Le délai électromécanique représente le délai entre l'activation électrique du muscle et sa production de force. Ce délai (entre 6 et 80 ms dans la littérature) est influencé par plusieurs mécanismes (e.g., couplage excitation-contraction) et structures (e.g., tendon, aponévrose). Seulement, leur contribution dans le délai ne peut pas être déterminée directement par les méthodes classiques d'exploration de la fonction neuromusculaire.
Grâce à la technique d'échographie ultrarapide (fréquence d'échantillonnage = 4000 Hz), cette étude a permis de quantifier *in vivo* le délai entre : i) l'artefact de stimulation et le début de mouvement des fascicules musculaires, ii) le début de mouvement des fascicules et le début de mouvement de l'insertion myotendineuse (i.e., extrémité proximale du tendon), et iii) le début de mouvement de l'insertion myotendineuse et le début de production de la force au niveau du pied. Ainsi, la contribution relative du couplage excitation-contraction et de la fraction active de la composante élastique série (52,5 ± 6,0 %), de l'aponévrose (20,3 ± 10,7%) et du tendon (27,6 ± 11,4%) au délai électromécanique a pu être déterminée.

Publications : 1 article publié dans une revue indexée ISI
Contrats de recherche : 1 subvention de recherche de l'Association Française contre les Myopathies
Encadrement : 1 étudiant de Licence STAPS 3ème année (stage recherche)

Chapitre 4 – Projets de recherche

Comme cela est déjà le cas pour les études présentées dans la partie 3 de ce mémoire d'habilitation à diriger des recherches, les perspectives de recherche détaillées ci-après s'inscrivent dans le programme scientifique du laboratoire « Motricité, Interactions, Performance » (EA 4334). Dans ce contexte, je propose de développer des travaux s'inscrivant dans la continuité de ceux déjà réalisés (Partie 4.1 « Électromyographie et analyse des coordinations musculaires » et partie 4.2 « Évaluation électromyographique de la fatigue neuromusculaire »).

Que ce soit pour l'étude des coordinations musculaires ou de la fatigue neuromusculaire, la présentation des travaux déjà réalisés (partie 3.1 et 3.3 de ce mémoire d'habilitation à diriger des recherches) met clairement en évidence des limites méthodologiques qui rendent l'interprétation des résultats délicate. Par exemple, l'étude menée au cours d'un exercice fatigant de pédalage (Dorel *et al.*, 2009) suggère des compensations musculaires sans que les résultats EMG suffisent à le démontrer. Lorsqu'il s'agit de déterminer un seuil EMG de la fatigue, on est limité par l'incapacité de détecter des compensations intermusculaires. Pour aller plus loin dans ces travaux, il me paraît donc primordial de pouvoir quantifier la force produite par le muscle (et non du couple de force estimé au niveau d'une articulation). C'est pour cette raison que je présenterai, dans une troisième partie (Partie 4.3), le développement d'un axe de recherche portant sur l'estimation de la force musculaire et l'étude de sa transmission. Un effort particulier sera consenti en faveur du développement de cet axe qui paraît particulièrement porteur.

Le développement de ces axes de recherche n'exclut pas la participation à d'autres protocoles de recherche portant sur des thématiques qui me passionnent tout autant (e.g., étude des muscles respiratoires) mais qui ne peuvent pas être menés au sein du laboratoire « Motricité, Interactions, Performance ».

4.1. Électromyographie et analyse des coordinations musculaires

4.1.1. Hétérogénéité spatiale du recrutement musculaire.

Classiquement, les enregistrements de l'activité électromyographique de surface en mode bipolaire se font au moyen de deux électrodes espacées de 2 cm, placées selon la direction supposée des fibres musculaires entre la zone distale et la zone d'innervation du muscle (cf. recommandations SENIAM « Surface Electromyography for the Non-Invasive Assessment of Muscles » ; http://www.seniam.org/). Cette modalité d'enregistrement présuppose que l'activité EMG mesurée est représentative de l'activité myoélectrique du muscle entier. Or, plusieurs études menées au cours d'un exercice isométrique font état d'une activation non homogène du muscle (Jensen *et al*., 1993; Kleine *et al*., 2000; Farina *et al*., 2008) (Figure 24). Des travaux menés chez l'animal (Hoffer *et al.*, 1987) et plus récemment chez l'Homme (Campanini *et al.*, 2007; Wakeling, 2009) rapportent également des variations spatiales de l'activité musculaire au cours de tâches de locomotion. Ce phénomène serait certainement lié à une distribution non homogène des différents types de fibres musculaires et/ou à une compartimentation du muscle en fonction des avantages biomécaniques [e.g., angle de pennation; (Chanaud *et al.*, 1991)].

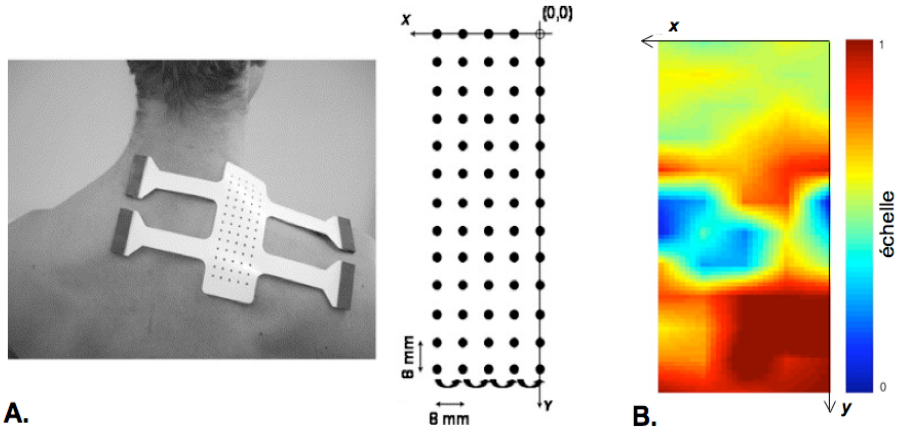

Figure 24. A, Exemple de matrices d'électrodes permettant d'enregistrer l'activité EMG sur 64 voies. B, cartographie du niveau d'activité EMG obtenue par l'utilisation de cette matrice d'électrodes au cours d'une tâche isométrique. L'activité est ici normalisée en pourcentage de l'activité maximale mesurée sur la carte. Cet exemple illustre bien que le niveau d'activité n'est pas homogène sur toute la surface du muscle. D'après Farina *et al*. (2006).

Il paraît donc important de quantifier cette variabilité liée au placement des électrodes. Cette information est essentielle pour toutes les études s'intéressant à décrire les patrons d'activité musculaire au cours de différents mouvements, à l'instar des études que nous avons présentées dans la partie 3.1 de ce mémoire d'Habilitation à Diriger des Recherches. Nous pouvons supposer qu'une partie des différences interindividuelles mises en évidence dans nos études (Hug *et al.*, 2004a; Hug *et al.*, 2008b) est dûe à une variabilité liée au placement des électrodes. Nous proposons donc d'utiliser des matrices d'électrodes de 64 voies (Figure 24) avec un amplificateur EMG approprié (EMG-128, LISiN – OT Bioelettronica, Torino, Italie) pour enregistrer l'activité EMG de certains muscles des membres inférieurs au cours d'un mouvement de pédalage. Le choix des muscles étudiés pourrait se faire en fonction de la variabilité interindividuelle mise en évidence précédemment (Hug *et*

al., 2004a; Hug *et al.*, 2008b). Ainsi, nous pourrions enregistrer un muscle présentant de faibles différences interindividuelles, le *Vastus lateralis* et un muscle présentant de fortes différences interindividuelles, le *Tibialis anterior*. Dans un premier temps, l'hétérogénéité spatiale sera quantifiée au cours d'un exercice de pédalage sous-maximal. Ensuite, il est envisagé de faire varier les contraintes du mouvement (i.e., cadence, puissance) et d'étudier leur influence sur le recrutement du muscle, d'un point de vue spatial.

Faisabilité : Le laboratoire « Motricité, Interactions, Performance » va prochainement (novembre 2009) faire l'acquisition d'un amplificateur EMG 128 canaux (EMG-128, LISiN – OT Bioelettronica, Torino, Italie), ce qui nous permettra d'être autonome sur cet axe de recherche. Dans le cadre d'une collaboration avec l'Institut National du Sport et de l'Education Physique (INSEP), il nous a déjà été possible d'utiliser cet outil (juillet 2009).

4.1.2. Identification des synergies musculaires.

Le système moteur possède un grand nombre de degrés de liberté (e.g., nombre de muscles, nombre d'articulations, etc.). Se pose alors la question de la manière de contrôler ces degrés de liberté pour produire un mouvement. Comme l'a proposé Bernstein (1967), le système nerveux central assemblerait les degrés de liberté en différentes synergies de façon à rendre le système contrôlable. De là découle la notion de synergie musculaire qui peut être définie comme l'activation simultanée de plusieurs muscles fonctionnellement liés. En d'autres termes, une synergie musculaire permet de regrouper des muscles en unités fonctionnelles. Quelques études récentes ont utilisé différents traitements statistiques [e.g., analyse en composantes principales (ACP), analyse en composantes indépendantes (ACI) ou factorisation matricielle non négative (NNMF)] pour extraire des synergies musculaires à partir de l'enregistrement de l'activité électromyographique de plusieurs muscles [pour revue, voir Bizzi *et al*. (2008)]. Chaque synergie est alors caractérisée par son profil d'activation et le poids que représente chacun des muscles dans cette synergie (Figure 25).

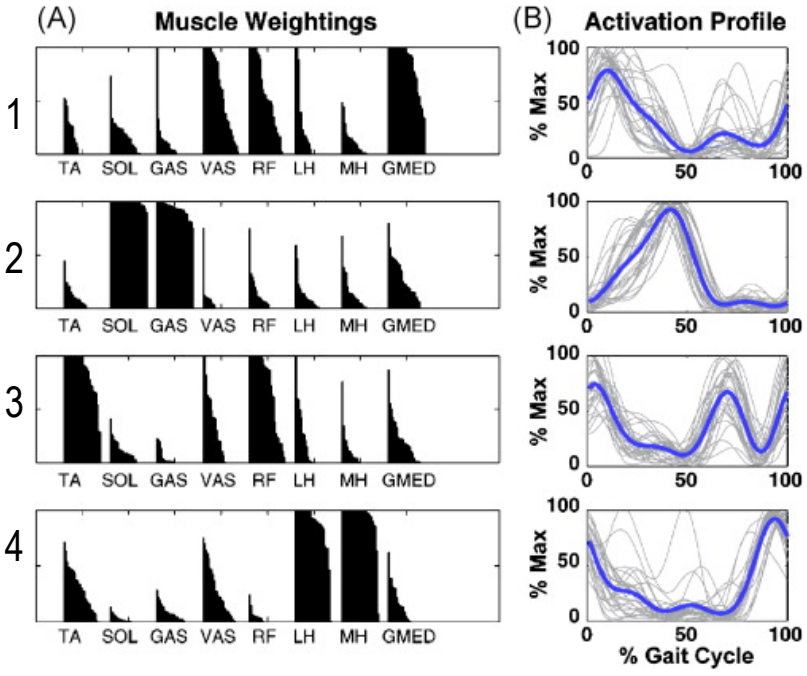

Figure 25. Identification des synergies musculaires au cours d'une activité de locomotion. Une factorisation matricielle non négative des signaux électromyographiques obtenus sur 8 muscles des membres inférieurs a permis d'identifier 4 synergies musculaires. Chacune des quatre synergies est représentée par le poids des muscles (A, i.e., représentation de chacun des muscles dans cette synergie) et un profil d'activation (B). Les régions noires représentant le poids des muscles sont en réalité formées de 28 histogrammes (12 sujets x 2 membres inférieurs). Un rectangle parfait indiquerait alors aucune différence entre les sujets/membres. D'après Neptune *et al.* (2009).

Ainsi, l'identification des synergies musculaires permettrait d'appréhender l'organisation de la commande nerveuse (pour revue, voir Ting et McKay, (2007)). Par exemple, il a été montré que l'activité EMG obtenue sur 32 muscles au cours de la marche peut être caractérisée par la combinaison de cinq synergies musculaires (Cappellini *et al.*, 2006). Des observations récentes réalisées chez la grenouille désafférentée suggèrent que ces synergies musculaires représentent ce que l'on appelle les « central pattern generators » et seraient capables de générer des patrons moteurs en l'absence d'information afférente (Cheung *et al.*, 2005). Enfin, les profils d'activité de ces synergies musculaires sont peu sensibles aux contraintes de la tâche et relativement similaires entre les sujets, bien que les poids soient plus variables (Ivanenko *et al.*, 2004; Cheung *et al.*, 2005). Cette nouvelle approche de traitement des signaux EMG sera utilisée dans le cadre des travaux de thèse de Nicolas Turpin, que je co-encadre. En complément d'une comparaison classique des patrons d'activité EMG (24 muscles du haut et bas du corps) obtenus chez des rameurs experts et des sédentaires, cette approche devrait nous permettre de révéler des différences d'organisation motrice (i.e., nombre de synergies musculaires, patrons d'activité des synergies musculaires, etc.) entre ces deux populations de sujets.

Nous appliquons actuellement ce type de traitement à des signaux EMG enregistrés dans le cadre d'une étude ayant déjà fait l'objet d'une publication (Hug *et al.*, 2008a). Dans cette dernière, nous avions mis en évidence, par l'enregistrement de l'activité EMG de 10 muscles du membre inférieur chez une population de cyclistes entraînés, une variabilité interindividuelle des patrons d'activité EMG, davantage marquée sur les muscles biarticulaires (cf. Chapitre 3.1.3). Une question se pose alors : la variabilité interindividuelle mise en évidence sur certains muscles implique-t-elle aussi une variabilité des synergies musculaires (et donc du programme moteur) ? En d'autres termes, est-ce que le mouvement de pédalage est réalisé par la combinaison du même nombre de synergies et des mêmes synergies chez une population de cyclistes entraînés ? En utilisant une factorisation matricielle, nous avons extrait trois synergies musculaires pour chacun des cyclistes étudiés (Figure 27, A)[10] ce qui paraît cohérent avec les résultats obtenus par simulation [Raash et Zajac, (1999) ; Figure 26]. Nous avons rapporté une faible variabilité interindividuelle concernant le profil d'activation de chacune de ces trois synergies. *A contrario*, nos résultats montrent davantage de variabilité interindividuelle des poids de certains muscles (e.g., *Rectus femoris, Gastrocnemius medialis, Biceps femoris, Semitendinosus*) dans les synergies (Figure 27, B) .

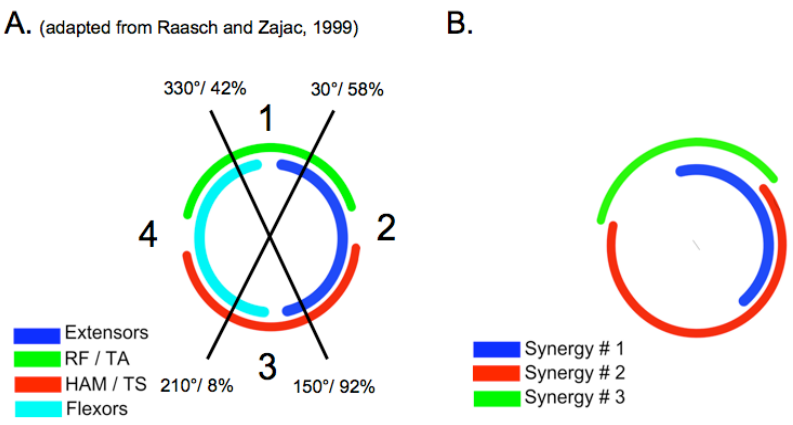

Figure 26. Représentation schématique des résultats obtenus par simulation (Raash et Zajac,1999) (A) et ceux que nous avons obtenus (B). L'absence d'une quatrième synergie dans notre étude peut s'expliquer par le fait que nous n'avons pas enregistré l'activité EMG de muscles monarticulaires fléchisseurs du genou/de la hanche.

[10] Hug, F., Turpin, N., Guével, A., Dorel, S. Is interindividual variability of EMG patterns in trained cyclists related to different muscle synergies? *Journal of Neurophysiology*. En révision majeure – août 2009.

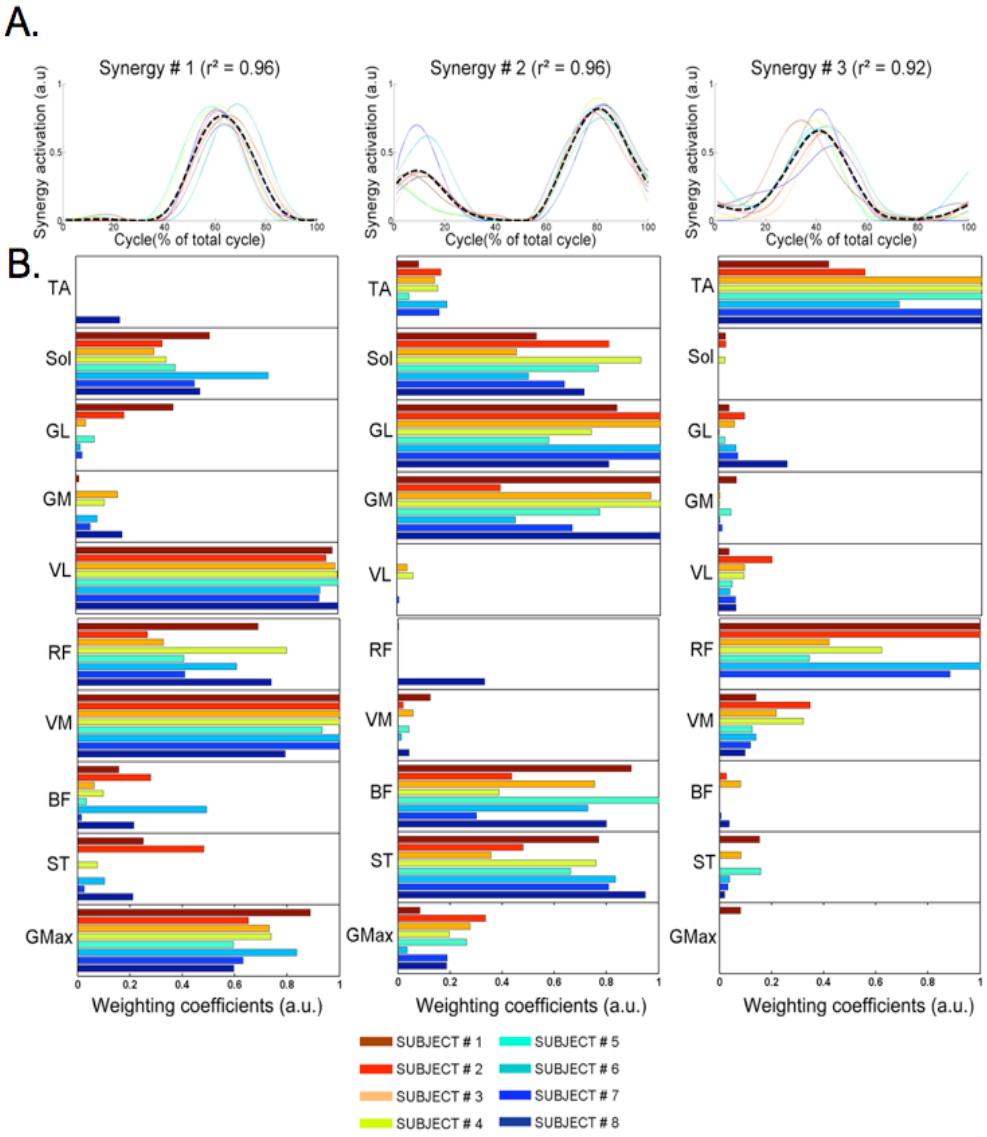

Figure 27. Extraction de trois synergies musculaires chez 8 cyclistes entraînés à partir de l'activité EMG de 10 muscles enregistrée sur 40 cycles consécutifs. A) Le patron d'activation de chacune des 3 synergies identifiées est représenté pour chaque sujet. 0% représente le point mort bas (manivelle dans la position verticale, pédale en bas). Chaque patron est normalisé par rapport à l'activité maximale mesurée au cours des 40 cycles. La courbe en pointillés représente le patron moyen de tous les sujets. r^2 indique le degré de corrélation entre tous les patrons. B) Pour chaque sujet, le poids des muscles dans chaque synergie est représenté. GMax, *Gluteus maximus* ; ST, *Semitendinosus* ; BF, *Biceps femoris* (chef long) ; VM, *Vastus medialis* ; VL, *Vastus lateralis* ; GM, *Gastrocnemius medialis* ; GL, *Gastrocnemius lateralis* ; SOL, *Soleus* ; TA, *Tibialis anterior*.

Faisabilité : Comme en témoignent les résultats présentés ci-dessus (article en révision dans *Journal of Neurophysiology*), le développement méthodologique nécessaire à l'identification des synergies musculaires est actuellement en cours. Il est réalisé dans le cadre de la thèse de Mr Nicolas TURPIN (2008-2011), que je co-encadre. Cet axe de recherche est financé par la Région des Pays de la Loire (Projet OPERF2A « Optimisation de la performance et interactions homme-machine en sport automobile et en aviron »).

4.2. Évaluation électromyographique de la fatigue neuromusculaire

4.2.1. Détermination du seuil électromyographique de la fatigue.

Comme nous l'avons déjà souligné dans ce mémoire (partie 3.3.3), de nombreuses études se sont intéressées à déterminer le seuil électromyographique de la fatigue[11] (EMG_{FT}) au cours d'exercices de pédalage (deVries *et al.*, 1982; Matsumoto *et al.*, 1991; Moritani *et al.*, 1993; Graef *et al.*, 2008) ou d'efforts isométriques (Hendrix *et al.*, 2009a; Hendrix *et al.*, 2009b). Puisque ce seuil est déterminé à partir d'exercices d'intensité et de durée sous maximales, cet axe de recherche est particulièrement intéressant, notamment pour des populations de sujets pathologiques qui ne peuvent pas être évaluées sur des exercices menés jusqu'à épuisement, et ce pour éviter les effets délétères liés à ce type de sollicitation. Cependant, dans la littérature, aucun critère de validité n'est fixé pour la détermination de ce seuil. Bien que les études déterminent un seuil EMG de la fatigue pour la grande majorité des sujets, on peut légitimement s'interroger sur la validité de ces résultats. Par exemple, en se basant sur le tableau de résultats fourni par Hendrix et al. (2009b), nous avons calculé l'erreur standard de chaque seuil déterminé par ces auteurs. Pour deux sujets (sur 10 sujets testés), cette erreur est supérieure à 9% de la contraction maximale volontaire (Figure 28).

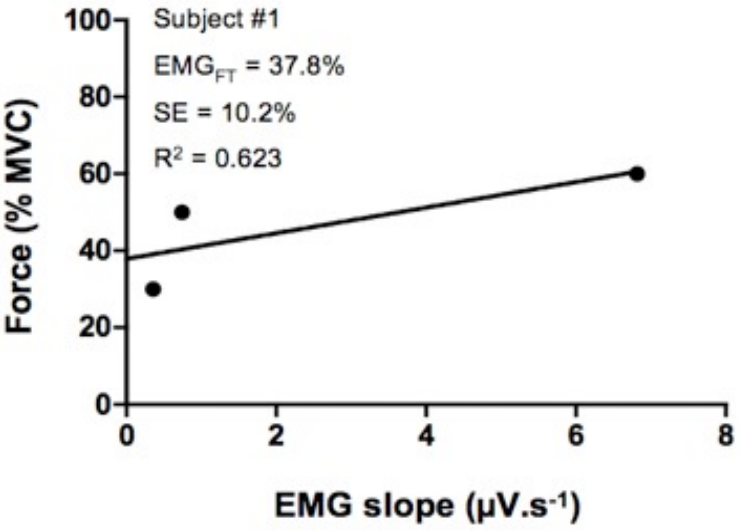

Figure 28. Exemple d'un seuil EMG de la fatigue déterminé d'après les résultats obtenus par Hendrix *et al.* (2009). Il s'agit du sujet #1 du tableau 2 publié par ces auteurs. MVC, contraction maximale volontaire.

Cette précision ne nous semble pas satisfaisante dans la perspective d'utiliser ce seuil comme indice d'évaluation de la fonction musculaire. En effet, dans ce cas il devra être suffisamment sensible pour détecter de petites variations entre les sujets ou au cours d'un programme d'entraînement/réentraînement. En utilisant des critères de validité (e.g., erreur standard < 5% de la contraction maximale volontaire), nous n'avons pas été en mesure de déterminer un seuil EMG de la fatigue pour la plupart de nos sujets (Hug *et al.*, 2009 ; cf. chapitre 3.3.3).

[11] Pour rappel, le seuil électromyographique de la fatigue est généralement défini comme la plus haute intensité d'exercice pouvant être maintenue sans apparition de la fatigue neuromusculaire.

Nous proposons plusieurs hypothèses pour expliquer cette incapacité de détecter un seuil valide :

1) Le concept de seuil EMG de la fatigue est basé sur la relation linéaire entre l'augmentation du niveau d'activité EMG et le temps au cours d'un exercice sous-maximal. Or, cette relation n'est pas forcément linéaire (Hug *et al.*, 2004b) ;

2) Le seuil EMG de la fatigue est déterminé au cours d'exercices impliquant plusieurs muscles. Or, au cours d'un exercice fatigant, on peut observer des compensations inter-musculaires (Kouzaki *et al.*, 2002) susceptibles d'interférer dans la détermination du seuil ;

3) Comme souligné dans la partie précédente, il existe une variabilité spatiale du recrutement musculaire. Il est important de prendre en compte cette variabilité lorsqu'il s'agit d'étudier l'évolution des paramètres EMG au cours d'un exercice fatigant. En effet, quelques études ont démontré que l'évolution du niveau d'activité EMG au cours d'un exercice sous-maximal mené jusqu'à épuisement varie de manière très différente en fonction de l'emplacement des électrodes (Zijdewind *et al.*, 1995; Farina *et al.*, 2008) (Figure 29). De surcroît, Zijdewing et al. (1995) n'ont pas été en mesure de localiser un site qui, chez tous les sujets, présente la même évolution du niveau d'activité EMG. Dans ces conditions il apparaît alors impossible de déterminer convenablement un seuil EMG de la fatigue en enregistrant l'activité EMG de manière trop localisée ;

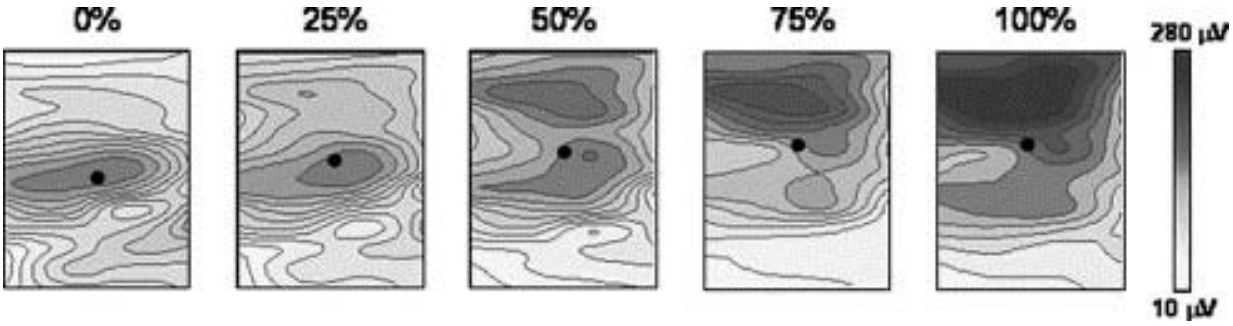

Figure 29. Représentation spatiale du niveau d'activité EMG (RMS) mesuré sur le *Trapezius* (configuration identique à celle présentée sur la figure 24, A) à 0, 25, 50, 75 et 100% d'un exercice de temps limite. Le rond noir représente le centre de gravité du niveau d'activité EMG. L'échelle de gris est la même pour toutes les figures. Sur cet exemple, l'enregistrement classique (2 électrodes – détection bipolaire) de l'activité EMG dans la partie supérieure de cette cartographie aurait montré une augmentation du niveau d'activité EMG au cours de l'exercice alors que l'enregistrement dans la partie inférieure n'aurait pas montré de modification du niveau d'activité EMG. D'après Farina *et al*. (2008).

4) Le concept de seuil EMG de la fatigue repose sur l'hypothèse que la fatigue neuromusculaire induit une augmentation progressive du niveau d'activité EMG au cours d'un exercice maintenu à une intensité constante. Or, de nombreux travaux ont démontré que d'autres facteurs (physiologiques et non-physiologiques) peuvent également être la cause de cette variation [pour revue, voir Farina *et al*. (2004)].

Nous proposons de mettre en place un protocole expérimental évitant les écueils évoqués ci-dessus :

1) Pour pallier aux limites induites par la relation possiblement non-linéaire entre l'augmentation du niveau d'activité EMG et le temps, nous proposons d'utiliser « l'aera ratio » introduit par Merletti *et al*. (1991) au lieu de la pente de la régression linéaire.

L'area ratio est défini selon la formule :

$$\text{Area ratio (AE)} = A/R$$

où R correspond à l'aire du rectangle dont la longueur est définie par la durée de l'exercice et la largeur par la valeur du niveau d'activité EMG du début de l'exercice (Y_0) et une valeur maximale égale à x fois la valeur initiale (Y_1). A correspond à l'aire située en-dessous de la relation EMG *vs.* temps (Figure 30).

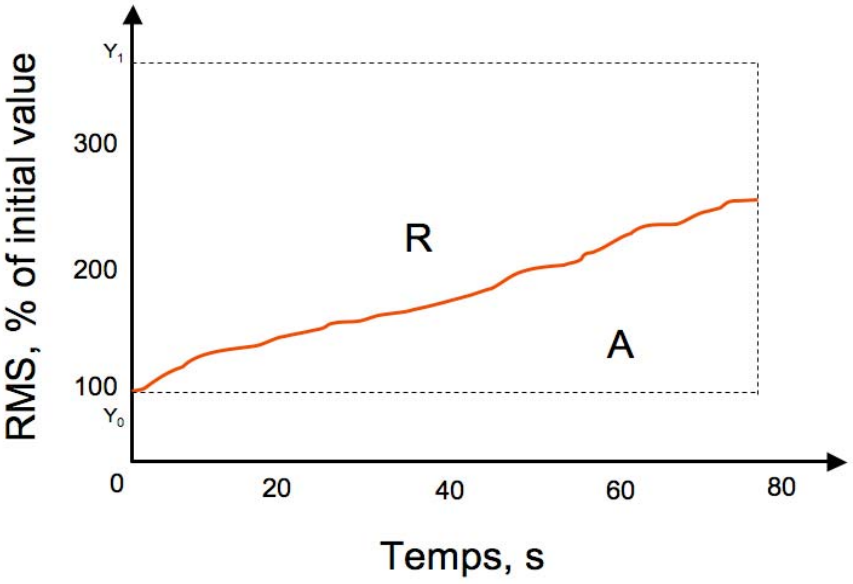

Figure 30. Représentation des aires considérées dans le calcul de l'aera ratio pour l'évolution du RMS en fonction du temps. Y_0 correspond à la valeur initiale du RMS et Y_1 à la valeur maximale ici égale à 4 fois la valeur initiale. Plus le niveau d'activité augmente et plus l'aera ratio augmente. Le seuil EMG de la fatigue correspondrait à un aera ratio=0.

L'avantage du calcul de l'area ratio réside dans le fait qu'il n'est pas établi à partir d'un modèle prédéterminé de l'évolution du signal EMG (e.g., régression linéaire) comme cela est le cas dans la méthode classique de détection du seuil EMG de la fatigue.

2) Dans un second temps, parce que des compensations intermusculaires peuvent intervenir au cours d'un exercice fatigant, il faudrait idéalement utiliser une tâche n'impliquant qu'un muscle principal. Par exemple, le premier *Dorsal interosseus* est responsable d'environ 93% de la force maximale produite au cours de l'adduction de l'index et l'*Adductor pollicis* est le principal muscle impliqué dans l'adduction du pouce (environ 80% de la force maximale) (Chao *et al.*, 1989). Étant donnée la contribution importante de ces deux muscles dans leurs actions respectives, ils pourraient être étudiés dans les futurs travaux. Néanmoins, même au sein de ces muscles de faible volume, la distribution spatiale du recrutement musculaire n'est pas homogène (Zijdewind *et al.*, 1995). Pour cette raison nous proposons d'utiliser un amplificateur EMG multicanaux couplé à une matrice (ou un vecteur) d'électrodes permettant d'enregistrer l'activité EMG sur toute la surface du muscle. Si un protocole combinant l'utilisation de l'area ratio et des matrices d'électrodes lors d'une tâche d'adduction de l'index (ou du pouce) permet de déterminer un seuil EMG de la fatigue valide (erreur standard < 5% de la contraction maximale volontaire), il pourrait alors être intéressant de poursuivre ces travaux, et par exemple, de comparer ce seuil entre des populations de sujets sains et des populations de sujets pathologiques (e.g., myopathes).

Faisabilité : Le laboratoire « Motricité, Interactions, Performance » va prochainement (novembre 2009) faire l'acquisition d'un amplificateur EMG 128 canaux (EMG-128, LISiN – OT Bioelettronica, Torino, Italie), ce qui nous permettra d'être autonome sur cet axe de recherche. Dans le cadre d'une collaboration avec l'Institut National du Sport et de l'Education Physique (INSEP), il nous a déjà été possible d'utiliser cet outil (juillet 2009). Un étudiant que je co-encadre, inscrit en 2ème année de master (2009-2010), aura la charge de conduire ce protocole de recherche.

4.2.2. Prédiction de l'endurance limite.

La fatigue musculaire étant un processus continu et progressif dont les manifestations myoélectriques peuvent être observées dès le début de l'exercice (De Luca, 1984), de nombreuses études ont essayé de prédire la durée maximale pendant laquelle un sujet peut maintenir un niveau de force requis (i.e., le temps limite) à partir des évolutions précoces du signal EMG (calculées sur des durées inférieures au temps limite) mesurées au cours d'exercices sous-maximaux (pour revue, voir la thèse de S. Boyas, 2007[12]). À l'instar du seuil EMG de la fatigue, cet axe de recherche est particulièrement intéressant pour des populations de sujets pathologiques qui ne peuvent pas être évaluées sur des exercices menés jusqu'à épuisement. Seulement, les résultats de ces travaux sont décevants puisqu'ils n'ont pas démontré la capacité de prédire l'endurance limite avec une précision satisfaisante. En effet, bien que certaines études rapportent une régression linéaire significative entre l'évolution précoce des paramètres EMG (souvent la fréquence médiane) et le temps limite (Mannion et Dolan, 1994; Dolan *et al.*, 1995; Merletti et Roy, 1996; Maisetti *et al.*, 2002), le coefficient de détermination de cette régression (témoignant de la précision de la prédiction) est faible, i.e., entre 0,27 et 0,74. En plus des hypothèses déjà exposées précédemment pour expliquer l'incapacité de déterminer précisément un seuil EMG de la fatigue, nous formulons l'hypothèse que les populations testées dans ces études sont trop homogènes en termes d'aptitudes physiques. En effet, à l'instar de la relation entre VO_2max et performance, il est probable que les évolutions précoces de l'EMG ne permettent pas de prédire le temps limite chez une population homogène de sujets. Nous proposons donc d'étudier la capacité de prédire le temps limite au cours de la même tâche que celle présentée dans la partie précédente, chez une population de sujets hétérogènes en termes d'aptitudes physiques.

Faisabilité : le protocole de recherche présenté dans la partie 4.2.1 de ce mémoire servira de support à l'étude de la prédiction de l'endurance limite. Ces deux projets pourront donc être menés de front.

[12] Boyas, S. Analyse des évolutions du signal électromyographique en vue de la prédiction de l'endurance limite lors de tâches mono- et multi-segmentaires. 2007. Thèse de doctorat (Université de Nantes).

4.3. Estimation de la force musculaire et étude de sa transmission

4.3.1. Estimation de la force produite par le muscle.

Comme évoqué précédemment, plusieurs facteurs physiologiques et non-physiologiques sont susceptibles de faire varier le niveau d'activité EMG. Le signal EMG ne permet donc pas d'estimer le niveau de force développé par un muscle. Cette limite est d'autant plus gênante lorsqu'il s'agit d'interpréter les modifications du niveau d'activité EMG au cours d'un exercice fatigant comme cela est le cas dans certaines de nos études (cf. partie 3.1 et 3.3). En effet, dans ce contexte, une augmentation du niveau d'activité EMG peut être liée (entre autre) à : i) une augmentation du nombre d'unités motrices recrutées pour augmenter le niveau de force produit par le muscle, ii) une augmentation du nombre d'unités motrices recrutées pour compenser l'altération de la fonction contractile (i.e., la fatigue) ou iii) les deux combinées. Ainsi, réussir à quantifier les efforts musculaires serait un atout indéniable pour toutes les études que nous menons, et bien au-delà. En effet, l'estimation de la force musculaire est un problème ouvert, notamment en biomécanique, et intéresse donc de nombreuses équipes de recherche. Des études ont tenté de quantifier cette force par une approche de modélisation (Buchanan *et al.*, 2004; Erdemir *et al.*, 2007) sans toutefois être en mesure de valider ces modèles. Réussir à quantifier la force musculaire serait alors une avancée indéniable pour cette validation.

Davis *et al*. (2003) ont observé, sur le muscle isolé, une bonne corrélation entre la pression intramusculaire et la force générée par le muscle. Ce résultat suggère que la dureté (élasticité) du muscle est liée à la force qu'il produit. Le module d'élasticité d'un tissu biologique peut être mesuré par différentes techniques d'élastographie[13]. La technique d'élastographie statique consiste à appliquer une contrainte externe (σ) uniformément à la surface d'un solide et à mesurer la déformation (ε) induite. Plus un matériau est dur et moins cette déformation est importante. La relation contrainte/déformation est donnée par : $\sigma = E\varepsilon$ (E étant le module d'élasticité). Lorsqu'il s'agit d'évaluer la dureté du tissu humain (e.g., le muscle), on est limité par l'impossibilité d'appliquer une contrainte uniforme sur l'ensemble de la zone étudiée. On peut alors utiliser la technique d'élastographie impulsionnelle qui consiste à exciter le milieu par une impulsion mécanique brève induisant de ce fait la formation de deux types d'ondes mécaniques : les ondes de compression qui se déplacent très vite (1500 m/s) dans les tissus en les comprimant de proche en proche et les ondes de cisaillement qui se déplacent plus lentement (1 à 10 m/s). La vitesse des ondes de cisaillement est directement reliée à la dureté du tissu selon l'équation $\mu = \rho C^2$ (μ étant le module d'élasticité de cisaillement, ρ la masse volumique du milieu et C la vitesse de propagation des ondes de cisaillement). L'utilisation d'un transducteur ultrasonore atteignant une fréquence d'échantillonnage entre 1000 et 2000 Hz permet alors de calculer la vitesse de propagation de cette onde de cisaillement dans l'axe du faisceau ultrasonore (i.e., axe transversal du muscle), et donc de déterminer

[13] désigne l'ensemble des techniques d'imagerie (e.g., échographie, imagerie par résonance magnétique) traitant de l'élasticité des tissus. Toutes les approches reposent sur les trois mêmes étapes : i) génération d'une contrainte, ii) imagerie du tissu pour analyser les effets de la contrainte, i.e., la déformation et ii) détermination d'un paramètre relié à la dureté du tissu. Si le module d'élasticité peut être déterminé, la technique est dite quantitative. Pour revue voir la thèse de J.L. Gennisson (2003 - http://pastel.paristech.org/00000487/)

le module d'élasticité de cisaillement (i.e., la dureté du tissu). Cette technique d'élastographie impulsionnelle 1D (puisqu'il n'y a qu'un transducteur ultrasonore) a été récemment utilisée pour évaluer la relation entre le module d'élasticité de cisaillement du muscle et : i) le niveau d'activité EMG (Nordez *et al.*, 2008) et ii) le niveau du couple passif (Nordez *et al.*, 2008). Cependant, le faible coefficient de détermination de la relation entre le module d'élasticité de cisaillement et le niveau d'activité EMG rapporté par Gennisson *et al.* (2005) (R^2=0.55) et la faible répétabilité des mesures mise en évidence par Nordez *et al.* (2008) soulignent les limites de l'élastographie impulsionnelle 1D. Deux hypothèses principales ont été avancées pour expliquer ces résultats : i) puisque les fibres musculaires bougent au cours de la contraction, les mesures d'élastographie ne sont pas réalisées sur le même échantillon musculaire et ii) il est difficile de standardiser la vibration mécanique. Une nouvelle technique, nommée Supersonic Shear Imaging (SSI) (Bercoff *et al.*, 2004) commercialisée avec l'échographe créé par Supersonic Imagine (et à ce jour, uniquement avec cet échographe), permettrait de résoudre certains problèmes posés par l'élastographie impulsionnelle et donc potentiellement d'améliorer la précision et la répétabilité de la mesure. Le concept de la SSI repose sur deux principes clefs (Figure 31). Le premier est que la génération des ondes de cisaillement ne se fait plus par l'application d'une impulsion externe mais directement *via* le signal ultrasonore. Brièvement, les ultrasons sont focalisés successivement à des profondeurs différentes pour créer des poussées par pression de radiation (pushs). En régime supersonique (quand la source se déplace plus vite que les ondes qu'elle génère), les ondes de cisaillement s'ajoutent de manière cohérente le long d'un « cône de Mach ». Le second principe de la méthode SSI est la mesure du déplacement de ces ondes de cisaillement par échographie ultrarapide (fréquence d'acquisition jusqu'à 20 000 Hz).

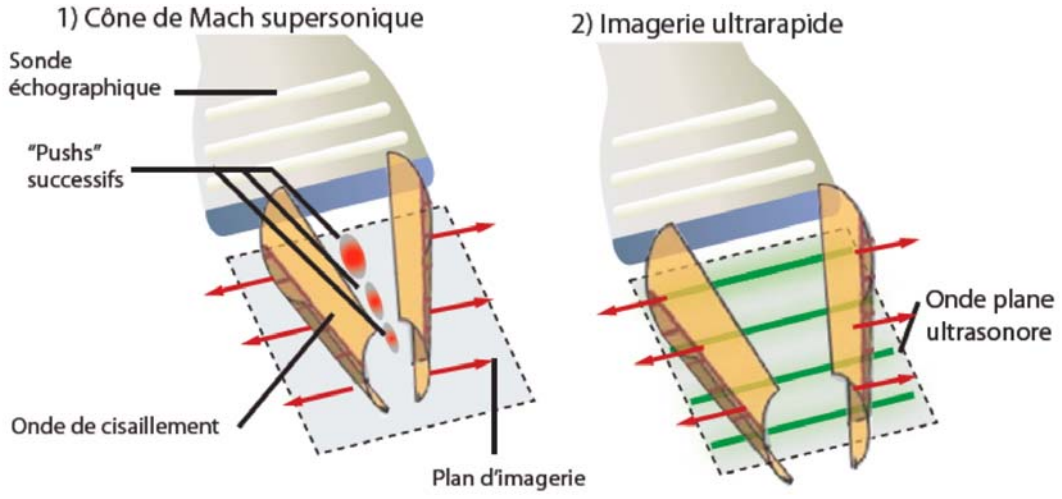

Figure 31. Principe de la technique « Supersonic Shear Imaging » (SSI). 1) Les ultrasons sont focalisés successivement à des profondeurs différentes pour créer des poussées par pression de radiation ("pushs"). Les interférences constructives des ondes de cisaillement forment un cône de Mach supersonique (dans lequel la vitesse de la source est supérieure à celle de l'onde générée) et une onde plane de cisaillement est crée. 2) L'échographe passe ensuite en mode d'imagerie ultrarapide pour suivre l'onde de cisaillement qui se propage dans le milieu. D'après la thèse de T. Deffieux (2008)[14].

[14] Deffieux, T. Palpation par force de radiation ultrasonore et échographie ultrarapide : applications à la caractérisation tissulaire in vivo. 2008. Thèse de doctorat. Université de Paris 7.

Dans le cadre d'une démonstration, la société Supersonic Imagine (Aix-en-provence, France) a mis à notre disposition un échographe Aixplorer disposant de la technologie SSI pour une durée de 3 jours (juillet 2009). En collaboration avec le Dr Antoine NORDEZ, nous avons mis à profit cette période pour tester la précision et la répétabilité de la technique SSI pour estimer le niveau d'activité du muscle *Biceps brachial*[15]. Six sujets ont été placés sur un ergomètre Biodex 3 et disposaient d'un feedback visuel du couple de force développé par les fléchisseurs du coude. Il leur a été demandé de réaliser deux rampes isométriques (espacées de 3 minutes de récupération) consistant en une augmentation du couple de force de 0 à 40% de la contraction maximale volontaire sur une période de 30 secondes. L'activité EMG et le module d'élasticité de cisaillement du *Biceps brachial* ont été enregistrés en continu. La Figure 32 présente un exemple de la carte d'élasticité qui a été obtenue toutes les secondes pendant l'exercice.

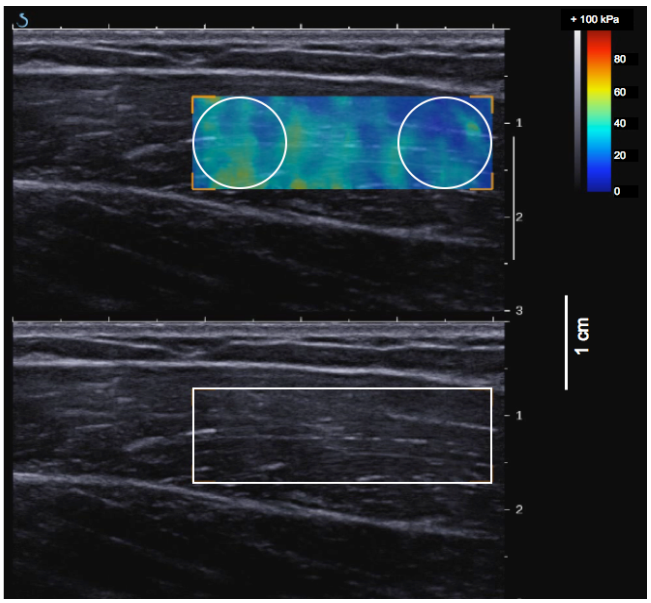

Figure 32. Exemple d'une carte d'élasticité obtenue par la technique SSI. À partir de l'image échographique brute (en bas) nous avons choisi une zone d'intérêt (rectangle blanc) au sein de laquelle une cartographie du module d'élasticité de cisaillment a été mesurée (en haut). Le logiciel de traitement fourni avec l'échographe permet de calculer la valeur moyenne du module d'élasticité de cisaillement sur deux régions circulaires. Nous avons ensuite moyenné ces deux valeurs afin d'obtenir une valeur la plus représentative possible du module d'élasticité du *Biceps brachial*.

Les résultats mettent en évidence une régression linéaire significative entre le module d'élasticité de cisaillement et le niveau d'activité EMG pour chacune des deux rampes des six sujets (R^2=0.94±0.05, de 0.82 à 0.98 ; Figure 33). Une bonne répétabilité a également été observée.

Les résultats de cette étude préliminaire sont très encourageants puisqu'ils démontrent très nettement la supériorité de cette technique par rapport à l'élastographie impulsionnelle 1D (meilleure précision et meilleure répétabilité de la mesure du module d'élasticité). Néanmoins, ces expérimentations ont mis en avant une limitation de la version commerciale de l'échographe puisque les mesures du module d'élasticité de cisaillement saturent à 100 kPa, ce qui ne nous a pas permis de traiter les résultats sur la totalité des rampes isométriques (en moyenne, le module d'élasticité de cisaillement a pu être mesuré jusqu'à 28±7 % de la MVC). Il semblerait que ce problème puisse être réglé simplement par les ingénieurs de Supersonic Imagine. Il sera donc intéressant de reproduire cette étude pour des niveaux d'activités musculaires plus élevés.

[15] Nordez, A., Hug, F. Muscle shear elastic modulus measured using supersonic shear imaging is highly related to muscle activity level: preliminary results. *Journal of Biomechanics*. Soumis – août 2009.

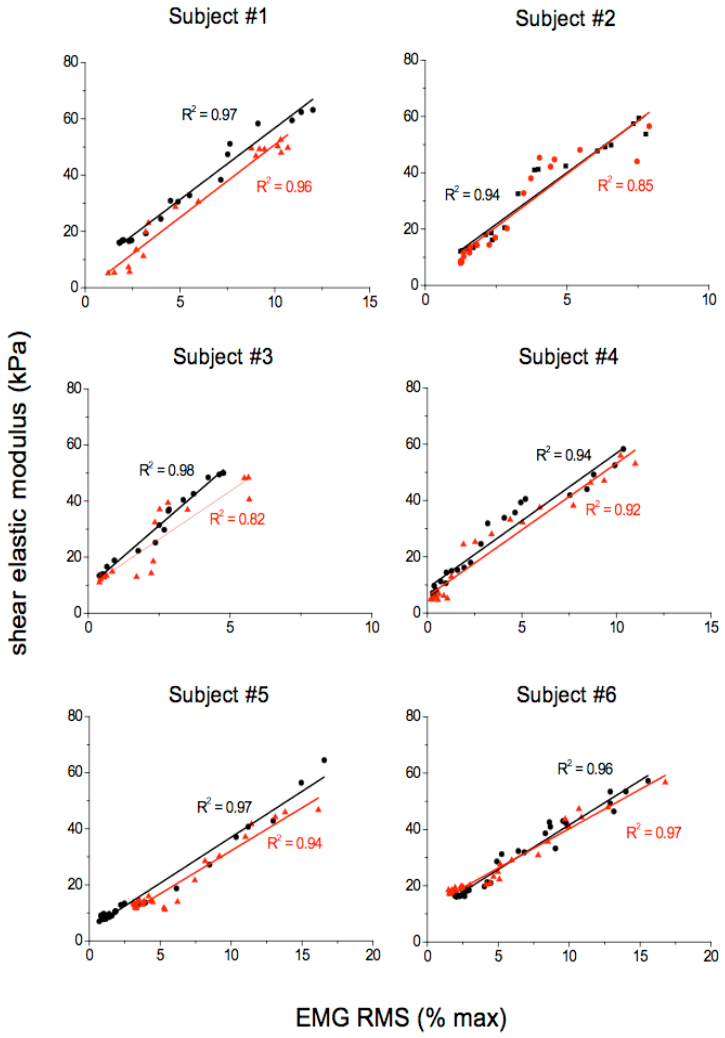

Figure 33. Régressions linéaires obtenues entre le module d'élasticité de cisaillement (shear elastic modulus) et la valeur normalisée (en % du niveau d'activité maximale) du niveau d'activité EMG (EMG RMS) pour les deux rampes isométriques des six sujets. En noir, rampe 1 et en rouge, rampe 2.

Puisqu'à terme, l'objectif de l'utilisation de cette technique est l'estimation de la force musculaire, au delà de la relation entre le module d'élasticité de cisaillement et le niveau de contraction (i.e., activité EMG), nous devrons explorer directement la relation entre le module d'élasticité de cisaillement et la force produite. Puisque le niveau de force produit par un muscle ne peut pas être mesuré directement chez l'Homme, cette phase expérimentale devra être conduite chez l'animal. Nous proposons donc, dans le cadre d'une collaboration avec les Drs Patrick DECHERCHI et Tanguy MARQUESTE (Institut des Sciences du mouvement Humain, Université de Aix-Marseille II), d'établir, *in vivo*, la relation entre le module d'élasticité de cisaillement mesuré par la technique SSI et le niveau de force produit par stimulation électrique d'un muscle de lapin (e.g., un muscle penné, *le Gastrocnemius* et un muscle fusiforme, *le Tiabialis anterior*). Dans le cas d'une relation linéaire, comme le suggère la littérature (Dresner *et al.*, 2001), nous pourrons raisonnablement envisager l'utilisation de la technique SSI pour estimer la force musculaire. Une deuxième étape consistera alors à établir l'influence de la longueur du muscle sur cette relation. Enfin, dans un troisième temps il pourrait être envisagé d'étudier l'influence de la fatigue musculaire sur cette relation en fatiguant préalablement le muscle par une stimulation électrique basse fréquence (LFF). Nous pourrions également comparer l'évolution du module d'élasticité de cisaillement au cours d'un protocole de fatigue (i.e., LFF) à la chute de force bien connue dans ce contexte. En

effet, le fluage du tendon observé au cours de ce type d'exercice (Mademli et Arampatzis, 2005) modifie l'angle de pennation des fascicules musulaires (dans le cas d'un muscle penné) et donc les propriétés mécaniques du muscle. Ces modifications devraient influencer le module d'élasticité de cisaillement indépendamment de la force produite par le muscle et donc potentiellement empêcher l'estimation de la force dans ce contexte. Cependant, nous formulons l'hypothèse que ces modifications sont mineures au regard de l'influence de la chute de force produite sur le module de cisaillement.

Parallèlement à ces travaux de validation chez l'animal, nous envisageons de poursuivre les travaux déjà engagés chez l'Homme (Nordez et Hug, soumis, J Biomech). Comme évoqué précédemment, la première étape consistera à compléter la relation entre le module d'élasticité de cisaillement et le niveau d'activité EMG en explorant des niveaux d'activité plus élevés (jusqu'à 100 %). Nous envisageons également d'étudier la relation entre le module d'élasticité de cisaillement et la force produite par stimulation électrique du muscle. La myostimulation devrait nous permettre de stimuler sélectivement un muscle. Chacune de ces deux études sera réalisée à la fois sur un muscle fusiforme (e.g., *Biceps brachial*) et un muscle penné (e.g., *Gastrocnemius medialis*).

Faisabilité : Le développement de cet axe de recherche est conditionné par l'acquisition d'un échographe Aixplorer (Supersonic Imagine, Aix-en-Provence, France ; 140 000 euros) doté de la technologie Supersonic Shear Imaging (SSI). Dans cette optique, une demande de financement a été déposée à la région Pays de la Loire (juillet 2009 ; 70 000 euros) et deux autres le seront prochainement à l'Association Française contre les Myopathies (AFM, octobre 2009 ; 50 000 euros) et l'Agence Nationale pour la Recherche (ANR, programme jeune chercheur , novembre 2009; 70 0000 euros).

Une collaboration avec l'équipe « plasticité des systèmes nerveux et musculaire » de l'Institut des Sciences du mouvement Humain – UMR 6233 (Université de Aix-Marseille, Drs Patrick DECHERCHI et Tanguy MARQUESTE) est envisagée.

Si les demandes de financement effectuées nous permettent de faire l'acquisition de l'échographe, nous prévoyons le recrutement d'un étudiant en thèse à court terme.

4.3.2. Transmission de la force, délai électromécanique.

Pour être totalement exhaustif dans le lien entre l'activité myoélectrique et le couple de force habituellement mesurée au niveau d'une articulation, il est important, au-delà de l'estimation de la force produite au niveau d'un muscle de pouvoir étudier sa transmission.

Ce projet de recherche s'inscrit dans la continuité de l'étude déjà réalisée (Nordez *et al.*, 2009b) dans le cadre du contrat de recherche avec l'Association Française contre les Myopathies (AFM ; contrat n°14084). Il s'agissait de quantifier, au cours de contractions musculaires évoquées par myostimulation, la part des différentes structures (e.g., tendon, aponévrose) et mécanismes (e.g., couplage excitation-contraction) impliqués dans le délai électromécanique (cf. chapitre 3.4). Ce travail a permis de valider une méthodologie qui présente

des perspectives de recherche intéressantes pour l'étude de la transmission de la force musculaire au squelette, classiquement attribuée aux propriétés mécaniques des structures de la composante élastique série. Outre l'intérêt « fondamental », cet axe de recherche est particulièrement intéressant puisque la méthodologie non-invasive développée pourrait permettre à terme de suivre l'état clinique de patients atteints de myopathies comme les dystrophies. En effet, de nombreuses études ont montré des modifications importantes de la raideur musculaire (Cornu *et al.*, 1998, 2001) ou du couplage E-C (De Luca *et al.*, 2001) chez ces patients. Ainsi, la méthode proposée devrait représenter un moyen pertinent d'évaluation des effets d'une pathologie, de suivi de son évolution, ainsi que de suivi longitudinal des effets de protocoles de réhabilitation ou de thérapies.

Dans un premier temps, il pourrait être intéressant d'appliquer la méthodologie précédemment décrite (Nordez *et al.*, 2009b) à une contraction musculaire volontaire. En effet, cette modalité de contraction est connue pour induire un délai électromécanique plus élevé (22,8 ± 8,2 ms lors d'une flexion plantaire pour Hopkins *et al*., 2007) que celui obtenu lors d'une contraction musculaire évoquée électriquement (11,6 ± 1,3 ms lors d'une flexion plantaire pour Nordez *et al*., 2009b). Certains auteurs ont tenté d'expliquer cette différence par les modalités différentes de recrutement des unités motrices (Hopkins *et al.*, 2007), sans que cette hypothèse n'ait pu être vérifiée. En effet, lors d'une contraction volontaire, l'ordre de recrutement des différents types d'unités motrices répond au principe de taille de Henneman[16] ce qui n'est plus le cas lors d'une contraction évoquée électriquement. Dans cette modalité toutes les unités motrices sont recrutées simultanément. Sachant que la vitesse de raccourcissement est plus élevée pour les fibres musculaires rapides que pour les fibres musculaires lentes, on peut alors supposer que le recrutement d'unités motrices rapides dès le début de la contraction explique le délai électromécanique plus court généralement relevé lors d'une contraction induite électriquement. Si la modalité de recrutement des unités motrices est la cause de cette différence de délai entre ces deux modes de contractions, ceci devrait pouvoir être observé *via* l'échographie ultrarapide par une modification du délai entre le début d'activité électrique et le début de mouvement des fascicules musculaires. Nous envisageons donc de déterminer le début de mouvement des fascicules musculaires et de l'insertion myotendineuse sur le *Biceps brachial* et de déterminer ainsi, à l'instar de ce qui a été fait dans la précédente étude, la part des différentes structures (e.g., tendon, aponévrose) et mécanismes (e.g., couplage excitation-contraction) impliqués dans le délai électromécanique. Une précaution devra être prise afin de ne pas modifier de délai-électromécanique artificiellement. En effet, nous avons montré (Nordez *et al.*, 2009b) que le début de mouvement des fascicules musculaires et de l'insertion myotendineuse est dû à la production de force des fibres musculaires recrutées en premier, i.e., celles situées à proximité du point moteur. De ce fait, le placement des électrodes de recueil de l'activité EMG peut réduire artificiellement le délai électromécanique si elles sont situées à distance du point moteur (e.g., considérant une vitesse de propagation de 4 m/s, le potentiel d'action musculaire parcourt 2 cm en 5 ms). Pour cette étude, nous proposons donc d'utiliser un vecteur d'électrode EMG (8 électrodes – distance inter-électrodes = 5 mm) centré sur le point moteur, ce qui nous permettra de déterminer précisément le temps correspondant à l'apparition du potentiel d'action musculaire.

[16] Lors d'une contraction musculaire volontaire les petites unités motrices sont recrutées avant les grandes.

Dans un deuxième temps, nous nous proposons d'utiliser l'échographie ultrarapide pour étudier certains facteurs susceptibles de modifier le délai électromécanique, dont la fatigue musculaire. En effet, certains travaux rapportent une augmentation du délai électromécanique après un exercice fatigant (Zhou *et al.*, 1995; Pääsuke *et al.*, 1999; Kubo *et al.*, 2001). Cependant, la méthodologie employée dans ces études ne permet pas de déterminer les structures ou mécanismes impliqués dans cette augmentation. Alors que certaines suggèrent une augmentation de la durée du couplage excitation-contraction (Zhou *et al.*, 1995; Pääsuke *et al.*, 1999), d'autres expliquent cette augmentation par une modification des propriétés mécaniques de la composante élastique série (Kubo *et al.*, 2001). En effet, certains travaux ont mis en évidence une modification des propriétés mécaniques du muscle (Nordez *et al.*, 2009c), de l'ensemble tendon-aponévrose (Mademli et Arampatzis, 2005) et du tendon (Kubo *et al.*, 2001) au cours d'une contraction fatigante. Nous envisageons donc de déterminer le début de mouvement des fascicules musculaires et de l'insertion myotendineuse en réponse à une stimulation électrique du muscle (et/ou d'une contraction volontaire si les résultats de l'étude présentée précédemment sont concluants) avant et après un exercice mené jusqu'à épuisement (e.g., à 40 % de la contraction maximale volontaire). Ce protocole permettrait de déterminer directement le rôle de la fraction passive de la CES (i.e., tendon et aponévrose) dans l'augmentation possible du délai électromécanique observée suite à un exercice fatigant.

Pour ces études, nous envisageons de poser un accéléromètre (i.e., enregistrement de l'activité mécanomyographique, MMG) sur le muscle pour comparer le début de mouvement des fascicules musculaires déterminé par les enregistrements échographiques et le début de l'activité MMG à la surface du muscle. Si ces valeurs sont proches et/ou évoluent de la même manière en fonction des contraintes imposées au système neuromusculaire, nous disposerons alors d'un moyen simple et peu onéreux de séparer la contribution de la composante passive de la CES du reste des structures (i.e., composante active de la CES) et mécanismes (i.e., couplage excitation-contraction ; transmission synaptique). Nous pourrions alors envisager le développement d'un outil simple et peu onéreux combinant des électrodes EMG et un accéléromètre.

Faisabilité : L'étude du délai électromécanique est actuellement poursuivie dans le cadre d'une collaboration avec le laboratoire de Géophysique Interne et Tectonophysique (Université de Grenoble, Dr Stefan CATEHLINE).

Conclusion

Ces projets de recherche ont pour vocation de compléter les travaux déjà développés et présentés dans le chapitre 3 de ce mémoire d'Habilitation à Diriger des Recherches. Mais au-delà, ils s'inscrivent dans une démarche d'amélioration des connaissances fondamentales et de transfert vers le milieu médical et sportif (i.e.,évaluation de la fonction neuromusculaire, optimisation de la performance).

L'apport d'une nouvelle technique de recueil de l'activité EMG (utilisation de matrices et/ou vecteurs d'électrodes) et d'une nouvelle méthodologie de traitement des signaux EMG (identification des synergies musculaires) nous permettra de compléter les travaux portant sur les coordinations musculaires. Parmi ces travaux, la quantification des différences interindividuelles m'intéresse tout particulièrement car elle me paraît être un préambule à la question de l'amélioration de la technique de pédalage. En effet, cette dernière ne pourra être abordée que lorsque nous auront identifié précisément les techniques individuelles et leur relation avec la performance.

L'utilisation d'un amplificateur EMG multicanaux (i.e., matrices et ou vecteurs d'électrodes) devrait également nous permettre de revisiter le concept de seuil électromyographique de la fatigue qui nous paraît potentiellement intéressant pour l'évaluation de la fonction neuromusculaire chez des patients ne pouvant pas réaliser un exercice fatigant (e.g., myopathes). Cette évaluation pourrait être, à terme, complétée par l'évaluation du délai électromécanique par l'imagerie échographique ultrarapide telle que présentée dans le troisième axe de recherche de ce chapitre.

Outre l'étude du délai électromécanique, le troisième axe de recherche intègre la thématique de l'estimation de la force musculaire, de loin la plus porteuse à mes yeux. En effet, la technique SSI présentée précédemment semble particulièrement prometteuse. L'estimation de la force musculaire a pour vocation de répondre à certaines interrogations posées par les travaux déjà réalisés en complétant les informations fournies par l'électromyographie de surface. Mais au-delà, la capacité d'estimer la force musculaire permettrait d'envisager de nombreux travaux dans le domaine de la physiologie neuromusculaire et la biomécanique.

Bibliographie

Basmajian JV, De Luca CJ. 1985. Muscle alive (electromyography). Baltimore: Williams & Wilkins.
Beau JHS, Maissiat JH. 1843. Recherches sur le mécanisme des mouvements respiratoires (deuxième article). Archives Générales de Médecine:265-295.
Bercoff J, Tanter M, Fink M. 2004. Supersonic shear imaging: a new technique for soft tissue elasticity mapping. IEEE Trans Ultrason Ferroelectr Freq Control 51:396-409.
Bernstein N. 1967. Coordination and regulation of movements. pergamon press.
Bigland-Ritchie B, Woods JJ. 1974. Integrated EMG and oxugen uptake during dynamic contractions of human muscles. J Appl Physiol 36:475-479.
Bizzi E, Cheung VC, d'Avella A, Saltiel P, Tresch M. 2008. Combining modules for movement. Brain Res Rev 57:125-133.
Bouisset S, Maton B. 1995. Muscles, posture et mouvement. In: Hermann, editor. p 292-314.
Brochard L, Harf A, Lorino H, Lemaire F. 1989. Inspiratory pressure support prevents diaphragmatic fatigue during weaning from mechanical ventilation. Am Rev Respir Dis 139:513-521.
Buchanan TS, Lloyd DG, Manal K, Besier TF. 2004. Neuromusculoskeletal modeling: estimation of muscle forces and joint moments and movements from measurements of neural command. J Appl Biomech 20:367-395.
Campanini I, Merlo A, Degola P, Merletti R, Vezzosi G, Farina D. 2007. Effect of electrode location on EMG signal envelope in leg muscles during gait. J Electromyogr Kinesiol 17:515-526.
Capelli C, Rosa G, Butti F, Ferretti G, Veicsteinas A, di Prampero PE. 1993. Energy cost and efficiency of riding aerodynamic bicycles. Eur J Appl Physiol Occup Physiol 67:144-149.
Cappellini G, Ivanenko YP, Poppele RE, Lacquaniti F. 2006. Motor patterns in human walking and running. J Neurophysiol 95:3426-3437.
Cavanagh PR, Komi PV. 1979. Electromechanical delay in human skeletal muscle under concentric and eccentric contractions. Eur J Appl Physiol Occup Physiol 42:159-163.
Chanaud CM, Pratt CA, Loeb GE. 1991. Functionally complex muscles of the cat hindlimb. V. The roles of histochemical fiber-type regionalization and mechanical heterogeneity in differential muscle activation. Exp Brain Res 85:300-313.
Chao EYS, An KN, Cooner WP, Linscheid RL. 1989. In: Biomechanis of hand. Singapore: World scientific. p 31-51.
Chen HY, Liau JJ, Wang CL, Lai HJ, Jan MH. 2009. A novel method for measuring electromechanical delay of the vastus medialis obliquus and vastus lateralis. Ultrasound Med Biol 35:14-20.
Cheung VC, d'Avella A, Tresch MC, Bizzi E. 2005. Central and sensory contributions to the activation and organization of muscle synergies during natural motor behaviors. J Neurosci 25:6419-6434.
Chiti L, Biondi G, Morelot-Panzini C, Raux M, Similowski T, Hug F. 2008. Scalene muscle activity during progressive inspiratory loading under pressure support ventilation in normal humans. Respir Physiol Neurobiol 164:441-448.
Cobb S, Forbes A. 1923. Electromyographic studies of muscular fatigue in man. Am J Phys 65:234-251.
Cornu C, Goubel F, Fardeau M. 1998. Stiffness of knee extensors in Duchenne muscular dystrophy. Muscle Nerve 21:1772-1774.
Cornu C, Goubel F, Fardeau M. 2001. Muscle and joint elastic properties during elbow flexion in Duchenne muscular dystrophy. J Physiol 533:605-616.
Davenport WB, Root WL. 1958. An introduction to the theory of random signals and noise. New York: McGraw.
Davis J, Kaufman KR, Lieber RL. 2003. Correlation between active and passive isometric force and intramuscular pressure in the isolated rabbit tibialis anterior muscle. J Biomech 36:505-512.
De Luca A. 1979. Physiology and mathematics of myoelectric signals. IEEE Trans Biomed Eng 26:313-325.
De Luca A, Pierno S, Liantonio A, Cetrone M, Camerino C, Simonetti S, Papadia F, Camerino DC. 2001. Alteration of excitation-contraction coupling mechanism in extensor digitorum longus muscle fibres of dystrophic mdx mouse and potential efficacy of taurine. Br J Pharmacol 132:1047-1054.
De Luca CJ. 1984. Myoelectrical manifestations of localized muscular fatigue in humans. Crit Rev Biomed Eng 11:251-279.
De Troyer A, Estenne M. 1984. Coordination between rib cage muscles and diaphragm during quiet breathing in humans. J Appl Physiol 57:899-906.
De Troyer A, Peche R, Yernault JC, Estenne M. 1994. Neck muscle activity in patients with severe chronic obstructive pulmonary disease. Am J Respir Crit Care Med 150:41-47.
Dedering A, Roos af Hjelmsater M, Elfving B, Harms-Ringdahl K, Nemeth G. 2000. Between-days reliability of subjective and objective assessments of back extensor muscle fatigue in subjects without lower-back pain. J Electromyogr Kinesiol 10:151-158.
Deffieux T, Gennisson JL, Nordez A, Tanter M, Fink M. 2006. Ultrafast imaging of in vivo muscle contraction using ultrasound. Appl Phys Let 89:184107-184111.
Deffieux T, Gennisson JL, Tanter M, Fink M. 2008. Assessment of the mechanical properties of the musculoskeletal system using 2-D and 3-D very high frame rate ultrasound. IEEE Trans Ultrason Ferroelectr Freq Control 55:2177-2190.
deVries HA, Moritani T, Nagata A, Magnussen K. 1982. The relation between critical power and neuromuscular fatigue as estimated from electromyographic data. Ergonomics 25:783-791.
Dolan P, Mannion AF, Adams MA. 1995. Fatigue of the erector spinae muscles. A quantitative assessment using "frequency banding" of the surface electromyography signal. Spine (Phila Pa 1976) 20:149-159.

Dorel S, Couturier A, Hug F. 2008. Intra-session repeatability of lower limb muscles activation pattern during pedaling. J Electromyogr Kinesiol 18:857-865.
Dorel S, Drouet JM, Couturier A, Champoux Y, Hug F. 2009. Changes of pedaling technique and muscle coordination during and exhaustive exercise. Med Sci Sports Exerc 41:1277-1286.
Dresner MA, Rose GH, Rossman PJ, Muthupillai R, Manduca A, Ehman RL. 2001. Magnetic resonance elastography of skeletal muscle. J Magn Reson Imaging 13:269-276.
Drouet JM, Champoux Y, Dorel S. 2008. Development of multi-patform instrumented force pedals for track cycling. The engineering of sport 7:49-51.
Duc S, Bertucci W, Pernin JN, Grappe F. 2006. Muscular activity during uphill cycling: Effect of slope, posture, hand grip position and constrained bicycle lateral sways. J Electromyogr Kinesiol.
Erdemir A, McLean S, Herzog W, van den Bogert AJ. 2007. Model-based estimation of muscle forces exerted during movements. Clin Biomech (Bristol, Avon) 22:131-154.
Ericson M. 1986. On the biomechanics of cycling. A study of joint and muscle load during exercise on the bicycle ergometer. Scand J Rehabil Med Suppl 16:1-43.
Falla D, Dall'Alba P, Rainoldi A, Merletti R, Jull G. 2002. Repeatability of surface EMG variables in the sternocleidomastoid and anterior scalene muscles. Eur J Appl Physiol 87:542-549.
Farina D, Leclerc F, Arendt-Nielsen L, Buttelli O, Madeleine P. 2008. The change in spatial distribution of upper trapezius muscle activity is correlated to contraction duration. J Electromyogr Kinesiol 18:16-25.
Farina D, Merletti R, Enoka RM. 2004. The extraction of neural strategies from the surface EMG. J Appl Physiol 96:1486-1495.
Friden J, Lieber RL, Thornell LE. 1991. Subtle indications of muscle damage following eccentric contractions. Acta Physiol Scand 142:523-524.
Gamet D, Duchene J, Goubel F. 1996. Reproducibility of kinetics of electromyogram spectrum parameters during dynamic exercise. Eur J Appl Physiol Occup Physiol 74:504-510.
Gandevia SC. 2001. Spinal and supraspinal factors in human muscle fatigue. Physiol Rev 81:1725-1789.
Garland SJ, Enoka RM, Serrano LP, Robinson GA. 1994. Behavior of motor units in human biceps brachii during a submaximal fatiguing contraction. J Appl Physiol 76:2411-2419.
Garland SJ, Griffin L, Ivanova T. 1997. Motor unit discharge rate is not associated with muscle relaxation time in sustained submaximal contractions in humans. Neurosci Lett 239:25-28.
Gnehm P, Reichenbach S, Altpeter E, Widmer H, Hoppeler H. 1997. Influence of different racing positions on metabolic cost in elite cyclists. Med Sci Sports Exerc 29:818-823.
Graef JL, Smith AE, Kendall KL, Walter AA, Moon JR, Lockwood CM, Beck TW, Cramer JT, Stout JR. 2008. The relationships among endurance performance measures as estimated from VO2PEAK, ventilatory threshold, and electromyographic fatigue threshold: a relationship design. Dyn Med 7:15.
Granata KP, Ikeda AJ, Abel MF. 2000. Electromechanical delay and reflex response in spastic cerebral palsy. Arch Phys Med Rehabil 81:888-894.
Gregor RJ, Broker JP, Ryan MM. 1991. The biomechanics of cycling. Exerc Sport Sci Rev 19:127-169.
Gregor RJ, Cavanagh PR, LaFortune M. 1985. Knee flexor moments during propulsion in cycling--a creative solution to Lombard's Paradox. J Biomech 18:307-316.
Grosset JF, Piscione J, Lambertz D, Perot C. 2009. Paired changes in electromechanical delay and musculo-tendinous stiffness after endurance or plyometric training. Eur J Appl Physiol 105:131-139.
Hendrix CR, Housh TJ, Johnson GO, Mielke M, Camic CL, Zuniga JM, Schmidt RJ. 2009a. Comparison of critical force to EMG fatigue thresholds during isometric leg extension. Med Sci Sports Exerc 41:956-964.
Hendrix CR, Housh TJ, Johnson GO, Weir JP, Beck TW, Malek MH, Mielke M, Schmidt RJ. 2009b. A comparison of critical force and electromyographic fatigue threshold for isometric muscle actions of the forearm flexors. Eur J Appl Physiol 105:333-342.
Hettinga FJ, De Koning JJ, Broersen FT, Van Geffen P, Foster C. 2006. Pacing strategy and the occurrence of fatigue in 4000-m cycling time trials. Med Sci Sports Exerc 38:1484-1491.
Hoffer JA, Sugano N, Loeb GE, Marks WB, O'Donovan MJ, Pratt CA. 1987. Cat hindlimb motoneurons during locomotion. II. Normal activity patterns. J Neurophysiol 57:530-553.
Hopkins JT, Feland JB, Hunter I. 2007. A comparison of voluntary and involuntary measures of electromechanical delay. Int J Neurosci 117:597-604.
Housh TJ, deVries HA, Johnson GO, Housh DJ, Evans SA, Stout JR, Evetovich TK, Bradway RM. 1995. Electromyographic fatigue thresholds of the superficial muscles of the quadriceps femoris. Eur J Appl Physiol Occup Physiol 71:131-136.
Housh TJ, Perry SR, Bull AJ, Johnson GO, Ebersole KT, Housh DJ, deVries HA. 2000. Mechanomyographic and electromyographic responses during submaximal cycle ergometry. Eur J Appl Physiol 83:381-387.
Houtz SJ, Fischer FJ. 1959. An analysis of muscle action and joint excursion during exercise on a stationary bicycle. J Bone Joint Surg Am 41-A:123-131.

Hug F, Bendahan D, Le Fur Y, Cozzone PJ, Grelot L. 2004a. Heterogeneity of muscle recruitment pattern during pedaling in professional road cyclists: a magnetic resonance imaging and electromyography study. Eur J Appl Physiol 92:334-342.

Hug F, Dorel S. 2009. Electromyographic analysis of pedaling: A review. J Electromyogr Kinesiol 19:182-198.

Hug F, Drouet JM, Champoux Y, Couturier A, Dorel S. 2008a. Interindividual variability of electromyographic patterns and pedal force profiles in trained cyclists. Eur J Appl Physiol 104:667-678.

Hug F, Faucher M, Kipson N, Jammes Y. 2003a. EMG signs of neuromuscular fatigue related to the ventilatory threshold during cycling exercise. Clin Physiol Funct Imaging 23:208-214.

Hug F, Faucher M, Marqueste T, Guillot C, Kipson N, Jammes Y. 2004b. Electromyographic signs of neuromuscular fatigue are concomitant with further increase in ventilation during static handgrip. Clin Physiol Funct Imaging 24:25-32.

Hug F, Laplaud D, Lucia A, Grelot L. 2006a. A comparison of visual and mathematical detection of the electromyographic threshold during incremental pedaling exercise: a pilot study. J Strength Cond Res 20:704-708.

Hug F, Laplaud D, Lucia A, Grelot L. 2006b. EMG threshold determination in eight lower limb muscles during cycling exercise: a pilot study. Int J Sports Med 27:456-462.

Hug F, Laplaud D, Savin B, Grelot L. 2003b. Occurrence of electromyographic and ventilatory thresholds in professional road cyclists. Eur J Appl Physiol 90:643-646.

Hug F, Nordez A, Guevel A. 2009. Can the electromyographic fatigue threshold be determined from superficial elbow flexor muscles during an isometric single-joint task? Eur J Appl Physiol.

Hug F, Raux M, Prella M, Morelot-Panzini C, Straus C, Similowski T. 2006c. Optimized analysis of surface electromyograms of the scalenes during quiet breathing in humans. Respir Physiol Neurobiol 150:75-81.

Hull ML, Butler P. 1981. Analysis of quadriceps loading in bicycle. In: engineers Asom, editor. Biomechanics symposium. New York. p 263-266.

Hull ML, Jorge M. 1985. A method for biomechanical analysis of bicycle pedalling. J Biomech 18:631-644.

Hunter SK, Critchlow A, Shin IS, Enoka RM. 2004. Fatigability of the elbow flexor muscles for a sustained submaximal contraction is similar in men and women matched for strength. J Appl Physiol 96:195-202.

Ivanenko YP, Poppele RE, Lacquaniti F. 2004. Five basic muscle activation patterns account for muscle activity during human locomotion. J Physiol 556:267-282.

Jensen C, Vasseljen O, Westgaard RH. 1993. The influence of electrode position on bipolar surface electromyogram recordings of the upper trapezius muscle. Eur J Appl Physiol Occup Physiol 67:266-273.

Jorge M, Hull ML. 1986. Analysis of EMG measurements during bicycle pedalling. J Biomech 19:683-694.

Katz B, Miledi R. 1965. The Measurement of Synaptic Delay, and the Time Course of Acetylcholine Release at the Neuromuscular Junction. Proc R Soc Lond B Biol Sci 161:483-495.

Keenan KG, Farina D, Maluf KS, Merletti R, Enoka RM. 2005. Influence of amplitude cancellation on the simulated surface electromyogram. J Appl Physiol 98:120-131.

Kleine BU, Schumann NP, Stegeman DF, Scholle HC. 2000. Surface EMG mapping of the human trapezius muscle: the topography of monopolar and bipolar surface EMG amplitude and spectrum parameters at varied forces and in fatigue. Clin Neurophysiol 111:686-693.

Korff T, Romer LM, Mayhew I, Martin JC. 2007. Effect of pedaling technique on mechanical effectiveness and efficiency in cyclists. Med Sci Sports Exerc 39:991-995.

Kouzaki M, Shinohara M, Masani K, Kanehisa H, Fukunaga T. 2002. Alternate muscle activity observed between knee extensor synergists during low-level sustained contractions. J Appl Physiol 93:675-684.

Kubo K, Kanehisa H, Kawakami Y, Fukunaga T. 2001. Effects of repeated muscle contractions on the tendon structures in humans. Eur J Appl Physiol 84:162-166.

LaFortune MA, Cavanagh PR. 1983. Effectivenes and efficiency during cycling riding. In: Biomechanics VIII-B: international series on biomechanics. Human Kinetics. p 928-936.

Laplaud D, Hug F, Grelot L. 2006. Reproducibility of eight lower limb muscles activity level in the course of an incremental pedaling exercise. J Electromyogr Kinesiol 16:158-166.

Lariviere C, Arsenault AB, Gravel D, Gagnon D, Loisel P, Vadeboncoeur R. 2002. Electromyographic assessment of back muscle weakness and muscle composition: reliability and validity issues. Arch Phys Med Rehabil 83:1206-1214.

Larsson B, Karlsson S, Eriksson M, Gerdle B. 2003. Test-retest reliability of EMG and peak torque during repetitive maximum concentric knee extensions. J Electromyogr Kinesiol 13:281-287.

Larsson B, Mansson B, Karlberg C, Syvertsson P, Elert J, Gerdle B. 1999. Reproducibility of surface EMG variables and peak torque during three sets of ten dynamic contractions. J Electromyogr Kinesiol 9:351-357.

Lepers R, Millet GY, Maffiuletti NA. 2001. Effect of cycling cadence on contractile and neural properties of knee extensors. Med Sci Sports Exerc 33:1882-1888.

Li L, Caldwell GE. 1998. Muscle coordination in cycling: effect of surface incline and posture. J Appl Physiol 85:927-934.

Li L, Caldwell GE. 1999. Coefficient of cross correlation and the time domain correspondence. J Electromyogr Kinesiol 9:385-389.

Lucia A, Hoyos J, Pardo J, Chicharro JL. 2000. Metabolic and neuromuscular adaptations to endurance training in professional cyclists: a longitudinal study. Jpn J Physiol 50:381-388.

Lucia A, San Juan AF, Montilla M, CaNete S, Santalla A, Earnest C, Pérez M. 2004. In professional road cyclists, low pedaling cadences are less efficient. Med Sci Sports Exerc 36:1048-1054.

Lucia A, Vaquero AF, Perez M, Sanchez O, Sanchez V, Gomez MA, Chicharro JL. 1997. Electromyographic response to exercise in cardiac transplant patients: a new method for anaerobic threshold determination? Chest 111.

Mademli L, Arampatzis A. 2005. Behaviour of the human gastrocnemius muscle architecture during submaximal isometric fatigue. Eur J Appl Physiol 94:611-617.

Magnusson SP, Narici MV, Maganaris CN, Kjaer M. 2008. Human tendon behaviour and adaptation, in vivo. J Physiol 586:71-81.

Maisetti O, Guevel A, Legros P, Hogrel JY. 2002. Prediction of endurance capacity of quadriceps muscles in humans using surface electromyogram spectrum analysis during submaximal voluntary isometric contractions. Eur J Appl Physiol 87:509-519.

Mannion AF, Dolan P. 1994. Electromyographic median frequency changes during isometric contraction of the back extensors to fatigue. Spine (Phila Pa 1976) 19:1223-1229.

Matsumoto T, Ito K, Moritani T. 1991. The relationship between anaerobic threshold and electromyographic fatigue threshold in college women. Eur J Appl Physiol Occup Physiol 63:1-5.

Merletti R, Lo Conte L, Orizio C. 1991. Indices of muscle fatigue. J Electromyogr Kinesiol 1:20-33.

Merletti R, Roy S. 1996. Myoelectric and mechanical manifestations of muscle fatigue in voluntary contractions. J Orthop Sports Phys Ther 24:342-353.

Morimoto S, Takemori S. 2007. Initial mechanomyographical signals from twitching fibres of human skeletal muscle. Acta Physiol (Oxf) 191:319-327.

Moritani T, Takaishi T, Matsumoto T. 1993. Determination of maximal power output at neuromuscular fatigue threshold. J Appl Physiol 74:1729-1734.

Mornieux G, Stapelfeldt B, Gollhofer A, Belli A. 2008. Effects of pedal type and pull-up action during cycling. Int J Sports Med 29:817-822.

Muraoka T, Muramatsu T, Fukunaga T, Kanehisa H. 2004. Influence of tendon slack on electromechanical delay in the human medial gastrocnemius in vivo. J Appl Physiol 96:540-544.

Neptune RR, Clark DJ, Kautz SA. 2009. Modular control of human walking: a simulation study. J Biomech 42:1282-1287.

Neptune RR, Kautz SA, Hull ML. 1997. The effect of pedaling rate on coordination in cycling. J Biomech 30:1051-1058.

Nordez A, Catheline S, Hug F. 2009a. Re: A novel method for measuring electromechanical delay on the vastus medialis obliquus and vastus lateralis. Ultrasound Med Biol 35:878; author reply 879.

Nordez A, Gallot T, Catheline S, Guevel A, Cornu C, Hug F. 2009b. Electromechanical delay revisited using very high frame rate ultrasound. J Appl Physiol 106:1970-1975.

Nordez A, Gennisson JL, Casari P, Catheline S, Cornu C. 2008. Characterization of muscle belly elastic properties during passive stretching using transient elastography. J Biomech 41:2305-2311.

Nordez A, Guevel A, Casari P, Catheline S, Cornu C. 2009c. Assessment of muscle hardness changes induced by a submaximal fatiguing isometric contraction. J Electromyogr Kinesiol 19:484-491.

Norman RW, Komi PV. 1979. Electromechanical delay in skeletal muscle under normal movement conditions. Acta Physiol Scand 106:241-248.

Origenes MMt, Blank SE, Schoene RB. 1993. Exercise ventilatory response to upright and aero-posture cycling. Med Sci Sports Exerc 25:608-612.

Orizio C, Esposito F, Sansone V, Parrinello G, Meola G, Veicsteinas A. 1997. Muscle surface mechanical and electrical activities in myotonic dystrophy. Electromyogr Clin Neurophysiol 37:231-239.

Paasuke M, Ereline J, Gapeyeva H. 1999. Neuromuscular fatigue during repeated exhaustive submaximal static contractions of knee extensor muscles in endurance-trained, power-trained and untrained men. Acta Physiol Scand 166:319-326.

Pääsuke M, Ereline J, Gapeyeva H. 1999. Neuromuscular fatigue during repeated exhaustive submaximal static contractions of knee extensor muscles in endurance-trained, power-trained and untrained men. Acta Physiol Scand 166:319-326.

Pardee NE, Winterbauer RH, Allen JD. 1984. Bedside evaluation of respiratory distress. Chest 85:203-206.

Petrofsky JS. 1979. Frequency and amplitude analysis of the EMG during exercise on the bicycle ergometer. Eur J Appl Physiol Occup Physiol 41:1-15.

Pulkovski N, Schenk P, Maffiuletti NA, Mannion AF. 2008. Tissue Doppler imaging for detecting onset of muscle activity. Muscle Nerve 37:638-649.

Raasch CC, Zajac FE. 1999. Locomotor strategy for pedaling: muscle groups and biochemical functions. J Neurophysiol 82:515)525.

Rainoldi A, Galardi G, Maderna L, Comi G, Lo Conte L, Merletti R. 1999. Repeatability of surface EMG variables during voluntary isometric contractions of the biceps brachii muscle. J Electromyogr Kinesiol 9:105-119.

Raper AJ, Thompson WT, Jr., Shapiro W, Patterson JL, Jr. 1966. Scalene and sternomastoid muscle function. J Appl Physiol 21:497-502.

Ryan MM, Gregor RJ. 1992. EMG profiles of lower extremity muscles during cycling at constant workload and cadence. J Electromyogr Kinesiol 2:69-80.

Sanderson DJ. 1991. The influence of cadence and power output on the biomechanics of force application during steady-rate cycling in competitive and recreational cyclists. J Sports Sci 9:191-203.
Sanderson DJ, Black A. 2003. The effect of prolonged cycling on pedal forces. J Sports Sci 21:191-199.
Sandow A. 1952. Excitation-contraction coupling in muscular response. Yale J Biol Med 25:176-201.
Sassoon CS, Foster GT. 2001. Patient-ventilator asynchrony. Curr Opin Crit Care 7:28-33.
Smith AE, Walter AA, Herda TJ, Ryan ED, Moon JR, Cramer JT, Stout JR. 2007. Effects of creatine loading on electromyographic fatigue threshold during cycle ergometry in college-aged women. J Int Soc Sports Nutr 4:20.
Straus C, Similowski T, Zelter M, Derenne JP. 1998. Mécanismes et diagnostic des dyspnées. In: Encyclop. Med. Chir. Paris: Elsevier. p 6-090-E-015.
Taylor AD, Bronks R. 1994. Electromyographic correlates of the transition from aerobic to anaerobic metabolism in treadmill running. Eur J Appl Physiol Occup Physiol 69:508-515.
Ting LH, McKay JL. 2007. Neuromechanics of muscle synergies for posture and movement. Curr Opin Neurobiol 17:622-628.
Tobin MJ, Jubran A, Laghi F. 2001. Patient-ventilator interaction. Am J Respir Crit Care Med 163:1059-1063.
van Bolhuis BM, Gielen CC. 1999. A comparison of models explaining muscle activation patterns for isometric contractions. Biol Cybern 81:249-261.
van Ingen Schenau GJ, Boots PJM, de Groots G, Snackers RJ, van Woensel WWLM. 1992. The constrained control of force and position in multi-joint movements. Neuroscience 46:197-207.
van Soest AJ, Schwab AL, Bobbert MF, van Ingen Schenau GJ. 1993. The influence of the biarticularity of the gastrocnemius muscle on vertical-jumping achievement. J Biomech 26:1-8.
Wakeling JM. 2009. The recruitment of different compartments within a muscle depends on the mechanics of the movement. Biol Lett 5:30-34.
Wren TA, Patrick Do K, Rethlefsen SA, Healy B. 2006. Cross-correlation as a method for comparing dynamic electromyography signals during gait. J Biomech 39:2714-2718.
Zajac FE. 1989. Muscle and tendon: properties, models scaling, and application to biomechanics and motor control. Crit Rev Biomed Eng 17:359-411.
Zhou S, Lawson DL, Morrison WE, Fairweather I. 1995. Electromechanical delay in isometric muscle contractions evoked by voluntary, reflex and electrical stimulation. Eur J Appl Physiol Occup Physiol 70:138-145.
Zijdewind I, Kernell D, Kukulka CG. 1995. Spatial differences in fatigue-associated electromyographic behaviour of the human first dorsal interosseus muscle. J Physiol 483:499-509.

Annexes

Électromyographie et analyse des coordinations musculaires

Hug, F., Dorel, S.
Electromyographic analysis of pedaling: a review. *Journal Electromyography and Kinesiology*. 2009. 19(2) : 182-198.

Laplaud, D., Hug, F., Grélot, L.
Reproducibility of eight lower limb muscles activity level in the course of an incremental pedalling exercise. *Journal of Electromyography and Kinesiology*. 2006. 16(2):158-166.

Dorel, S., Couturier, A., Hug, F.
Intra-session repeatability of lower limb muscles activation pattern during pedaling. *Journal of Electromyography and Kinesiology*. 2008. 18(5) : 857-865.

Hug, F., Drouet, JM., Champoux, Y., Couturier, A., Dorel, S.
Inter-individual variability of EMG patterns and pedal force profiles in trained cyclists. *European Journal of Applied Physiology* 2008. 104(4) : 667-678.

Dorel, S., Drouet, JM., Champoux, Y., Couturier, A., Hug, F.
Changes of pedaling technique and muscle coordination during an exhaustive exercise. *Medecine & Science in Sports & Exercise.* 2009. 41(6) : 1277-1286.

Dorel, S., Couturier, A., Hug, F.
Influence of different racing positions on mechanical and electromyographic patterns during pedaling. *Scandinavian Journal of Medicine & Science in Sports*. 2009. 19 : 44-54.

Électromyographie et détection d'une charge mécanique imposée au système respiratoire

Hug, F., Raux, M., Prella, M., Morelot-Panzini, C., Straus, C., Similowski T.
Optimized analysis of surface electromyograms of the scalenes during quiet breathing in humans. *Respiratory Physiology and Neurobiology*. 2006. 25;150(1):75-81.

Chiti, L., Biondi, G., Morélot-Panzini, C., Raux, M., Similowski, T., Hug, F.
Scalene muscle activity during progressive inspiratory loading under pressure support ventilation on normal humans. *Respiratory Physiology and Neurobiology*. 2008. 164(3) : 440-447.

Électromyographie et évaluation de la fatigue neuromusculaire

Hug, F., Laplaud, D., Lucia, A., Grélot, L.
Comparison of visual and mathematical detection of the EMG threshold during incremental pedalling exercise. *Journal of Strength and Conditionning Research*. 2006. 20(3):704-708.

Hug, F., Laplaud, D., Lucia, A., Grélot, L.
EMG threshold determination in 8 lower limb muscles during cycling exercise: a pilot study. I*nternational Journal of Sports Medicine*. 2006. 27(6):456-462.

Hug, F., Nordez, A., Guével, A.
Can the electromyographic fatigue threshold be determined from superficial elbow flexor muscles during an isometric single-joint task ? *European Journal of Applied Physiology.* 2009. 107(2) : 193-201.

Caractérisation du délai électromécanique

Nordez, A., Catheline, S., Hug, F.
A novel method for measuring electromechanical delay on the vastus medialis obliquus and vastus lateralis. *Ultrasound in Medicine and Biology*. 2009. 35(5) : 172 – lettre à l'éditeur.

Nordez, A., Gallot, T., Catheline, S., Guevel, A., Cornu, C., Hug, F.
Electromechanical delay revisited using very high frame rate ultrasound. *Journal of Applied Physiology*. 2009. 106(6) : 1970-1975.

Available online at www.sciencedirect.com
ScienceDirect
Journal of Electromyography and Kinesiology 19 (2009) 182–198
JOURNAL OF ELECTROMYOGRAPHY AND KINESIOLOGY
www.elsevier.com/locate/jelekin

Review

Electromyographic analysis of pedaling: A review

François Hug [a,*], Sylvain Dorel [b]

[a] University of Nantes, Nantes Atlantic Universities, Laboratory "Motricity, Interactions, Performance" (JE 2438), F-44000 Nantes, France
[b] National Institute for Sports and Physical Education (INSEP), Laboratory of Biomechanics and Physiology, F-75012 Paris, France

Received 3 July 2007; received in revised form 30 October 2007; accepted 30 October 2007

Abstract

Although pedaling is constrained by the circular trajectory of the pedals, it is not a simple movement. This review attempts to provide an overview of the pedaling technique using an electromyographic (EMG) approach. Literature concerning the electromyographic analysis of pedaling is reviewed in an effort to make a synthesis of the available information, and to point out its relevance for researchers, clinicians and/or cycling/triathlon trainers. The first part of the review depicts methodological aspects of the EMG signal recording and processing. We show how the pattern of muscle activation during pedaling can be analyzed in terms of muscle activity level and muscle activation timing. Muscle activity level is generally quantified with root mean square or integrated EMG values. Muscle activation timing is studied by defining EMG signal onset and offset times that identify the duration of EMG bursts and, more recently, by the determination of a lag time maximizing the cross-correlation coefficient. In the second part of the review, we describe whether the patterns of the lower limb muscles activity are influenced by numerous factors affecting pedaling such as power output, pedaling rate, body position, shoe–pedal interface, training status and fatigue. Some research perspectives linked to pedaling performance are discussed throughout the manuscript and in the conclusion.

Keywords: Cycling; Rehabilitation; Electromyography; Activation; Pattern; Muscle; EMG

Contents

* Corresponding author. Address: University of Nantes, UFR STAPS, Laboratory "Motricity, Interactions, Performance", JE 2438, 25 bis boulevard Guy Mollet, BP 72206, 44322 Nantes cedex 3, France. Tel.: +33 (0)2 51 83 72 24; fax: +33 (0)2 51 83 72 10.
E-mail address: francois.hug@univ-nantes.fr (F. Hug).

1050-6411/$ - see front matter © 2007 Elsevier Ltd. All rights reserved.
doi:10.1016/j.jelekin.2007.10.010

1. Introduction

In 1817, Baron von Drais invented a walking machine that would help him get around the royal gardens faster. In 1855, the french engineers Michaux and Lallement added the pedals and by the beginning of the 20th century the general design of the bicycle was similar to that of today. Ever since, millions of bicycles are used daily for transportation, recreational or competitive cycling. Because stationary bicycles (cycle ergometers) allow controlled test conditions and easy measurements of numerous physiological variables (*e.g.* heart rate, respiratory gas exchanges, etc.), physiologists have developed different types of ergometers for testing physical fitness and performing applied physiology research. The first ergometers were described at the beginning of the 20th century (Krogh, 1913). They have been further developed and improved (Von Dobeln, 1954; Atkins and Nicholson, 1963) and have recently been made partially programmable (Torres et al., 1975; Giezendanner et al., 1983). These cycle ergometers are also used for prescribing exercise for patients with heart disease (Cooper and Hasson, 1970; Shafer, 1971), rheumatoid arthritis (Nordemar et al., 1976), cancer-related fatigue (Lucia et al., 2003) and Chronic Obstructive Pulmonary Disease (Busch and McClements, 1988), etc.

Unlike running or swimming, pedaling is more standardized since the bicycle constrains lower extremity movements. The activation pattern of lower limb muscles allows both the force production and its optimal orientation on the pedals. With a complete understanding of the "standard" muscle activation patterns, physiotherapists and cycling trainers can focus on a particular phase of the pedaling action to train a particular muscle group. Furthermore, it has been shown that specific patterns of muscle activation during a pedaling exercise can influence cardiovascular, plasma metabolite and endocrine responses both during and after exercise, even when the metabolic demand is held constant (Deschenes et al., 2000). Therefore, to improve rehabilitation protocols and cycling performance it is of primary importance to have a complete knowledge of the activation pattern of lower limb muscles during pedaling. The information required to understand the pedaling movement include identifying the lower limb muscles which are activated and precisely knowing their level/timing of activation. Associated to kinetic and kinematic analyses, it represents a means to elucidate the role of each of the muscles along the crank cycle. In addition, it is important to know how the coordination strategies adapt to various constraints such as power output, pedaling rate, body position, shoe–pedal interface, training status and fatigue.

Overall, this article attempts to provide an overview of the pedaling technique using an electromyographic approach. Literature concerning the electromyographic analysis of pedaling is reviewed in an effort to make a synthesis of the available information and to point out its relevance for researchers, clinicians and/or cycling/triathlon trainers. We first depict methodological aspects of the EMG signal recording and processing and then describe whether the patterns of the lower limb muscles activity are influenced by numerous constraints. Some research perspectives linked to pedaling performance are discussed throughout the manuscript and in the conclusion.

2. The use of electromyography

2.1. Detection and interpretation of EMG signals

For more than two centuries, physiologists have known and acted on Galvani's revelation that skeletal muscles contract when stimulated electrically and, conversely, that a detectable current is detectable when they contract (Basmajian and De Luca, 1985). The extraction of information from the electrical signal generated by the activated muscles (electromyography; EMG) has been regarded as an easy way to gain access to the less accessible activity of motor control centers. Electromyographic techniques are now well accepted by the research community, and their usage is spreading as an assessment tool in sport and applied physiology. EMG can be recorded invasively, by wires or needles inserted directly into the muscle, or non-invasively, by recording electrodes placed over the skin surface overlying the investigated muscle. With wire electrodes, the volume of muscle from which signal is recorded is relatively small (few cubic millimeters) and thus, may not be representative of the total muscle mass involved in the exercise. Conversely, surface EMG provides information from a large mass of muscle tissue (though the superficial fibers contribute more than deep fibers) and thus is more directly correlated to the mechanical outcome (Frigo and Shiavi, 2004). Therefore, use of this latter modality is preferable in healthy sedentary subjects and in athletes,

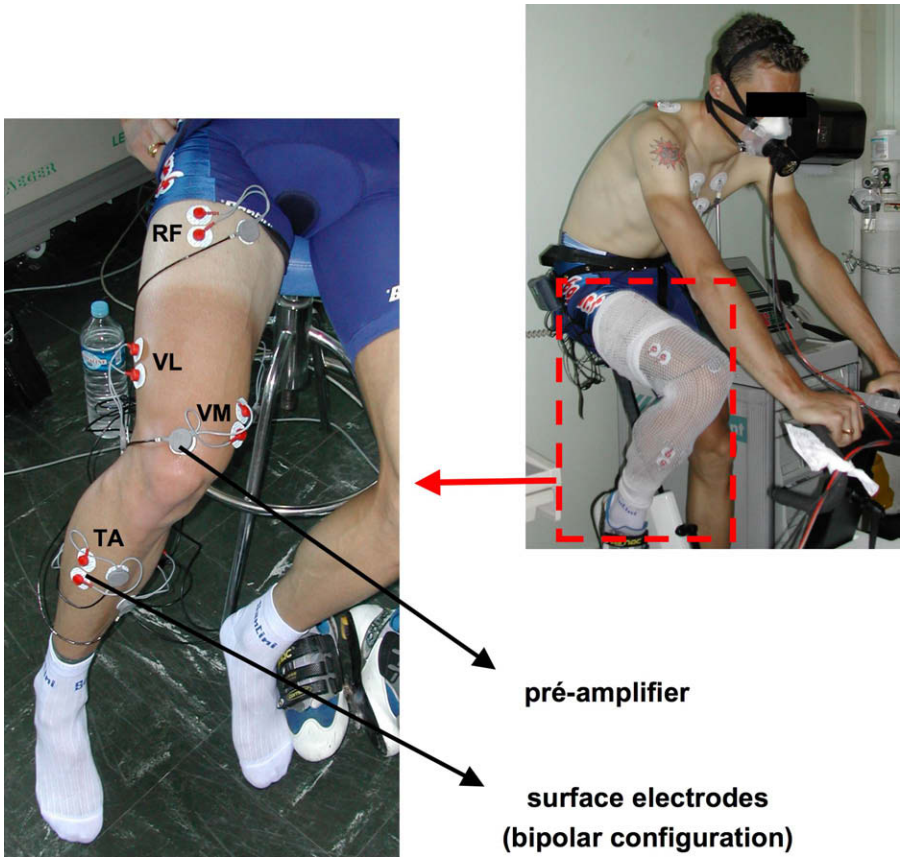

Fig. 1. Example of experimental design to study the lower limb muscle activation patterns during pedaling. Motion artifacts are reduced/eliminated by carefully fixing all the cables (a net bandage can be put around the lower limbs) and/or by using pre-amplifiers close to the electrodes.

despite some limitations and drawbacks. In fact, surface EMG is mainly related to the neural output from the spinal cord and thus to the number of activated motor units and their discharge rate. However, various factors can influence the signal and must be taken into consideration for a proper interpretation. The main physiological factors that influence the surface EMG are fiber membrane properties (*e.g.* muscle fiber conduction velocity) and motor unit properties (*e.g.* firing rates). Other factors considered as non-physiological can also influence the signal as crosstalk (contamination by a nearby muscle's electrical activity) and motion artifacts (induced by the movements of the electrodes and/or cables). Even if motion artifacts can be eliminated by carefully fixing all the cables and by using pre-amplifiers close to the electrodes (Fig. 1), avoiding crosstalk is more difficult. However, the use of double differential electrode configuration (van Vugt and van Dijk, 2001) and/or a proper localization of the surface electrodes on the muscle (Hermens et al., 2000) may diminish it. Accordingly, recommendations for correct electrode placement over the intended muscle have been provided by SENIAM concerted action (Hermens et al., 2000). A typical example of EMG signals recording during pedaling is depicted in the videoclip (supplementary material) attached to the electronic version of this article.

2.2. Determination of muscle activity level and normalization procedures

The pattern of muscle activation during a specific movement, and in a rhythmic human motion such as pedaling can be analyzed in terms of activity level and/or activation timing (Fig. 2). Muscle activity level during pedaling is generally quantified with the root mean square value (RMS) (Duc et al., 2006; Laplaud et al., 2006; Dorel et al., 2007) or integrated EMG (EMGi) values (Ericson, 1986; Jorge and Hull, 1986; Takaishi et al., 1998). Note that RMS is recommended compared to integrated EMG (Basmajian and De Luca, 1985). In order to compare the muscular activity between different muscles and between different subjects, numerous authors use and recommend an EMG normalization (Ericson, 1986; Marsh and Martin, 1995). In most cases, EMG activity recorded during the test situation is expressed relative to that previously recorded during a brief (*i.e.* less than 5 s) isometric maximal voluntary contraction (IMVC) (Ericson, 1986; Marsh and Martin, 1995). Because it is not obvious that the reference EMG values recorded during IMVC can be used to represent the maximal neural drive during pedaling, this type of normalization is strongly criticized on the basis of possible misinterpretations (Mirka, 1991). For instance, by using this method, Hautier et al. (2000) reported an activity level

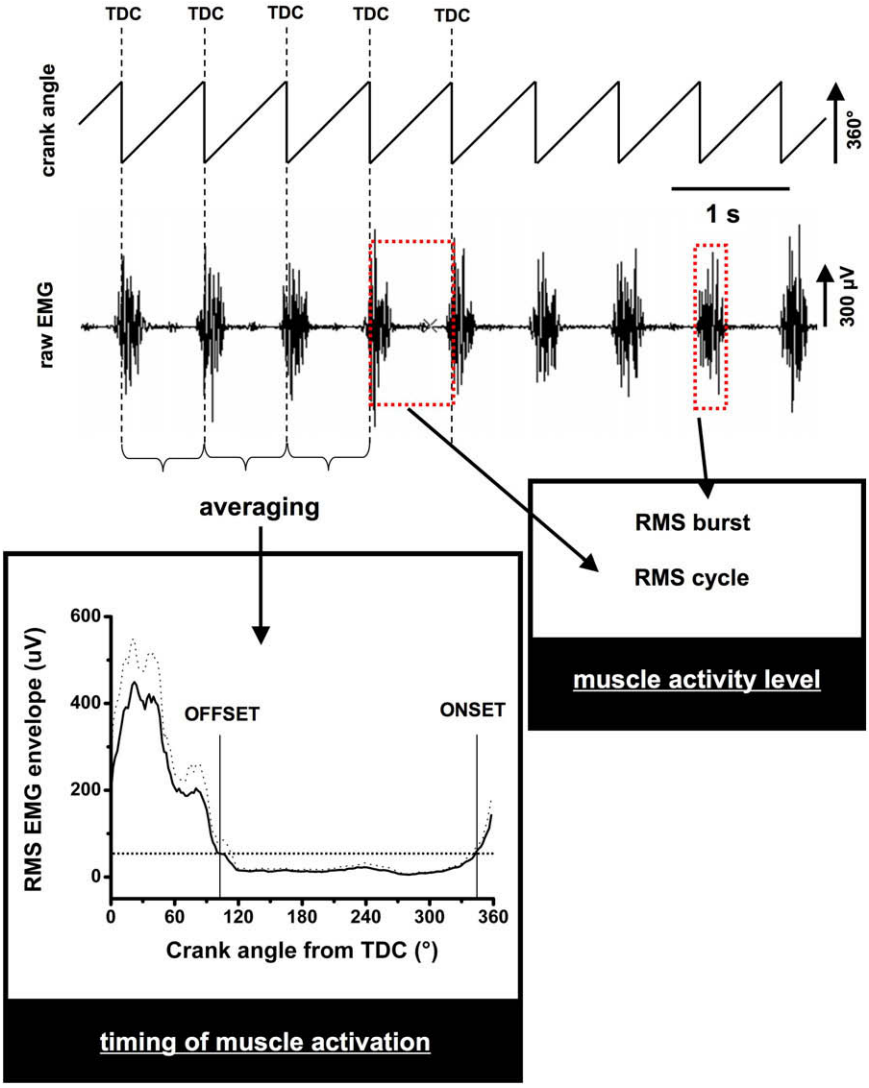

Fig. 2. Example of surface electromyographic signal processing to study the lower limb muscle activation patterns during pedaling. Crank angle and EMG signals are synchronized. The muscle activity level is easily identified by the calculation of EMG RMS over one complete cycle (*i.e.* 0–360°; RMS cycle) and/or by the calculation EMG RMS over the period of muscle activity (*i.e.* EMG burst). For the study of muscle activation timing, raw EMG data are root mean squared (RMS) with a time averaging period of 25 ms to produce a linear envelope. A linear interpolation technique is then used to obtain a mean value of EMG RMS for each degree of rotation. Finally, these data are averaged over various consecutive pedaling cycles in order to get a representative EMG RMS linear envelope. Solid lines indicate the EMG RMS envelope and the dashed curves are 1 standard deviation above the mean. Onset and offset values are determined from this averaged pattern using an EMG threshold value fixed at 20% of the peak EMG recorded during the cycle (horizontal dashed line). TDC, top dead center (0°).

above 100% of IMVC (*i.e.* 126.2%) for VL during a brief maximal cycling exercise. To take into account the specificity of the cycling posture, Hunter et al. (2002) proposed to use more specific isomeric tasks performed on the cycle ergometer. More recently, Rouffet and Hautier (2007) recommended a novel approach based on a cycling torque–velocity test in order to better control the posture (*i.e.* joint angle and muscle length), the type of contraction, and the role of each muscle. Despite presenting an original normalization procedure for future studies, different aspects concerning the activation of lower limb muscles during such a maximal pedaling exercise remain to be elucidated due to the lack of detailed information. In order to adequately discuss the field we can raise the following questions: (1) what is the influence of the power–velocity combination on the maximal reference value of activation obtained for the different muscles? (2) How this influence as well as the influence of the free acceleration of the movement allowed during the sprint should be taken into account by researchers, with the view of obtaining a reference value used to study the activation of the lower limb muscles during submaximal exercises during which both these factors are controlled? (3) What is the influence of the time interval and smoothing process used to calculate the maximal reference EMG value during the sprint exercise on the normalization procedure and how can this be optimized? (4) How

can it be determined that the level of activation during the sprint reflects the maximal neural drive of the different lower limb muscles? (5) Is it rational to assume that all of the subjects have the same ability to maximally activate all of the lower limb muscles during such a specific exercise (and especially the bi-articular muscles)? This last point is important because it could lead to misinterpretations concerning the inter-individual variability of the normalized EMG values. Various studies focusing on EMG profiles normalize the EMG patterns in respect to the peak (named peak dynamic method; Ryan and Gregor, 1992; Dorel et al., 2007) or mean (named mean dynamic method; Winter and Yack, 1987) value measured over the complete cycle. However, it should be kept in mind that these normalization procedures only inform the researcher or clinician about the level of activity displayed by a muscle over a pedaling cycle (*i.e.* shape of the EMG pattern) in relation to the peak or average activity. Thus, it does not inform on muscle activation level that is required during pedaling. Overall, to date, there is no agreement on the best normalization procedure to be adopted (Burden and Bartlett, 1999). This methodological aspect concerning normalization of EMG signal processing will be of primary interest to improve interpretation of EMG signals in future studies which aim to quantitatively compare the activity of different muscles in the same subject or to quantitatively describe the inter-subject variability of muscle activation levels. Nevertheless, for studies which examine the alteration of EMG responses of the different muscles induced by independent factors (such as body position, workload, etc.) in the same session, the normalization procedure has a lower influence on the analysis and its necessity remains to be established.

2.3. Determination of muscle activation timing

Muscle activation timing is generally studied from a representative EMG profile obtained by averaging various consecutive cycles and by smoothing. This mean EMG profile generally depicts the evolution of the RMS envelope throughout the crank cycle (Fig. 2). Detecting a bottom or top dead center signal of the crank (BDC and TDC, respectively) permits to display EMG profiles as function of time expressed in percentage of the total duration of the complete cycle. This method allows the comparison with other pedaling cycles of different durations. However, due to the slight variations of the crank velocity, especially if the pedaling rate is not maintained constant (e.g. during a sprint), it is recommended to synchronize the EMG signal with a continuous mechanical measurement of the crank position. Timing parameters generally determined from this EMG profile include signal onset and offset times that identify the duration of EMG bursts (Jorge and Hull, 1986; Li and Caldwell, 1998; Chapman et al., 2006, 2007; Duc et al., 2006; Dorel et al., 2007). Usually, an EMG threshold value (fixed at 15–25% of the peak EMG recorded during the cycle, or 1, 2 or 3 standard deviations beyond mean of baseline activity) is chosen for onset and offset detection (Fig. 2). It allows identification of the EMG activity regions as a function of the crank angle as it rotates from the highest pedal position (0°, TDC) to the lowest (180°, BDC) and back to TDC to complete a 360° crank cycle. However, because this identification can be disputable with some EMG patterns and strongly dependant of the threshold level used, some authors visually adjust and raise this threshold in the cases for which it is considered inappropriate (Li and Caldwell, 1998; Duc et al., 2006). This approach has two limitations. First, the determination is largely subjective and thus, there is a lack of agreement between investigators as to the "correct" threshold (Hodges and Bui, 1996). Second, information about the shape of the EMG signals (*i.e.* level of activation changes across the crank cycle) is not taken into account. The peak of EMG activity (EMG_{peak}) and the crank angle at which this peak value occurs (Li and Caldwell, 1998; Duc et al., 2006) also attempt to quantitatively and qualitatively characterize the EMG burst. However, these values remain influenced to a large extent by the signal processing employed, and specifically by the smoothing method. As a consequence some discrepancies in the onset, the offset or the angle corresponding to EMG_{peak} for a given muscle could appear between the studies. For these reasons, some authors propose to calculate a coefficient of cross-correlation to give an objective estimation of the similarity of two activity patterns of the same muscle obtained in two different conditions (with lag time = 0; Li and Caldwell, 1998; Dorel et al., 2007). Recently, this method has been used to calculate the lag time (k_{max}) maximizing the coefficient of cross-correlation and its 95% confidence interval to determine phase shift based on the entire EMG profile (Li and Caldwell, 1999). However, to the best of our knowledge, the results obtained with the cross-correlation technique have not been compared to the onset and offset results. Theoretically, if two EMG patterns are very similar in terms of shape and burst duration despite a shift in time, the same value of k_{max} can be expected as the computed relative onset and offset changes. Conversely, if the burst duration changes, differences in the results obtained with both methods could appear. Fig. 3 depicts the EMG profile of the *Gastrocnemius medialis* muscle obtained during pedaling in two different body positions (*i.e.* dropped posture, DP and upright posture, UP). As illustrated by this figure, due to the decrease of the burst duration from DP to UP, offset of activation (with threshold level fixed at 20% of the peak EMG) appears 20° earlier in UP condition, whereas the onset remains unchanged. By taking into account the two complete EMG profiles the cross-correlation technique and k_{max} calculation lead to a total shift of 4° from DP to UP. It remains controversial in this typical example to describe the timing difference between both conditions by a total shift of activation (*i.e.* only by 4°),

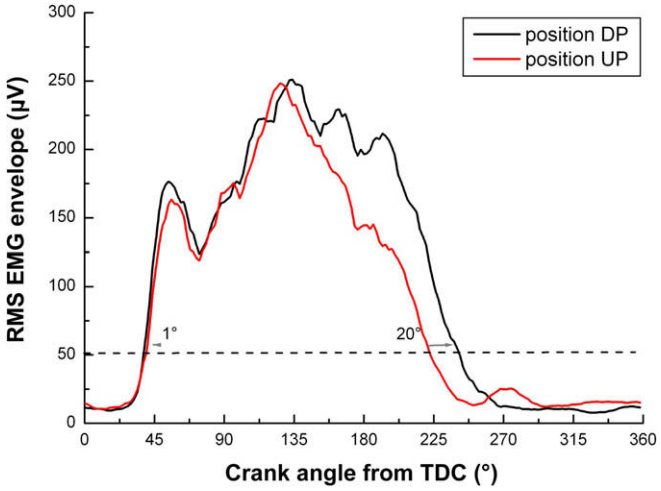

Fig. 3. Illustration of potential differences between onset/offset and the coefficient of cross-correlation determination. Example curves of *Gastrocnemius medialis* EMG linear envelopes obtained during pedaling in two different body positions (*i.e.* Dropped posture, DP and Upright posture, UP) are depicted. Dashed lines indicate the threshold for onset and offset at 20% of the peak EMG. Offset appears 20° earlier in UP condition, whereas the onset is not modified. By taking into account the two complete EMG profiles the cross-correlation technique and k_{max} calculation lead to a total shift of 4° from DP to UP.

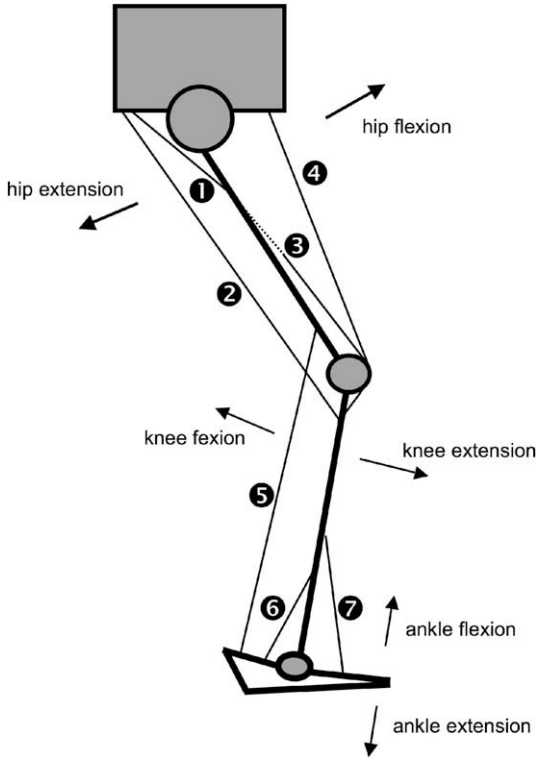

Fig. 4. Schematic representation of bone insertions of the main lower limb muscles implicated in pedaling. (1) *Gluteus maximus* (hip extensor); (2) *Semimembranosus* and *Biceps femoris* long head (hip extensors/knee flexors); (3) *Vastus medialis* and *Vastus lateralis* (knee extensors); (4) *Rectus femoris* (knee extensor/hip flexor); (5) *Gastrocnemius lateralis* and *Gastrocnemius medialis* (knee flexors/ankle extensors); (6) *Soleus* (ankle extensor) and (7) *Tibialis anterior* (ankle flexor).

whereas the two curves clearly demonstrated a similarity in the beginning of activation, but with a significant decrease in the duration in the UP condition. As a consequence, despite its indisputable methodological benefits, the cross-correlation technique should be used carefully and certainly to complement to the classical on-off method and the visual inspection of the EMG profiles.

3. Characterization of the lower limb muscle activation patterns during pedaling

3.1. Typical lower limb muscles activity level

To the best of our knowledge, Houtz and Fischer (1959) were the first to record surface electromyograms during pedaling. They studied all the major surface lower limb muscles (14 muscles) except the *soleus* and stated that these muscles are activated in an orderly and coordinated way. However, this work was performed on a limited number of subjects (three subjects) further casting doubt on the conclusions provided by the authors. More recently, numerous investigators have reported EMG analyses of pedaling (Ericson, 1986; Jorge and Hull, 1986; Ryan and Gregor, 1992; Hug et al., 2004a,b; Duc et al., 2006; Hug et al., 2006a,b; Dorel et al., 2007). Muscles typically sampled are the *Gluteus maximus* (GMax), *Rectus femoris* (RF), *Vatsus lateralis* (VL) *Vatsus medialis* (VM), *Semimembranosus* (SM), *Semitendinosus* (ST), *Biceps femoris* (BF, long head), *Gastrocnemius lateralis* (GL) and *Gastrocnemius medialis* (GM), *Tibialis anterior* (TA), and *Soleus* (SOL). Fig. 4 depicts the general anatomy and action of these muscles. Using a standard normalization procedure, Ericson (1986) showed that a workload of 120 W (corresponding to approximately 54% of the maximum aerobic power) induces an EMG activity level of 45%, 44% and 32% of IMVC for respectively VM, VL and SOL (three mono-articular muscles). EMG activity level is lower for bi-articular muscles such as RF and GL (respectively, 22% and 18% of the IMVC values).

It is important to note that the activation pattern of deeper muscles (*e.g. Tibialis posterior*, *Flexor digitorum longus*, *Adductor magnus*, *Vatsus intermedius*, *Psoas*, etc.) can only be recorded with intramuscular electrodes (*i.e.* wire electrodes). However, due to its invasive nature, this technique was used in very few studies (Juker et al., 1998; Chapman et al., 2006; Chapman et al., 2007) and in only few muscles (*Tibialis posterior*, *Psoas*). Some authors used ^{1}H transverse relaxation time (T2) during Magnetic Resonance Imaging (MRI) of thigh muscles as an index of muscle activity level (Hug et al., 2004a, 2006a,b; Akima et al., 2005; Endo et al., 2007). Despite the opportunity to study deep muscles, this technique only gives indirect indications of muscle activity level, and does not permit a precise comparison between the muscles. Thus, information about the recruitment of deep lower limb muscles during pedaling are scarce.

3.2. Typical lower limb muscles activation timing

As mentioned previously, to examine the pattern of muscle activation, important variables of interest are the starting (onset) and ending (offset) crank angles of the EMG bursts. Figs. 5 and 6 depict respectively the averaged patterns and typical onset and offset values for 10 lower limb muscles. The GMax is active from TDC to about 130°, which is inside the region of the power stroke (25–160°) (Jorge and Hull, 1986; Dorel et al., 2007). *Vastii* (VL and VM) are activated from just before TDC to just after 90° (Houtz and Fischer, 1959; Jorge and Hull, 1986; Dorel et al., 2007). Note that the onset of activity for RF is earlier than for *Vastii* (about 270°) and that termination of activity is just about 90° (Jorge and Hull, 1986; Dorel et al., 2007). The region of activity of TA is in the second half of the upstroke phase (from BDC to TDC) from almost 270° (*i.e.* −90°) to slightly after TDC (Jorge and Hull, 1986; Dorel et al., 2007). Activity of the *Gastrocnemii* muscles (GL and/or GM, depending on the study) begins just after the termination of TA activity (about 30°) and finishes just before the onset of TA activity (about 270°) (Faria and Cavanagh, 1978; Jorge and Hull, 1986; Dorel et al., 2007). SOL is activated during the downstroke phase (*i.e.* 0° to 180°) from 45° to 135° (Dorel et al., 2007). The results concerning the muscles of the hamstrings group (BF, SM and ST) are more controversial. Some authors showed an activation region beginning just after TDC to BDC (Dorel et al., 2007) while others showed a longer activation region from about TDC to about 270° (Jorge and Hull, 1986). Ryan and Gregor (1992) clearly reported the two different patterns described above for BF activation during pedaling (the two patterns described above). In a recent study, we also observed two distinct patterns for TA, GL and SOL (Dorel et al., 2007). In fact, in some subjects (2–8 of 12) these muscles displayed two distinct bursts of activation (Fig. 7). These differences may be related to: (1) inter-subject variability of the pedaling technique (Ryan and Gregor, 1992; Hug et al., 2004a,b), (2) discrepancies between the studies concerning the determination of onset and offset values as mentioned in Section 2.3 (Li and Caldwell, 1999) and/or (3) modifications of several constraints (*e.g.* body position, pedaling rate, shoe–pedal interface, etc.) as further detailed in this review.

3.3. Lower limb muscles function and coordination

Based on the information described above (*i.e.* level and timing of muscle activation patterns) and, in some case, on kinematic/kinetic variables, some studies examined the functional roles of the lower limb muscle during pedaling. As hypothesized by various authors, they may have different roles depending on how many joints the muscles traverse. Ryan and Gregor (1992) noted that the mono-articular muscles (GMax, VL, VM, TA, and SOL) play a relatively invariant role as primary power producers. Conversely, the bi-articular muscles (BF, ST, SM, RF, GM, and GL) behave differently and with greater variability (Ryan and Gregor, 1992; Hug et al., 2004a). According to the theory proposed by van Ingen Schenau et al. (1992), and largely reported in the literature following this study, these muscles appear to be primarily active in the transfer of energy between joints at critical times in the pedaling cycle and in the control of the direction of force production on the pedal.

Lombard (1903) was the first to observe antagonistic contraction during knee extension movement. Indeed, during the propulsive phase of pedaling, several agonist/antagonist muscles pairs activate together. This action occurs between the joint torque necessary to contribute to joint power and the torque necessary to establish the direction of the force on the pedal. Co-activation of mono-articular agonists and their bi-articular antagonists appears to provide the unique solution for these conflicting requirements (van Ingen Schenau et al., 1992); moreover, co-contraction of antagonistic muscles may also provide joint stability by reducing bone displacement and rotation (Hirokawa, 1991) or by equalizing the pressure distribution in the articular surface (Solomonow et al., 1988). For instance, Sanderson et al. (2000) noted that if pedal force is high and cadence is slow eversion of the foot with inward rotation of the tibia through the cycle would lead to stress in the knee. Based on this observation, co-activation may help to relieve this stress. For all these reasons, a decrease of the co-activation level would not necessarily be linked to a more efficient pedaling movement.

3.4. Repeatability of lower limb muscle activation patterns

Assessment of intra-session repeatability of muscle activation pattern is of considerable relevance for research settings, especially when used to determine the effects of various constraints (*e.g.* pedaling rate, fatigue, body position, etc.). Even if the methodological problems, due to electrode replacement, are avoided when EMG measurements of a same session are compared (as is the case found in the major part of studies using EMG in cycling), the question of whether a personal muscle strategy is able to be adopted and maintained stable throughout the experimental cycling session still remains of great importance. However, assessment of reproducibility of lower limb muscle activation patterns during pedaling has been investigated only a few times. Houtz and Fischer (1959) were the first to suggest a high reproducible pattern during pedaling (in three subjects). Later, Laplaud et al. (2006) showed a high day-to-day reproducibility of the activity level (*i.e.* RMS value) of eight lower limb muscles during progressive cycling exercise performed until exhaustion. However, this study did not focus on the timing variables (*i.e.* onset, offset and EMG profile). To the best of our knowledge, only Dorel et al. (2007) demonstrated a good intra-session repeatability of 10 lower limb muscle activation patterns during pedaling, both in terms of muscle activity level and muscle activation timing.

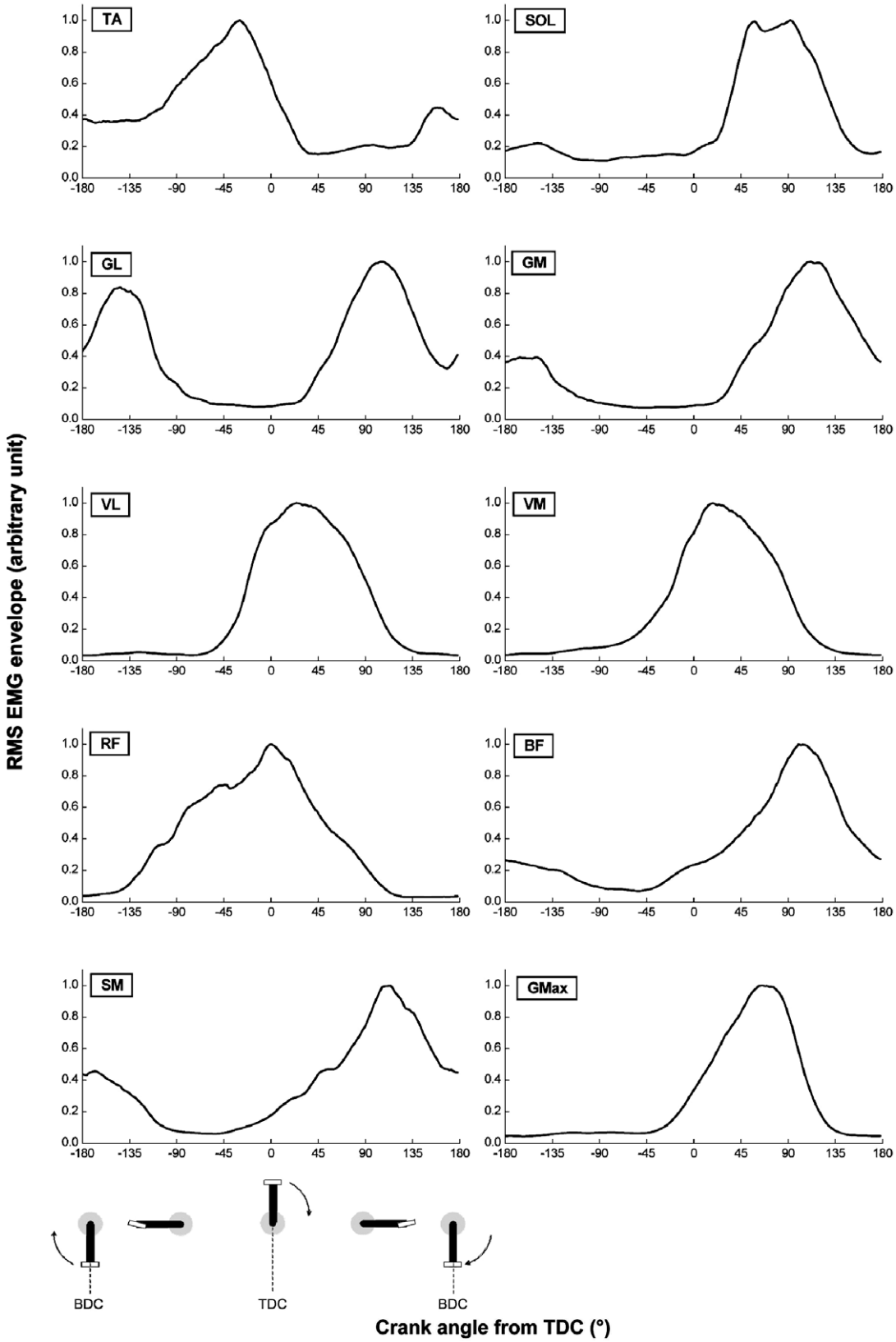

Fig. 5. Ensemble curves of EMG RMS linear envelope for 10 lower limb muscles. The EMG RMS envelopes were averaged over 45 consecutive cycles across 12 triathletes who were asked to pedal at the power output associated to the first ventilatory threshold (238 ± 23 W). For each subject, magnitudes were normalized to the maximal RMS value obtained during the cycle. TDC, top dead center (0°); BDC, bottom dead center (180°). GMax, *Gluteus maximus*; SM, *Semimembranosus*; BF, *Biceps femoris* (long head); VM, *Vastus medialis*; RF, *Rectus femoris*; VL, *Vastus lateralis*; GM, *Gastrocnemius medialis*; GL, *Gastrocnemius lateralis*; SOL, *Soleus*; TA, *Tibialis anterior*. Material published by Dorel et al. (2007).

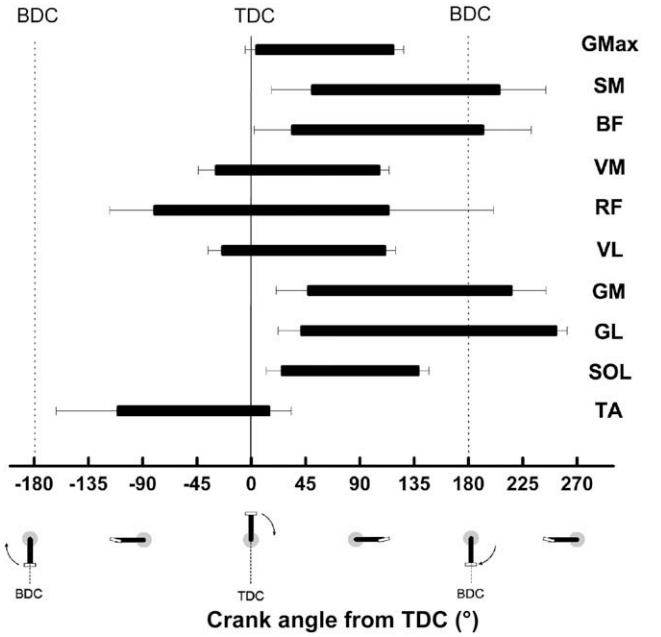

Fig. 6. Mean onset, offset and duration of EMG activity phase indicated by horizontal bars for 10 lower limb muscles. These results were obtained in 12 triathletes who were asked to pedal at the power output associated to the first ventilatory threshold (238 ± 23 W). Only the main burst is depicted when two bursts were observed. TDC, top dead center (0°); BDC, bottom dead center (180°). GMax, *Gluteus maximus*; SM, *Semimembranosus*; BF, *Biceps femoris* (long head); VM, *Vastus medialis*; RF, *Rectus femoris*; VL, *Vastus lateralis*; GM, *Gastrocnemius medialis*; GL, *Gastrocnemius lateralis*; SOL, *Soleus*; TA, *Tibialis anterior*. Material published by Dorel et al. (2007).

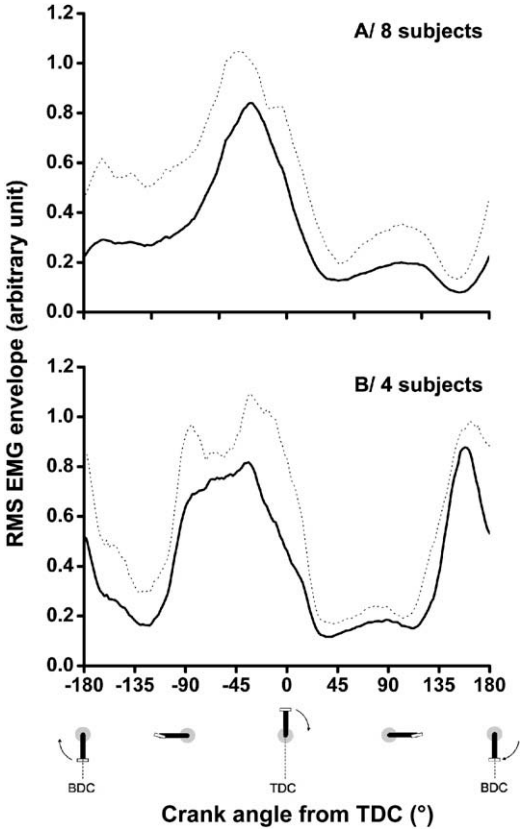

Fig. 7. Example of two different patterns obtained in a group of 12 triathletes for the *Tibialis anterior*. EMG RMS envelopes were averaged over 90 consecutive cycles across 8 and 4 triathletes (for respectively the pattern A and B) who were asked to pedal at 150 W. For each subject, magnitudes were normalized to the maximal RMS value obtained during the cycle. Solid lines indicate the EMG RMS envelope and the dashed curves are 1 standard deviation above the mean. TDC, top dead center (0°); BDC, bottom dead center (180°). Material published by Dorel et al. (2007).

4. Which factors can influence the EMG patterns during pedaling?

4.1. Power output

The power output (expressed in Watt) can be modified by a change in the pedaling rate, mechanical load or both. The following focuses only on the EMG changes induced by manipulations of the mechanical load (*i.e.* resistance imposed by the cyclo-ergometer) without a change in the pedaling rate.

Recordings of EMG activity of some lower limb muscles during a progressive pedaling test performed until exhaustion have shown an increase of EMG activity level with respect to power output (Bigland-Ritchie and Woods, 1974; Taylor and Bronks, 1994; Lucia et al., 1997; Hug et al., 2003; Hug et al., 2006a,b). Some studies reported a linear relationship between the RMS (or EMGi) and the workload level (Bigland-Ritchie and Woods, 1974; Taylor and Bronks, 1994). Others have shown a non-linear increase of RMS (or EMGi) after a certain workload was reached (Lucia et al., 1997; Hug et al., 2003, 2006a,b). However, because the exercises were performed until exhaustion, it is difficult to dissociate the effects of the increase of power output and the occurrence of muscle fatigue on the EMG activity level (further detailed in Section 4.6). During constant-load exercises performed at different intensities (separated by a sufficient period of recovery to avoid fatigue), Ericson (1986) reported increased EMG activity level of the main lower limb muscles (GMax, VL, RF, VM, BF, ST, GM) as power output increased from 120 to 240 W (pedaling rate: 60 rpm) and suggested that GMax activity is greatly influenced by the workload level. Sarre et al. (2003) confirmed these results showing a significant power effect on the EMG activity level of three knee extensor muscles (VM, VL, RF) at three different power outputs expressed as a percentage of the maximal aerobic power (60%, 80% and 100%). However, at low intensities and when the difference between the power outputs is lower (*e.g.* from 83 to 125 W), EMG activity level in *Gastrocnemius* seems to be unchanged (Jorge and Hull, 1986). This result is confirmed by those obtained by Hug et al. (2004a), who showed, during a progressive pedaling exercise, a constant GM activation during the initial stages (from the beginning to about 70% of the maximal aerobic power). It would confirm that this bi-articular muscle is active to transfer energy between joints in the pedaling

cycle and/or to control the direction of force production rather than as a primary power producer.

To the best of our knowledge, few studies have focused on the effects of power output on muscle activation timing. Jorge and Hull (1986) suggested that EMG activity patterns are not strongly influenced by mechanical load. Further research is needed to confirm this point.

Among the new informations that can be extracted from surface EMG and that has not been described previously in this review, muscle fiber conduction velocity (MFCV) is a physiological parameter that is related to the fiber membrane and contractile properties. Because lower threshold motor units have a lower conduction velocity than higher threshold motor units, MFCV can provide indications on motor unit recruitment strategies (Farina et al., 2004a,b). Using linear adhesive arrays of eight electrodes, Farina et al. (2004a) measured MFVC on two thigh muscles (VL and VM) at two different workload levels. They showed that MFVC increases in respect to mechanical load, indicating progressive recruitment of large, high conduction velocity motor units with increasing muscle force.

4.2. Pedaling rate

As mentioned above, a given power output can be obtained at a variety of pedaling rates (also referred to as "cadence"), resulting in a number of cadence–resistance combinations. We will only focus on the EMG changes induced by manipulations of cadence at constant power output.

Pedaling rate is widely accepted as an important factor that affects cycling performance (Faria et al., 2005a,b). For this reason, numerous investigators have quantified the EMG activity level in various lower limb muscles over a large range of pedaling rates (Suzuki et al., 1982; Ericson, 1986; Marsh and Martin, 1995; Neptune et al., 1997; MacIntosh et al., 2000; Baum and Li, 2003; Sarre et al., 2003; Li and Baum, 2004; Lucia et al., 2004). Ericson (1986) reported increased muscle activity on GMax, VM, SM, GM and SOL as pedaling rate was increased from 40 to 100 rpm. However, they showed no change of the level of activation for RF and BF. Neptune et al. (1997) recorded EMG activity of eight lower limb muscles at 250 W across pedaling rates ranging from 45 to 120 rpm. They reported that GM, BF, SM and VM increased their EMG activity level systematically as the pedaling rate increased. In contrast, the EMG–cadence relationship of GMax and SOL showed a quadratic trend with a minimum of EMG activity at pedaling rates near 90 rpm, while RF and TA EMG activities were not affected significantly by cadence. Sarre et al. (2003) showed no significant cadence effect on VL and VM EMG activity levels while RF EMG activity was significantly greater at lower pedaling rates of approximately 60 rpm. In a more recent study, Lucia et al. (2004) tested a population of professional cyclists at about 370 W. They reported contradictory results in this highly trained population, showing a decrease of EMG activity level in VL and GMax with increasing pedaling rate. Overall, even if most of the studies reported an increase of EMG activity level on *Gastrocnemii* and SM in relation to a pedaling rate increase, conflicting results exist with the other muscles. These discrepancies could be explained by differences in the training status of the subjects, the range of cadences tested, and the levels of power output. For instance, the power output was fixed at 120 W in the study performed by Ericson (1986), whereas Sarre et al. (2003) fixed the power output from about 222 W to about 370 W. MacIntosh et al. (2000) averaged EMG activity (RMS values) for seven muscles (GMax, BF, RF, VM, TA, GM, SOL) within each subject. Then, they tested the subjects at four power outputs (100, 200, 300, and 400 W) at each cadence: 50, 60, 80, 100, and 120 rpm. Their results confirmed that the level of muscle activation is modified by the cadence at a given power output. Furthermore, they showed that minimum EMG activity level occurs at a progressively higher cadence as power output increases. For instance, minimal EMG amplitude was observed at less than 60 rpm for 100 W, and close to 100 rpm for 400 W. These results suggest that, at a given submaximal power output, there is a cadence with minimal level of muscle activation. However, it should be kept in mind that these authors averaged RMS values for seven muscles. For this reason, their results can not be extended to each lower limb muscle since each of them responds differently to pedaling rate modifications.

As pedaling rate increases, significant linear trends for peak EMG activity to shift earlier in the pedaling cycle have been reported in various muscles (VL, RF, BF, SOL, and GM) (Marsh and Martin, 1995). Most of these results have been further confirmed by Neptune et al. (1997) who showed that EMG onset and offset of five muscles (GMax, BF, RF, SM, and VM) systematically advanced as pedaling rate increased except for SOL which shifted later in the crank cycle. The time delay between the electrical event (*i.e.* EMG activity) and the related mechanical output (*i.e.* force) (called electromechanical delay, EMD) has been suggested to be relatively constant and within the range 30–100 ms (Cavanagh and Komi, 1979). Assuming the EMD is 100 ms, it corresponds to about 1/10th of a pedaling cycle (*i.e.* 36°) at 60 rpm and to 1/6th of a pedaling cycle (*i.e.* 60°) at 100 rpm. In this line, it was hypothesized that muscle activation must occur progressively earlier as pedaling rate increases in order to develop pedal force in the same crank cycle sector (Li and Baum, 2004). However, Sarre and Lepers (2006) recently showed that peak torque shifts forward in crank cycle as cadence increases (about 10° between 50 and 75 rpm at 37.5% of the maximal aerobic power) suggesting that this central strategy, consisting of earlier muscle activation as cadence increases, is only partial. Moreover, during sprint cycling (at higher pedaling rates), Samozino et al. (2007) showed that, despite an earlier activation of VL and GM, force production occurred later in the crank cycle, during a less effective crank cycle sector. For these authors,

it could partly explain the decrease in power output beyond optimal pedaling rate during sprint cycling.

4.3. Shoe–pedal interface

Bicycle pedals represent two of the five attachment sites between the body and the bicycle. Because they are the primary site of energy transfer from rider to bicycle, the pedal naturally became a focal point for scientists. Platform pedals (also called standard pedals) refer to any flat pedal without a cage. They are used with traditional soft-soled shoes by most recreational riders and by patients involved in rehabilitation therapy. In contrast, toe-clip and clipless pedals are used with hard-soled shoes that are specially adapted for them. Note that nowadays, most of the amateur and professional cyclists use clipless pedals. While standard pedals only permit the application of a positive effective force during the downstroke phase of the crank cycle, toe-clip and clipless pedals also permit (theoretically) the application of a positive effective pedal force from BDC to TDC (*i.e.* during the upstroke phase).

Very few studies have focused on the effects of the shoe–pedal interface on the lower limb muscle activation patterns. Ericson (1986) compared EMG activity level of 11 lower limb muscles during pedaling with standard and toe-clip pedals. He found a higher activity level in RF, BF, and TA when the toe-clip pedals were used. In contrast, it induced lower activity level in VM, VL, and SOL, while the other muscles (hamstrings, *Gastrocnemii*, and GMax) were not affected. More recently, Cruz and Bankoff (2001) compared clipless *vs*. toe-clip pedals. They showed a lower EMG activity in SM and ST (hamstring muscles) with clipless pedals and, in contrast, a higher activity in BF and GL. However, this later study was performed in only four subjects, at a pedaling rate of 100 rpm and at an unknown power output. For these reasons, these results should be taken with caution. Furthermore, these two studies only reported changes of EMG activity level and neither showed EMG activation timing. This later variable is crucial, especially for bi-articular muscles, for linking the quantitative changes of EMG patterns with putative pedaling coordination changes. In addition, considering that a positive relationship exists between negative crank torque and pedaling rate (Neptune et al., 1997), it could be hypothesized that the effects of shoe–pedal interface on the EMG patterns are strongly related to the pedaling rate.

4.4. Body position

A proper position on the bicycle is paramount for both cyclists interested in performance and patients involved in rehabilitation therapy. The most common changes in body position are due to saddle height and trunk orientation (*i.e.* the angle between the trunk and the line connecting the center of the hip joint and the crank axis). Another posture change occurs when the rider switches from a seated to a standing posture to decrease the strain on the lower back muscles. Thus, several authors have been interested in determining the modifications in the activation pattern of the lower limb muscles induced by these changes in body position (Ericson, 1986; Jorge and Hull, 1986; Juker et al., 1998; Li and Caldwell, 1998; Savelberg et al., 2003; Duc et al., 2006).

Saddle height is defined as the vertical distance between the top of the saddle and the center of the pedal axle measured when the pedal is down and the crank arm is in line with the seat tube. Because it is of considerable relevance for both cycling performance and rehabilitation protocols, the effects of saddle height on physiological responses have been extensively explored (Houtz and Fischer, 1959; Hamley and Thomas, 1967; Ericson, 1986; Jorge and Hull, 1986). First, Hamley and Thomas (1967) reported that a saddle height equal to 100% of the trochanter length is the most efficient when oxygen uptake is taken as a criterion. Later, Jorge and Hull (1986) showed an increase in the level of muscle activity for quadriceps (VL, RF, VM) and hamstrings (BF, SM) when the saddle was lowered to 95% of this "optimal" height. In contrast, Ericson (1986) showed that changes in saddle height were not related to activity changes in the quadriceps (RF and VM). These discrepancies could be easily explained by the differences in power output used in these studies and in the methods used to determine the saddle height [*i.e.* 100% *vs.* 95% of the trochanter length for Jorge and Hull (1986) and 102% *vs.* 120% of the distance between the ischial tuberosity and the medial malleolus of the distal part of the tibia for Ericson (1986)].

In an effort to reduce the drag force, competitive cyclists can use a clip-on aero-handlebar during time-trial events. Decreasing the frontal area, this more crouched upper body position (*i.e.* areo-posture) allows a lower wind resistance (Capelli et al., 1993) compared to conventional postures (*i.e.* upright posture or dropped posture). However, in rehabilitation, patients preferred a more upright posture because it offers a more stable position. To the best of our knowledge, only one study focused on the effects of trunk orientation on the activation pattern of lower limb muscles (Savelberg et al., 2003). They showed that GMax was significantly more activated in a crouched position compared to an upright posture. Despite the fact that this position was not comparable to a standard competitive aero-position, these results could partly explain the higher metabolic cost of pedaling reported by some authors in aero-posture (Gnehm et al., 1997). Further research is needed to confirm this point.

Pedaling on a graded surface is an important part of road cycling competition. In addition to change the rider's orientation to gravitational forces, uphill cycling is often accompanied by a switch between seated and standing posture. Li and Caldwell (1998) first showed that the change of cycling grade from 0% to 8% (without body position change) does not induce a significant change the activation pattern of lower limb muscles (Fig. 8). This result was later

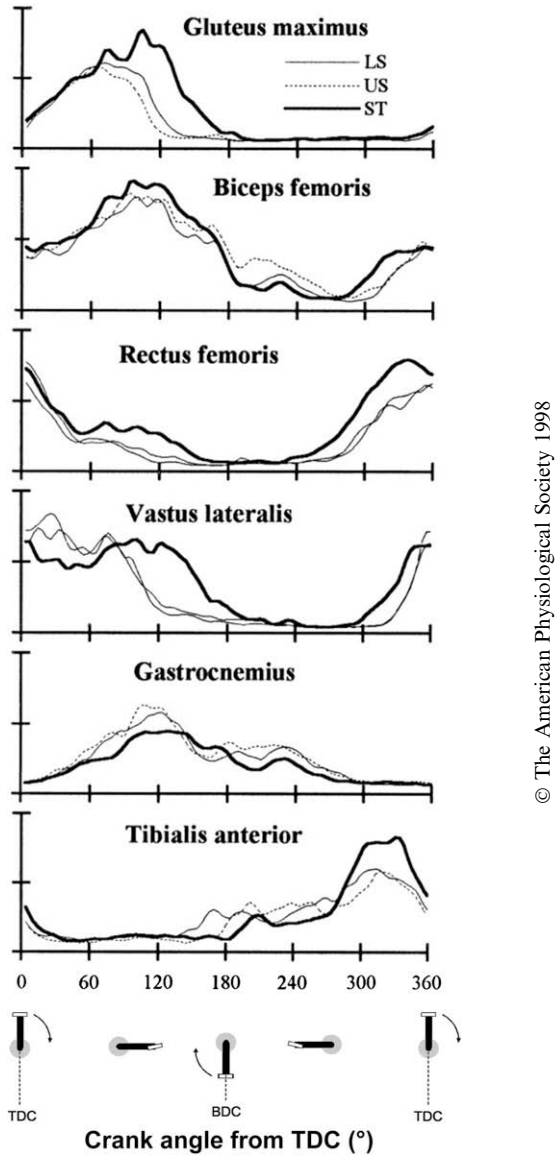

Fig. 8. Ensemble average curves of EMG linear envelope for six lower limb muscles for three positions. LS, level seated; US, uphill seated; ST, uphill standing. All curves in one panel here used same arbitrary units on vertical axes. Reprinted from Li and Caldwell (1998) with permission.

confirmed by Duc et al. (2006). In contrast, the change of pedaling posture from seated to standing affects the intensity and timing of EMG activity of the main lower limb muscles involved in pedaling (Li and Caldwell, 1998; Duc et al., 2006) (Fig. 8). For instance, Li and Caldwell (1998) observed a greater activation for GMax, RF and TA and a longer duration of GMax, RF and VL activity (Fig. 8). It was supposed that this greater and longer GMax activation in standing help to stabilize the pelvis due to the removal of the saddle support.

4.5. Training status

Highly trained road cyclists (*i.e.* professional or elite cyclists) cover about 30,000–35,000 km/year including training and competition (Lucia et al., 1998; Faria et al., 2005a,b) corresponding to about 25 h/week. Numerous studies provided evidence that repeated performance of a movement task facilitates neuromuscular adaptations, which result in more skilled movement (Schneider et al., 1989; Osu et al., 2002). Therefore, some authors wondered if the high volume of training observed in elite/professional cyclists induces the adoption of a pedaling skill in terms of lower limb muscle activation patterns (Ryan and Gregor, 1992; Takaishi et al., 1998; Hug et al., 2004a; Chapman et al., 2006; Chapman et al., 2007).

Based on physiological measurements (Coyle et al., 1991), cycling efficiency (Boning et al., 1984) and/or preferred cadence (Marsh and Martin, 1995), some studies have suggested differences in muscle recruitment patterns between untrained and highly trained cyclists. Marsh and Martin (1995) compared the EMG patterns of five lower limb muscles (VL, RF, BF, SOL and GM) between cyclists and non-cyclists of comparable aerobic aptitudes. Their results showed no significant difference between the two groups for any of the muscles tested. In contrast, Takaishi et al. (1998) suggested that cyclists have a certain pedaling skill regarding the positive utilization of knee flexors (BF) up to the higher cadences, which would contribute to a decrease in peak pedal force and which would alleviate muscle activity for the knee extensors (VL and VM). In this line, using MRI technique, Hug et al. (2006a) recently showed a selective hypertrophy of BF in professional road cyclists suggesting a possible cause–effect relationship between BF activation and hypertrophy, associated with a specific pedaling skill. However, as mentioned above, BF (long head) is a bi-articluar muscle involved in knee flexion and hip extension. Because Takaishi et al. (1998) calculated EMGi values on 20-s samples, without depicting EMG activity in respect to the crank angle, they were not able to precisely distinguish if the higher BF EMG activity measured in cyclists was linked to a higher knee flexion, hip extension or both. Recording leg muscles, less implied in power production than hip and knee extensors, Chapman et al. (2007) showed lower muscle co-activation, a lower individual variance and a lower population variance in highly trained cyclists compared to novices.

To the best of our knowledge only one study was performed on professional road cyclists (*i.e.* in the top-400 "Union Cycliste International" ranking) (Hug et al., 2004a). Using two complementary techniques (surface EMG and functional MRI), they reported that the high degree of expertise of these cyclists is not linked to the production of a common pattern of pedaling. Striking differences between these expert cyclists were observed for two bi-articular muscles: RF and ST. These results are in accordance with those reported by Ryan and Gregor (1992) on 18 experienced cyclists. However, no other details concerning the cycling experience of the subjects were done in this later study. Further research is needed to explore the link between this heterogeneity of muscle recruitment patterns and the mechanical efficiency. It would also be interesting

to study the effects of a specific cycling training program (*e.g.* with EMG feedback) on the activation pattern of the lower limb muscles (*i.e.* a cross sectional study in opposition to the transversal ones depicted in this paragraph).

4.6. Fatigue

Muscular fatigue was defined as the "failure to maintain the force output, leading to a reduced performance" (Asmussen, 1979). In this view, fatigue occurs suddenly at the point of task failure, but the maximal force-generating capacity of muscles starts to decline progressively during exercise so that fatigue really begins before the muscles fail to performed the required task (Gandevia, 2001). Hence, a more realistic definition of fatigue is "any exercise-induced reduction in the ability to exert muscle force or power, regardless or whether or not the task can be sustained" (Bigland-Ritchie and Woods, 1984). The evolution may be fast or slow, depending on the effort perform, and will lead sooner or later to mechanically detectable changes of performance. Many factors that contribute to this evolution affect the surface EMG signal and can be detected through it.

Classically, the EMG activity progressively increases during the course of a continuous isometric exercise of given force maintained until exhaustion (Edwards and Lippold, 1956). Following Edwards and Lippold (1956), many authors explain the increased EMG amplitude to the recruitment of additional motor units that take place to compensate the decrease in force of contraction that occurs in the fatigued muscle fibers. Others attribute the increased EMG amplitude to an increased firing frequency and/or synchronization of motor unit recruitment (see review of Gandevia, 2001) or to slowing of muscle fiber action potential conduction velocity (Linstrom et al., 1970). This increased EMG amplitude was also reported in quadriceps muscles during fatiguing constant-load pedaling exercises (Petrofsky, 1979; Housh et al., 2000; Saunders et al., 2000; Sarre and Lepers, 2005). Hettinga et al. (2006) studied changes in power output and EMGi during a 4000-m cycling time-trial. Their results showed a decrease in mechanical power output near the end of the time-trial accompanied by an increase in EMGi for VL and BF muscles. They concluded that this EMGi increase was consistent with a peripheral locus of fatigue, but because EMGi was calculated over every each successive 200-m, no specific EMG patterns were depicted and thus, it is impossible to know where EMG activity was increased in respect to the crank cycle.

As mentioned above, the rise of EMG activity in the course of a fatiguing constant-load exercise could be mainly attributed to progressive recruitment of additional motor units, as fatigue occurs. However, it could also be assumed that fatigue induces changes of the coordination of the lower limb muscles. Hence, it is difficult to dissociate the effects of neuromuscular fatigue and the putative changes of lower limb muscle coordination patterns. For instance, Psek and Cafarelli (1993) examined the activation of antagonist muscles under fatigue conditions and found that fatigue of VL increases BF activation (which acts as an antagonist in knee extension movement). In contrast, Hautier et al. (2000) showed a decrease in co-activation as agonist force was lost during repeated sprint cycling suggesting that muscle coordination could be efficiently adapted to the loss of contractile force due to local muscle fatigue. This result was later confirmed by Sarre and Lepers (2005) in the course of a 1-h constant load exercise performed at 65% of maximal power tolerated. In order to better isolate the direct effects of neuromuscular fatigue from the changes of muscles coordination, it is possible to measure neural (M Wave, voluntary activation, RMS) and contractile (muscular twitch) properties of a muscles group at various instants of a constant-load pedaling exercise. In this way, Lepers et al. (2002) measured neural and contractile properties of the quadriceps (VM and VL) at each hour of a 5-h cycling exercise (power output fixed at 55% of maximal aerobic power). Their results suggested that the contractile properties are significantly altered after the first hour, whereas the central drive is more impaired toward the latter stages of this long-duration exercise (Fig. 9). Another possible strategy to counteract the effects of fatigue consists of modifying the activation timing of the muscles utilized for performing the movement. Pääsuke et al. (1999) demonstrated that the electromechanical delay increases with fatigue. In consequence, various authors hypothesized that muscle activation timing might also be influenced (Knaflitz and Molinari, 2003; Billaut et al., 2005; Sarre and Lepers, 2005). Billaut et al. (2005) reported an earlier antagonist activation (BF) with fatigue occurrence, while other authors failed to show any significant change (Knaflitz and Molinari, 2003; Sarre and Lepers, 2005). Further studies using the different timing variables are needed to clarify the influence of fatigue on the coordination of the lower limb muscles.

It is a classic notion that muscle fiber conduction velocity decreases during a fatiguing exercise (De Luca, 1984). Spectral analysis aims at an indirect estimation of MFCV changes over time (De Luca, 1984) and is also used to study muscle fatigue (Merletti et al., 1990) and to infer changes in motor unit recruitment (Solomonow et al., 1990). Characteristic spectral frequencies can be computed by a classic periodogram (Merletti and Lo Conte, 1997), or by advanced methods such as wavelet analysis (Karlsson et al., 2000). This latter method may be more appropriate than the classic approach when the signals are nonstationary (Farina et al., 2004b). In support of this idea, von Tscharner (2002) adopted a wavelet analysis and showed that the shifting of the frequency components that occurred with fatigue is very specific for certain periods during the crank revolution. He concluded that these spectral analysis would reflect a systematic change of the motor unit recruitment pattern with pedal position and with fatigue. However, spectral analysis of EMG signals in dynamic contractions has been shown to be poorly associated with neural (*e.g.* recruitment strategies) and muscular

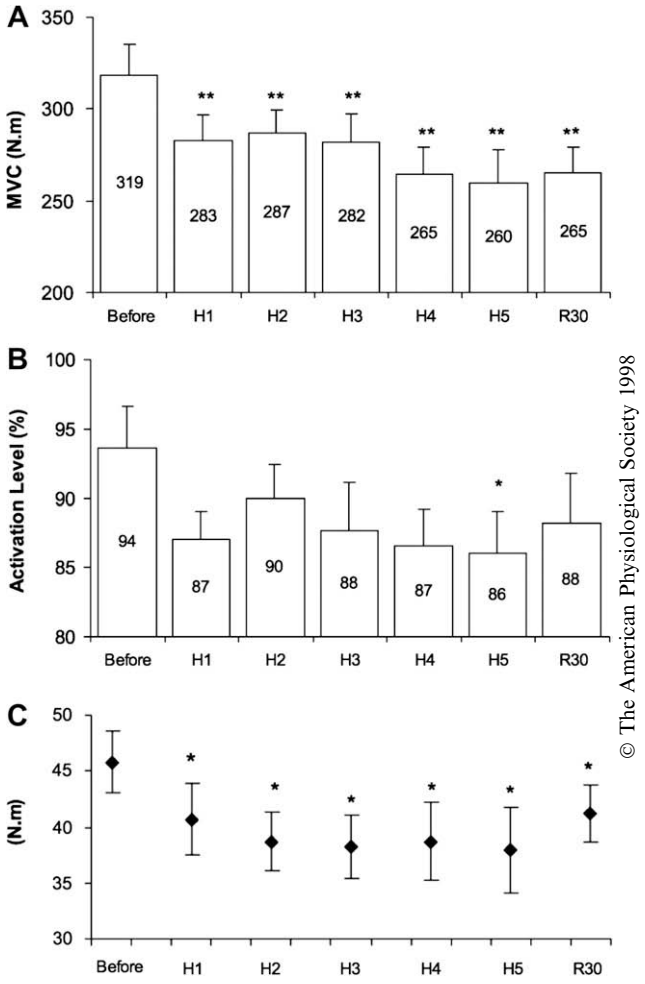

Fig. 9. Time course of changes in the neuromuscular properties of the quadriceps muscle during a 5-h cycling exercise performed at 55% of maximal aerobic power. Isometric maximal voluntary contraction torque (A), activation level estimated by the superimposed twitch method (B) and the maximal twitch torque (C) before, during (H1, 60th min; H2, 120th min; H3, 180th min; H4, 240th min), immediately after (H5, 300th min), and 30-min after the 5-h cycling exercise. Values are means ± SE. Statistically significant compared with before exercise values: *, $p < 0.05$ and **, $p < 0.01$. Adapted from Lepers et al. (2002) with permission.

(*e.g.* muscle fiber conduction velocity) factors in non-fatiguing and fatiguing contractions (Farina, 2006). Thus, the use of spectral analysis of EMG during pedaling should not be suggested. For this reason, a more direct technique based on multichannel EMG detection may be used for MFCV estimation. Using this technique, Farina et al. (2004a) showed a trend of decreasing conduction velocity on VL and VM during a fatiguing cycling exercise.

5. Conclusion and perspectives

Although pedaling is constrained by the circular trajectory of the pedals, it is not a simple movement. Individual patterns of lower limb muscles activation are fairly stereotypical at given pedaling conditions. However, we showed that the level and/or timing of muscle activation change as a function of numerous factors such as power output, pedaling rate, body position, shoe–pedal interface, training status and fatigue.

The majority of EMG studies concerning pedaling have been published since 2000 (33 out of 62 found in Pubmed with "pedaling" and "EMG"). This can be explained by recent advances in technology. Indeed, new EMG acquisition systems permit easy recordings of high quality surface EMG in several muscles (up to 16) during unrestricted movements, even in natural situations (and with wireless electrodes for very recent systems). Nevertheless, to date, the majority of the studies have been performed in laboratory and thus have used stationary cycle ergometers. This type of cycle ergometers constrains the lateral bicycle motion that occurs naturally in road cycling. Because this constraint could potentially affect the pedaling movement, it would be important to compare the lower limb muscles activity pattern during pedaling on a stationary bicycle and on a conventional bicycle used in a natural situation.

Another direction for future research is the evaluation of new devices which continue to be developed and may enhance cycling performance. For instance, a new transmission system (Power Cranks™) that uncouples the right and left cranks offers a variant on the standard pedaling task. Based on empirical observations, numerous cyclists are using this new device during training sessions. It seems important that trainers precisely know what acute and chronic changes in the pattern of lower limb muscle activity are induced by the use of such a device.

It is evident from the more recent history of movement studies that an interdisciplinary approach is needed. In this context, it is not possible to limit the description of human movement to one particular aspect. In this line, we should be establishing link(s) between electromyographic and mechanical patterns during pedaling. For example, instrumented pedals offer the possibility of determining the mechanical effectiveness of pedaling. Considering that 1-h of pedaling corresponds to about 4800 crank revolutions (at 80 rpm), it could be postulated that even a small increase in pedaling effectiveness would induce significant gains in performance. However, it is important to note that this mechanical effectiveness cannot be dissociated from the neuromuscular efficiency. Indeed, an optimal mechanical pattern (with high efficiency) is not necessarily linked to an optimal neuromuscular efficiency and thus to an optimal gross efficiency, etc. It is postulated that direct EMG measurements (*i.e.* direct biofeedback) would be useful (and easily used by coaches and clinicians) for improving the activation pattern of the lower limb muscles and thus, the rehabilitation/training programs.

Acknowledgements

This study was funded in part by "La fondation d'entreprise de la Française Des Jeux" and the French Ministry of Sport (Contract No. 06-046). The authors thank Dr. Antoine Couturier for their constructive remarks.

Appendix A. Supplementary data

Supplementary data associated with this article can be found, in the online version, at doi:10.1016/j.jelekin.2007.10.010.

References

Akima H, Kinugasa R, Kuno S. Recruitment of the thigh muscles during sprint cycling by muscle functional magnetic resonance imaging. Int J Sport Med 2005;26:245–52.

Asmussen E. Muscle fatigue. Med Sci Sport 1979;11:313–21.

Atkins AR, Nicholson JD. An accurate constant-work-rate ergometer. J Appl Physiol 1963;18:205–8.

Basmajian JV, De Luca CJ. Muscle alive (electromyography). Baltimore: Williams & Wilkins; 1985.

Baum BS, Li L. Lower extremity muscle activities during cycling are influenced by load and frequency. J Electromyogr Kinesiol 2003;13:181–90.

Bigland-Ritchie B, Woods JJ. Integrated EMG and oxygen uptake during dynamic contractions of human muscles. J Appl Physiol 1974;36:475–9.

Bigland-Ritchie B, Woods JJ. Changes in muscle contractile properties and neural control during human muscular fatigue. Muscle Nerve 1984;7:691–9.

Billaut F, Basset FA, Falgairette G. Muscle coordination changes during intermittent cycling sprints. Neurosci Lett 2005;380:265–9.

Boning D, Gonen Y, Maassen N. Relationship between work load, pedal frequency, and physical fitness. Int J Sport Med 1984;5:92–7.

Burden A, Bartlett R. Normalisation of EMG amplitude: an evaluation and comparison of old and new methods. Med Eng Phys 1999;21:247–57.

Busch AJ, McClements JD. Effects of a supervised home exercise program on patients with severe chronic obstructive pulmonary disease. Phys Ther 1988;68:469–74.

Capelli C, Rosa G, Butti F, Ferretti G, Veicsteinas A, di Prampero PE. Energy cost and efficiency of riding aerodynamic bicycles. Eur J Appl Physiol Occup Physiol 1993;67:144–9.

Cavanagh PR, Komi PV. Electromechanical delay in human skeletal muscle under concentric and eccentric contractions. Eur J Appl Physiol Occup Physiol 1979;42:159–63.

Chapman AR, Vicenzino B, Blanch P, Knox JJ, Hodges PW. Leg muscle recruitment in highly trained cyclists. J Sport Sci 2006;24:115–24.

Chapman AR, Vicenzino B, Blanch P, Hodges PW. Patterns of leg muscle recruitment vary between novice and highly trained cyclists. J Electromyogr Kinesiol 2007.

Cooper JA, Hasson J. Clinical pathologic conference. Am Heart J 1970;80:824–30.

Coyle EF, Feltner ME, Kautz SA, Hamilton MT, Montain SJ, Baylor AM, et al.. Physiological and biomechanical factors associated with elite endurance cycling performance. Med Sci Sport Exerc 1991;23:93–107.

Cruz CF, Bankoff AD. Electromyography in cycling: difference between clipless pedal and toe clip pedal. Electromyogr Clin Neurophysiol 2001;41:247–52.

De Luca CJ. Myoelectrical manifestations of localized muscular fatigue in humans. Crit Rev Biomed Eng 1984;11:251–79.

Deschenes MR, Kraemer WJ, McCoy RW, Volek JS, Turner BM, Weinlein JC. Muscle recruitment patterns regulate physiological responses during exercise of the same intensity. Am J Physiol Regul Integr Comp Physiol 2000;279:R2229–36.

Dorel S, Couturier A, Hug F. Intra-session repeatability of lower limb muscles activation pattern during pedaling. J Electromyogr Kinesiol 2007.

Duc S, Bertucci W, Pernin JN, Grappe F. Muscular activity during uphill cycling: effect of slope, posture, hand grip position and constrained bicycle lateral sways. J Electromyogr Kinesiol 2006.

Edwards RG, Lippold OC. The relation between force and integrated electrical activity in fatigued muscle. J Physiol 1956;132:677–81.

Endo MY, Kobayakawa M, Kinugasa R, Kuno S, Akima H, Rossiter HB, et al. Thigh muscle activation distribution and pulmonary VO2 kinetics during moderate, heavy and severe intensity cycling exercise in humans. Am J Physiol Regul Integr Comp Physiol 2007.

Ericson M. On the biomechanics of cycling. A study of joint and muscle load during exercise on the bicycle ergometer. Scand J Rehabil Med Suppl 1986;16:1–43.

Faria IE, Cavanagh PR. What are my muscles doing? The physiology and biomechanics of cycling. Wiley; 1978. p. 23–50.

Faria EW, Parker DL, Faria IE. The science of cycling: factors affecting performance – part 2. Sport Med 2005a;35:313–37.

Faria EW, Parker DL, Faria IE. The science of cycling: physiology and training – part 1. Sport Med 2005b;35:285–312.

Farina D. Interpretation of the surface electromyogram in dynamic contractions. Exerc Sport Sci Rev 2006;34:121–7.

Farina D, Macaluso A, Ferguson RA, De Vito G. Effect of power, pedal rate, and force on average muscle fiber conduction velocity during cycling. J Appl Physiol 2004a;97:2035–41.

Farina D, Merletti R, Enoka RM. The extraction of neural strategies from the surface EMG. J Appl Physiol 2004b;96:1486–95.

Frigo C, Shiavi R. Applications in movement and gait analysis. Electromyography: physiology, engineering and noninavasive applications. Wiley–Interscience, Hoboken; 2004. p. 381–97.

Gandevia SC. Spinal and supraspinal factors in human muscle fatigue. Physiol Rev 2001;81:1725–89.

Giezendanner D, Di Prampero PE, Cerretelli P. A programmable electrically braked ergometer. J Appl Physiol 1983;55:578–82.

Gnehm P, Reichenbach S, Altpeter E, Widmer H, Hoppeler H. Influence of different racing positions on metabolic cost in elite cyclists. Med Sci Sport Exerc 1997;29:818–23.

Hamley EJ, Thomas V. Physiological and postural factors in the calibration of the bicycle ergometer. J Physiol 1967;191:55P–6P.

Hautier CA, Arsac LM, Deghdegh K, Souquet J, Belli A, Lacour JR. Influence of fatigue on EMG/force ratio and cocontraction in cycling. Med Sci Sport Exerc 2000;32:839–43.

Hermens HJ, Freriks B, Disselhorst-Klug C, Rau G. Development of recommendations for SEMG sensors and sensor placement procedures. J Electromyogr Kinesiol 2000;10:361–74.

Hettinga FJ, De Koning JJ, Broersen FT, Van Geffen P, Foster C. Pacing strategy and the occurrence of fatigue in 4000-m cycling time trials. Med Sci Sport Exerc 2006;38:1484–91.

Hirokawa S. Three-dimensional mathematical model analysis of the patellofemoral joint. J Biomech 1991;24:659–71.

Hodges PW, Bui BH. A comparison of computer-based methods for the determination of onset of muscle contraction using electromyography. Electroencephalogr Clin Neurophysiol 1996;101:511–9.

Housh TJ, Perry SR, Bull AJ, Johnson GO, Ebersole KT, Housh DJ, et al.. Mechanomyographic and electromyographic responses during submaximal cycle ergometry. Eur J Appl Physiol 2000;83:381–7.

Houtz SJ, Fischer FJ. An analysis of muscle action and joint excursion during exercise on a stationary bicycle. J Bone Joint Surg Am 1959;41-A:123–31.

Hug F, Laplaud D, Savin B, Grelot L. Occurrence of electromyographic and ventilatory thresholds in professional road cyclists. Eur J Appl Physiol 2003;90:643–6.

Hug F, Bendahan D, Le Fur Y, Cozzone PJ, Grelot L. Heterogeneity of muscle recruitment pattern during pedaling in professional road cyclists: a magnetic resonance imaging and electromyography study. Eur J Appl Physiol 2004a;92:334–42.

Hug F, Faucher M, Marqueste T, Guillot C, Kipson N, Jammes Y. Electromyographic signs of neuromuscular fatigue are concomitant with further increase in ventilation during static handgrip. Clin Physiol Funct Imag 2004b;24:25–32.

Hug F, Laplaud D, Lucia A, Grelot L. EMG threshold determination in eight lower limb muscles during cycling exercise: a pilot study. Int J Sport Med 2006a;27:456–62.

Hug F, Marqueste T, Le Fur Y, Cozzone PJ, Grelot L, Bendahan D. Selective training-induced thigh muscles hypertrophy in professional road cyclists. Eur J Appl Physiol 2006b;97:591–7.

Hunter AM, St Clair Gibson A, Lambert M, Noakes TD. Electromyographic (EMG) normalization method for cycle fatigue protocols. Med Sci Sport Exerc 2002;34:857–61.

Jorge M, Hull ML. Analysis of EMG measurements during bicycle pedalling. J Biomech 1986;19:683–94.

Juker D, McGill S, Kropf P. Quantitative intramuscular myoelectric activity of lumbar portions of psoas and the abdominal wall during cycling. J Appl Biomech 1998;14:428–38.

Karlsson S, Yu J, Akay M. Time–frequency analysis of myoelectric signals during dynamic contractions: a comparative study. IEEE Trans Biomed Eng 2000;47:228–38.

Knaflitz M, Molinari F. Assessment of muscle fatigue during biking. IEEE Trans Neural Syst Rehabil Eng 2003;11:17–23.

Krogh A. A bicycle ergometer and respiration apparatus for the experimental study of muscular work. Scand Arch Physiol 1913;30: 375–94.

Laplaud D, Hug F, Grelot L. Reproducibility of eight lower limb muscles activity level in the course of an incremental pedaling exercise. J Electromyogr Kinesiol 2006;16:158–66.

Lepers R, Maffiuletti NA, Rochette L, Brugniaux J, Millet GY. Neuromuscular fatigue during a long-duration cycling exercise. J Appl Physiol 2002;92:1487–93.

Li L, Baum BS. Electromechanical delay estimated by using electromyography during cycling at different pedaling frequencies. J Electromyogr Kinesiol 2004;14:647–52.

Li L, Caldwell GE. Muscle coordination in cycling: effect of surface incline and posture. J Appl Physiol 1998;85:927–34.

Li L, Caldwell GE. Coefficient of cross correlation and the time domain correspondence. J Electromyogr Kinesiol 1999;9:385–9.

Linstrom L, Magnusson R, Petersen I. Muscular fatigue and action potential conduction velocity changes studied with frequency analysis of EMG signals. Electromyography 1970;4:341–56.

Lombard WP. The action of two-joint muscles. Am Physiol Educ Rev 1903;8:141–5.

Lucia A, Vaquero AF, Perez M, Sanchez O, Sanchez V, Gomez MA, et al.. Electromyographic response to exercise in cardiac transplant patients: a new method for anaerobic threshold determination?. Chest 1997:111.

Lucia A, Pardo J, Durantez A, Hoyos J, Chicharro JL. Physiological differences between professional and elite road cyclists. Int J Sport Med 1998;19:342–8.

Lucia A, Earnest C, Perez M. Cancer-related fatigue: can exercise physiology assist oncologists?. Lancet Oncol 2003;4:616–25.

Lucia A, San Juan AF, Montilla M, CaNete S, Santalla A, Earnest C, et al.. In professional road cyclists, low pedaling cadences are less efficient. Med Sci Sport Exerc 2004;36:1048–54.

MacIntosh BR, Neptune RR, Horton JF. Cadence, power, and muscle activation in cycle ergometry. Med Sci Sport Exerc 2000;32:1281–7.

Marsh AP, Martin PE. The relationship between cadence and lower extremity EMG in cyclists and noncyclists. Med Sci Sport Exerc 1995;27:217–25.

Merletti R, Lo Conte LR. Surface EMG signal processing during isometric contractions. J Electromyogr Kinesiol 1997;7:241–50.

Merletti R, Knaflitz M, De Luca CJ. Myoelectric manifestations of fatigue in voluntary and electrically elicited contractions. J Appl Physiol 1990;69:1810–20.

Mirka GA. The quantification of EMG normalization error. Ergonomics 1991;34:343–52.

Neptune RR, Kautz SA, Hull ML. The effect of pedaling rate on coordination in cycling. J Biomech 1997;30:1051–8.

Nordemar R, Berg U, Ekblom B, Edstrom L. Changes in muscle fibre size and physical performance in patients with rheumatoid arthritis after 7 months physical training. Scand J Rheumatol 1976;5:233–8.

Osu R, Franklin DW, Kato H, Gomi H, Domen K, Yoshioka T. Short- and long-term changes in joint co-contraction associated with motor learning as revealed from surface EMG. J Neurophysiol 2002;88: 991–1004.

Pääsuke M, Ereline J, Gapeyeva H. Neuromuscular fatigue during repeated exhaustive submaximal static contractions of knee extensor muscles in endurance-trained, power-trained and untrained men. Acta Physiol Scand 1999;166:319–26.

Petrofsky JS. Frequency and amplitude analysis of the EMG during exercise on the bicycle ergometer. Eur J Appl Physiol Occup Physiol 1979;41:1–15.

Psek JA, Cafarelli E. Behavior of coactive muscles during fatigue. J Appl Physiol 1993;74:170–5.

Rouffet DM, Hautier CA. EMG normalization to study muscle activation in cycling. J Electromyogr Kinesiol 2007.

Ryan MM, Gregor RJ. EMG profiles of lower extremity muscles during cycling at constant workload and cadence. J Electromyogr Kinesiol 1992;2:69–80.

Samozino P, Horvais N, Hintzy F. Why does power output decrease at high pedaling rates during sprint cycling?. Med Sci Sport Exerc 2007;39:680–7.

Sanderson DJ, Hennig EM, Black AH. The influence of cadence and power output on force application and in-shoe pressure distribution during cycling by competitive and recreational cyclists. J Sport Sci 2000;18:173–81.

Sarre G, Lepers R. Neuromuscular function during prolonged pedalling exercise at different cadences. Acta Physiol Scand 2005;185:321–8.

Sarre G, Lepers R. Cycling exercise and the determination of electromechanical delay. J Electromyogr Kinesiol. 2006;17:617–21.

Sarre G, Lepers R, Maffiuletti N, Millet G, Martin A. Influence of cycling cadence on neuromuscular activity of the knee extensors in humans. Eur J Appl Physiol 2003;88:476–9.

Saunders MJ, Evans EM, Arngrimsson SA, Allison JD, Warren GL, Cureton KJ. Muscle activation and the slow component rise in oxygen uptake during cycling. Med Sci Sport Exerc 2000;32:2040–5.

Savelberg HHCM, Van de Port IGL, Willems PJB. Body configuration in cycling affects muscle recruitment and movement pattern. J Appl Biomech 2003;19:310–24.

Schneider K, Zernicke RF, Schmidt RA, Hart TJ. Changes in limb dynamics during the practice of rapid arm movements. J Biomech 1989;22:805–17.

Shafer N. Indoor cycling for the cardiac patient. JAMA 1971;215:1985.

Solomonow M, Baratta R, Zhou BH, D'Ambrosia R. Electromyogram coactivation patterns of the elbow antagonist muscles during slow isokinetic movement. Exp Neurol 1988;100:470–7.

Solomonow M, Baten C, Smit J, Baratta R, Hermens H, D'Ambrosia R, et al.. Electromyogram power spectra frequencies associated with motor unit recruitment strategies. J Appl Physiol 1990;68:1177–85.

Suzuki S, Watanabe S, Homma S. EMG activity and kinematics of human cycling movements at different constant velocities. Brain Res 1982;240:245–58.

Takaishi T, Yamamoto T, Ono T, Ito T, Moritani T. Neuromuscular, metabolic, and kinetic adaptations for skilled pedaling performance in cyclists. Med Sci Sport Exerc 1998;30:442–9.

Taylor AD, Bronks R. Electromyographic correlates of the transition from aerobic to anaerobic metabolism in treadmill running. Eur J Appl Physiol Occup Physiol 1994;69:508–15.

Torres PF, Whipp BJ, Steen SN, Wasserman K. A sinusoidal load generator for use in cycle ergometry. J Appl Physiol 1975;38:554–7.

van Ingen Schenau GJ, Boots PJM, de Groots G, Snackers RJ, van Woensel WWLM. The constrained control of force and position in multi-joint movements. Neuroscience 1992;46:197–207.

van Vugt JP, van Dijk JG. A convenient method to reduce crosstalk in surface EMG. Clin Neurophysiol 2001;112:583–92.

Von Dobeln W. A simple bicycle ergometer. J Appl Physiol 1954;7:222–4.

von Tscharner V. Time-frequency and principal-component methods for the analysis of EMGs recorded during a mildly fatiguing exercise on a cycle ergometer. J Electromyogr Kinesiol 2002;12:479–92.

Winter DA, Yack HJ. EMG profiles during normal human walking: stride-to-stride and inter-subject variability. Electroencephalogr Clin Neurophysiol 1987;67:402–11.

François Hug received his Ph.D. from the university of Aix-Marseille II, France in December 2003. In 2004–2005, he was in a post-doctoral position at the University Paris VI (Laboratory of Respiratory Physiopathology), France. In 2005–2006, he was researcher at the National Institute for Sports (INSEP), France. He is currently assistant professor at the University of Nantes (Laboratory Motricity, Interactions, Performance), France. He has published four national and nineteen international papers in peer-review periodicals. His research interests focus on (1) the metabolic and neuromuscular adaptations of trained cyclists, (2) the neuromuscular adaptations to fatigue and (3) EMG activity of respiratory muscles submitted to mechanical/metabolic loads.

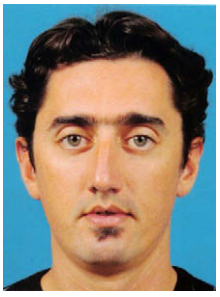

Sylvain Dorel received his Ph.D. in "Motor Function in Human" from the University of St-Etienne, France in December 2004 (Laboratory of Physiology, PPEH, St-Etienne and Laboratory of Biomechanics and Human Modeling, LBMH, Lyon). After a post-doctoral position at the University Lyon I as a teaching and research assistant (CRIS), he is currently researcher at the National Institute for Sports (INSEP), Paris, France. His research interests focus on the neuromuscular adaptations, mechanical characteristics (kinetics and kinematics), and performance (1) during maximal cycling exercise and (2) during sub-maximal exercise in response to the occurrence of fatigue or in relation with alterations of the posture or material.

Available online at www.sciencedirect.com
SCIENCE DIRECT®
Journal of Electromyography and Kinesiology 16 (2006) 158–166
JOURNAL OF ELECTROMYOGRAPHY AND KINESIOLOGY
www.elsevier.com/locate/jelekin

Reproducibility of eight lower limb muscles activity level in the course of an incremental pedaling exercise

David Laplaud [a,*], François Hug [a,b,c], Laurent Grélot [a]

[a] *UPRES EA 3285, " Déterminants Physiologiques de l'Activité Physique", Institut Fédératif de Recherche Etienne-Jules Marey, Faculté des Sciences du Sport, Université de la méditerranée (Aix-Marseille II), CC 910-163 Avenue de Luminy, 13288 Marseille Cedex 9, France*
[b] *UPRES EA 2201, "Laboratoire de Physiopathologie Respiratoire", Institut Fédératif de Recherche Jean Roche, Faculté de médecine, Université de Aix-Marseille II, Marseille, France*
[c] *UPRES EA 2397, "Laboratoire de Physiopathologie Respiratoire", Université de Paris VI Pierre et Marie Curie, Paris, France*

Received 23 June 2004; received in revised form 21 April 2005; accepted 26 April 2005

Abstract

Despite the wide use of surface electromyography (EMG) recorded during dynamic exercises, the reproducibility of EMG variables has not been fully established in a course of a dynamic leg exercise. The aim of this study was to investigate the reproducibility of eight lower limb muscles activity level during a pedaling exercise performed until exhaustion.

Eight male were tested on two days held three days apart. Surface EMG was recorded from *vastus lateralis*, *rectus femoris* (RF), *vastus medialis*, *semimembranosus*, *biceps femoris*, *gastrocnemius lateral*, *gastrocnemius medianus* and *tibialis anterior* during incremental exercise test. The root mean square, an index of global EMG activity, was averaged every five crank revolutions (corresponding to about 3 s at 85 rpm) throughout the tests.

Despite inter-subjects variations, we showed a high reproducibility of the activity level of lower limb muscles during a progressive pedaling exercise performed until exhaustion. However, RF muscle seemed to be the less reproducible of the eight muscles investigated during incremental pedaling exercise. These results suggest that each subject adopt a personal muscle activation strategy in a course of an incremental cycling exercise but fatigue phenomenon can induce some variations in the most fatigable muscles (RF).

Keywords: Surface electromyography; Reproducibility; RMS; Progressive exercise

1. Introduction

Surface electromyography (EMG) is widely used to assess the level of activation in working muscles and to detect the early signs of neuromuscular fatigue. For instance, an increase in the root mean squares (RMS), an index of the global EMG activity, is thought to reflect the recruitment of additional motor units as well as an increase in motor unit rate coding to compensate for the deficit of contractility resulting from the impairment of fatigued motor units [23]. Assessment of the reliability of EMG variables is of considerable relevance for the clinical and experimental use of such a technique.

During static exercises (isometric contractions), many authors have demonstrated the good reproducibility of neuromuscular indices such as amplitude of integrated EMG (EMGi), RMS, median frequency (MF) or mean power frequency (MPF) of the EMG power spectrum and/or muscle fiber conduction velocity [4,6,7,14,15,19–21,25].

In contrast, despite the wide use of EMG recorded during dynamic exercises, the repeatability of EMG

* Corresponding author. Tel.: +33 3 83 97 31 31; fax: +33 3 83 97 80 72.
E-mail address: david.laplaud@auxilia.fr (D. Laplaud).

1050-6411/$ - see front matter © 2005 Elsevier Ltd. All rights reserved.
doi:10.1016/j.jelekin.2005.04.002

variables has not been fully established in this experimental condition. Indeed, to the best of our knowledge, only few studies showed the reproducibility of the EMG parameters during isokinetic repeated contractions [16,17] or throughout an incremental cycling exercise performed until exhaustion [8]. However, in the former, only few muscles (*vastus medialis*, *vastus lateralis* and *rectus femoris*) were recorded. In this context, there is a lack of information about the reliability of EMG parameters of various muscles involved in a cycling exercise.

In a previous EMG and MRI study, we have showed significant differences in the eight lower limb muscles activity level recorded during various cycling exercises in professional road cyclists [11]. These results suggested the use of different pedaling strategies in a homogeneous group of professional road cyclists. However, in this previous work, the reproducibility of the measured indices has not been studied. Then, the question remains to be answered if a proper reliable muscle activation strategy depending on physiological characteristics is adopted or if the subjects can use different strategies with day to day variability.

In this context, the aim of this study was to investigate the reproducibility of eight lower limb muscles activity level during a pedaling exercise performed until exhaustion.

2. Materials and methods

2.1. Subjects

Eight male healthy subjects (age: 27 ± 1 years; height: 180 ± 10 cm; body mass: 78 ± 9 kg), volunteered for the present study. Each subject gave informed consent. Subjects were not engaged in regular athletic activities during leisure time. The experiment was conducted in accordance with the code of ethics of the World Medical Association (Declaration of Helsinki).

2.2. Protocol

2.2.1. Incremental cycling test

Each subject performed twice the same incremental cycling test until exhaustion on an electrically-braked cycle-ergometer (Excalibur sport, Lode®, Netherlands). The two tests (i.e. Test 1 and Test 2) were separated by three days during which the subjects refrained from strenuous physical activity. Each test consisted of a 3-min constant level warm up period (at 100 W) after which the power output (PO) was increased by 25 W min^{-1}. Subjects wore cycling shoes with clip-less pedals and maintained pedal cadence within the 75–85 rev min^{-1} range. A cadence monitor was placed in view of the subject during each test. A designated investigator was placed in charge of monitoring the subjects in order to insure that they maintained the required pedaling cadence throughout the duration of the test. The tests were terminated upon volitional exhaustion of the subjects and/or when cadence could not be maintained at a minimum of 75 rev min^{-1}. At the beginning of each experiment, the height of the saddle and handlebars was adjusted to obtain a conventional cycling posture. Considering that muscle activity can be influenced by the position of the subject as previously described [5], special care was taken to place each subject in the same position on the cycle-ergometer during the two tests.

2.2.2. EMG recording

During the two incremental cycling exercises, EMG activity was continuously recorded from eight muscles of the right lower limb: *vastus lateralis* (VL), *rectus femoris* (RF), *vastus medialis* (VM), *semimembranosus* (SM), *biceps femoris* (BF), *gastrocnemius lateral* (GL), *gastrocnemius medianus* (GM) and *tibialis anterior* (TA). A pair of adhesive electrodes (Universal Ag/AgCl electrodes, Contrôle Graphique Medical®, France) was attached to the skin at a constant inter-electrode distance of 20 mm and was located according to the recommendations of SENIAM [10]. Inter-electrode impedance was kept below 2000 Ω by careful skin shaving and abrasion with an ether pad. The wires connected to the electrodes were well secured with tape to avoid artifacts from lower limb movements. In order to test the between days stability of EMG parameters, the position of each electrode was marked with an indelible marker.

EMG was recorded with a ME3000P8 amplifier (Mega Electronics Ltd.®, Finland). The EMG signals were pre-amplified (375×) close to the electrodes. The raw EMG signals were band pass filtered between 20 and 480 Hz, amplified, an analog-to-digital converted at a sampling rate of 1 kHz. Fig. 1 depicts an individual example of the raw EMG signals obtained in the eight lower limb muscles over five cranks revolutions. For each muscle, a mean RMS data was numerically computed for each cycle (i.e. period of muscle activity visually determined) and they were averaged every 5 cycles throughout the tests. For each subject and each muscle, the calculated RMS values were also expressed as a percentage of the maximal value (RMS_{max}) recorded during each incremental exercise. For the sake of clarity, relative RMS values were calculated at given times of exercise (at the warming up period, 40%, 60%, 80% and 100% of peak power output).

2.3. Statistical analysis

All statistics were performed using the statistical packages SPSS for windows (version 10.1). Results were expressed as means ± standard deviation (SD). For all statistical comparisons outlined below, the level of

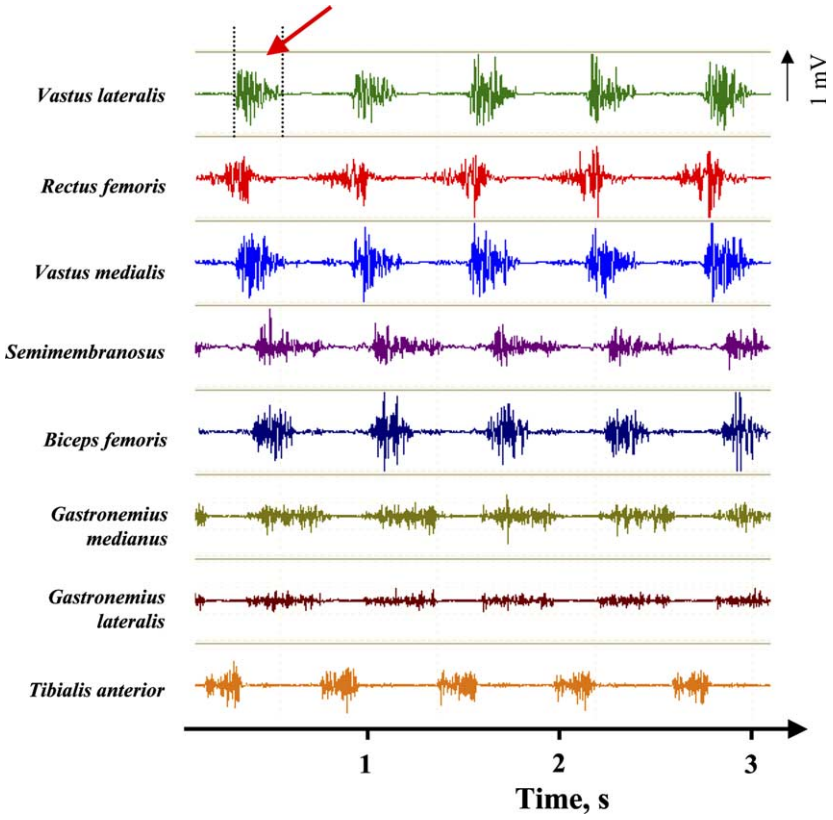

Fig. 1. Individual example of raw EMG signals recorded during the pedaling exercises. Arrow indicates an example of cycle (i.e. muscle activation period) used for the mean RMS calculation.

significance was set at 0.05. Possible differences in RMS values between repeated tests were assessed with a Wilcoxon's test. The same test was used to compare the peak power output (PPO) and mean pedaling cadence in Test 1 and Test 2.

In order to asses the test–retest reproducibility of RMS values, both absolute and relative indices should be determined. The standard error of measurement (SEM, defined as the square root of mean square error with trials) and the coefficient of variation (CV, i.e. standard deviation/mean, in %) can be used to estimate an absolute measure of reliability [4], whereas intra-class correlation coefficient (ICC, i.e. the ratio between intra-class variance and total variance) is a relative and dimensionless reliability variable [2]. Thus, we determined SEM, and ICC for RMS values obtained between Test 1 and Test 2. Moreover, inter-subjects variability was assessed with CV analysis, if CV values were lesser than 12% a good variability was considered [27]. According to Sleivert and Wenger (1994), when ICC ranged between 0.80 and 1.00 a good reproducibility exists, when ICC ranged between 0.60 and 0.79 a fair reproducibility exists and when ICC is less than 0.60 the reproducibility is poor [26]. On the other hand, an ICC value above 0.80 is acceptable for clinical work [3].

Further analysis of EMG reliability was accomplished by applying the procedures suggested by Bland and Altman [1]. For this analysis, the mean difference (bias) and SD of the differences between the mean values of RMS obtained in Test 1 and Test 2 were calculated. The data were shown graphically comparing the difference between the two tests against their average value in W. The mean difference (bias) was indicated in the graph.

3. Results

3.1. General results

There is no significant difference between the two tests (Test 1 and Test 2) concerning the PPO reached by the subjects (300 ± 32 W vs. 300 ± 32 W, respectively; $p > 0.99$, ICC = 1) or in their mean pedaling rate (80 ± 4 vs. 82 ± 3 rpm, respectively).

3.2. Reproducibility of the muscles activity level during progressive pedaling exercises

We found very low variation concerning the contraction time of each muscle between the subjects (CV = 1.8%), between all the cycles recorded during an incremental exercise (CV = 0.9%) and between the two tests (CV = 1.2%).

The reproducibility of the muscles activity level was compared between Test 1 and Test 2. The absolute and normalized RMS values were calculated at given times of the exercise (40%, 60%, 80% and 100% of PPO). Each obtained value was compared between Test 1 and Test 2 using a Wilcoxon's test. We found no significant difference of absolute and normalized RMS values for the eight muscles investigated (except for normalized RMS values of VL obtained at 40% of PPO).

According to ICC and SEM analysis, Table 1 reported a good reproducibility of RMS values for all the muscles investigated except for VL.

Moreover, ICC and SEM values showed a good reproducibility of the normalized RMS values in percentage of RMS_{max} for VL, VM, SM, BF and TA (Table 1). The relative values of RMS calculated for the RF seemed to be not reproducible between the two tests (ICC value always lesser than 0.60, high SEM values). ICC values showed a weak reproducibility for GL and GM normalized RMS values obtained for the low intensities (i.e. 40% and 60% of PPO). Nevertheless, the reproducibility of the normalized RMS values of these two muscles increased with the intensity (Table 1).

If only ICC was considered, there appears a lack of reproducibility for all muscles at 100% of PPO. Nevertheless, at 100% of PPO, SEM values were very low suggesting a good reproducibility.

Fig. 2 shows normalized RMS values recorded throughout the two incremental pedaling exercises at different exercise intensities for each studied muscles. The analysis of the inter-subjects CV values reported a

Table 1
Reproducibility of the absolute and normalized RMS measurements between Test 1 and Test 2 of eight lower limb muscles implied in pedaling activity at different percentage of the maximal power output reached (PPO)

	% PPO	Absolute RMS values (μV)			Normalized RMS values (%RMS_{max})		
		p	ICC	SEM	*p*	ICC	SEM
VL	40	NS	0.83	12.77	0.001	1.00	0.03
	60	NS	0.22	39.80	NS	0.94	0.05
	80	NS	−0.07	29.51	NS	0.89	0.06
	100	NS	0.73	37.34	NS	0.46	0.04
RF	40	NS	0.68	38.76	NS	0.11	0.17
	60	NS	0.54	46.61	NS	−0.41	0.16
	80	NS	0.95	23.12	NS	0.05	0.13
	100	NS	0.97	22.73	NS	−0.43	0.02
VM	40	NS	0.80	31.29	NS	0.92	0.09
	60	NS	0.71	16.74	NS	0.85	0.07
	80	NS	0.97	13.90	NS	0.76	0.06
	100	NS	0.98	17.74	NS	−4.15	0.04
SM	40	NS	0.94	6.40	NS	0.90	0.05
	60	NS	0.87	11.33	NS	0.82	0.08
	80	NS	0.85	13.23	NS	0.96	0.04
	100	NS	0.84	19.33	NS	0.29	0.03
BF	40	NS	0.92	10.34	NS	0.67	0.15
	60	NS	0.78	17.10	NS	0.85	0.07
	80	NS	0.87	19.47	NS	0.84	0.06
	100	NS	0.87	17.88	NS	−0.28	0.08
GL	40	NS	0.82	20.45	NS	0.61	0.11
	60	NS	0.94	15.93	NS	−0.22	0.11
	80	NS	0.96	18.17	NS	0.91	0.05
	100	NS	0.92	25.88	NS	0.002	0.05
GM	40	NS	0.86	11.62	NS	0.28	0.10
	60	NS	0.87	11.40	NS	0.35	0.07
	80	NS	0.99	4.24	NS	0.76	0.05
	100	NS	0.97	9.59	NS	0.79	0.08
TA	40	NS	0.82	19.60	NS	0.96	0.06
	60	NS	0.74	16.27	NS	0.89	0.10
	80	NS	0.91	11.78	NS	0.96	0.07
	100	NS	0.79	24.33	NS	0.91	0.01

ICC, intraclass correlation coefficient; SEM, standard error measurement. *Vastus lateralis* (VL), *vastus medialis* (VM), *rectus femoris* (RF), *semimembranosus* (SM), *biceps femoris* (BF), *gastrocnemius lateralis* (GL), *gastrocnemius medianus* (GM), *tibialis anterior* (TA).

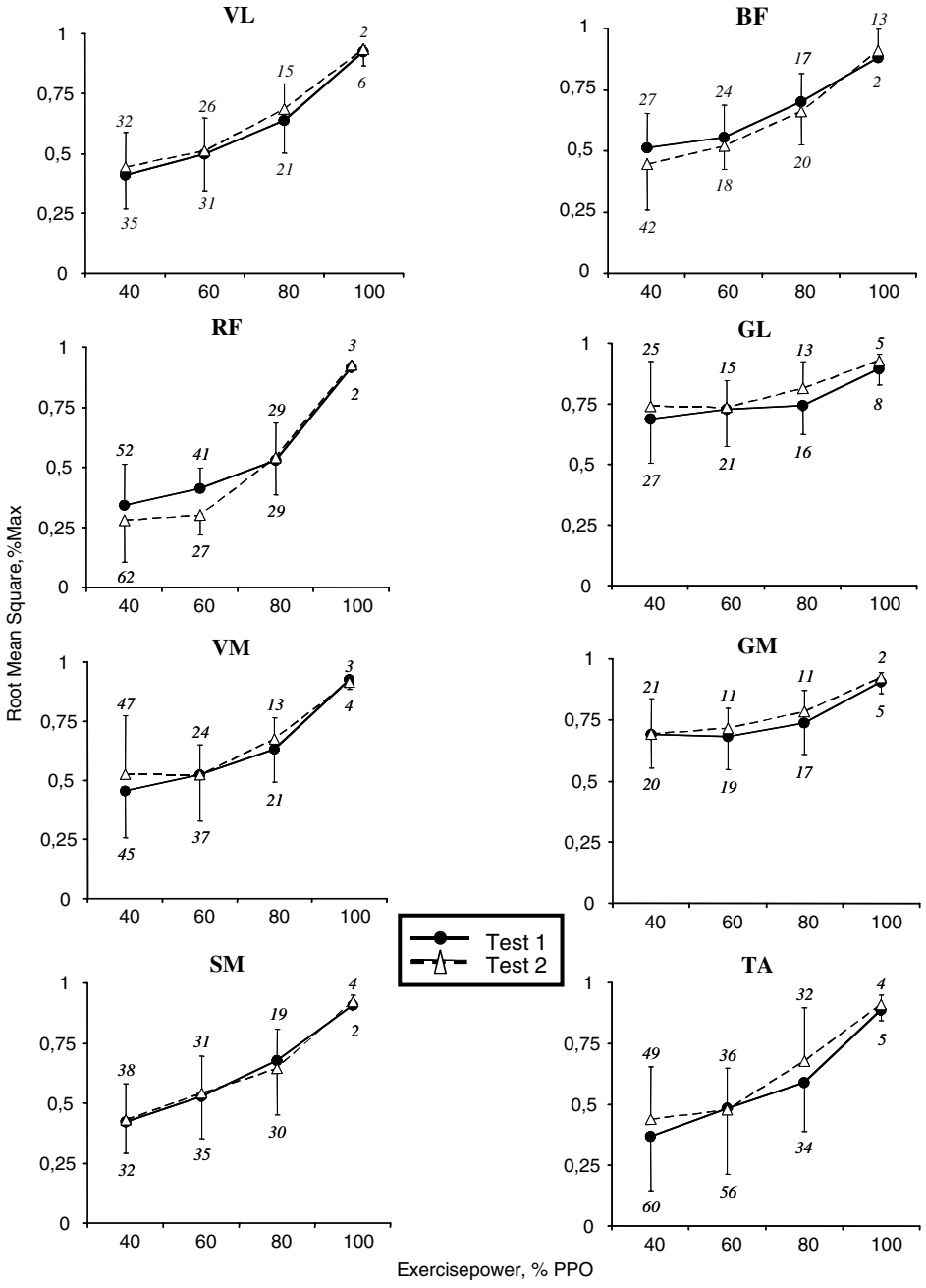

Fig. 2. Time-dependent changes in root mean square (RMS) values during the two incremental cycling exercises. Results are presented as means (SD) for each muscle. RMS values are expressed relative to the maximum RMS value (RMS_{max}). Time-points are as follows: warming up period, 40%, 60%, 80% and 100% of the time to exhaustion. For each averaged value, the variation coefficient between the subjects is indicated. *Vastus lateralis* (VL), *vastus medialis* (VM), *rectus femoris* (RF), *semimembranosus* (SM), *biceps femoris* (BF), *gastrocnemius lateralis* (GL), *gastrocnemius medianus* (GM), *tibialis anterior* (TA).

wide variability for all the muscles studied especially for the lower intensities of the incremental tests (Fig. 2).

The Bland and Altman procedure confirmed the results reported by ICC, and SEM, that is for absolute RMS values a good reliability in seven of the eight muscles investigated and for normalized RMS values a weak reliability in RF, GL and GM (at least at the onset of exercise) (Figs. 3 and 4).

4. Discussion

To the best of our knowledge, this is the first study which showed a high reproducibility of the activity level of lower limb muscles during a progressive pedaling exercise performed until exhaustion. However, RF muscle seemed to be the less reproducible of the eight muscles investigated during incremental pedaling exercise.

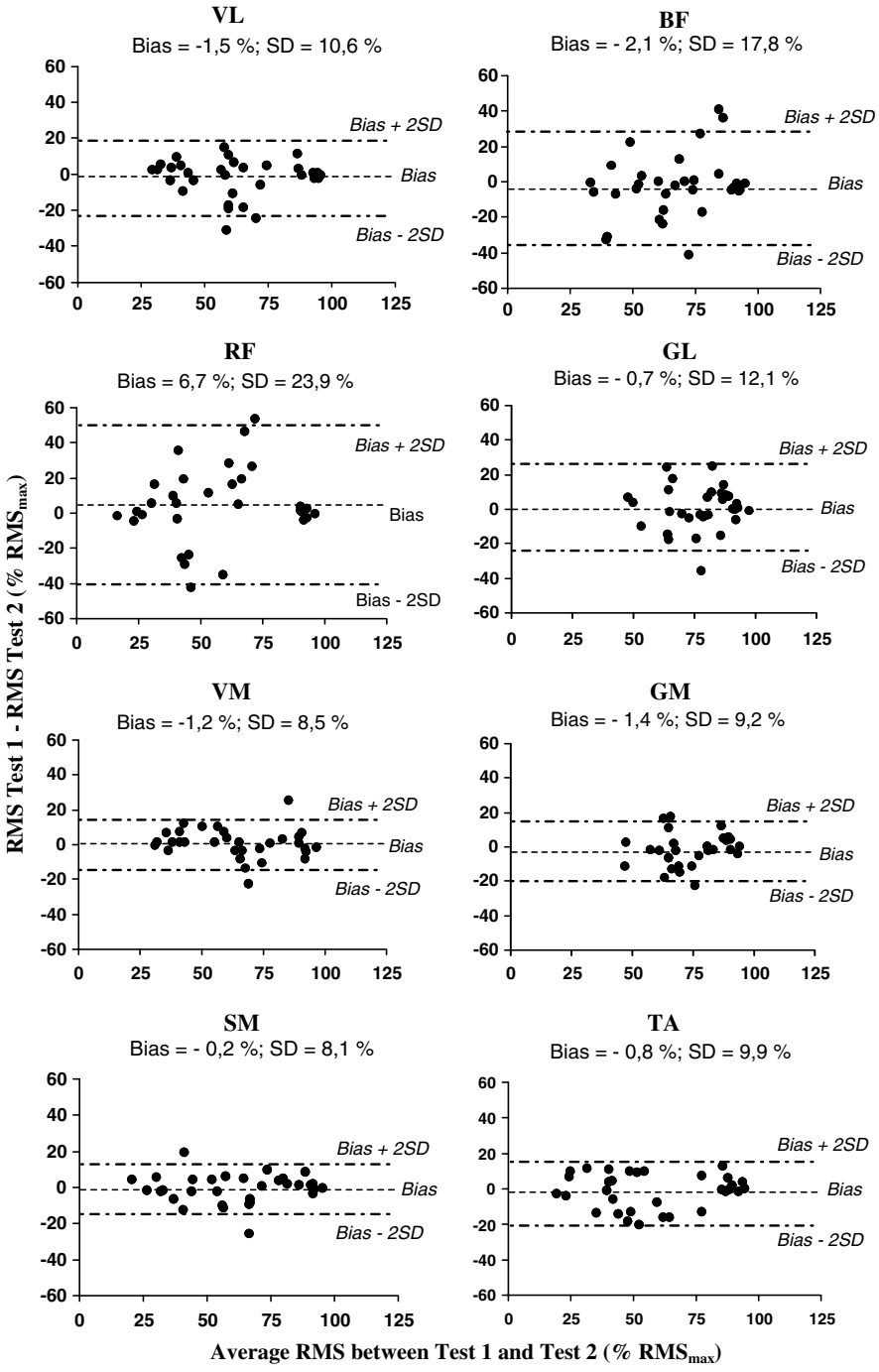

Fig. 3. Bland and Altman procedures applied to normalized values recorded during the two tests. *Vastus lateralis* (VL), *vastus medialis* (VM), *rectus femoris* (RF), *semimembranosus* (SM), *biceps femoris* (BF), *gastrocnemius lateralis* (GL), *gastrocnemius medianus* (GM), *tibialis anterior* (TA).

The results of the present study reported a good reproducibility of the EMG activity level of various lower limb muscles implied in pedaling between Test 1 and Test 2. Indeed, ICC values reported for absolute and normalized RMS values were higher than the aforementioned ICC references values (ICC ranged from 0.60 to 1.00), except in absolute RMS values of VL and in normalized RMS values of RF, GL and GM. ICC was used to express the relative reliability, while absolute reliability required the use of SEM. The SEM was expressed in actual units and the smaller the SEM, the greater the reliability [2]. According to those authors, the use of a single index was not sufficient to assess the measurement reliability [2]. If the ICC values of normalized RMS values were observed, there appeared a lack of reproducibility in the majority of the muscles

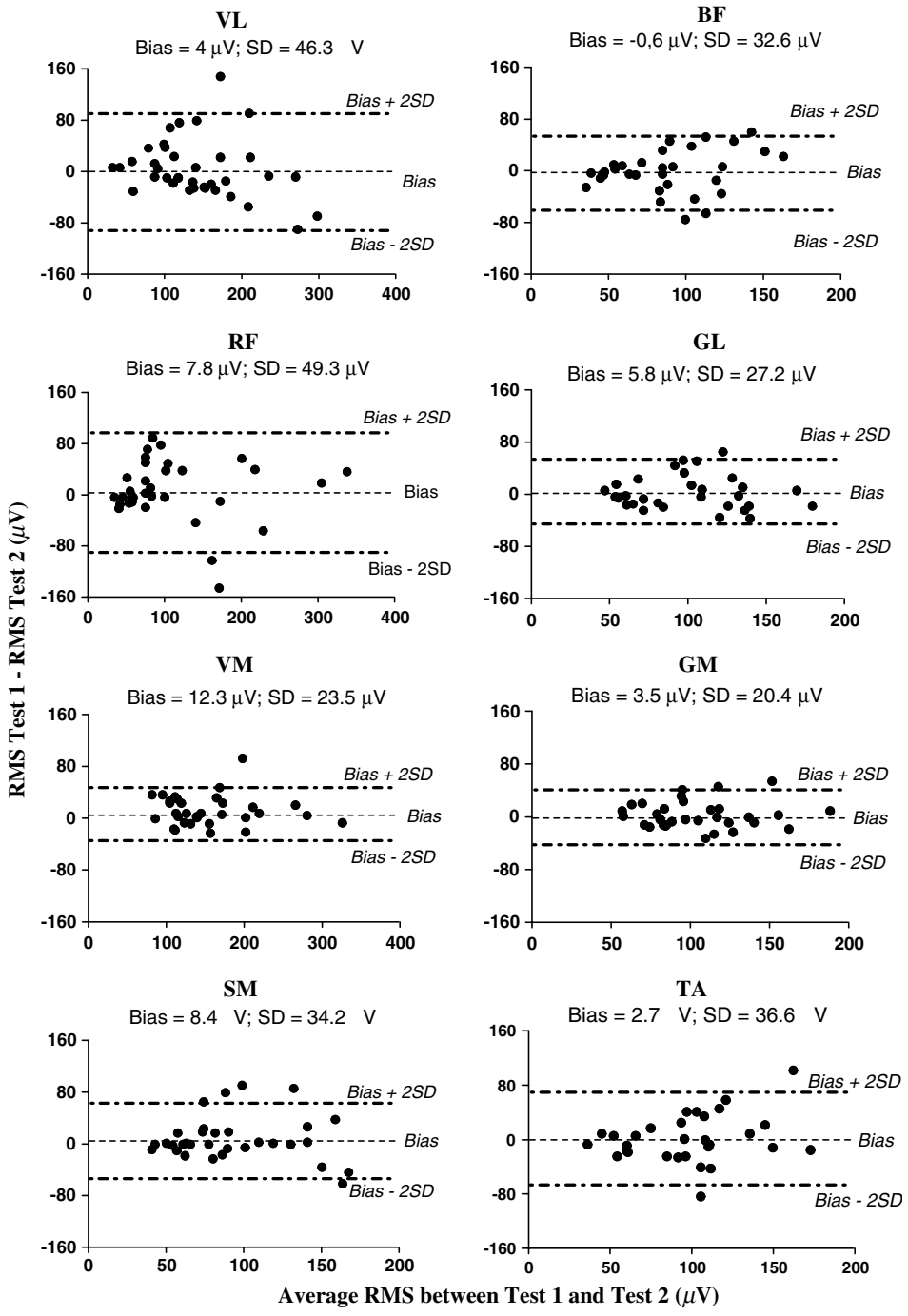

Fig. 4. Bland and Altman procedures applied to absolute values recorded during the two tests. *Vastus lateralis* (VL), *vastus medialis* (VM), *rectus femoris* (RF), *semimembranosus* (SM), *biceps femoris* (BF), *gastrocnemius lateralis* (GL), *gastrocnemius medianus* (GM), *tibialis anterior* (TA).

studied when the subjects reached PPO. However, if SEM values were analyzed, those values reported a good reproducibility. This discrepancy between ICC and SEM values were due to the fact that at the end of the test all the subjects finished with normalized RMS values of 90–100%, therefore, the inter-subject variance was near or even lower than the intra-subject variance. Thus, the ICC became close to 0 or even negative. According to ICC and SEM analysis, the present results reported a good reproducibility of the absolute and normalized RMS values recorded throughout an incremental exercise test.

Several normalization procedures for EMG values have been used. A standardization using EMG changes associated with a maximal voluntary isometric contraction has been reported [5,18] and strongly criticized on

the basis of possible misinterpretation [22]. On the other hand, standardization with respect to EMG changes recorded at 0 W could lead to overestimation of end-of-exercise activity when a given muscle was not activated at all at the onset of exercise. In order to avoid such misinterpretations of EMG data, RMS values were normalized with respect to the RMS_{max} value recorded during the incremental exercise as previously reported [8,13].

Surface electromyography is commonly used for assessment of muscular function during different types of dynamic exercise such as cycling, running or isokinetic repeated contractions. To the best of our knowledge, few studies have investigated the reproducibility during dynamic exercise, especially during an incremental cycling exercise performed until exhaustion [8]. Indeed, most of the studies related to EMG parameters reliability referred to static exercise and reported a good reliability of EMG parameters. Several studies showed that during static exercise there was a good reliability for MF and/or MPF recorded on back muscles [4,15], *vastus lateralis* [19,20,24], *tibialis anterior* [19,20], *vastus medialis* [19] or *rectus femoris* [14,19]. In order to assess the reliability of the EMG parameters during a dynamic exercise, some authors recorded these EMG parameters during isokinetic exercise. Larsson et al. [17] investigated the reproducibility of the MPF of the power spectrum and RMS recorded in RF, VL and VM toward three sets of ten maximal contractions separated by 1 h. The same authors have recently studied the reliability of the same EMG parameters for the VL, RF, VM and BF toward two sets of 100 isokinetic contractions separated by 7–8 days [16]. In these two studies, there appeared a good reliability of the EMG parameters (MPF and RMS). Others have also investigated the reliability of EMG parameters and specially RMS during incremental exercise [8]. Gamet et al. [8] reported a good reproducibility of the profile of the total power spectrum (PEMG) recorded in RF during an incremental cycling exercise performed until exhaustion. Moreover, Gollhofer et al., [9] reported a high reliability of the amplitude of integrated EMG recorded in GM, TA and *soleus* implied in stretch-shortening cycle. Thus, on the whole our results were in agreement with these previous studies. Furthermore, our results showed that RMS values of the lower extremity muscles recorded, among the most implied in pedaling exercise, were highly reproducible in the course of an incremental exercise test performed until exhaustion. As shown in Fig. 2, the RMS values increased throughout the incremental exercise in all muscles. However, RF was the muscle which exhibited the higher variance and seemed to be the less reproducible (Fig. 2). This phenomenon could be partly attributed to kinesiological differences, as the RF is a biarticular muscle involved in both leg extension and thigh flexion. On the other hand, differences in muscle fibre composition cannot be excluded, the *rectus femoris* being comprised a high percentage of fatigable fast twitch fibres [12]. In this line, a recent studies showed a poor reproducibility of median frequency values recorded on RF in a course of an isometric exercise demonstrating a greater rate of fatigue in this muscle [19]. This result was also in accordance with a previous magnetic resonance imaging (MRI) and EMG study which showed heterogeneity of RF recruitment during pedaling in professional road cyclists [11].

5. Conclusion

The results of the present study revealed the good reproducibility of the muscular activity level recorded throughout an incremental. These results suggested that each subject could adopt a personal muscle activation strategy in a course of an incremental cycling exercise but fatigue phenomenon can induce some variations in the most fatigable muscles (RF).

Acknowledgements

This work was supported by grants from ASO (Amaury Sport Organisation – Société du Tour de France). The authors are grateful to Duane Button (University of Manitoba, Canada) and Dr. Tanguy Marqueste (University of Aix-Marseille II, France) for their English language revisions.

References

[1] J. Bland, D. Altman, Statistical method for assesing agreement between two methods of clinical measurement, Lancet 8 (1) (1986) 307–310.
[2] A. Bruton, J.H. Conway, S.T. Holgate, Reliability: what is it, and how is it measured? Physiotherapy 86 (2) (2000) 94–99.
[3] D.P. Currier, Elements of Research in Physical Therapy, third ed., Williams and Wilkins, Baltimore, 1990.
[4] A. Dedering, M. Roos af Hjelmsater, B. Elfving, K. Harms-Ringdahl, G. Nemeth, Between-days reliability of subjective and objective assessments of back extensor muscle fatigue in subjects without lower-back pain, J. Electromyogr. Kinesiol. 10 (3) (2000) 151–158.
[5] M. Ericson, On the biomechanics of cycling. A study of joint and muscle load during exercise on the bicycle ergometer, Scan J. Rehabil. Med. Suppl. 16 (1986) 1–43.
[6] D. Falla, P. Dall'Alba, A. Rainoldi, R. Merletti, G. Jull, Repeatability of surface EMG variables in the sternocleidomastoid and anterior scalene muscles, Eur. J. Appl. Physiol. 87 (6) (2002) 542–549.
[7] D. Farina, D. Zagari, M. Gazzoni, R. Merletti, Reproducibility of muscle-fiber conduction velocity estimates using multichannel surface EMG techniques, Muscle Nerve 29 (2) (2004) 282–291.
[8] D. Gamet, J. Duchene, F. Goubel, Reproducibility of kinetics of electromyogram spectrum parameters during dynamic exercise, Eur. J. Appl. Physiol. Occup Physiol. 74 (6) (1996) 504–510.

[9] A. Gollhofer, G.A. Horstmann, D. Schmidtbleicher, D. Schonthal, Reproducibility of electromyographic patterns in stretch-shortening type contractions, Eur. J. Appl. Physiol. Occup. Physiol. 60 (1) (1990) 7–14.
[10] H.J. Hermens, B. Freriks, R. Merletti, D. Stegeman, J. Blok, G. Rau, C. Disselhorst-Klug, G. Hägg, SENIAM 8: European Recommandations of Surface Electromyography, Roessingh Research and Development, 1999.
[11] F. Hug, D. Bendahan, Y. Le Fur, P.J. Cozzone, L. Grelot, Heterogeneity of muscle recruitment pattern during pedaling in professional road cyclists: a magnetic resonance imaging and electromyography study, Eur. J. Appl. Physiol. (2004).
[12] M.A. Johnson, J. Polgar, D. Weightman, D. Appleton, Data on the distribution of fibre types in thirty-six human muscles. An autopsy study, J. Neurol. Sci. 18 (1) (1973) 111–129.
[13] L. Knutson, G. Soderberg, B. Ballantyne, W.R. Clarke, A study of various normalization procedures for within day electromyographic data, J. Electromyogr. Kinesiol. 4 (1994) 47–59.
[14] J. Kollmitzer, G.R. Ebenbichler, A. Kopf, Reliability of surface electromyographic measurements, Clin. Neurophysiol. 110 (4) (1999) 725–734.
[15] C. Lariviere, A.B. Arsenault, D. Gravel, D. Gagnon, P. Loisel, Evaluation of measurement strategies to increase the reliability of EMG indices to assess back muscle fatigue and recovery, J. Electromyogr. Kinesiol. 12 (2) (2002) 91–102.
[16] B. Larsson, S. Karlsson, M. Eriksson, B. Gerdle, Test–retest reliability of EMG and peak torque during repetitive maximum concentric knee extensions, J. Electromyogr. Kinesiol. 13 (3) (2003) 281–287.
[17] B. Larsson, B. Mansson, C. Karlberg, P. Syvertsson, J. Elert, B. Gerdle, Reproducibility of surface EMG variables and peak torque during three sets of ten dynamic contractions, J. Electromyogr. Kinesiol. 9 (5) (1999) 351–357.
[18] A. Marsh, P. Martin, The relationship between cadence and lower extremity EMG in cyclists and noncyclists, Med. Sci. Sport. Exerc. 27 (1995) 217–225.
[19] S. Mathur, J.J. Eng, D.L. MacIntyre, Reliability of surface EMG during sustained contractions of the quadriceps, J. Electromyogr. Kinesiol. 15 (1) (2005) 102–110.
[20] R. Merletti, A. Fiorito, L.R. Lo Conte, C. Cisari, Repeatability of electrically evoked EMG signals in the human *vastus medialis* muscle, Muscle Nerve 21 (2) (1998) 184–193.
[21] R. Merletti, L. Lo Conte, D. Sathyan, Repeatability of electrically evoked myoelectric signals in the human *tibialis anterior* muscle, J. Electromyogr. Kinesiol. 5 (1995) 67–80.
[22] G. Mirka, The quantification of EMG normalization error, Ergonomics 34 (1991) 343–352.
[23] T. Moritani, H.A. deVries, Reexamination of the relationship between the surface integrated electromyogram (IEMG) and force of isometric contraction, Am. J. Phys. Med. 57 (6) (1978) 263–277.
[24] A. Rainoldi, J.E. Bullock-Saxton, F. Cavarretta, N. Hogan, Repeatability of maximal voluntary force and of surface EMG variables during voluntary isometric contraction of quadriceps muscles in healthy subjects, J. Electromyogr. Kinesiol. 11 (6) (2001) 425–438.
[25] A. Rainoldi, G. Galardi, L. Maderna, G. Comi, L. Lo Conte, R. Merletti, Repeatability of surface EMG variables during voluntary isometric contractions of the *biceps brachii* muscle, J. Electromyogr. Kinesiol. 9 (2) (1999) 105–119.
[26] G.G. Sleivert, H.A. Wenger, Reliability of measuring isometric and isokinetic peak torque, rate of torque development, integrated electromyography, and tibial nerve conduction velocity, Arch. Phys. Med. Rehabil. 75 (12) (1994) 1315–1321.
[27] A.D. Taylor, R. Bronks, Reproducibility and validity of the quadriceps muscle integrated electromyogram threshold during incremental cycle ergometry, Eur. J. Appl. Physiol. Occup. Physiol. 70 (3) (1995) 252–257.

David Laplaud received his Ph.D. degree in exercise physiology from Poitiers University, France, in december 2001. His research topics concern the determination of the electromyographic and ventilatory thresholds. He actually develops rehabilitation programs for chronic obstructive pulmonary disease (COPD) patients. david.laplaud @auxilia.fr.

François Hug received his Ph.D. degree in exercise physiology from Aix-Marseille II University, France in december 2003. He is actually in a post-doctoral position in the Laboratory of Physiopathology (UPRES EA 2397), Paris, France. His research interests focus on metabolic and neuromuscular adaptations of professional road cyclists, neuromuscular adaptations to fatigue and recruitment pattern of respiratory muscles. francois_hug@hotmail.com and http://perso.wanadoo.fr/francois.hug/.

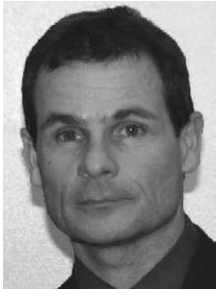

Laurent Grélot received his Ph.D. degree in neurophysiology from Aix-Marseille III University, France, in 1989. He is actually the Head of the Department of Sport Physiology (UPRES EA 3285) and the director of the Faculty of Sport Sciences, Marseilles, France. He is also director of the "doping observatory" since 2000. His main research topics concern neurophysiology, doping and exercise physiology.

Available online at www.sciencedirect.com
ScienceDirect
Journal of Electromyography and Kinesiology 18 (2008) 857–865
JOURNAL OF ELECTROMYOGRAPHY AND KINESIOLOGY
www.elsevier.com/locate/jelekin

Intra-session repeatability of lower limb muscles activation pattern during pedaling

Sylvain Dorel [a], Antoine Couturier [a], François Hug [a,b,*]

[a] National Institute for Sports (INSEP), Laboratory of Biomechanics and Physiology, F-75012 Paris, France
[b] University of Nantes, Nantes Atlantic Universities, Laboratory "Motricity, Interactions, Performance" (JE 2438), F-44000 Nantes, France

Received 29 December 2006; received in revised form 6 March 2007; accepted 6 March 2007

Abstract

Assessment of intra-session repeatability of muscle activation pattern is of considerable relevance for research settings, especially when used to determine changes over time. However, the repeatability of lower limb muscles activation pattern during pedaling is not fully established. Thus, we tested the intra-session repeatability of the activation pattern of 10 lower limb muscles during a sub-maximal cycling exercise.

Eleven triathletes participated to this study. The experimental session consisted in a reference sub-maximal cycling exercise (*i.e.* 150 W) performed before and after a 53-min simulated training session (mean power output = 200 ± 12 W). Repeatability of EMG patterns was assessed in terms of muscle activity level (*i.e.* RMS of the mean pedaling cycle and burst) and muscle activation timing (*i.e.* onset and offset of the EMG burst) for the 10 following lower limb muscles: gluteus maximus (GMax), semimembranosus (SM), Biceps femoris (BF), vastus medialis (VM), rectus femoris (RF), vastus lateralis (VL), gastrocnemius medianus (GM) and lateralis (GL), soleus (SOL) and tibialis anterior (TA).

No significant differences concerning the muscle activation level were found between test and retest for all the muscles investigated. Only VM, SOL and TA showed significant differences in muscle activation timing parameters. Whereas ICC and SEM values confirmed this weak repeatability, cross-correlation coefficients suggest a good repeatability of the activation timing parameters for all the studied muscles.

Overall, the main finding of this work is the good repeatability of the EMG pattern during pedaling both in term of muscle activity level and muscle activation timing.

Keywords: Triathletes; Reproducibility; Root mean square; Cycling; Training

1. Introduction

Surface electromyographic (EMG) techniques for non-invasive muscle activation study are well accepted by the research community and spreading in sport and clinical physiology as assessment tools. The pattern of muscle activation during a specific movement and in rhythmic human motion as pedaling can be analyzed in terms of muscle activity level and/or muscle activation timing. Muscle activity level is quantified with the Root Mean Square (RMS) (Duc et al., 2006; Laplaud et al., 2006) or integrated EMG (EMGi) values (Ericson, 1986; Jorge and Hull, 1986). Muscle activation timing is generally studied by defining signal onset and offset times that identify the duration of EMG bursts (Jorge and Hull, 1986; Li and Caldwell, 1998). Using these indicators, numerous studies have described the pattern of lower limb muscles activation during pedaling (Houtz and Fischer, 1959; Ericson, 1986; Jorge and Hull, 1986; Lucia et al., 2004; Duc et al., 2005; Duc et al., 2006; Hettinga et al., 2006). Some of them have

* Corresponding author. Present address: University of Nantes, UFR STAPS, Laboratory "Motricity, Interactions, Performance", JE 2438, 25 bis boulevard Guy Mollet, BP 72206, 44322 Nantes cedex 3, France. Tel.: +33 (0)2 51837224; fax: +33 (0)2 51837210.
E-mail address: francois.hug@univ-nantes.fr (F. Hug).

1050-6411/$ - see front matter © 2007 Elsevier Ltd. All rights reserved.
doi:10.1016/j.jelekin.2007.03.002

showed changes in EMG magnitude and in temporal characteristics of EMG pattern (onset, offset and/or burst duration) in response to modifications of physiological (*i.e.* fatigue, exercise intensity...) or mechanical (*i.e.* pedaling rate, bicycle geometry, body orientations...) constraints (Ericson, 1986; Lucia et al., 2004; Duc et al., 2006).

Day to day reproducibility of various EMG parameters (*i.e.* integrated EMG, Root Mean Square, Median frequency, Mean power frequency) has been demonstrated during static (Rainoldi et al., 1999; Dedering et al., 2000; Falla et al., 2002; Lariviere et al., 2002) and dynamic isokinetic (Larsson et al., 1999; Larsson et al., 2003) exercises. Surprisingly, assessment of the reproducibility of muscle activation patterns during pedaling is not fully established. Recently, Laplaud et al. (2006) showed a high reproducibility of the activity level (*i.e.* RMS value) of eight lower limb muscles during progressive cycling exercise performed until exhaustion. The major limitation of this study lies in the fact that it only takes into account quantitative EMG variables (*i.e.* RMS or iEMG) without considering timing variables (*i.e.* onset and offset). Moreover, even if the day to day reproducibility suggests good intra-session repeatability, it was never been clearly established for both quantitative and qualitative variables defining the EMG pattern of the main lower limb muscles.

Assessment of intra-session repeatability of muscles activation pattern is of considerable relevance for research settings, especially when used to determine changes over time in the same subject. Even if the methodological problems due to electrode replacement are reduced when EMG measurements of a same session are compared (it is the case of the major part of studies using EMG in cycling), the question remains to be answered whether a personal muscle activation strategy is adopted and maintained stable throughout a cycling session. Houtz and Fischer (1959) were the first to suggest a high reproducible activity pattern during pedaling, but this pilot study enrolled only three subjects.

The aim of this study was to test intra-session repeatability of the activation pattern of 10 lower limb muscles during a sub-maximal pedaling exercise performed at a constant power output. Trained triathletes were tested before and after a simulated cycling training session performed at a low intensity. The EMG pattern was analyzed both in term of muscle activity level and muscle activation timing.

2. Materials and methods

2.1. Subjects

Eleven male triathletes whose anthropometrical and physiological characteristics are presented in Table 1 volunteered to participate to this study. They performed a cycling training volume of 6600 ± 2223 km per year and had a 9 ± 5 years of competitive experience. None of them had recent or ancient pathology of limb muscles or joints. The test procedures were explained to the subjects before they gave their informed consent. The experimental design of the study was approved by the Ethical Committee of Saint-Germain-en-Laye (acceptance no. 06016) and was done in accordance with the Declaration of Helsinki. All subjects were instructed to refrain from intense physical activities during the two days before testing and were naive concerning the nature of the experiment.

Table 1
Morphological and physiological characteristics of the triathletes ($n = 11$)

	Age (year)	BM (kg)	Height (cm)	BMI	$\dot{V}O_{2max}$ (mL min^{-1} kg^{-1})	MAP (W)	VT_1 (%MAP)	VT_2 (%MAP)
Mean	31	72.7	181	22.1	62.3	389	57	82
SD	8.4	6.8	8	1.7	9.1	39	4	4

BM, body mass; BMI, body mass index; MAP, maximal aerobic power; VT_1 and VT_2, first and second ventilatory thresholds expressed in percentage of MAP.

2.2. Exercise protocol

The testing protocol consisted of two sessions conducted in the following order: (1) an incremental cycling exercise performed until exhaustion in order to determine the physical and physiological aptitudes of our population; (2) an experimental session consisted in a reference sub-maximal cycling exercise performed before and after a simulated training session to assess the repeatability of the EMG pattern of the main lower limb muscles. This session was organized one week after the first one and both were performed on the same electronically braked cycle ergometer (Excalibur Sport, Lode®, Netherlands). It was equipped with standard crank (length = 170 mm) and subjects used their own clipless pedals. Vertical and horizontal position of the saddle, handlebar height and stem length were set to match the usual position of the participants.

During the first visit, each subject performed an incremental pedaling exercise, starting at 100 W with workload increments of 25 W min^{-1}. Subjects freely chose their pedaling rate (rpm). The incremental exercise was stopped when the power output could not be maintained (*i.e.* exhaustion). Throughout this exercise trial, a gas exchange analyser (K4B2, Cosmed®, Italy) computed breath-by-breath data of $\dot{V}E$, $\dot{V}O_2$, $\dot{V}CO_2$, and the ventilatory equivalents for O_2 ($\dot{V}E.\dot{V}O_2^{-1}$) and CO_2 ($\dot{V}E.\dot{V}CO_2^{-1}$). According to Reinhard et al. (1979), the first ventilatory threshold (VT_1) corresponded to the time value at which $\dot{V}E/\dot{V}O_2$ exhibited a systematic increase without a concomitant increase in $\dot{V}E/\dot{V}CO_2$ and the second ventilatory threshold (VT_2) was determined by using the criteria of an increase in both $\dot{V}E/\dot{V}O_2$ and $\dot{V}E/\dot{V}CO_2$. Two independent observers detected VT_1 and VT_2 following the criteria previously described. If they did not agree, the opinion of a third investigator was included. The first power achieved when the maximal oxygen uptake was reached ($\dot{V}O_{2max}$) was referred as the maximal aerobic power (MAP).

During the second session, the subjects were asked, after a 10-min warm-up at 100 W, to perform two sub-maximal 5-min pedaling exercises at 150 W at the same constant preferred pedaling rate (±2 rpm) chosen at the end of the warm-up period. These two exercises (*i.e.* test and retest) were separated by a simulated trainning session of 53-min duration. It consisted on six pedaling bouts interspersed by active recovery at 150 W. The first three were completed at an intensity corresponding to the power output measured at VT_1+Δ20% of the difference between power

output measured at VT_1 and VT_2 (VT_1+Δ20%, 6-min duration and 5-min recovery between bouts). The last three were performed at an exercise intensity corresponding to the power output measured at VT_2 (2-min duration and 7-min recovery between bouts). These intensities were chosen in order to simulate a non-fatigable cycling training session.

2.3. Material and data collection

TTL rectangular pulses were delivered by the cycle ergometer each 2°. Additional TTL rectangular pulse permitted to detect the bottom dead centre of the right pedal (*i.e.* BDC: lowest position of the right pedal with crank arm angle = 180°). These data were digitized at a sampling rate of 2 kHz (USB data acquisition DT9800, Data translation®, USA).

Surface EMG activity was continuously recorded for the following 10 muscles of the right lower limb: *gluteus maximus* (GMax), *semimembranosus* (SM), *Biceps femoris* (BF), *vastus medialis* (VM), *rectus femoris* (RF), *vastus lateralis* (VL), *gastrocnemius medianus* (GM) and *lateralis* (GL), soleus (SOL) and *tibialis anterior* (TA). A pair of surface Ag/AgCl electrodes (Blue sensor, Ambu®, Denmark) was attached to the skin with a 2-cm inter-electrode distance. The electrodes were placed longitudinally with respect to the underlying muscle fibre arrangement and located according to the recommendations by SENIAM (Surface EMG for Non-Invasive Assessment of Muscles) (Hermens et al., 2000). Prior to electrode application, the skin was shaved and cleaned with alcohol in order to minimize impedance. The wires connected to the electrodes were well secured with adhesive tape to avoid movement-induced artifacts. Raw EMG signals were pre-amplified close to the electrodes (gain 375, bandwidth 8–500 Hz), and digitized at a sampling rate of 1 kHz (ME6000P16 by Mega Electronics Ltd®, Finland). BDC TTL rectangular pulses were simultaneously digitized for further synchronization with cycle ergometer data.

2.4. Data processing

All data were analyzed with custom written scripts (Origin 6.1, OriginLab Corporation, USA). The BDC TTL rectangular pulses were used to synchronize cycle ergometer crank angle and EMG data. Raw EMG data were root mean squared (RMS) with a time averaging period of 25 ms to produce linear envelope for each muscle activity pattern. EMG RMS was then re-sampled in order to obtain one value each 2° of crank displacement. Prior re-sampling, data were filtered with an anti-aliasing filter which cutoff frequency was dynamically computed according to Shannon Theorem (Shannon, 1949) (*i.e.* 2° TTL pulses half mean frequency). Linear interpolation technique was then used to obtain an EMG RMS value each degree of rotation. Finally, these data were averaged over 25 consecutive pedaling cycles in order to get representative EMG RMS linear envelopes for each muscle, each subject and each condition (test and retest). These values were expressed as a function of the crank arm angle as it rotated from the highest pedal position (0°, top dead centre: TDC) to the lowest (180°, bottom dead centre, BDC) and back to TDC to complete a 360° crank cycle. Fig. 1 depicts an individual example of mean EMG RMS envelopes obtained in the 10 lower limbs muscles for test and retest.

To quantify the muscle activity pattern, a series of classical variables were calculated from the EMG RMS linear envelope. The overall activity level was identified by the mean EMG RMS magnitude over one complete cycle (*i.e.* 0–360°, RMS_{cycle}) and by the mean EMG RMS magnitude over the period of muscle activation (*i.e.* burst, RMS_{burst}). A burst of muscle activation was defined as the muscle activity between the starting crank angle (onset) of the higher activity phase (*i.e.* period where the signal was above a threshold of 20% of the difference between peak and baseline EMG) and the end of this phase (offset) (Li and Caldwell, 1999). The technique of cross-correlation was used to measure the relative change in the temporal characteristics of neuromuscular activity (Li and Caldwell, 1998; Li and Caldwell, 1999; Wren et al., 2006). Therefore, the cross-correlation coefficients of EMG RMS curves between test and retest for each muscle were calculated according to the equation proposed by Li and Caldwell (1998) with a time lag equal to zero. The purpose was to estimate the test–retest reproducibility of linear envelope patterns of the different muscles by using this more recent approach for comparing signals.

2.5. Statistical analysis

All analyses were performed with the statistical package SPPS 11.0 and ORIGIN 6.1 software for Windows. Data were first tested for normality using Kolmogorov–Smirnov test with Dallal and Wilkinson approximation. Because the normality condition was verified, the results are expressed as mean ± standard deviation (±SD). Differences were considered significant when probability (p) of a type I error was below 5%. Paired t-test was used to evaluate possible differences in RMS_{cycle}, RMS_{burst}, onset and offset between test and retest. Intra-session repeatability of all these variables was also assessed using different absolute and relative indices. The standard error of measurement or typical error (SEM) was determined according to the recommendations of Hopkins (2000) to estimate an absolute measure of reliability: $SEM = S_{diff}/\sqrt{2}$, where S_{diff} is the standard deviation of the difference score obtained between test and retest. For quantitative variables such as RMS values, SEM was also expressed as a percentage of the grand mean (%SEM). The intra-class correlation coefficient (ICC, ratio between intra-class variance and total variance) was calculated from the formula: $SEM = SD \cdot \sqrt{(1 - ICC)}$ and hence $ICC = (SD^2 - SEM^2)/SD^2$, where SD^2 is the average of the between-subject variances obtained in test and retest ($SD^2 = 0.5 \cdot SD^2_{test} + 0.5 \cdot SD^2_{retest}$). ICC represents a relative and dimensionless reliability variable. According to Sleivert and Wenger (1994), when ICC ranged between 0.80 and 1.00 a good repeatability exists, when ICC ranged between 0.60 and 0.79 a fair repeatability exists and when ICC is less than 0.60 the repeatability is poor. On the other hand, an ICC value above 0.80 is considered acceptable for clinical work (Currier, 1990). Finally, as described above, the coefficient of cross-correlation was calculated to examine variability in terms of both timing and shape between pairs of EMG RMS envelopes.

3. Results

3.1. General results

Similar pedaling rate was maintained during test and retest (86.8 ± 6.2 and 88.8 ± 5.2 rpm, respectively) to achieve the work rate of 150 W. The mean power output maintained during the 53-min of simulated cycling training

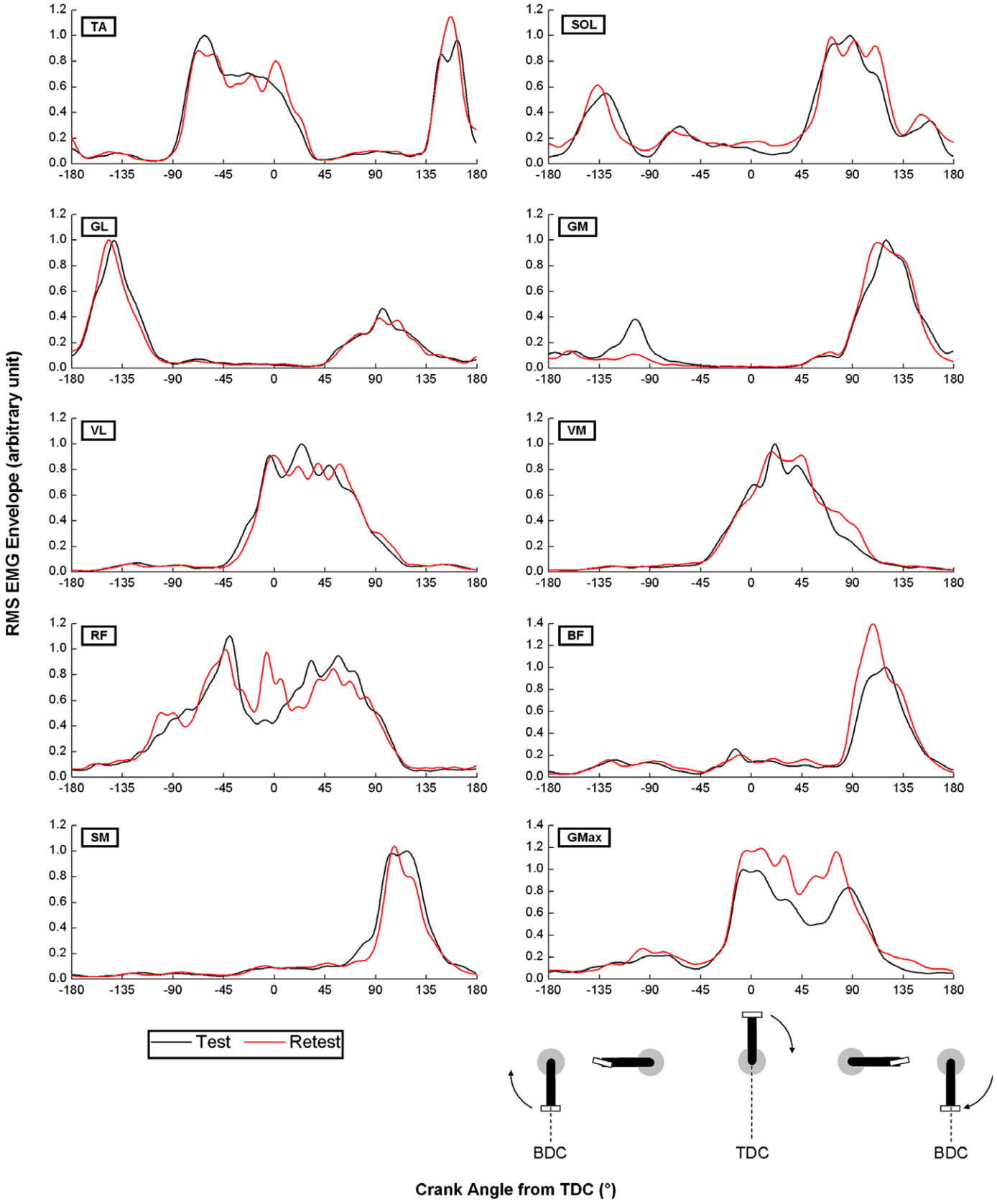

Fig. 1. Individual example of mean EMG RMS envelopes obtained in the 10 lower limbs muscles for test and retest. Test in black and retest in red. For sake of clarity, all the curves on one panel use same arbitrary unit on vertical axes (the first and second tests are normalized to maximal EMG obtained during the first test). TDC, top dead centre (0°); BDC, bottom dead centre (180°). (For interpretation of the references in colour in this figure legend, the reader is referred to the web version of this article.)

performed between test and retest was 200 ± 12 W (corresponded to 52 ± 3% of MPA). In some subjects (2–8), TA, GL and SOL displayed two distinct bursts of activation for both test and retest. In these few cases, we focused the analysis only on the main burst (*i.e.* the common burst for all the subjects). Due to the loss of signal for GMax in one subject, statistics concerning this muscle in the following parts were done with only 10 subjects.

3.2. Muscle activity level

No significant differences were found between test and retest for the 10 muscles investigated. Furthermore, the values of bias measured between test and retest concerning the RMS_{burst} and RMS_{cycle} values were small for each muscle except for GMax (Table 2). ICC and SEM analysis reported a good repeatability for 8 of the 10 muscles regarding RMS_{burst} and for 7 of the 10 muscles regarding RMS_{cycle} (Table 2). Overall, the activity level of both RF and GMax muscles seemed to be less repeatable as indicated by the lower ICC and higher SEM. A weak repeatability of the SOL activity level was also reported for RMS_{cycle}.

3.3. Muscle activation timing

Fig. 2 depicts the mean values of the muscle activation timing variables obtained for both tests. Among the 10 muscles tested, only VM, SOL and TA showed significant differences in muscle activation timing parameters (Table 3). For both VM and SOL the onset of activation occurred later for the retest. The activity of TA lasted longer after TDC for the retest. According to ICC and SEM analysis, for some muscles, results reported a lesser repeatability of onset (RF and TA) and offset (GMax, GL, BF and SOL) values. In contrast, the cross-correlation coefficients indicated a very high repeatability of the EMG activation pattern for all muscles (range: 0.942–0.988, Table 4). The lowest correlation scores were found for RF, and in a lower extent for TA.

4. Discussion

To the best of our knowledge, it is the first study which focuses on the repeatability of lower limb muscles activation pattern throughout a same experimental session (*i.e.* intra-session repeatability). The main finding of this investigation is the high repeatability of the EMG pattern both in terms of muscle activity level and muscle activation timing.

4.1. Methodological considerations

Surface EMG is influenced by a number of physiological properties such as motor unit discharge rates and muscle membrane characteristics, as well as non-physiological properties as electrode placement (Farina et al., 2004). Then, day to day variation in EMG recording may be associated with differences in electrodes re-application such as minor changes in the position of these electrodes over the muscles and/or differences in skin preparation (Kankaanpaa et al., 1998). Then, natural physiological variability of the EMG patterns should be identified in the course of tests performed in the same session. It is the reason why we have tested the pattern of lower limb muscles activation before and after a 53-min simulated training session. Because the subjects performed only three short bouts at both the power output corresponding to $VT_1+\Delta 20\%$ and VT_2 (*i.e.* 6 and 2 min respectively), we hypothetized that this pedaling exercise did not induce neuromuscular fatigue. In this line, Perrey et al. (2003) showed that triathletes, with a similar training status than those involved in the present work, were able to performed a 30-min pedaling exercise at VT_2.

Table 2
Repeatability of the selected RMS measurements between test and retest

Muscles	RMS_{burst}						RMS_{cycle}					
	Mean (SD)		Bias	SEM		ICC	Mean (SD)		Bias	SEM		ICC
	Test (μV)	Retest (μV)	μV	μV	%		Test (μV)	Retest (μV)	μV	μV	%	
GMax	54.4 (25.0)	48.7 (17.0)	−5.7	14.3	28.0	0.55	21.9 (11.6)	19.7 (8.5)	−2.3	7.4	35.4	0.48
SM	84.8 (37.9)	81.5 (36.8)	−3.3	9.8	12.0	0.93	35.1 (16.2)	32.2 (14.8)	−2.9	4.2	12.5	0.93
BF	56.8 (35.4)	53.9 (42.4)	−2.9	11.2	20.3	0.92	27.8 (11.6)	25.5 (11.3)	−2.4	3.3	12.3	0.92
VM	155.3 (35.7)	160.5 (45.6)	5.2	15.3	9.7	0.86	65.2 (16.8)	66.9 (21.3)	1.7	8.0	12.1	0.83
RF	52.4 (16.4)	53.7 (17.8)	1.3	10.1	19.1	0.65	27.7 (8.7)	28.8 (8.0)	1.1	5.3	18.9	0.59
VL	186.5 (44.4)	185.4 (59.9)	−1.1	23.1	12.4	0.81	73.5 (19.3)	73.9 (23.4)	0.4	8.6	11.7	0.84
GM	152.5 (80.2)	156.8 (101)	4.3	21.6	14.0	0.94	69.9 (33.0)	67.3 (42.2)	−2.6	13.0	18.9	0.88
GL	112.8 (45.1)	113.4 (53.4)	0.4	13.9	11.9	0.93	59.8 (24.4)	59.7 (25.0)	−0.1	6.7	11.0	0.93
SOL	91.7 (31.1)	89.2 (41.7)	−2.5	14.8	16.4	0.84	39.2 (11.5)	39.1 (13.0)	−0.1	7.9	20.2	0.58
TA	86.6 (49.9)	83.3 (51.4)	−3.3	5.7	6.7	0.99	38.1 (20.2)	39.7 (25.5)	1.6	5.9	15.2	0.93

RMS_{burst}, mean RMS magnitude during the higher activity phase; RMS_{cycle}, mean RMS magnitude for one complete cycle (from 0 to 360°). ICC, intraclass correlation coefficient; SEM, standard error of measurement. GMax, *gluteus maximus*; SM, *semimembranosus*, BF, *Biceps femoris*; VM, *vastus medialis*; RF, *rectus femoris*; VL, *vastus lateralis*; GM, *gastrocnemius medianus*; GL, *gastrocnemius lateralis*; SOL, *soleus* and TA, *tibialis anterior*.

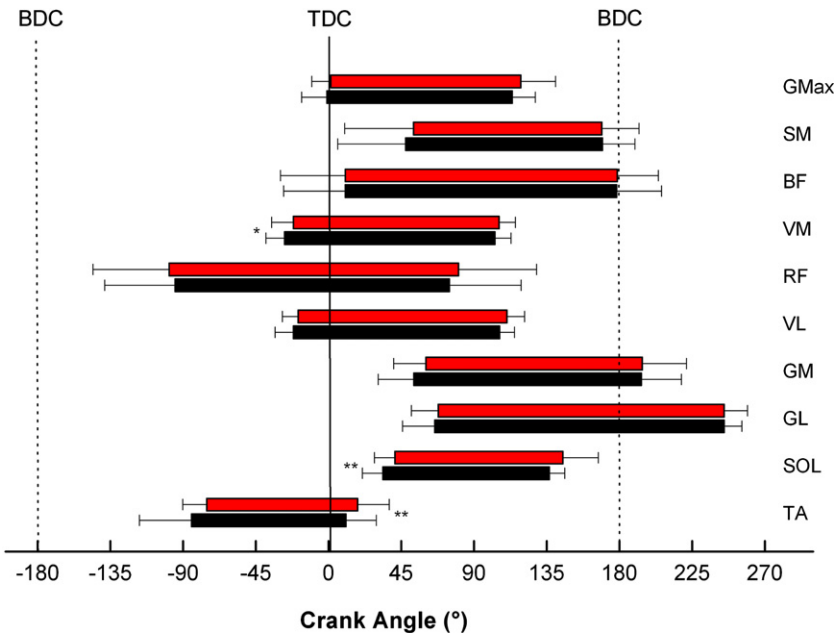

Fig. 2. Mean onset, offset and duration of higher EMG activity phase indicated by bars for the 10 muscles, displayed as a function of crank position. The second burst observed for some muscles and some subjects are voluntary not represented. TDC, top dead centre (0°); BDC, bottom dead centre (180°). Black bars: test; red bars: retest. $^{**}p < 0.01$, $^{*}p < 0.05$ significant difference between test and retest. (For interpretation of the references in colour in this figure legend, the reader is referred to the web version of this article.)

Table 3
Repeatability of the onset and the offset of the EMG bursts between test and retest

Muscles	Onset			Offset		
	p	SEM (°)	ICC	*p*	SEM (°)	ICC
GMax	NS	5.6	0.84	NS	7.3	0.63
SM	NS	5.2	0.98	NS	7.0	0.90
BF	NS	8.1	0.96	NS	12.5	0.78
VM	*	3.6	0.92	NS	3.5	0.88
RF	NS	11.9	0.93	NS	8.5	0.97
VL	NS	6.1	0.66	NS	6.9	0.54
GM	NS	7.9	0.86	NS	5.2	0.96
GL	NS	3.3	0.97	NS	13.7	−0.11
SOL	**	3.7	0.92	NS	15.7	0.14
TA	NS	16.1	0.59	**	4.6	0.94

Onset, Offset: starting crank angle and end crank angle of the higher activity phase. ICC, intra-class correlation coefficient; SEM, standard error of measurement; NS, no significant difference between test and retest; $^{**}p < 0.01$. $^{*}p < 0.05$ significant difference between test and retest. Mean values (SD) and bias are voluntary not depicted (see Fig. 2). GMax, *gluteus maximus*; SM, *semimembranosus*, BF, *Biceps femoris*; VM, *vastus medialis*; RF, *rectus femoris*; VL, *vastus lateralis*; GM, *gastrocnemius medianus*; GL, *gastrocnemius lateralis*; SOL, *soleus* and TA, *tibialis anterior*.

Table 4
Cross-correlation coefficients between EMG curves obtained for test and retest

Muscles	Cross-correlation coefficient (*r*)
	Test *vs.* retest
GMax	0.974
SM	0.977
BF	0.971
VM	0.988
RF	0.942
VL	0.984
GM	0.981
GL	0.971
SOL	0.970
TA	0.961

GMax, *gluteus maximus*; SM, *semimembranosus*, BF, *Biceps femoris*; VM, *vastus medialis*; RF, *rectus femoris*; VL, *vastus lateralis*; GM, *gastrocnemius medianus*; GL, *gastrocnemius lateralis*; SOL, *soleus* and TA, *tibialis anterior*.

4.2. Muscle activity level

When the test–retest repeatability indices of EMG activity level for all the muscles were compared, it was interesting to note there were no different trends between RMS_{cycle} and RMS_{burst} (Table 2). Since the pilot work performed by Houtz and Fischer (1959), only few studies have reported the reproducibility of EMG quantitative variables during pedaling. Bigland-Ritchie and Woods (1976) mentioned a high day to day reproducibility of the VL EMG amplitude but this observation was made only in two subjects. More recently, Gamet et al. (1996) reported a good week-to-week reproducibility of the profile of the total power spectrum (PEMG) recorded in RF during an incremental cycling exercise performed until exhaustion. Using a similar exercise protocol, Laplaud et al. (2006) demonstrated the good reproducibility of the activity level of eight lower limb muscles. Our results are in line with these studies reporting high ICC for both RMS_{cycle} and RMS_{burst} values. However, as showed in the previous studies, RF seems to be one of the least reproducible muscles. This phenomenon could be partly attributed to kinesiological differences, as RF is

a biarticular muscle involved in both leg extension and thigh flexion. Nevertheless, GMax and to a lesser extent SOL which are monoarticular muscles are also lesser repeatable. Keeping in mind that GMax is weakly activated at low power outputs (Ericson, 1986), our results also suggest an irregular recruitment of this muscle. However, it is important to note that these results only reflect the repeatability of surface EMG during a cycling exercise performed at a sub-maximal power output (150 W). Based on the results of the study of Laplaud et al. (2006) it remains difficult to evidence a clearly trend of SEM values in actual units to increase or decrease with power alteration. In the present study, SEM was expressed in actual units and in percentage of the grand mean (%SEM) in Table 2. Thus, one would put forth the hypothesis that %SEM reported here for all the muscles would be surestimated at this low intensity (almost 40% of MAP) compared to a higher. It could also partly explain the higher values of SEM in % of the RMS obtained for GMax and RF in comparison to other more activated muscles. Further studies are required to investigate whether the repeatability indices as a whole and particularly SEM% could be still better for exercise performed at higher power outputs.

4.3. Muscle activation timing

To examine the pattern of muscles activation, important variables of interest are the starting (onset) and ending (offset) crank angles of the EMG bursts. Despite the majority of the 10 muscles displayed a good repeatability for these variables, three muscles showed significant differences for onset (VM, SOL) or offset values (TA). However, as illustrated in Fig. 2 and statistically confirmed, these small differences in onset and offset (ranged 0.1–7.5° of crank rotation) did not lead to any significant modifications of the burst duration whatever the muscle considered. ICC and SEM values also showed fair and sometimes poor repeatability of the onset and/or offset for some muscles (Table 3).

In the present study, a threshold of 20% of the peak EMG was voluntary kept constant for all detections. Despite this value is in accordance with the literature, some methodological limitations remain concerning the identification of onset and offset of the bursts. Indeed, as well demonstrated by Li and Caldwell (1999), this identification could be disputable with some EMG patterns and dependant of the threshold level. In this line, it would be expected a better repeatability of these variables if the threshold value would have been visually adjusted and raised in the cases for which threshold was considered inappropriate (Li and Caldwell, 1998; Duc et al., 2006). Whatever the algorithms used for onset/offset times determination (Dankaerts et al., 2004; Morey-Klapsing et al., 2004), it remains difficult to dissociate natural variability of the EMG pattern and that inherent to the measurement method of these variables. Thus, as argued by some authors (Li and Caldwell, 1998; Li and Caldwell, 1999; Wren et al., 2006), the recent use of the cross-correlation could give a better objective estimation of the similarity of muscle activity patterns between two conditions. Using this method, we found high cross-correlation coefficients for all the muscles suggesting a good repeatability of the EMG pattern. Nevertheless, it is interesting to note that the lowest correlation scores were obtained for the muscles which also showed poor repeatability for onset and offset values (*i.e.* RF, TA and SOL).

4.4. Strategies of muscles activation

It is noteworthy that stable locomotion may be achieved despite significant variability in the muscle recruitment patterns (Bernstein, 1967). In this line, we previously reported heterogeneity of muscle recruitment pattern during pedaling in a population of highly trained cyclists (Hug et al., 2004). As mentioned in the "results" section, we found high interindividual differences concerning the EMG patterns for GL, TA and SOL muscles (*i.e.* one or two EMG bursts during the cycle), suggesting a relative heterogeneity of these muscle recruitment patterns. However, these inter-subject differences were observed in the same way for test and retest conditions. Associated with the good repeatability for all muscles mentioned above, it supports the hypothesis that each subject adopts a personal muscle activation strategy in a course of a sub-maximal pedaling exercise.

A better understanding of the fact that repeatability is not high as expected for some muscles (GMax and RF for instance) can be gained by placing that within the context of the complexity of the muscle coordination strategies (van Soest et al., 1993; Li and Caldwell, 1998). Based on knowledge and hypothesis about coordination or coactivation of lower limb muscles during pedaling, recruitment strategies of the different muscle groups as well as of the muscles sharing the same biomechanical function are unlimited. Therefore, small differences in the EMG pattern could be related not only to subject-specific pedaling techniques (inter-subjects variability) but also to a natural variation of this strategy over time for a given subject. Fig. 3 illustrates an example of the relative compensation appeared from test to retest condition between the activation patterns of three leg muscles composing the triceps surae (especially between GL and SOL in this case). This phenomenon leads to a very high repeatability of EMG pattern of the equivalent ankle extensor muscle group (Ankle-Ext, representing the sum of EMG patterns of GL, GM and SOL) which hence confirms the great stability of the functional role of these specific muscles. By extending this reflexion to our entire population and to the main muscles, ICC and SEM values were calculated for the quantitative EMG variables of the following muscle groups (Table 5): knee flexors (Knee-Flex: BF+SM), knee extensors (Knee-Ext-Tot: VL+VM+RF and Knee-Ext-Mono: VL+VM), and ankle extensors (Ankle-Ext: GM+GL+SOL). Despite the choice and the composition of muscles groups proposed here cannot be considered as exhaustive and cannot take

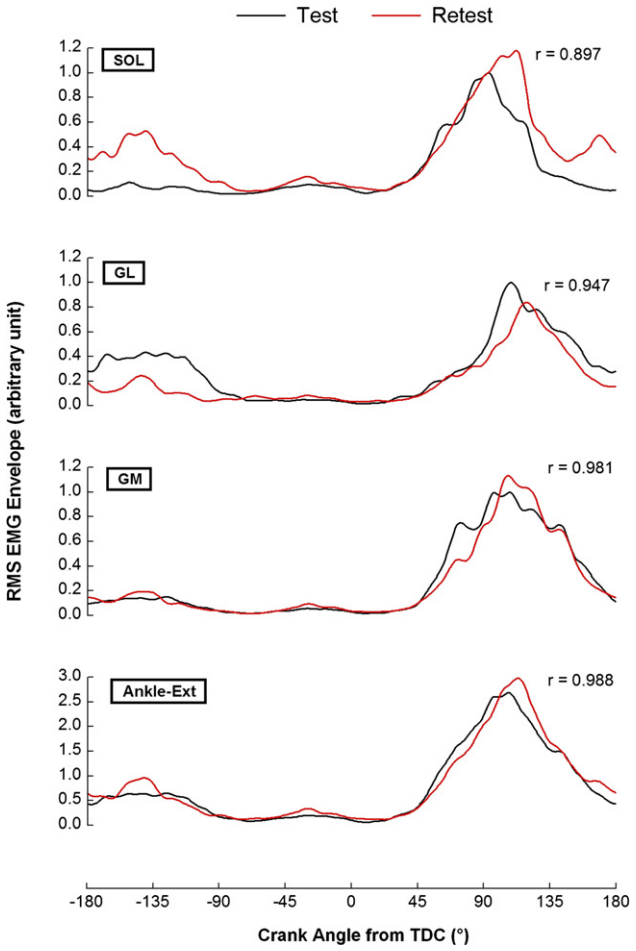

Fig. 3. Typical curves of RMS EMG envelope for each ankle extensor muscle (SOL, GL, GM) for test (in black) and retest (in red) conditions. The last graphic represents the soma of the three previous envelopes (Ankle-Ext). All the curves used same arbitrary unit on vertical axes (the first and second tests are normalized to maximal EMG obtained during the first test). Note the relative compensation between the activities of SOL and GL during the downstroke phase (45–180°) as well as during the first part of the upstroke phase (−180 to −90°) leading to a great similarity in the global activity pattern of the ankle extensor muscles group (Ankle-Ext). (For interpretation of the references in colour in this figure legend, the reader is referred to the web version of this article.)

into account all the complexity of muscle coordination, it is interesting to note the very low values of SEM (8.1–11.6%) and very high values of ICC (0.89–0.95) for all the muscles groups considered. The ICC and SEM values obtained for all muscles groups appears better than the values of each muscle considered individually. For instance we can note the very good value obtained for Knee-Ext-Tot (at least equivalent to the values of Knee-Ext-Mono) while this group included RF which showed one of the weakest repeatability. As a whole, these results can clearly be considered as an evidence for the compensation that seems to occur between the muscles of a same group and/or playing the same functional role in pedaling action. Accordingly, these results comfort the fact that recording the main lower limbs muscles (*i.e.* not only one agonist–antagonist pair of muscles per articulation) seems to be advised in future studies to give reliable information about potential modification in muscle coordination during cycling. It would be interesting in future studies to interpret the EMG patterns by also considering the possible alteration in mechanical aspects of the cycling task (orientation of the force on the pedals, relative compensation between the two limbs...).

Table 5
Repeatability of the selected RMS measurements of muscle activities, between test and retest, for the different muscles grouped in terms of their function: knee flexors, knee extensors and ankle extensors muscles groups

Muscles	$Mean_{burst}$			$Mean_{cycle}$		
	SEM		ICC	SEM		ICC
	μV	%		μV	%	
Knee-Flex	13.8	10.3	0.95	4.7	8.1	0.95
Knee-Ext-Tot	32.7	9.1	0.90	15.8	10.5	0.89
Knee-Ext-Mono	31	9.9	0.90	14.8	11.6	0.89
Ankle-Ext	32.8	10	0.94	14	9.3	0.94

$Mean_{burst}$ mean EMG magnitude during the higher activity phase; $Mean_{cycle}$ mean EMG magnitude for 1 cycle. ICC, intra-class correlation coefficient; SEM, standard error of measurement (absolute value or expressed as a percentage of the grand mean across trials). Knee-Flex: BF+SM; Knee-Ext-Tot: VL+VM+RF; Knee-Ext-Mono: VL+VM; Ankle-Ext: SOL+GM+GL.

4.5. Conclusion

The challenge of interpreting dynamic EMG is complicated by variability in the data. For this reason, it is important to recognize the natural variability associated with these physiological signals during pedaling in order to improve the interpretation of EMG activity. For instance, the knowledge about this EMG patterns repeatability may help for the interpretation of the numerous studies which focused on the changes of EMG burst duration and/or muscle activation timing in response to physiological (*i.e.* fatigue, exercise intensity) or mechanical (*i.e.* pedaling rate, bicycle geometry, body orientations...) constraints. It could be considered extending this study to spectral indices of the EMG signals.

Acknowledgements

This study was funded in part by "La fondation d'entreprise de la Française Des Jeux" and the French Ministry of Sport. The authors are grateful for the subjects for having accept to participate in this study.

References

Bernstein N. Coordination and regulation of movements. Pergamon Press; 1967.
Bigland-Ritchie B, Woods JJ. Integrated electromyogram and oxygen uptake during positive and negative work. J Physiol 1976;260:267–77.
Currier D. Elements of research in physical therapy. Baltimore; 1990.
Dankaerts W, O'Sullivan PB, Burnett AF, Straker LM, Danneels LA. Reliability of EMG measurements for trunk muscles during maximal and sub-maximal voluntary isometric contractions in healthy controls and CLBP patients. J Electromyogr Kinesiol 2004;14:333–42.

Dedering A, Roos af Hjelmsater M, Elfving B, Harms-Ringdahl K, Nemeth G. Between-days reliability of subjective and objective assessments of back extensor muscle fatigue in subjects without lower-back pain. J Electromyogr Kinesiol 2000;10:151–8.
Duc S, Bertucci W, Pernin JN, Grappe F. Muscular activity during uphill cycling: effect of slope, posture, hand grip position and constrained bicycle lateral sways. J Electromyogr Kinesiol 2006, in press. doi:10.1016/j.jelekin.2007.09.007.
Duc S, Villerius V, Bertucci W, Pernin JN, Grappe F. Muscular activity level during pedalling is not affected by crank inertial load. Eur J Appl Physiol 2005;95:260–4.
Ericson M. On the biomechanics of cycling. A study of joint and muscle load during exercise on the bicycle ergometer. Scand J Rehabil Med 1986;16:1–43.
Falla D, Dall'Alba P, Rainoldi A, Merletti R, Jull G. Repeatability of surface EMG variables in the sternocleidomastoid and anterior scalene muscles. Eur J Appl Physiol 2002;87:542–9.
Farina D, Merletti R, Enoka RM. The extraction of neural strategies from the surface EMG. J Appl Physiol 2004;96:1486–95.
Gamet D, Duchene J, Goubel F. Reproducibility of kinetics of electromyogram spectrum parameters during dynamic exercise. Eur J Appl Physiol Occup Physiol 1996;74:504–10.
Hermens HJ, Freriks B, Disselhorst-Klug C, Rau G. Development of recommendations for SEMG sensors and sensor placement procedures. J Electromyogr Kinesiol 2000;10:361–74.
Hettinga FJ, De Koning JJ, Broersen FT, Van Geffen P, Foster C. Pacing strategy and the occurrence of fatigue in 4000-m cycling time trials. Med Sci Sports Exerc 2006;38:1484–91.
Hopkins WG. Measures of reliability in sports medicine and science. Sports Med 2000;30:1–15.
Houtz SJ, Fischer FJ. An analysis of muscle action and joint excursion during exercise on a stationary bicycle. J Bone Joint Surg Am 1959;41-A:123–31.
Hug F, Bendahan D, Le Fur Y, Cozzone PJ, Grelot L. Heterogeneity of muscle recruitment pattern during pedaling in professional road cyclists: a magnetic resonance imaging and electromyography study. Eur J Appl Physiol 2004;92:334–42.
Jorge M, Hull ML. Analysis of EMG measurements during bicycle pedaling. J Biomech 1986;19:683–94.
Kankaanpaa M, Taimela S, Laaksonen D, Hanninen O, Airaksinen O. Back and hip extensor fatigability in chronic low back pain patients and controls. Arch Phys Med Rehabil 1998;79:412–7.
Laplaud D, Hug F, Grelot L. Reproducibility of eight lower limb muscles activity level in the course of an incremental pedaling exercise. J Electromyogr Kinesiol 2006;16:158–66.
Lariviere C, Arsenault AB, Gravel D, Gagnon D, Loisel P, Vadeboncoeur R. Electromyographic assessment of back muscle weakness and muscle composition: reliability and validity issues. Arch Phys Med Rehabil 2002;83:1206–14.
Larsson B, Karlsson S, Eriksson M, Gerdle B. Test–retest reliability of EMG and peak torque during repetitive maximum concentric knee extensions. J Electromyogr Kinesiol 2003;13:281–7.
Larsson B, Mansson B, Karlberg C, Syvertsson P, Elert J, Gerdle B. Reproducibility of surface EMG variables and peak torque during three sets of ten dynamic contractions. J Electromyogr Kinesiol 1999;9:351–7.
Li L, Caldwell GE. Muscle coordination in cycling: effect of surface incline and posture. J Appl Physiol 1998;85:927–34.
Li L, Caldwell GE. Coefficient of cross correlation and the time domain correspondence. J Electromyogr Kinesiol 1999;9:385–9.
Lucia A, San Juan AF, Montilla M, CaNete S, Santalla A, Earnest C, et al. In professional road cyclists, low pedaling cadences are less efficient. Med Sci Sports Exerc 2004;36:1048–54.
Morey-Klapsing G, Arampatzis A, Bruggemann GP. Choosing EMG parameters: comparison of different onset determination algorithms and EMG integrals in a joint stability study. Clin Biomech (Bristol, Avon) 2004;19:196–201.
Perrey S, Grappe F, Girard A, Bringard A, Groslambert A, Bertucci W, et al. Physiological and metabolic responses of triathletes to a simulated 30-min time-trial in cycling at self-selected intensity. Int J Sports Med 2003;24:138–43.
Rainoldi A, Galardi G, Maderna L, Comi G, Lo Conte L, Merletti R. Repeatability of surface EMG variables during voluntary isometric contractions of the biceps brachii muscle. J Electromyogr Kinesiol 1999;9:105–19.
Reinhard U, Muller PH, Schmulling RM. Determination of anaerobic threshold by the ventilation equivalent in normal individuals. Respiration 1979;38:36–42.
Shannon CE. Communication Theory of secrecy systems. Bell Syst Tech J 1949;28:656–715.
Sleivert GG, Wenger HA. Reliability of measuring isometric and isokinetic peak torque, rate of torque development, integrated electromyography, and tibial nerve conduction velocity. Arch Phys Med Rehabil 1994;75:1315–21.
van Soest AJ, Schwab AL, Bobbert MF, van Ingen Schenau GJ. The influence of the biarticularity of the gastrocnemius muscle on vertical-jumping achievement. J Biomech 1993;26:1–8.
Wren TA, Patrick Do K, Rethlefsen SA, Healy B. Cross-correlation as a method for comparing dynamic electromyography signals during gait. J Biomech 2006;39:2714–8.

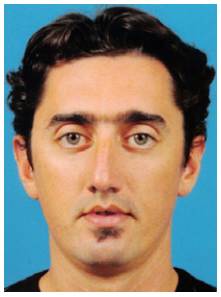

Sylvain Dorel received his Ph.D. in "Motor Function in Human" from the University of St-Etienne, France in December 2004 (Laboratory of Physiology, PPEH, St-Etienne and Laboratory of Biomechanics and Human Modeling, LBMH, Lyon). After a post-doctoral position at the University Lyon I as a teaching and research assistant (CRIS), he is currently researcher at the National Institute for Sports (INSEP), Paris, France. His research interests focus on the neuromuscular adaptations, mechanical characteristics (kinetics and kinematics), and performance (i) during maximal cycling exercise and (ii) during sub-maximal exercise in response to the occurrence of fatigue or in relation with alterations of the posture or material.

Antoine Couturier received his Ph.D. in Biomedical Engineering from the University of Lyon I, France in June 1999. He is a research engineer at the National Institute for Sports (INSEP), Paris, France. His work essentially focuses on signal processing, software development and electronics.

François Hug received his Ph.D. from the university of Aix-Marseille II, France in December 2003. In 2004–2005, he was in a post-doctoral position at the University Paris VI (Laboratory of Respiratory Physiopathology), France. In 2005–2006, he was researcher at the National Institute for Sports (INSEP), France. He is currently assistant professor at the University of Nantes (Laboratory Motricity, Interactions, Performance), France. He has published four national and seventeen international papers in peer-review periodicals. His research interests focus on (1) the metabolic and neuromuscular adaptations of trained cyclists, (2) the neuromuscular adaptations to fatigue and (3) EMG activity of respiratory muscles submitted to mechanical/metabolic loads.

Eur J Appl Physiol (2008) 104:667–678
DOI 10.1007/s00421-008-0810-y

ORIGINAL ARTICLE

Interindividual variability of electromyographic patterns and pedal force profiles in trained cyclists

François Hug · Jean Marc Drouet · Yvan Champoux · Antoine Couturier · Sylvain Dorel

Accepted: 18 June 2008 / Published online: 16 July 2008

Abstract The aim of this study was to determine whether high inter-individual variability of the electromyographic (EMG) patterns during pedaling is accompanied by variability in the pedal force application patterns. Eleven male experienced cyclists were tested at two submaximal power outputs (150 and 250 W). Pedal force components (effective and total forces) and index of mechanical effectiveness were measured continuously using instrumented pedals and were synchronized with surface electromyography signals measured in ten lower limb muscles. The intersubject variability of EMG and mechanical patterns was assessed using standard deviation, mean deviation, variance ratio and coefficient of cross-correlation ($\overline{R_0}$, with lag time = 0). The results demonstrated a high intersubject variability of EMG patterns at both exercise intensities for biarticular muscles as a whole (and especially for Gastrocnemius lateralis and Rectus femoris) and for one monoarticular muscle (Tibialis anterior). However, this heterogeneity of EMG patterns is not accompanied by a so high intersubject variability in pedal force application patterns. A very low variability in the three mechanical profiles (effective force, total force and index of mechanical effectiveness) was obtained in the propulsive downstroke phase, although a greater variability in these mechanical patterns was found during upstroke and around the top dead center, and at 250 W when compared to 150 W. Overall, these results provide additional evidence for redundancy in the neuromuscular system.

Keywords Pedaling · Heterogeneity · Mechanical · Electromyography · Muscle · Redundancy

F. Hug · A. Couturier · S. Dorel (✉)
Research Mission, Laboratory of Biomechanics and Physiology, National Institute for Sports and Physical Education (INSEP), 11 Avenue du Tremblay, 75012 Paris, France
e-mail: sylvain.dorel@insep.fr

F. Hug
Laboratory "Motricity, Interactions, Performance" (EA 4334), University of Nantes, Nantes Atlantic Universities, 44000 Nantes, France
e-mail: francois.hug@univ-nantes.fr

J. M. Drouet · Y. Champoux
VélUS Group, Department of Mechanical Engineering, Université de Sherbrooke, Sherbrooke, QC J1K2R1, Canada

Introduction

Variability in human movement has been the focus of numerous studies across multiple disciplines within the movement sciences. It is well documented that the nervous system has multiple ways of accomplishing a given motor task (Bernstein 1967). At the muscle level, there are multiple synergists as well as various combinations of agonist/antagonists that can contribute to the same end-effector trajectory and force pattern (van Bolhuis and Gielen 1999). This motor redundancy suggests that the nervous system could use different muscle activation patterns for a given movement.

Cycling task represents a typical multijoint movement characterized by several degrees of freedom. In contrast with other movements, the constant circular trajectory of the pedal constrains lower extremity displacement. Despite that, some studies have reported a high variability of electromyographic (EMG) patterns even when in trained cyclists (Ryan and Gregor 1992; Hug et al. 2004). Ryan and Gregor (1992) showed two distinct EMG patterns for the biceps femoris muscle within a population of 18 experienced cyclists (no other details about the training status of the subjects were mentioned). This study also pointed out

interindividual differences of the EMG patterns of ten lower limb muscles, especially apparent for biarticular muscles compared to monoarticular ones. Using two complementary techniques (surface EMG and functional magnetic resonance imaging) and using only quantitative analysis (i.e., mean RMS values across seven crank revolutions), Hug et al. (2004) confirmed these results showing that the high degree of expertise of professional road cyclists is not linked to the production of a common activation pattern of lower limb muscles. Striking differences in the level of activation among these expert cyclists were also observed for biarticular muscles: rectus femoris and semimembranosus.

From a mechanical standpoint, it is interesting to note that, for a given power output–pedaling rate combination, the effective force (or torque) profile as a function of the crank angle appears to be stereotypical (Gregor et al. 1985; van Ingen Schenau et al. 1992; Sanderson et al. 2000). On the other hand, it has been suggested that substantial differences exist between subjects regarding their power generation techniques (Gregor et al. 1991). To characterize the biomechanics of force application, it is important to note that the effective force (i.e., that which acts perpendicular to the bicycle crank and thus drives the crank around in its circle) represents only one component of the total force produced at the shoe/pedal interface. On the sagittal plane, a second ineffective component of the resultant force acts along the crank, and thus performs no useful external work (Fig. 1, Hull and Davis 1981). Instrumented pedals developed since 1970s (Dal Monte et al. 1973) offer the possibility of determining both components and allow the index of mechanical effectiveness (IE), defined as the ratio of the effective force to the total force exerted by the foot on the pedal (LaFortune and Cavanagh 1983), to be calculated. However, there is a lack of information concerning the intersubject variability of the index of mechanical effectiveness and total resultant force throughout the cycle. Finally, to our knowledge, no previous study has focused on the putative interindividual differences in all of these mechanical profiles as well as on the EMG patterns of the main lower limb muscles in the same population.

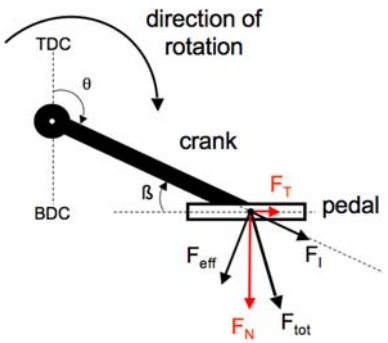

Fig. 1 Representation of the various forces applied on the pedal on a sagittal plane. Total force (F_{tot}) produced at the shoe/pedal interface is decomposed into two components: **a** effective force (F_{eff}) acts perpendicular to the bicycle crank and thus drives the crank around in its circle; **b** ineffective component (F_I) acts along the crank, and thus performs no useful external work. F_T and F_N, tangential and normal components of F_{tot} on the pedal

Thus, the purpose of the present study was to determine whether the relatively high interindividual variability in EMG patterns during pedaling is accompanied by variability in the pedal force application patterns. It was hypothesized that, in a population of trained cyclists, forces and IE profiles would exhibit a lower intersubject variability compared to EMG patterns. Cyclists were tested at two submaximal power outputs (i.e., 150 and 250 W). Pedal force components were measured continuously using instrumented pedals and were then synchronized with surface electromyography signals measured in ten lower limb muscles.

Methods

Subjects

Eleven male experienced cyclists whose anthropometrical and physiological characteristics are presented in Table 1 volunteered to participate in this study. The subjects had 8.5 ± 3 years of competitive experience. During the last season before the experimentation, they have covered an average of 14,000 ± 4,333 km. None of them had recent or ancient pathology of lower limb muscles or joints. They were informed of the possible risk and discomfort associated with the experimental procedures before they gave their written consent to participate. The experimental design of the study was approved by the Ethical Committee of Saint-Germain-en-Laye (acceptance no. 06016) and was done in accordance with the Declaration of Helsinki.

Exercise protocol

The testing protocol consisted of two sessions conducted in the following order: (1) incremental cycling exercise

Table 1 Anthropometric and physical characteristics of the subjects

	Mean ± SD	CV
Age (years)	20.5 ± 3.4	0.166
Height (cm)	180.6 ± 5.9	0.033
Body mass (kg)	68.5 ± 6.6	0.096
BMI (kg m^{-2})	21.0 ± 2.1	0.100
$\dot{V}O_{2\,max}$ (mL min^{-1} kg^{-1})	67.1 ± 9.2	0.137
MPT (Watts)	410.9 ± 30.1	0.073
MAP (Watts)	391.0 ± 22.3	0.057

BMI body mass index, *CV* Coefficient of variation, *MPT* maximal power tolerated, *MAP* maximal aerobic power, $\dot{V}O_{2max}$ maximal oxygen uptake

performed until exhaustion to characterize the population in terms of physical and physiological capacities; (2) experimental session consisting of two submaximal pedaling exercises.

During the first visit, in the 2 weeks preceding the experimental session, each subject performed an incremental cycling exercise (workload increments of 25 W min^{-1}; starting at 100 W) during which the usual respiratory and ventilatory parameters were measured breath-by-breath (K4B2, Cosmed®, Italy). The first power output achieved when the maximal oxygen uptake was reached ($\dot{V}O_{2\,max}$) was referred as the maximal aerobic power (MAP). Maximal power tolerated (MPT) was referred as the last stage entirely completed.

During the second session, subjects were asked, after a 10 min warm-up at 100 W, to pedal at 150 W for 6 min. This bout was immediately followed by a second one performed at 250 W for 3 min. Because of the training status of the subjects, the low workload level (i.e., 150 and 250 W representing about 38 and 63% of MAP, respectively) and the short duration of the exercises, this protocol was considered as nonfatiguing. For each of these two intensities, subjects were asked to keep a constant pedaling rate fixed at 95 rpm (±5 rpm). This value was chosen, because it represents the mean pedaling rate (94.6 ± 4.2 rpm) freely adopted by the subjects at the end of the warm-up of the incremental cycling exercise. One among the twelve cyclists (initially enrolled in the study) has not been included in this second session due to his higher pedaling rate (>2 SD from the mean). Surface electromyography and mechanical parameters were continuously recorded during this experimental session.

Material and data collection

Subjects exercised on an electronically braked cycle ergometer (Excalibur Sport, Lode®, Netherlands) equipped with standard crank (length = 170 mm) and with instrumented pedals described below. During both sessions, vertical and horizontal positions of the saddle, handlebar height and stem length were set to match the usual racing position of the participants (i.e., dropped posture).

A pedal dynamometer specifically designed for pedaling load measurements by VélUS group (Department of Mechanical Engineering, Sherbrooke University, Canada) was used to collect mechanical data. The instrumented pedal is compatible with LOOK CX7 clipless pedal using LOOK Delta cleat. The sagittal plane components of the total reaction force (F_{tot}) applied at the shoe/pedal interface were measured by using a series of eight strain gauges located within each pedal. F_{tot} was calculated from the measured Cartesian components (F_T, F_N) corresponding for the pedal to the horizontal forward and vertical upward forces, respectively (Fig. 1). Static calibration was performed by applying sequentially three degrees of freedom force and moment loads to measure the direct sensitivity (F_T and F_N) and both the calibratable and noncalibratable cross-sensitivity (Rowe et al. 1998). The maximum nonlinearity for both measured components is less than 0.4% full scale (FS) and the maximum hysteresis is less than 0.8% FS. Calibration revealed an error less than 0.7% FS when only the measured force components were applied. Application of unmeasured load components created an error less than 0.8% FS. An optical encoder with a resolution of 0.4° mounted on the pedal measured pedal angle (β) with respect to the crank orientation. A zero adjustment for both components of force and pedal angle was done before each session. The crank angle (θ) was calculated based on TTL pulses delivered each 2° by the cycle ergometer. Additional TTL pulse permitted to detect the bottom dead center of the right pedal (i.e., BDC: lowest position of the right pedal with crank arm angle = 180°). All these data were digitized at a sampling rate of 2 kHz (USB data acquisition, ISAAC instruments®, Québec, Canada) and stored on a computer.

Surface EMG activity was continuously recorded for the following ten muscles of the right lower limb: gluteus maximus (GMax), semimembranosus (SM), biceps femoris (BF), vastus medialis (VM), rectus femoris (RF), vastus lateralis (VL), gastrocnemius medialis (GM) and lateralis (GL), soleus (SOL) and tibialis anterior (TA). A pair of surface Ag/AgCl electrodes (Blue sensor, Ambu®, Denmark) was attached to the skin with a 2 cm interelectrode distance. The electrodes were placed longitudinally with respect to the underlying muscle fibers arrangement and located according to the recommendations by SENIAM (Surface EMG for Non-Invasive Assessment of Muscles) (Hermens et al. 2000). Prior to electrode application, the skin was shaved and cleaned with alcohol to minimize impedance. The wires connected to the electrodes were well secured with adhesive tape to avoid movement-induced artifacts. Raw EMG signals were preamplified close to the electrodes (gain 375, bandwidth 8–500 Hz), and simultaneously digitized with BDC TTL pulses at a sampling rate of 1 kHz (ME6000P16, Mega Electronics Ltd®, Finland).

Data processing

All data were analyzed with two custom-written scripts (Matlab, MathWorks®, USA, for mechanical data; and Origin 6.1, OriginLab Corporation®, USA, for EMG data and final processing). All mechanical data were smoothed by a 10 Hz third-order Butterworth low pass filter. Based on components F_N and F_T and pedal angle (β), F_{tot} was calculated by trigonometry and resolved into two components: one orthogonal to the crank (effective force F_{eff}) and another along the crank (ineffective force F_I). Instantaneous

index of mechanical effectiveness (IE) was determined as the ratio of the effective force to the total applied force at each point in the pedaling cycle (Sanderson 1991; Sanderson and Black 2003). A high pass filter (20 Hz) was applied on the EMG signals (Chart 5.4, AD instruments®, Hasting, UK) to diminish movement artifacts. EMG data were root-mean-squared (RMS) over a 25 ms moving window to produce linear envelope for each muscle activity pattern.

The BDC TTL pulses were used to synchronize EMG and mechanical signals of the right pedal. According to the procedure previously described (Dorel et al. 2008a, b), all data were smoothed, resampled (one value each one degree) and averaged over 30 consecutive pedaling cycles to get a representative mechanical profile (pedal forces and IE) and EMG RMS linear envelope for each muscle, each subject and each condition (i.e., 150 and 250 W). These values were expressed as a function of the crank arm angle as it rotated from the highest pedal position (0°, top dead center, TDC) to the lowest (180°, bottom dead center, BDC) and back to TDC to complete a 360° crank cycle. Except for the index of effectiveness (which is already expressed as a percentage), all the mechanical and EMG patterns were then normalized to the mean value calculated over the complete pedaling cycle as advised by various authors (Yang and Winter 1984; Shiavi et al. 1986, 1987; Burden et al. 2003). Finally, mean ensemble curves of EMG and mechanical patterns were calculated over the 11 subjects from these individual normalized patterns.

Assessment of interindividual variability

Measurements of the standard deviation (SD) of the mean ensemble curves have been used to define the amount of interindividual variability of the EMG and mechanical patterns as previously done for other locomotive patterns (Winter and Yack 1987; Ryan and Gregor 1992; Dingwell et al. 1999). The larger the distance between the mean + SD curve and the mean curve, the greater the variability in the EMG/mechanical pattern. Variability among subjects was also estimated calculating mean deviation (MD, Eq. 1) and variance ratio (VR, Eq. 2) over the complete cycle according to the following equations:

$$\mathrm{MD} = \frac{\sum_{i=1}^{k} |\sigma_i|}{k} \quad (1)$$

$$\mathrm{VR} = \frac{\sum_{i=1}^{k} \sum_{j=1}^{n} \left(X_{ij} - \overline{X}_i\right)^2 \Big/ k(n-1)}{\sum_{i=1}^{k} \sum_{j=1}^{n} \left(X_{ij} - \overline{X}\right)^2 \Big/ (kn-1)} \quad (2)$$

with $\overline{X} = \frac{1}{k}\sum_{i=1}^{k} \overline{X}_i$ where k is the number of intervals over the pedaling cycle (i.e., 360), n is the number of participants (i.e., 11), $\overline{X_i}$ is the mean of the normalized EMG/mechanical values obtained at the ith interval calculated over the eleven participants, σ_i is the standard deviation of the normalized EMG/mechanical values about $\overline{X_i}$ and X_{ij} is the normalized EMG/mechanical value at the ith interval for the jth participant.

In addition to MD, VR has been recently reported as an alternative interesting index for assessing intrasubject and intersubject variability (Burden et al. 2003; Rouffet and Hautier 2007). The lower the MD and VR values are, the lesser the variability in the EMG/mechanical patterns is.

In addition to this overall analysis, one of these indexes (i.e., VR) was also calculated for four functional angular sectors over the entire pedaling cycle (by adjusting the k value) to identify regions of greatest variability. For mechanical data, the following sectors were chosen: sector 1 represented 330°–30°; sector 2, 30°–150°; sector 3, 150°–210°; sector 4, 210°–330° (Fig. 2). From a functional point, sectors 1 and 3 correspond, respectively, to the top and bottom dead centers; sectors 2 and 4 correspond, respectively, to the main propulsive and recovery phases. Assuming a relatively constant delay (called electromechanical delay, EMD) of 50 ms (Cavanagh and Komi 1979) between the electrical event (i.e., EMG activity) and the related mechanical output (i.e., force), the angular sectors used for EMG data were shifted 28° earlier (i.e., the crank angular displacement due to EMD at 95 rpm): sector 1 represented 302°–2°; sector 2, 2°–122°; sector 3, 122°–182°; sector 4, 182°–302° (Fig. 2). This shift for EMG data due to the EMD permits to compare the same functional sectors between EMG and mechanical data as recommended by Vos et al. (1990).

Cross-correlation has been used as a method for objectively comparing the timing and shape of two EMG or mechanical patterns (Li and Caldwell 1999; Wren et al. 2006; Dorel et al. 2008a, b). The coefficient of cross-correlation ($\overline{R_0}$, with lag time = 0) was determined for each

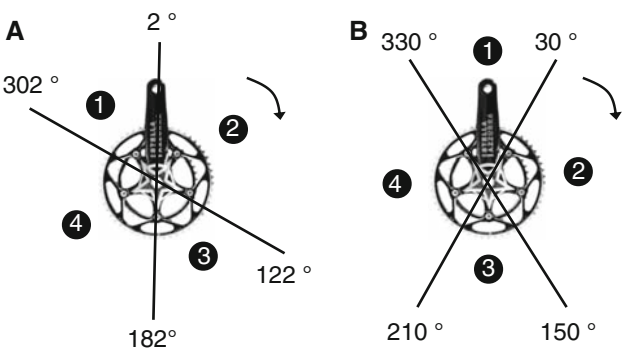

Fig. 2 Representation of the different angular sectors used for EMG (**a**) and mechanical (**b**) analysis. To compare the same (or approximatively the same) functional sectors between EMG and mechanical data, angular sectors used for EMG take into account an electromechanical delay (i.e., 50 ms)

pair of individual EMG patterns obtained for a given muscle and each pair of mechanical curves (i.e., number of combination: ${}_nC_2 = {}_{11}C_2 = 55$). Thus, in the perspective to characterize interindividual variability, a mean cross-correlation coefficient was calculated ($\overline{R_0}$ average of the 55 values) for each muscle and each mechanical variable (i.e., effective force, total force and index of mechanical effectiveness). Changing the magnitude of the curves without changing their shape does not affect $\overline{R_0}$ Higher $\overline{R_0}$ values indicated less variability in the shape and timing of the EMG/mechanical patterns (e.g., $\overline{R_0} = 1$ means that curves would exhibit exactly the same shape and timing).

Results

Average (±SD) EMG patterns for the ten muscles investigated are depicted in Figs. 3 and 4 (150 and 250 W, respectively). High interindividual variability is evident, especially for two biarticular muscles (GL and RF) and one

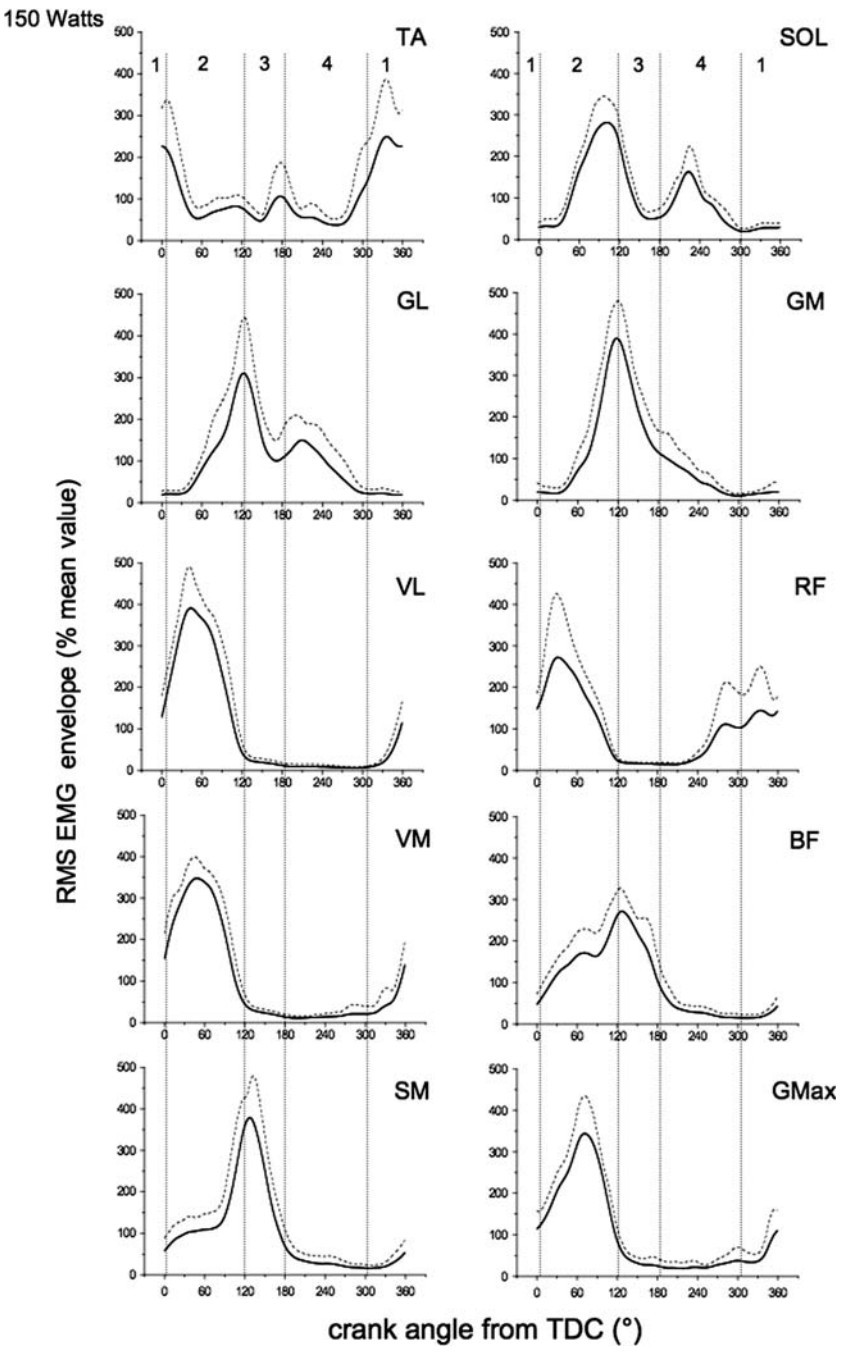

Fig. 3 RMS EMG envelope for ten lower limb muscles obtained during pedaling at 150 W. Each profile represents the mean (*solid line*) and the mean + standard deviation (*broken line*) obtained from averaging individual data across 30 consecutive pedaling cycle, normalizing to the mean RMS calculated over the complete pedaling cycle and further averaging across the 11 cyclists. *GMax* gluteus maximus, *SM* semimembranosus, *BF* biceps femoris, *VM* vastus medialis, *RF* rectus femoris, *VL* vastus lateralis, *GM* gastrocnemius medialis, *GL* gastrocnemius lateralis, *SOL* soleus, *TA* tibialis anterior. *Vertical lines* define the four angular sectors: *sector 1* (302°–2°), *sector 2* (2°–122°), *sector 3* (122°–182°), *sector 4* (182°–302°)

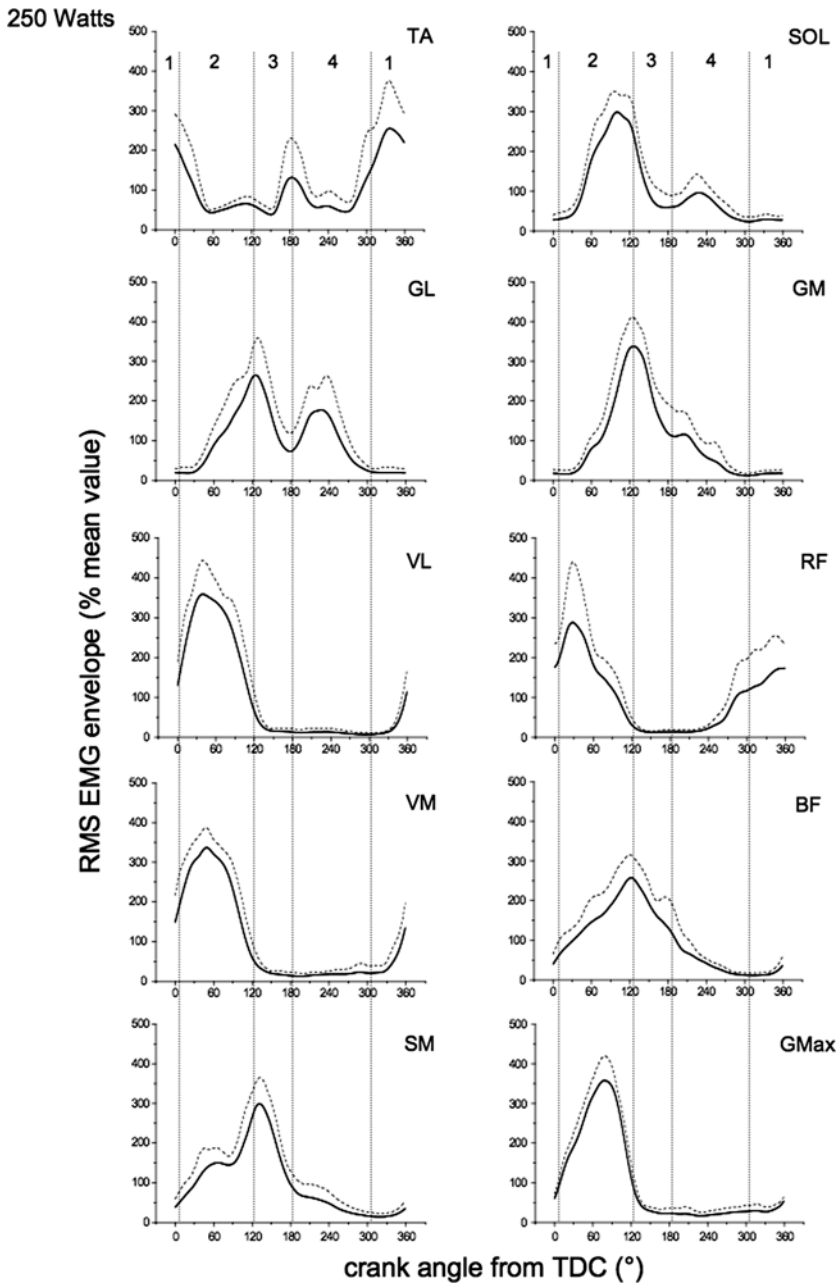

Fig. 4 RMS EMG envelope for ten lower limb muscles obtained during pedaling at 250 W. Each profile represents the mean (*solid line*) and the mean + standard deviation (*broken line*) obtained from averaging individual data across 30 consecutive pedaling cycle, normalizing to the mean RMS calculated over the complete pedaling cycle and further averaging across the 11 cyclists. *GMax* gluteus maximus, *SM* semimembranosus, *BF* biceps femoris, *VM* vastus medialis, *RF* rectus femoris, *VL* vastus lateralis, *GM* gastrocnemius medialis, *GL* gastrocnemius lateralis, *SOL* soleus, *TA* tibialis anterior. *Vertical lines* define the four angular sectors: *sector 1* (302°–2°), *sector 2* (2°–122°), *sector 3* (122°–182°), *sector 4* (182°–302°)

monoarticular muscle (TA). Overall, this result is confirmed by the lowest $\overline{R_0}$ and highest MD and VR for these three muscles (Fig. 5). Figure 6 depicts an exemple of two different patterns found in TA. Medium variability appeared for the three other biarticular muscles (BF, SM and GM). In contrast, low interindividual variability was found for the four monoarticular muscles (GMax, SOL, VL, VM) for which lower MD and VR and higher $\overline{R_0}$ values were observed. Detailed analysis for the different sectors described in Table 2 confirmed the high variability of RF and TA during their period of higher activity (i.e., sectors 1 and 2). With the exception of these muscles and to a lesser extent BF, the interindividual variability in sector 2 was relatively low for all other muscles and especially for GMax, SOL, VL and VM, which were greatly activated during this period. GL and BF depicted a non-negligible variability in sector 3 (i.e., during higher activity period) and also in sector 4. The other muscles, which were activated to some extent in sector 4, also exhibited a medium (GM, GL, RF) to high (SOL, TA) interindividual variability.

Average (±SD) effective force, total force and IE profiles are depicted in Fig. 7. As shown in Table 3, the ensemble-averaged mechanical profiles show lower variability than EMG patterns as confirmed by lower MD (ranging from 7.7 to 33.3%), lower VR (ranging from 0.017 to 0.088) and higher $\overline{R_0}$ (ranging from 0.922 to

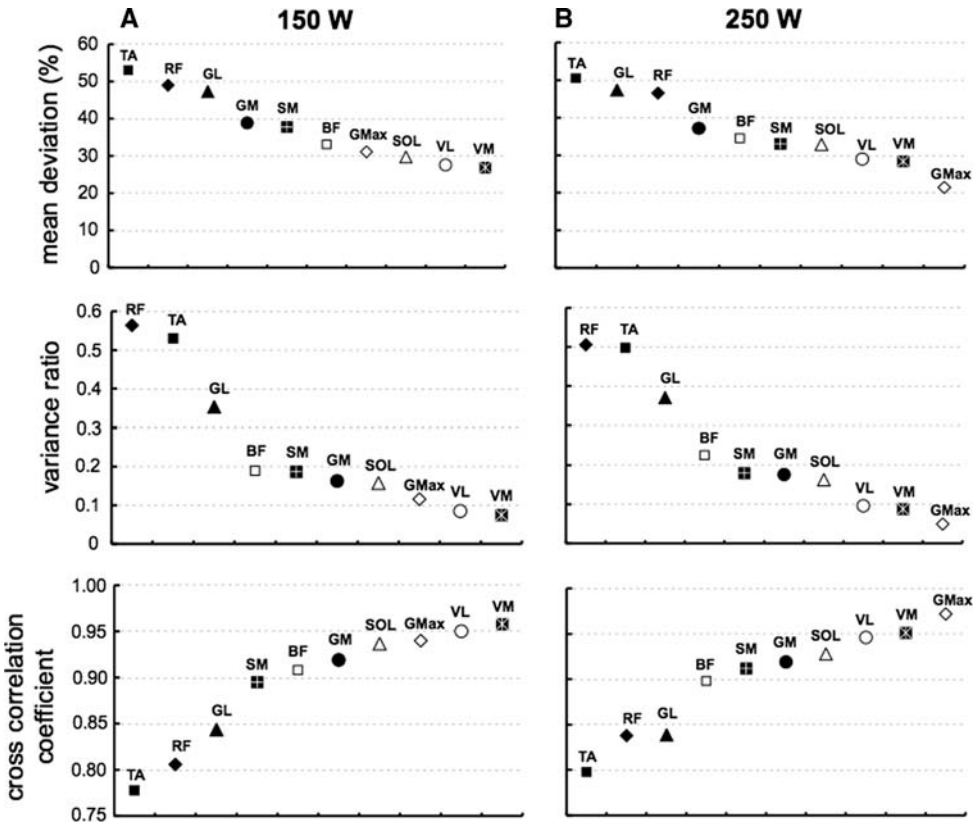

Fig. 5 Interindividual variability of complete cycle EMG RMS patterns for the ten muscles at both exercise intensities (**a** 150 W, **b** 250 W). *GMax* gluteus maximus, *SM* semimembranosus, *BF* biceps femoris, *VM* vastus medialis, *RF* rectus femoris, *VL* vastus lateralis, *GM* gastrocnemius medialis, *GL* gastrocnemius lateralis, *SOL* soleus, *TA* tibialis anterior

0.988). A very low VR value (0–0.086) for the three mechanical profiles (F_{eff}, F_{tot} and IE) was obtained in sector 2 corresponding to the propulsive downstroke phase (Table 4). F_{eff} was also very stable in sector 3 and became more variable in sector 4 and to a lesser extent in sector 1. F_{tot} presented medium interindividual variability during the three other sectors (especially in sector 3). In addition to the sector 2, IE also exhibited a very low to negligible interindividual variability in sectors 3 and 4. In contrast, a medium variability was apparent in sector 1.

Discussion

This is the first study to report on both EMG and pedal force variability in the same trained population. It shows high intersubject variability of EMG patterns at both exercise intensities (i.e., 150 and 250 W) for biarticular muscles as a whole (and specifically for GL and RF) and for one monoarticular muscle (TA). However, this heterogeneity of EMG patterns is not accompanied by a so high intersubject variability of pedal force application patterns.

Methodological aspects

EMG patterns of lower limb muscles during pedaling can be influenced by numerous factors such as power output, pedaling rate, body position, shoe–pedal interface and training status (for a review, see Hug and Dorel 2008). For this reason, all of these parameters were standardized. To allow appropriate comparisons between individuals, EMG patterns were normalized with respect to the mean value calculated over the complete cycle in line with numerous previous studies focusing on gait analysis (Winter and Yack 1987; Burden et al. 2003). However, it should be noted that this normalization procedure only provides information about the level of muscle activity in relation to the average activity over the pedaling cycle (i.e., shape of the EMG pattern). Thus, in contrast with methods referring to the isometric maximal voluntary contraction or the force–velocity test, this procedure does not allow to provide information on the absolute level of muscle activity required during pedaling. As these latter methods remain criticized on the basis of possible misinterpretations (Mirka 1991), the present study focused only on the intersubject variability in the shape and timing of EMG patterns over the pedaling cycle, in the same way as previous studies (Ryan and Gregor 1992; van Ingen Schenau et al. 1992; Chapman et al., 2007). Obviously, it would not seem appropriate to designate EMG variability as "high" in a muscle that is essentially not active at all. However, all the ten muscles recorded in this study showed a distinct phasic activity (Fig. 3) and were chosen for their role in the pedaling task as previously shown by various authors (Ericson 1986; Shan 2008).

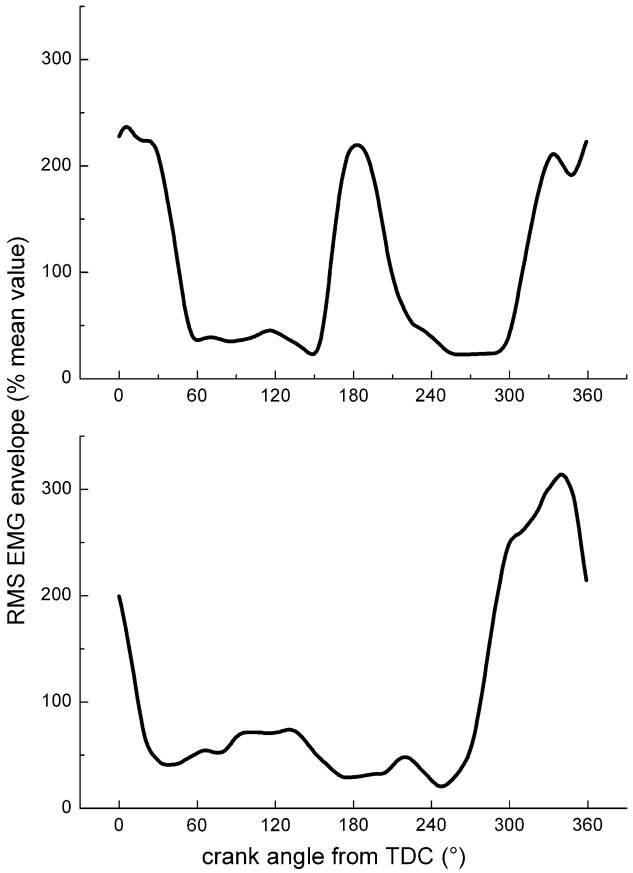

Fig. 6 Example of two different patterns observed for the tibialis anterior muscle. Each profile represents the mean obtained from averaging individual data across 30 consecutive pedaling cycles, normalizing to the mean RMS calculated over the complete pedaling cycle

Traditionally, the coefficient of variation (CV) allows the variability of a data set with a larger mean and a larger standard deviation to be compared with the variability of a data set with a smaller mean and associated with a smaller standard deviation (Ryan and Gregor 1992; Hug et al. 2004). However, CV is influenced greatly by the mean EMG value (i.e., denominator of CV formula) and could be overestimated in the sectors in which the muscle is not activated or is weak (e.g., between 180° and 300° for VL). For this reason, we chose to calculate MD and the variance ratio as recently proposed by Burden et al. (2003). The cross-correlation coefficient (with lag time = 0) were also calculated to compare the shape and timing of the individual EMG patterns as recently suggested by Wren et al. (2006). In the present study, this latter index was originally used to determine a robust mean cross correlation value ($\overline{R_0}$) considering all possible trial pairs to assess the intersubject variability. Finally, the advantage of this method was to be insensitive to signal amplitude and hence to provide a coefficient unaffected by this normalization procedure.

EMG patterns

Since considerable discussion is possible in view of the detailed EMG profiles depicted in Figs. 3 and 4, only major results will be discussed. A recent study (Dorel et al. 2008b) aimed to assess intrasession repeatability of EMG curves for ten lower limb muscles between two submaximal pedaling exercises (workload fixed at 150 W) performed before and after a 53-min simulated training session. Coefficients of cross-correlation ranging from 0.942 to 0.988 were reported. Interestingly, in the present study, for each muscle, at both 150 and 250 W, the calculated coefficient of cross-correlation (Fig. 5) is lower than those reported by Dorel et al. (2008b) suggesting that intersubject variability is higher than intrasession variability. However, it is noteworthy that muscles exhibiting the greater intersubject variability are the same as those exhibiting greater intraindividual variability.

Few studies have previously focused on heterogeneity of lower limb EMG patterns during pedaling (Ryan and Gregor 1992; Hug et al. 2004). Hug et al. (2004) did not report EMG profiles in respect to the crank cycle. In contrast, Ryan and Gregor (1992) depicted EMG profiles in ten lower limb muscles but did not provide a precise description of the training/physiological status of the subjects. Overall, our results are in accordance with those previously reported (Ryan and Gregor 1992; Hug et al. 2004) showing a high variability for biarticular muscles, especially for RF and GL. However, in contrast to Hug et al. (2004), we also reported a high variability for TA. This discrepancy could be explained by the fact that Hug et al. (2004) only reported information about the EMG activity level with respect to the crank cycle (they did not report EMG patterns). Thus, it could be hypothesized that TA variability is mainly linked to differences in shape and timing of the individual EMG patterns. In support of this idea, Ryan and Gregor (1992) reported and discussed three separate TA patterns. We also found highly different individual patterns for this muscle as shown in the example depicted in Fig. 6.

Our results confirmed that the EMG patterns of monoarticular muscles (with the exception of TA) are less variable: VL and VM are the lowest variable muscles at 150 W, while GMax is the lowest variable muscle at 250 W. It confirms that the GMax activity would be greatly influenced by workload level as suggested by Ericson (1986). The low variability of these monoarticular muscles could be explained by their role as primary power producers during pedaling (van Ingen Schenau et al. 1992). In contrast, according to the theory proposed by these authors, biarticular muscles appear to be active to transfer energy between joints at critical times in the pedaling cycle and to control the direction of force production. Thus, this high interindividual variability of EMG patterns reported in

Table 2 Inter-individual variability of EMG RMS patterns at four angular sectors for the ten muscles at both exercise intensities [(a) 150 W and (b) 250 W]

	TA	SOL	GL	GM	VL	RF	VM	BF	SM	GMax
(a) 150 W										
VR sector 1	0.966	–	–	–	0.353	1.358	0.470	–	–	0.684
VR sector 2	0.620	0.244	0.318	0.166	0.283	0.862	0.222	0.546	0.358	0.341
VR sector 3	0.900	0.430	0.551	0.397	–	–	–	0.547	0.356	–
VR sector 4	0.871	0.525	0.667	0.565	–	0.744	–	0.576	–	–
(b) 250 W										
VR sector 1	0.952	–	–	–	0.305	1.363	0.453	–	–	–
VR sector 2	0.537	0.242	0.309	0.189	0.384	0.822	0308	0.459	0.443	0.185
VR sector 3	0.768	0.507	0.548	0.391	–	–	–	0.673	0.382	–
VR sector 4	0.864	1.089	0.615	0.578	–	0.582	–	0.521	0.666	–

Omitted values appear when the mean activity over a sector was considered as negligible (i.e., <10% of the maximal activity over the complete cycle)

VR variance ratio, *GMax* gluteus maximus, *SM* semimembranosus, *BF* biceps femoris, *VM* vastus medialis, *RF* rectus femoris, *VL* vastus lateralis, *GM* gastrocnemius medialis, *GL* gastrocnemius lateralis, *SOL* soleus, *TA* tibialis anterior

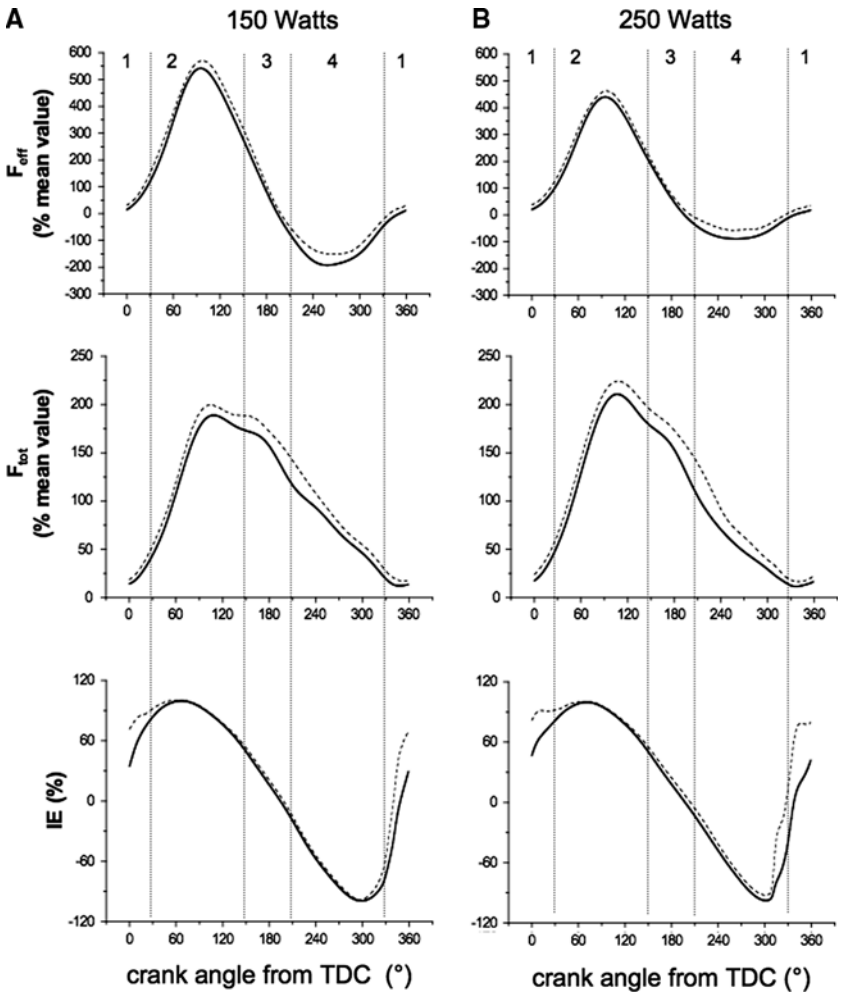

Fig. 7 Interindividual variability of effective force (F_{eff}), total force (F_{tot}) and index of mechanical effectiveness (IE) profiles at both exercise intensities (**a** 150 W, **b** 250 W). *Vertical lines* define the four angular sectors: *sector 1* (330°–30°), *sector 2* (30°–150°), *sector 3* (150°–210°), *sector 4* (210°–330°)

biarticular muscles in the present study appeared to support the contention suggested by these authors that the role of "fine tuning" the system and distributing energy among the segments of these muscles would lead to more variance. Note that the ankle is not considered as a major power-producing joint and TA has been proposed to enhance

ankle function in transmitting power to the crank (Ryan and Gregor 1992); therefore, this could explain the high variability found in this monoarticular muscle. Overall and consistent with the theory of van Ingen Schenau et al. (1992), one may wonder whether high interindividual variability of the EMG patterns reported in biarticular muscles could be linked to a variability in the direction of force vector on the pedals, and thus maybe to a heterogeneity of the mechanical effectiveness.

Pedal force profiles

To the best of our knowledge, this is the first study to focus on intersubject variability in pedal effective force, total force and IE profiles. Our results suggest a low intersubject variability corresponding with high cross-correlation coefficients and relatively low MD and VR values for F_{eff}, F_{tot} and IE profiles computed across the whole pedaling cycle (Table 3). Detailed analysis of the different sectors highlights the consistency in all the pedal mechanical variables during the major propulsive phase (sector 2). In the same way, the next part of the cycle (sector 3: BDC) is also consistent regarding F_{eff} and IE even if the F_{tot} demonstrated high variability. An important finding is the great variability in F_{eff} and F_{tot} during the upstroke phase (sector 4) supporting the assumption that effective force profiles for this period appear as individual like fingerprints for each subject (Kautz et al. 1991). This variability was also evident, although to a lesser extent, for F_{eff} and F_{tot} in the last sector (sector 1: TDC) and was associated with high variability in IE. Finally, our results show a greater variability in the pedaling technique at 250 W compared to 150 W (i.e., higher IE variability on the complete cycle, Table 3, Fig. 7; higher variability of F_{eff} and IE in sectors 1 and 4, Table 4). This result supports the hypothesis that a greater power output could lead to an increased variability specifically during the upstroke and TDC phases (Sanderson 1991).

Table 3 Inter-individual variability of complete cycle effective force (F_{eff}), total force (F_{tot}) and index of mechanical effectiveness (IE) profiles at both exercise intensities [(a) 150 W and (b) 250 W]

	F_{eff}	F_{tot}	IE
(a) 150 W			
MD (%)	30.3	12.2	7.7
VR	0.017	0.047	0.037
$\overline{R_0}$	0.988	0.987	0.962
(b) 250 W			
MD (%)	23.6	15.3	12.4
VR	0.019	0.059	0.088
$\overline{R_0}$	0.987	0.982	0.922

MD mean deviation, *VR* variance ratio, $\overline{R_0}$ cross-correlation coefficient

Table 4 Inter-individual variability of effective force (F_{eff}), total force (F_{tot}) and index of mechanical effectiveness (IE) profiles at four angular sectors at both exercise intensities [(a) 150 W and (b) 250 W]

	F_{eff}	F_{tot}	IE
(a) 150 W			
VR sector 1	0.197	0.359	0.243
VR sector 2	0.071	0.063	0.000
VR sector 3	0.064	0.547	0.005
VR sector 4	0.444	0.204	0.002
(b) 250 W			
VR sector 1	0.291	0.243	0.253
VR sector 2	0.058	0.086	0.000
VR sector 3	0.059	0.556	0.007
VR sector 4	0.699	0.366	0.036

VR variance ratio

EMG versus pedal force variability

Consistency in the pedal mechanical variables during sector 2 is in strong agreement with the fact that this sector is characterized by a low variability in EMG activation patterns especially obtained for the main power producer muscles (VL, VM, GMax). The relative variability in sectors 1 and 4 can also be interpreted in the context of the EMG results. Indeed, it is interesting to note that sector 1 is characterized by highest variability in both EMG and mechanical patterns. The most probable explanation would be the link around the TDC between the activation strategy of TA and RF muscles and the ability of subjects to effectively orientate the force and hence produce a high F_{eff} in this specific part of the cycle. The relationship is however less consistent around BDC (i.e., medium to high variability of BF, GL and TA versus negligible variability of F_{eff} and IE). Additionally, to attribute the great variability in mechanical parameters during the upstroke phase to the variability in EMG remains debatable when considering the very low global muscle activity level during this period. Furthermore, the functional role of the muscles, which are slightly activated during this sector, remains to be elucidated. As a whole, the relative variability in sectors 1 and 4, when the level of force is low, seems not to have a great impact on the intersubject variability calculated across the whole cycle. However, the implications of such variations should not be ignored in the context of long duration cycling exercises.

The difference in variability between pedal force and EMG (i.e., low variability of the mechanical variables

compared to EMG) could be explained by the fact that the musculoskeletal system has the characteristics of a low-pass filter. Although the myoelectrical signal has frequency components over 100 Hz, the force signal is of much lower frequencies (i.e., muscle force profiles are smoother than raw EMG profiles). There are many mechanisms that may cause this filtering, like excitation–contraction coupling and muscle/tendon viscoelasticity. However, for the EMG signal to be correlated with the muscle force, and as recommended by various authors (Buchanan et al. 2004), we used an EMG processing that permits to filter out the high-frequency components. Even if it is not possible to be sure that the filtering is sufficient, we think that the more plausible explanation for the difference in variability between pedal force and EMG is the redundancy of the neuromuscular system. In fact, lower limbs have more muscles than joints such that the same pedal force profile can be produced by various lower limb muscle patterns. Associated with the reproducibility of the EMG patterns during pedaling showed by Dorel et al. (2008b), our result suggests that each cyclist adopts a stable personal muscle activation strategy. However, some questions remain to be answered: how a muscle coordination pattern is selected from a large pool of valid alternatives? Is there an optimal coordination pattern or do the cyclists adopt their personal optimal coordination pattern?

Conclusion

This study shows high intersubject variability of EMG patterns at both exercise intensities (i.e., 150 and 250 W), especially for biarticular muscles. It suggests that despite their high and homogeneous level of expertise, cyclists adopt a personal muscle activation strategy during pedaling. However, this heterogeneity of EMG patterns is not accompanied by a so high intersubject variability in pedal force application patterns. Even if variability in EMG patterns is in line with the slight variability of the mechanical parameters observed during the upstroke phase and around the top dead center, the results of this work highlight that the flexibility at the muscle level as a whole is greater than that seen in the net effective torque that muscles induce at the level of the crank. Overall, these results provide additional evidence for redundancy in the neuromuscular system: the neuromuscular system has multiple ways of accomplishing a given motor task.

Acknowledgments This study was funded in part by "La fondation d'entreprise de la Française Des Jeux" and the French Ministry of Sport (contract no. 06-046). The authors are grateful for the subjects for having accepted to participate in this study.

References

Bernstein N (1967) Coordination and regulation of movements. Pergamon Press, New York

Buchanan TS, Lloyd DG, Manal K, Besier TF (2004) Neuromusculoskeletal modeling: estimation of muscle forces and joint moments and movements from measurements of neural command. J Appl Biomech 20:367–395

Burden AM, Trew M, Baltzopoulos V (2003) Normalisation of gait EMGs: a re-examination. J Electromyogr Kinesiol 13:519–532. doi:10.1016/S1050-6411(03)00082-8

Cavanagh PR, Komi PV (1979) Electromechanical delay in human skeletal muscle under concentric and eccentric contractions. Eur J Appl Physiol Occup Physiol 42:159–163. doi:10.1007/BF00431022

Chapman AR, Vicenzino B, Blanch P, Hodges PW (2007) Patterns of leg muscle recruitment vary between novice and highly trained cyclists. J Electromyogr Kinesiol 18(3):359–371

Dal Monte A, Manoni A, Fucci S (1973) Biomechanical study of competitive cycling: the forces exercised on the pedals. In: Press B (ed) Biomechanics III. pp 434–439

Dingwell JB, Ulbrecht JS, Boch J, Becker MB, O'Gorman JT, Cavanagh PR (1999) Neuropathic gait shows only trends towards increased variability of sagittal plane kinematics during treadmill locomotion. Gait Posture 10:21–29. doi:10.1016/S0966-6362(99)00016-8

Dorel S, Couturier A, Hug F (2008a) Influence of different racing positions on mechanical and electromyographic patterns during pedalling. Scand J Med Sci Sports (in press)

Dorel S, Couturier A, Hug F (2008b) Intra-session repeatability of lower limb muscles activation pattern during pedaling. J Electromyogr Kinesiol (in press)

Ericson M (1986) On the biomechanics of cycling. A study of joint and muscle load during exercise on the bicycle ergometer. Scand J Rehabil Med Suppl 16:1–43

Gregor RJ, Cavanagh PR, LaFortune M (1985) Knee flexor moments during propulsion in cycling—a creative solution to Lombard's Paradox. J Biomech 18:307–316. doi:10.1016/0021-9290(85)90286-6

Gregor RJ, Komi PV, Browning RC, Jarvinen M (1991) A comparison of the triceps surae and residual muscle moments at the ankle during cycling. J Biomech 24:287–297. doi:10.1016/0021-9290(91)90347-P

Hermens HJ, Freriks B, Disselhorst-Klug C, Rau G (2000) Development of recommendations for SEMG sensors and sensor placement procedures. J Electromyogr Kinesiol 10:361–374. doi:10.1016/S1050-6411(00)00027-4

Hug F, Dorel S (2008) Electromyographic analysis of pedaling: a review. J Electromyogr Kinesiol (in press)

Hug F, Bendahan D, Le Fur Y, Cozzone PJ, Grelot L (2004) Heterogeneity of muscle recruitment pattern during pedaling in professional road cyclists: a magnetic resonance imaging and electromyography study. Eur J Appl Physiol 92:334–342. doi:10.1007/s00421-004-1096-3

Hull ML, Davis RR (1981) Measurement of pedal loading in bicycling: I. Instrumentation. J Biomech 14:843–856. doi:10.1016/0021-9290(81)90012-9

Kautz SA, Feltner ME, Coyle EF, Baylor AM (1991) The pedaling technique of elite endurance cyclists: changes with increasing workload at constant cadence. Int J Sport Biomech 7:29–53

LaFortune MA, Cavanagh PR (1983) Effectiveness and efficiency during cycling riding. In: Biomechanics VIII-B: international series on biomechanics. Human Kinetics. pp 928–936

Li L, Caldwell GE (1999) Coefficient of cross correlation and the time domain correspondence. J Electromyogr Kinesiol 9:385–389. doi:10.1016/S1050-6411(99)00012-7

Mirka GA (1991) The quantification of EMG normalization error. Ergonomics 34:343–352. doi:10.1080/00140139108967318

Rouffet DM, Hautier CA (2008) EMG normalization to study muscle activation in cycling. J Electromyogr Kinesiol (in press)

Rowe T, Hull ML, Wang EL (1998) A pedal dynamometer for off-road bicycling. J Biomech Eng 120:160–164. doi:10.1115/1.2834297

Ryan MM, Gregor RJ (1992) EMG profiles of lower extremity muscles during cycling at constant workload and cadence. J Electromyogr Kinesiol 2:69–80. doi:10.1016/1050-6411(92)90018-E

Sanderson DJ (1991) The influence of cadence and power output on the biomechanics of force application during steady-rate cycling in competitive and recreational cyclists. J Sports Sci 9:191–203

Sanderson DJ, Black A (2003) The effect of prolonged cycling on pedal forces. J Sports Sci 21:191–199. doi:10.1080/0264041031000071010

Sanderson DJ, Hennig EM, Black AH (2000) The influence of cadence and power output on force application and in-shoe pressure distribution during cycling by competitive and recreational cyclists. J Sports Sci 18:173–181. doi:10.1080/026404100365072

Shan G (2008) Biomechanical evaluation of bike power saver. Appl Ergon 39:37–45

Shiavi R, Bourne J, Holland A (1986) Automated extraction of activity features in linear envelopes of locomotor electromyographic patterns. IEEE Trans Biomed Eng 33:594–600. doi:10.1109/TBME.1986.325841

Shiavi R, Bugle HJ, Limbird T (1987) Electromyographic gait assessment, Part 1: adult EMG profiles and walking speed. J Rehabil Res Dev 24:13–23

van Bolhuis BM, Gielen CC (1999) A comparison of models explaining muscle activation patterns for isometric contractions. Biol Cybern 81:249–261. doi:10.1007/s004220050560

van Ingen Schenau GJ, Boots PJM, de Groots G, Snackers RJ, van Woensel WWLM (1992) The constrained control of force and position in multi-joint movements. Neuroscience 46:197–207. doi:10.1016/0306-4522(92)90019-X

Vos EJ, Mullender MG, van Ingen Schenau GJ (1990) Electromechanical delay in the vastus lateralis muscle during dynamic isometric contractions. Eur J Appl Physiol Occup Physiol 60:467–471. doi:10.1007/BF00705038

Winter DA, Yack HJ (1987) EMG profiles during normal human walking: stride-to-stride and inter-subject variability. Electroencephalogr Clin Neurophysiol 67:402–411. doi:10.1016/0013-4694(87)90003-4

Wren TA, Do KP, Rethlefsen SA, Healy B (2006) Cross-correlation as a method for comparing dynamic electromyography signals during gait. J Biomech 39:2714–2718. doi:10.1016/j.jbiomech.2005.09.006

Yang JF, Winter DA (1984) Electromyographic amplitude normalization methods: improving their sensitivity as diagnostic tools in gait analysis. Arch Phys Med Rehabil 65:517–521

Changes of Pedaling Technique and Muscle Coordination during an Exhaustive Exercise

SYLVAIN DOREL[1], JEAN-MARC DROUET[2], ANTOINE COUTURIER[1], YVAN CHAMPOUX,[2] and FRANÇOIS HUG[1,3]

[1]*Research Mission, Laboratory of Biomechanics and Physiology, National Institute for Sports (INSEP), Paris, FRANCE;* [2]*VélUS Group, Department of Mechanical Engineering, University of Sherbrooke, Sherbrooke, Québec, CANADA; and* [3]*Laboratory « Motricity, Interactions, Performance (EA 4334)», University of Nantes, Nantes Atlantic Universities, Nantes, FRANCE*

ABSTRACT

DOREL, S., J.-M. DROUET, A. COUTURIER, Y. CHAMPOUX, and F. HUG. Changes of Pedaling Technique and Muscle Coordination during an Exhaustive Exercise. *Med. Sci. Sports Exerc.*, Vol. 41, No. 6, pp. 1277–1286, 2009. **Purpose**: Alterations of the mechanical patterns during an exhaustive pedaling exercise have been previously shown. We designed the present study to test the hypothesis that these alterations in the biomechanics of pedaling, which occur during exhaustive exercise, are linked to changes in the activity patterns of lower limb muscles. **Methods**: Ten well-trained cyclists were tested during a limited time to exhaustion, performing 80% of maximal power tolerated. Pedal force components were measured continuously using instrumented pedals and were synchronized with surface EMG signals measured in 10 lower limb muscles. **Results**: The results confirmed most of the alterations of the mechanical patterns previously described in the literature. The magnitude of the root mean squared of the EMG during the complete cycle (RMS_{cycle}) for tibialis anterior and gastrocnemius medialis decreased significantly ($P < 0.05$) from 85% and 75% of T_{lim}, respectively. A higher RMS_{cycle} was obtained for gluteus maximus ($P < 0.01$) and biceps femoris ($P < 0.05$) from 75% of T_{lim}. The k values that resulted from the cross-correlation technique indicated that the activities of six muscles (gastrocnemius medialis, gastrocnemius lateralis, tibialis anterior, vastus lateralis, vastus medialis, and rectus femoris) were shifted forward in the cycle at the end of the exercise. **Conclusions**: The large increases in activity for gluteus maximus and biceps femoris, which are in accordance with the increase in force production during the propulsive phase, could be considered as instinctive coordination strategies that compensate for potential fatigue and loss of force of the knee extensors (i.e., vastus lateralis and vastus medialis) by a higher moment of the hip extensors. **Key Words:** EMG, EFFECTIVENESS, FORCE, TORQUE, CYCLIST, FATIGUE

During an exhaustive exercise, the maximal force-generating capacity of muscles declines progressively, which suggests that fatigue begins before the muscles are no longer able to perform the required task (for review, see [9]). Depending on the effort exerted, the progression may be fast or slow and will lead sooner or later to changes of performance that are mechanically detectable. Several studies have focused on the occurrence of neuromuscular fatigue during different pedaling exercises (2,6,10, 12,20,26,28). Among these, reductions of maximal voluntary contractions of the quadriceps have been reported during long-duration submaximal cycling exercises (>2 h) (18,19). These reductions have been associated with both central and peripheral mechanisms such as decreases in maximal muscle activation and peak twitch torque. However, these studies did not focus on alterations of EMG activity during the exercise. Other authors have focused on the alterations in EMG activity levels of some lower limb muscles during time trial events (1,3,6,12), fatiguing constant-load exercises (13,23), or repeated sprints (2,10). Most of these studies found that there was a significant increase in the EMG/power ratio for some lower limb muscles (e.g., vastus lateralis and vastus medialis). This increase suggests that additional motor units (MU) are recruited to compensate for the decrease in the force of contraction that occurs in fatigued muscle fibers, which is generally observed during continuous isometric exercises

Address for correspondence: François Hug, Ph.D., Laboratory « Motricity, Interaction, Performance » (EA 4334), University of Nantes, UFR STAPS, 25 bis boulevard Guy Mollet, BP 72206, 44322 Nantes cedex 3, France; E-mail: francois.hug@univ-nantes.fr.
Submitted for publication July 2008.
Accepted for publication December 2008.

0195-9131/09/4106-1277/0
MEDICINE & SCIENCE IN SPORTS & EXERCISE®

DOI: 10.1249/MSS.0b013e31819825f8

that require maintaining a given force until exhaustion (7). However, these studies reported only changes of EMG activity level, and none showed complete EMG patterns (i.e., EMG activity with respect to the crank angle, which could have provided valuable information about the timing of muscle activation). This variable is crucial for linking the quantitative changes of EMG patterns with putative changes in pedaling coordination.

Literature concerning the influence of fatigue on muscle coordination during submaximal cycling exercise is scarce. The few studies (16,26) that have focused on the timing of muscle activation during fatiguing exercises showed that the timing of onset and offset of EMG bursts is not altered by fatigue. However, in these two studies, only a few muscles were investigated (four muscles for Sarre and Lepers [26] and three muscles for Knaflitz and Molinari [16]), and the exercises were not performed to complete exhaustion. In a limited time to exhaustion performed at 80% of the maximal power output reached during an incremental exercise, Sanderson and Black (25) showed an alteration in the mechanical pattern at the end of the test (i.e., a less effective force application during the recovery phase and an increase in force during the propulsive phase). These results strongly suggest that muscle coordination is modified with fatigue. Thus, the purpose of the present study was to investigate the evolution of the pedaling technique during a submaximal exercise performed until exhaustion on the basis of both the biomechanics of pedaling and the EMG activity of the main lower limb muscles. We tested the hypothesis that alterations in the application of pedal forces that occur during the exhaustive exercise (25) are linked to changes in the activity patterns of lower limb muscles.

MATERIALS AND METHODS

Subjects. Ten trained male cyclists volunteered to participate in this study. The mean ±SD age, height, and body mass were 20.8 ± 3.3 yr, 180.5 ± 6.0 cm, and 68.9 ± 6.0 kg, respectively. The mean percentage body fat was 10 ± 2.5%. Mean $\dot{V}O_{2max}$ and maximal power tolerated (MPT) reached during the incremental cycling exercise were 65.3 ± 7.4 $mL \cdot min^{-1} \cdot kg^{-1}$ and 412 ± 31.9 W, respectively. The participants had an average of 9 ± 3 yr of competitive experience, and their yearly training distance averaged approximately 14,000 ± 4333 km. They were informed of the possible risk and discomfort associated with the experimental procedures before they gave their written consent. The experimental design of the study was approved by the Ethical Committee of Saint-Germain-en-Laye (acceptance no. 06016) and was done in accordance with the Declaration of Helsinki.

Exercise protocol. The exercise protocol for this study is summarized by Figure 1. In brief, the protocol consisted of two sessions conducted in the following order: 1) incremental cycling exercise performed until exhaustion to characterize the population in physical and physiological capacities; 2) experimental session consisting of a constant-load exercise performed until exhaustion.

During the first visit, 8 to 10 d preceding the experimental session, each subject performed an incremental cycling exercise (workload increments of 25 $W \cdot min^{-1}$, starting at 100 W) during which respiratory and ventilatory parameters (i.e., $\dot{V}O_2$, $\dot{V}_E$, $\dot{V}CO_2$) were measured breath-by-breath (K4B2; Cosmed®, Rome, Italy). The MPT, defined as the last stage that was completed entirely, was used to calculate the appropriate workload imposed by the cycle ergometer for the second test.

During the second session, subjects were asked, after a standardized warm-up (i.e., 10 min at 100 W, 6 min at 150 W, and 3 min at 250 W) and a recovery period (i.e., 3 min at 100 W and 3 min of rest), to perform a cycling exercise at a constant power output equal to 80% of their MPT for as long as possible. Subjects were asked to keep a constant pedaling rate (i.e., the pedaling rate freely adopted at the end of the warm-up session). The test continued until the complete exhaustion: either until the cyclists voluntarily chose to stop the exercise or until they were no longer able to maintain their initial test cadence (±3 rpm), which was considered as a failure to maintain the required task (i.e., the target power output at a constant cadence). Surface EMG and mechanical parameters were recorded continuously during this experimental session.

Material and data collection. Subjects exercised on an electronically braked cycle ergometer (Excalibur Sport; Lode®, Groningen, the Netherlands) equipped with standard cranks (length = 170 mm) and with instrumented pedals that

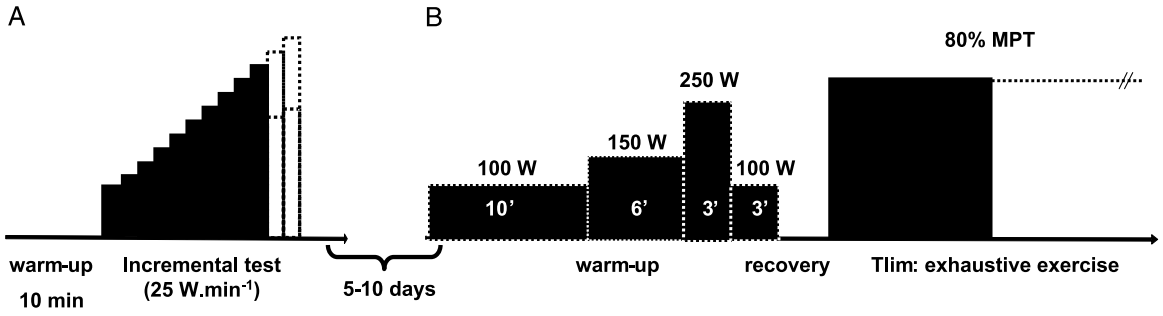

FIGURE 1—Experimental setup for the first (*A*) and the second sessions (*B*).

are described below. Throughout both sessions, vertical and horizontal positions of the saddle, handlebar height, and stem length were set to match the usual racing position of the participants (i.e., dropped posture). A pedal dynamometer, specifically designed for measuring pedal loads (VélUS group, Department of Mechanical Engineering, Sherbrooke University, Canada), was used to collect mechanical data (15). This instrumented pedal is compatible with LOOK CX7 clipless pedal using LOOK Delta cleat. The sagittal plane components of the total reaction force (F_{tot}) applied at the shoe/pedal interface were measured using a series of eight strain gauges located within each pedal. F_{tot} was calculated from the measured Cartesian components (F_T, F_N), which corresponded to the horizontal forward and vertical upward forces on the pedal, respectively. An optical encoder with a resolution of 0.4° mounted on the pedal-measured pedal angle (β) with respect to the crank orientation. Zero adjustments for both components of force and pedal angle were done before each session. The crank angle (Θ) was calculated on the basis of Transistor-Transistor Logic (TTL) pulses delivered each 2° by the cycle ergometer. Additional TTL pulses allowed the detection of the bottom dead center of the right pedal (i.e., BDC: lowest position of the right pedal with crank arm angle = 180°). All these data were digitized at a sampling rate of 2 kHz (USB data acquisition; ISAAC Instruments®, Québec, Canada) and were stored on a computer.

Surface EMG activity was continuously recorded for the following 10 muscles of the right lower limb: gluteus maximus (GMax), semimembranosus (SM), biceps femoris (BF), vastus medialis (VM), rectus femoris (RF), vastus lateralis (VL), gastrocnemius medialis (GM) and lateralis (GL), soleus (SOL), and tibialis anterior (TA). For each muscle, a pair of surface Ag/AgCl electrodes (Blue sensor; Ambu®, Ballerup, Denmark) was attached to the skin with a 2-cm interelectrode distance. The electrodes were placed longitudinally with respect to the underlying muscle fibers' arrangement and located according to the recommendations by the Surface EMG for Noninvasive Assessment of Muscles project (11). Before electrode application, the skin was shaved and cleaned with alcohol to minimize impedance. The wires connected to the electrodes were well secured with adhesive tape to avoid movement-induced artifacts. Raw EMG signals were preamplified close to the electrodes (gain of 375, in the bandwidth of 8–500 Hz) and digitized simultaneously with BDC TTL pulses at a sampling rate of 1 kHz (ME6000P16; Mega Electronics Ltd®, Kuopio, Finland).

Data processing. All data were analyzed with two custom-written scripts (MATLAB, Natick, MA, (MathWorks®) for mechanical data and Origin 6.1 (OriginLab Corporation®, Northampton, MA,) for EMG data and final processing). All mechanical data were smoothed by a 10-Hz third-order butterworth low-pass filter. On the basis of the components F_N and F_T and pedal angle (β), F_{tot} was calculated by trigonometry and resolved into two components: one orthogonal to the crank (effective force, F_{eff}) and another along the crank (ineffective force, F_I; Fig. 2). The instantaneous index of mechanical effectiveness (IE) was determined as the ratio of the effective force to the total applied force at each point in the pedaling cycle (24,25). A high-pass filter (20 Hz) was applied on the raw EMG signals (Chart 5.4; AD Instruments®, Hasting, United Kingdom) to diminish movement artifacts. Then, the root mean squared (RMS) of the EMG was calculated during a 25-ms window to produce a linear envelope for each muscle activity pattern.

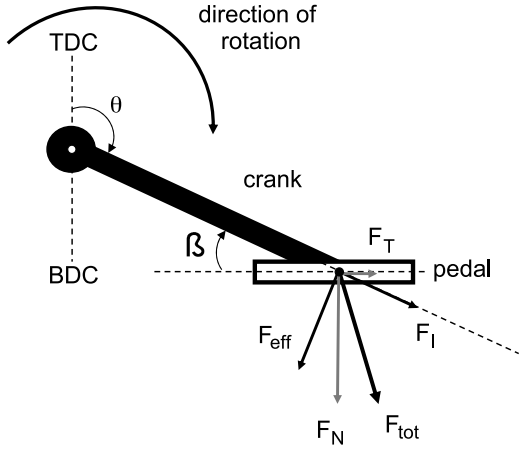

FIGURE 2—Representation of the various forces applied on the pedal on a sagittal plane. Total force (F_{tot}) produced at the shoe/pedal interface is decomposed into two components: effective force (F_{eff}) acts perpendicular to the bicycle crank and drives the crank around in its circle; the ineffective component (F_I) acts along the crank and performs no useful external work.

The BDC TTL pulses were used to synchronize the EMG and mechanical signals of the right pedal. All data were smoothed, resampled (one value per degree), and averaged during 30 consecutive pedaling cycles to get representative mechanical profiles (pedal forces and index of effectiveness) and EMG RMS linear envelopes (5). The values were expressed as a function of the angle of the crank arm as it rotated from the highest pedal position (0°, top dead center (TDC)) to the lowest (180°, BDC) and back to TDC to complete a 360° crank cycle. This procedure was repeated every 10% of the total exercise duration (from 5% to 95% of total time) to show the evolution of the patterns for each mechanical variable, muscle, and subject throughout the exhaustive exercise. The mean pattern, which was obtained by averaging the first two patterns (obtained at 5% and 15% of T_{lim}), was considered as the "reference pattern" and was used to characterize the starting values.

The following mechanical parameters were calculated or identified from the force profiles: the maximal (peak) value of the effective force exerted during the downstroke ($F_{eff\text{-}max}$, N), the minimal value exerted during the upstroke ($F_{eff\text{-}min}$, N), and the angle of the arm crank that corresponded to $F_{eff\text{-}max}$ (Angle$F_{eff\text{-}max}$,°) and $F_{eff\text{-}min}$ (Angle-$F_{eff\text{-}min}$,°). The overall index of mechanical effectiveness on the complete crank cycle (IE_{cycle}) was determined as the

ratio of the linear impulse of F_{eff} to the linear integral of F_{tot} (17,25). For improving the timing analysis, mean values of the main mechanical variables (F_{eff}, F_{tot}, and IE) were calculated for four angular sectors during the entire pedaling cycle: sector 1 represented 330°–30°; sector 2, 30°–150°; sector 3, 150°–210°; and sector 4, 210°–330°. From a functional standpoint, sectors 1 and 3 correspond to the top and bottom dead centers, respectively; sectors 2 and 4 correspond to the main propulsive and recovery phases, respectively.

To quantify the muscle activity pattern, a series of classic variables was calculated from the EMG RMS linear envelope. The overall activity level was identified by the magnitude of the mean EMG RMS during the complete cycle (RMS_{cycle}). The muscle activation timing analysis by the cross-correlation technique was used to measure the relative change in the temporal characteristics of EMG activity (4,14,21). The cross-correlation coefficients of the EMG RMS curves between the reference pattern (start) and the subsequent patterns (from 25% to 95% of T_{lim}) were calculated for each muscle according to the equation proposed by Li and Caldwell (21) with lag time equal to zero. Then, the magnitude of a significant angle shift between each pair of signals was found by assessing the k value at which the cross-correlation coefficient was maximized. The k values that resulted from this objective approach for comparing signals represented an interesting estimation of the time effect on the shift of the linear envelope EMG patterns in the pedaling cycle.

Statistical analysis. All analyses were performed with ORIGIN 6.1 software for Windows. First, data were tested for normality using the Kolmogorov–Smirnov test. After the normality condition was verified, the results were expressed as mean ± SD. One-way ANOVA with repeated measures was used to test the effect of time on the mechanical and EMG variables. When significant F ratios were found, all the means (from 25% to 95% of T_{lim}) were compared with the control value (e.g., start reference) using a Dunnett *post hoc* test. Differences were considered significant when probability (P) of a type I error was ≤5%.

RESULTS

The exhaustive exercise was achieved at a mean power output of 327 ± 23 W, a mean pedaling rate of 95 ± 8 rpm, and lasted 13.8 ± 6.0 min. There was a significant increase in the

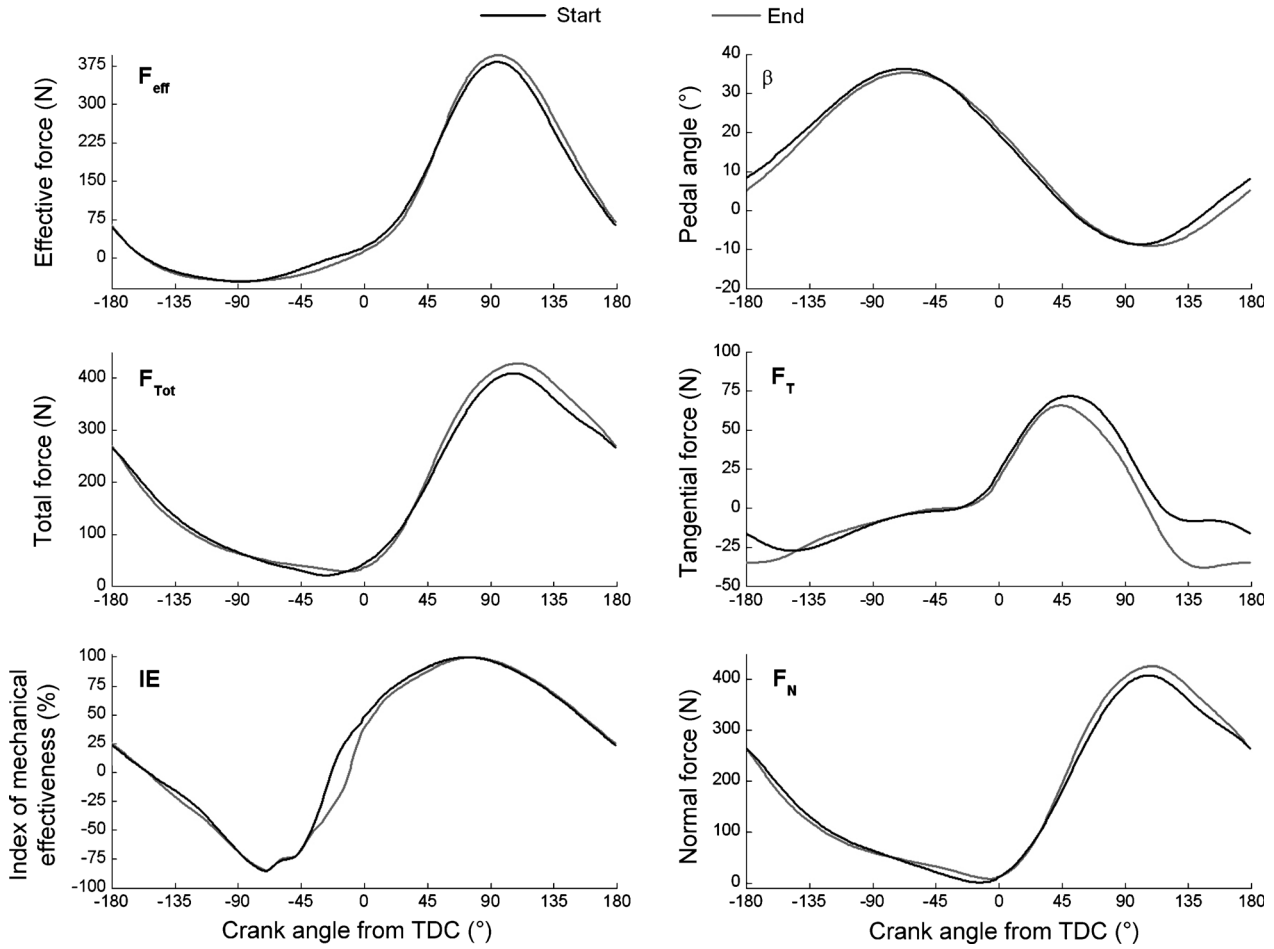

FIGURE 3—Mechanical patterns obtained at the start (*black lines*) and at the end (*gray lines*) of the exhaustive pedaling exercise. Pedal angle is expressed in reference to the horizontal.

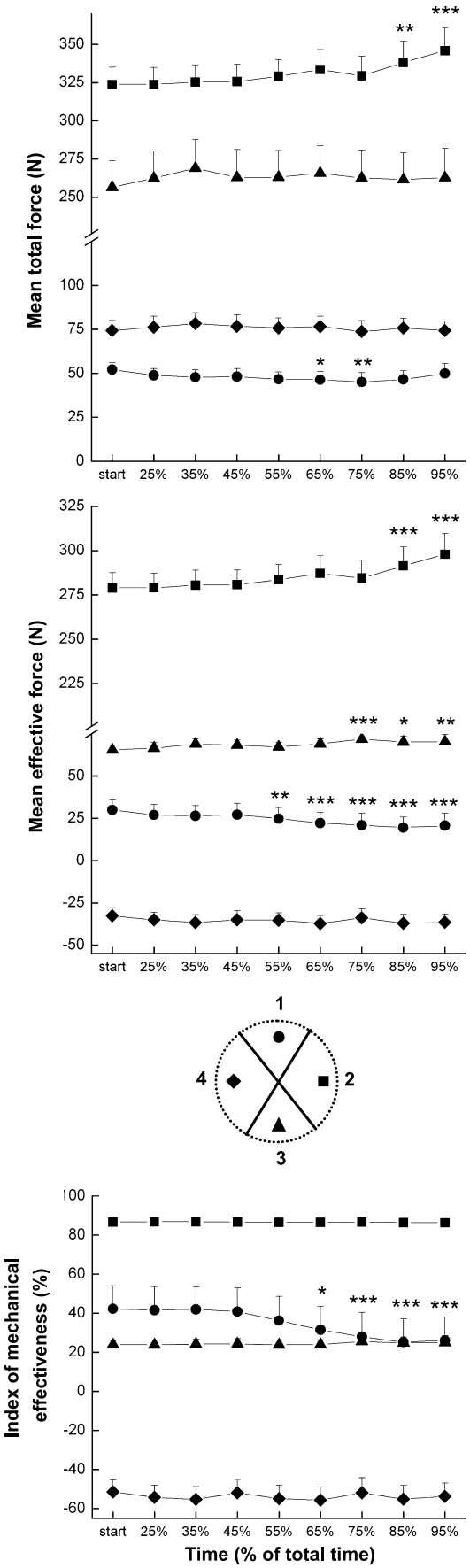

$F_{eff\text{-}max}$ (377.9 ± 34.2 and 401.3 ± 45.2 N for the start and the end of exercise, respectively, $P < 0.01$), whereas no difference was observed for $F_{eff\text{-}min}$ (−55.7 ± 17.7 vs −57.7 ± 15.1 N; Fig. 3). The angle corresponding to $F_{eff\text{-}max}$ ($AngleF_{eff\text{-}max}$) was not significantly different between the start and the end of exercise (95.1 ± 4.5° vs 94.9 ± 4.6°, respectively), whereas the angle corresponding to $F_{eff\text{-}min}$ ($AngleF_{eff\text{-}min}$) was significantly higher at the end (283.7 ± 29.1°) than at the start (275.3 ± 25.8°, $P < 0.05$). The overall index of mechanical effectiveness was not significantly different between the start and the end of the exercise (53.4 ± 6.4% vs 53.9 ± 7.4%, respectively).

Detailed analysis for the different sectors described in Figure 4 exhibited significant decreases of F_{tot}, F_{eff}, and IE in sector 1 from 65%, 55%, and 65% of T_{lim}, respectively, compared with the start value ($P < 0.05$ to $P < 0.001$). The significant decreases observed in F_{eff} and IE persisted until the end of the exercise, whereas the decrease for F_{tot} was observed only for 65% and 75% of T_{lim}. In sector 2, F_{eff} and F_{tot} were significantly higher at 85% and 95% of T_{lim} compared with the start value ($P < 0.001$). F_{eff} was increased in sector 3 from 75% of T_{lim} ($P < 0.05$ to $P < 0.001$). No alteration was observed in sector 4 for these three variables.

The evolution of the mean ensemble curves of the EMG RMS linear envelopes between the start ("reference pattern") and the end of the exercise (95% of T_{lim}) is depicted in Figure 5. Among the 10 muscles tested, only 4 displayed significant differences in mean EMG RMS between the start and the end of exercise (Fig. 6). RMS_{cycle} for TA and GM decreased significantly ($P < 0.05$) from 85% and 75% of T_{lim}, respectively. A higher RMS_{cycle} was obtained for GMax ($P < 0.01$) and BF ($P < 0.05$) from 75% of T_{lim}. The k values that resulted from the cross-correlation technique indicated that the activities of six muscles were shifted forward in the cycle at the end of the exercise (Fig. 7). Significant forward shifts were observed from 55%, 65%, and 75% of T_{lim} for the activation patterns of GM, TA, and GL, respectively. The activation patterns of knee extensors were also shifted forward significantly from 75% (VL and VM) and 85% (RF) of T_{lim}.

DISCUSSION

This study shows alterations in patterns of force application during exhaustive exercise, as previously reported by Sanderson and Black (25). These alterations are accompanied by changes in the activity patterns of some lower limb muscles, suggesting that some adjustments are made in the coordination of muscles with the occurrence of fatigue.

FIGURE 4—Evolution of the mean total force, mean effective force, and index of mechanical effectiveness during the exhaustive pedaling exercise. These evolutions are depicted for each functional sector. Asterisks indicate significant differences from the start value ($^{*}P < 0.05$, $^{**}P < 0.01$, $^{***}P < 0.001$).

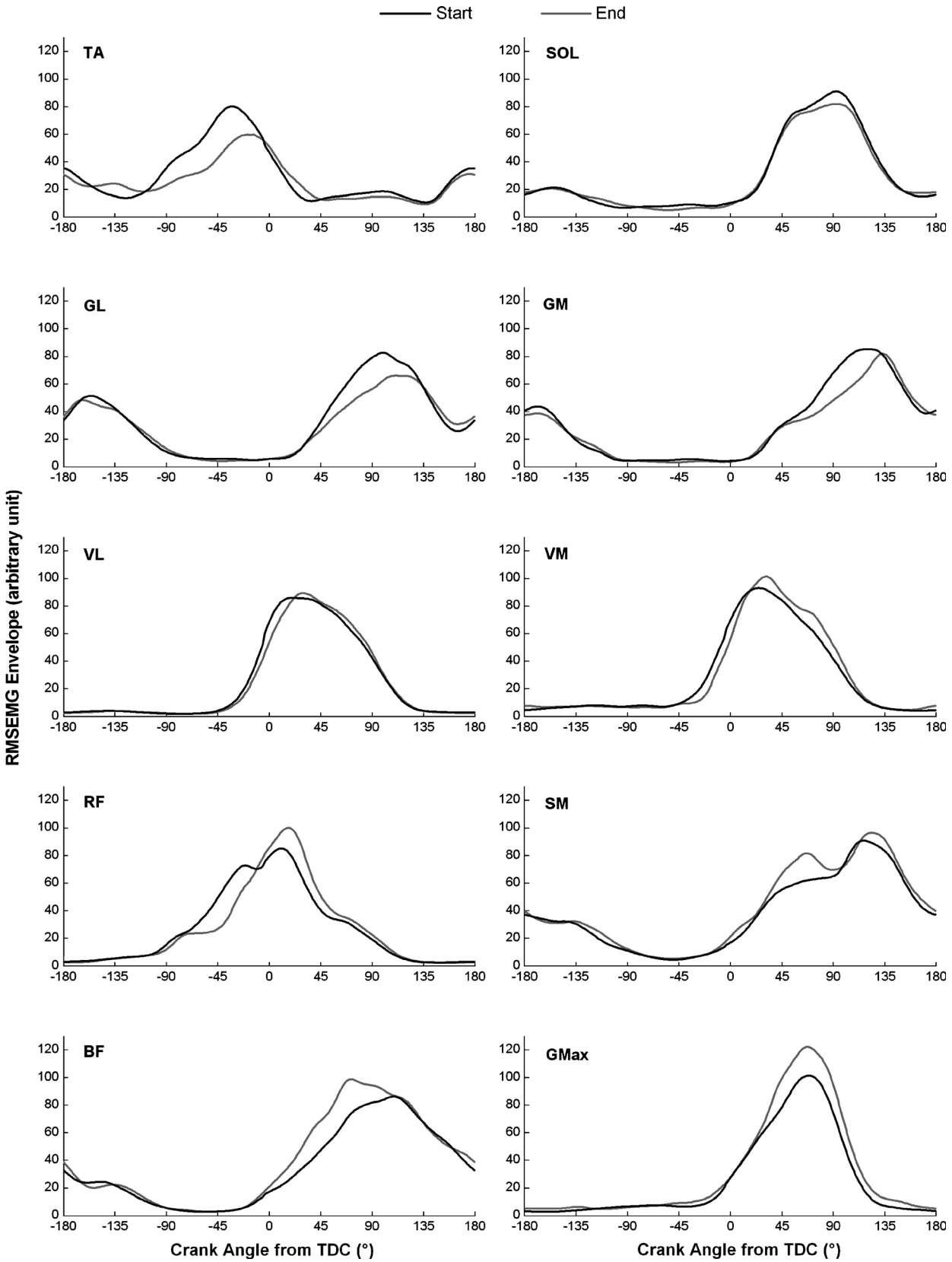

FIGURE 5—RMS EMG envelope for 10 lower limb muscles obtained at the start (*black lines*) and at the end (*gray lines*) of the exhaustive pedaling exercise. Each profile represents the mean obtained from averaging individual data across 30 consecutive pedaling cycles, normalizing to the mean RMS calculated during the complete pedaling cycle at the start condition ("reference pattern"), and further averaging across the 10 cyclists. BF, biceps femoris; GL, gastrocnemius lateralis; GM, gastrocnemius medialis; GMax, gluteus maximus; RF, rectus femoris; SM, semimembranosus; SOL, soleus; TA, tibialis anterior; VL, vastus lateralis; VM, vastus medialis.

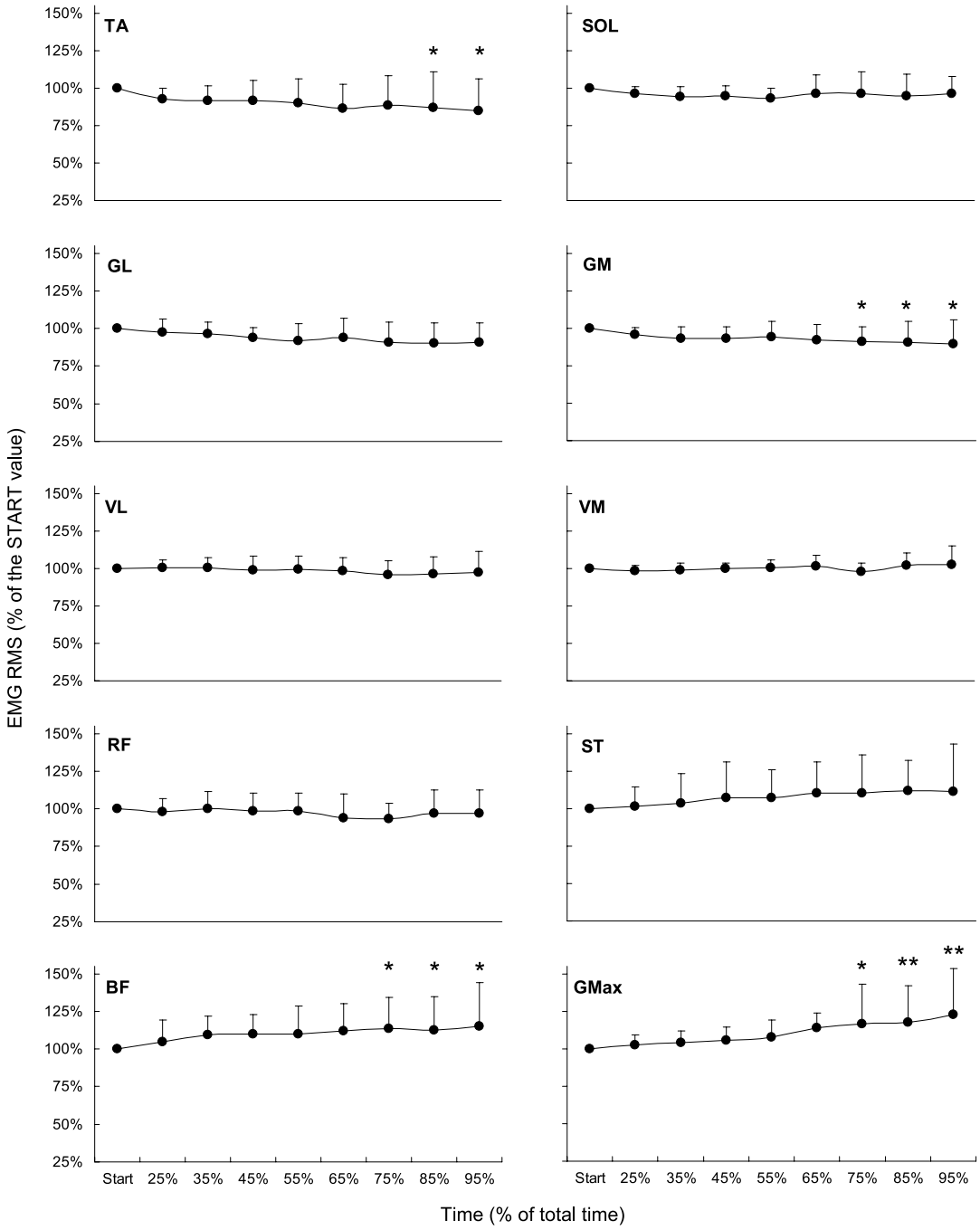

FIGURE 6—Evolution of the EMG RMS for the 10 lower limb muscles during the exhaustive pedaling exercise. BF, biceps femoris; GL, gastrocnemius lateralis; GM, gastrocnemius medialis; GMax, gluteus maximus; RF, rectus femoris; SM, semimembranosus; SOL, soleus; TA, tibialis anterior; VL, vastus lateralis; VM, vastus medialis. Asterisks indicate significant difference from the start value ($^{*}P < 0.05$, $^{**}P < 0.01$).

The increase in the effective force that was observed in our study, especially during the propulsive phase (sector 2), agrees with the increase in total force production, whereas the decrease in effective force around the TDC (sector 1) may be better explained by a lower ability to orient the force in this sector efficiently (i.e., a decrease in IE). These changes in the pattern of force application are in agreement with those previously reported by Sanderson and Black (25). Even if a decrease in the minimal value of the effective force (during the upstroke phase) has not been observed in the present study, the decrease in the mean F_{eff} during the TDC phase (zone 1) and the increase in the mean F_{eff} during the propulsive phase (zone 2) associated with the 6.1% increase of $F_{eff\text{-}max}$ confirmed the results from Sanderson and Black (25). These results seem to agree with the adjustments in muscle coordination strategy.

As mentioned in the introduction, the rise of EMG activity during a fatiguing constant-load exercise for a given

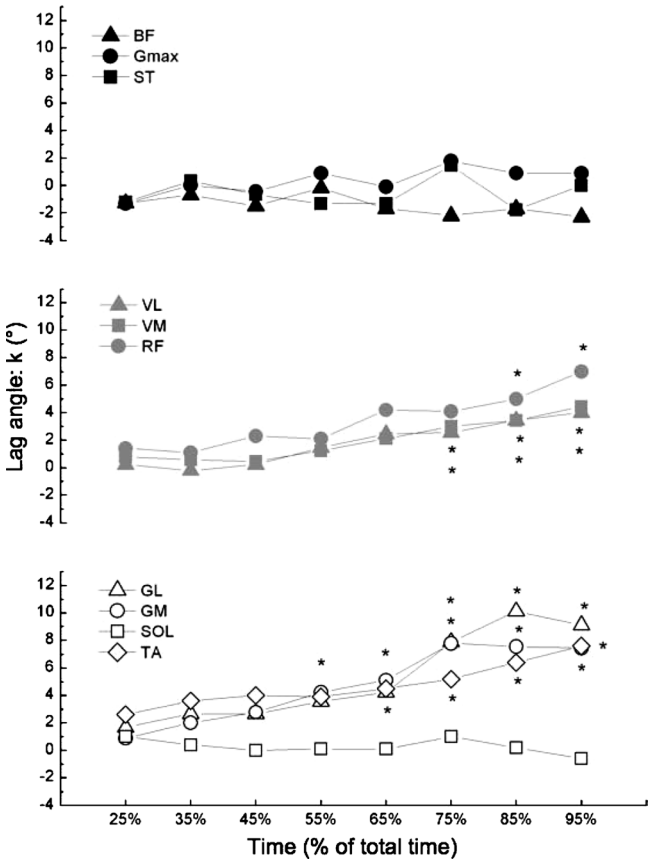

FIGURE 7—Angle shift of the complete EMG patterns assessed by the cross-correlation technique. The magnitude of a significant shift (lag angle) between each pair of signals was found by assessing the *k* value at which the cross-correlation coefficient was maximized. Each value for a given muscle results from the cross-correlation between the pattern obtained at the period of time considered and the reference pattern (obtained at the start of the exercise). BF, biceps femoris; GL, gastrocnemius lateralis; GM, gastrocnemius medialis; GMax, gluteus maximus; RF, rectus femoris; SM, semimembranosus; SOL, soleus; TA, tibialis anterior; VL, vastus lateralis; VM, vastus medialis. Asterisks indicate significant difference from the start value ($^*P < 0.05$).

muscle can be attributed to the progressive recruitment of additional motor units to compensate for the decrease in the force of contraction that occurs in the fatigued muscle fibers that make up this muscle. In this way, several studies have shown increased EMG amplitude in the quadriceps during fatiguing constant-load pedaling exercises (13,23,26,27). At first sight, the results of the these studies are not in agreement with the results obtained in the present study and others (22), where no modifications of VL and/or VM activities were observed. Nevertheless, the absence of any change in EMG activity level of a given muscle does not necessarily indicate that there is no decrease in the production of force at this muscle level, and hence, there is an absence of fatigue. Indeed, the same EMG activity level for a given muscle (e.g., VL and VM in our study) could be linked to a lesser force production because of the alteration of contractile properties. In this way, Lepers et al. (20) showed a significant decrease in maximal twitch tension (i.e., alteration of the contractile properties) of the quadriceps muscle group after 30 min of cycling at 80% of the maximal aerobic power. On the basis of this result, we can be reasonably hypothesized that similar alterations of the contractile properties of the quadriceps occurred during our exhaustive pedaling exercise. Nevertheless, because the mean load had to be kept constant, an increase in the activity of other power-producer muscles, such as the hip extensors, could have partly compensated for the loss of force production by the knee extensors. Our results, which show a 29% increase in the EMG activity level for GMax and a 15% increase for BF (i.e., mainly during the propulsive phase; Fig. 5), seem to be in line with this assumption. The RMS increase observed in these muscles (and especially in GMax) could be a result of: 1) a change of muscle coordination strategy (compensation of the loss of force production by knee extensors), 2) a progressive recruitment of additional motor units to compensate for the alteration of contractile properties, or 3) both. However, Ericson (8) showed that GMax activity level during a submaximal exercise is much lower than that for VM muscle (e.g., 40% vs 80% of maximal EMG activity at 240 W). Moreover, Sanderson and Black (25) reported an increase in maximum hip extensor moment at the end of a similar pedaling exercise. Taken together, these two pieces of information strongly suggest that the increases of GMax and BF activities, rather than manifesting fatigue in these muscles, mainly contribute to counteract the lesser production of force by the quadriceps muscles. Finally, it is interesting to note that this higher activity of hip extensors could certainly also help increase the propulsive force during the downstroke phase.

The lower EMG activity level of GM at the end of the exercise is consistent with the results of Bini et al. (3), which show no change of GM activity during a fatiguing exercise, despite a significant increase of power output thereby suggesting that these biarticular muscles are certainly not fatigued. This decrease of activity, which occurs primarily during phase 2 (i.e., the propulsive phase; Fig. 5), does not have much influence on the mechanical patterns (F_{eff} and F_{tot}) because this biarticular muscle is weakly activated and is not a great power producer during pedaling (8). However, this decrease in the activity of the plantar flexors could partly explain some changes observed in the distribution of tangential and normal pedal forces and in the pedal angle (Fig. 3): an increase in the normal component and a lower and more negative tangential force associated with a decrease in the pedal angle, suggesting a more pronounced dorsiflexion position of the ankle during the propulsive and BDC phases.

As mentioned above for GM and GL, a possible strategy for counteracting the effects of fatigue is to modify the activation timing of the muscles used in performing the movement. Billaut et al. (2) reported an earlier BF activation with fatigue occurrence, whereas most other authors showed no significant change (16,26). In our case, our results show a shift forward of the EMG patterns along the

crank cycle for six muscles: 4° for VL and VM and 7°–9° for TA, GM, GL, and RF). These differences in findings can be explained by the methods used to determine the muscles activation timing because all the previous studies chose an EMG threshold value for onset and offset detection fixed at 15%–25% of the peak EMG recorded during the cycle, or 1, 2, or 3 SD beyond the mean of baseline activity. This method can be questionable for some EMG patterns. Indeed, that is strongly dependant of the threshold level used, and information about the shape of the EMG signals (i.e., level of activation changes across the crank cycle) is not taken into account. The present study used a more objective method to examine the phase shift of the entire EMG patterns: the cross-correlation technique that detects more subtle variations in timing (for more details, see [21]).

The lower effective force observed around the TDC is in line with a decrease in mechanical effectiveness in this critical part of the pedaling cycle. All the EMG results concerning muscles acting in this phase are in agreement with this alteration and could partly account for the decrease of force production, i.e., the decrease of TA activity level and the shift forward of VL, VM, and RF. Moreover, an inspection of the RF pattern (Fig. 5) exhibits a decrease in the initial part of the activity period and an increase in the final part, clearly suggesting a lower activity as hip flexor in the first part of TDC phase and a higher activity as knee extensors during the beginning of the downstroke phase. Taken together, these adjustments in muscle coordination could largely explain the deterioration of effectiveness and, hence, the decrease in the effective force in this part of the cycle.

CONCLUSION AND PRACTICAL IMPLICATIONS

The pedaling technique is altered during a high-intensity exhaustive exercise, which leads to a higher downstroke effective force and lower mechanical effectiveness and effective force around the top dead center at the end of the effort. The occurrence of fatigue induces significant alterations in muscle coordination, which could be strongly related to these modifications. Whereas the decrease of GM activity seems to have moderate influence on the effective force profile, the decreases in TA and RF (as hip flexor) are in agreement with the decrease in mechanical effectiveness around the top dead center. The large increases of activity in GMax and BF, which are in accordance with the increase in force production during the propulsive phase, could be considered as instinctive coordination strategies that compensate for potential fatigue and loss of force of the knee extensors (i.e., VL and VM) with a higher moment of the hip extensors. The question of benefits of these adaptations is open to discussion. Further investigations using direct neuromuscular fatigue measurements are needed to better understand the alteration of the EMG response and to better separate the influence of muscle fatigue (i.e., alteration of contractile properties) from adjustments in the coordination strategy. From a practical point of view, the mechanical adaptations observed in our study (i.e., higher downstroke effective force and lower mechanical effectiveness and effective force around the top dead center at the end of the effort) question the pertinence to perform a specific training program to improve mechanical patterns and more specifically, the ability to pull up the pedal more efficiently. Considering that 1 h of pedaling corresponds to approximately 4800 crank revolutions (at 80 rpm), it could be postulated that even a small increase in pedaling effectiveness would induce significant gains in performance. Moreover, if the increase in GMax and BF activity is really an instinctive coordination strategy that compensates for potential fatigue and loss of force of the knee extensors with a higher moment of the hip extensors, we can hypothesize that an earlier recruitment of these muscles would be more efficient to delay fatigue occurrence. For such purpose, direct biofeedback of EMG and mechanical measurements would be useful for improving the activity pattern of the lower limb muscles and, thus, the training programs.

This study was funded in part by “La fondation d’entreprise de la Française Des Jeux” and the French Ministry of Sport (contract no. 06–046).

The authors are grateful for the subjects for having accepted to participate in this study and for Dr. Henry Vandewalle for his medical assistance. They also thank Dr. Christophe Hausswirth for the constructive discussions and advices. The results of the present study do not constitute endorsement by ACSM.

REFERENCES

1. Ansley L, Schabort E, St Clair Gibson A, Lambert MI, Noakes TD. Regulation of pacing strategies during successive 4-km time trials. *Med Sci Sports Exerc*. 2004;36(10):1819–25.
2. Billaut F, Basset FA, Falgairette G. Muscle coordination changes during intermittent cycling sprints. *Neurosci Lett*. 2005;380(3): 265–9.
3. Bini RR, Carpes FP, Diefenthaeler F, Mota CB, Guimaraes AC. Physiological and electromyographic responses during 40-km cycling time trial: relationship to muscle coordination and performance. *J Sci Med Sport*. 2008;11(4):363–70.
4. Dorel S, Couturier A, Hug F. Influence of different racing positions on mechanical and electromyographic patterns during pedalling. *Scand J Med Sci Sports*. 2009;19(1):44–54.
5. Dorel S, Couturier A, Hug F. Intra-session repeatability of lower limb muscles activation pattern during pedaling. *J Electromyogr Kinesiol*. 2008;18(5):857–65.
6. Duc S, Betik AC, Grappe F. EMG activity does not change during a time trial in competitive cyclists. *Int J Sports Med*. 2005;26:(2): 145–50.
7. Edwards RG, Lippold OC. The relation between force and integrated electrical activity in fatigued muscle. *J Physiol*. 1956; 132(3):677–81.

8. Ericson M. On the biomechanics of cycling. A study of joint and muscle load during exercise on the bicycle ergometer. *Scand J Rehabil Med Suppl*. 1986;16:1–43.
9. Gandevia SC. Spinal and supraspinal factors in human muscle fatigue. *Physiol Rev*. 2001;81(4):1725–89.
10. Hautier CA, Arsac LM, Deghdegh K, Souquet J, Belli A, Lacour JR. Influence of fatigue on EMG/force ratio and cocontraction in cycling. *Med Sci Sports Exerc*. 2000;32(4):839–43.
11. Hermens HJ, Freriks B, Disselhorst-Klug C, Rau G. Development of recommendations for SEMG sensors and sensor placement procedures. *J Electromyogr Kinesiol*. 2000;10(5):361–74.
12. Hettinga FJ, De Koning JJ, Broersen FT, Van Geffen P, Foster C. Pacing strategy and the occurrence of fatigue in 4000-m cycling time trials. *Med Sci Sports Exerc*. 2006;38(8):1484–91.
13. Housh TJ, Perry SR, Bull AJ, et al. Mechanomyographic and electromyographic responses during submaximal cycle ergometry. *Eur J Appl Physiol*. 2000;83(4–5):381–7.
14. Hug F, Dorel S. Electromyographic analysis of pedaling: a review. *J Electromyogr Kinesiol*. 2009;19(2):182–98.
15. Hug F, Drouet JM, Champoux Y, Couturier A, Dorel S. Inter-individual variability of electromyographic patterns and pedal force profiles in trained cyclists. *Eur J Appl Physiol*. 2008;104(4): 667–78.
16. Knaflitz M, Molinari F. Assessment of muscle fatigue during biking. *IEEE Trans Neural Syst Rehabil Eng*. 2003;11(1):17–23.
17. LaFortune MA, Cavanagh PR. Effectiveness and efficiency during cycling riding. *Biomechanics VIII-B: International Series on Biomechanics.* Chicago (IL): Human Kinetics; 1983. p. 928–36.
18. Lepers R, Hausswirth C, Maffiuletti N, Brisswalter J, van Hoecke J. Evidence of neuromuscular fatigue after prolonged cycling exercise. *Med Sci Sports Exerc*. 2000;32(11):1880–6.
19. Lepers R, Maffiuletti NA, Rochette L, Brugniaux J, Millet GY. Neuromuscular fatigue during a long-duration cycling exercise. *J Appl Physiol*. 2002;92(4):1487–93.
20. Lepers R, Millet GY, Maffiuletti NA. Effect of cycling cadence on contractile and neural properties of knee extensors. *Med Sci Sports Exerc*. 2001;33(11):1882–8.
21. Li L, Caldwell GE. Coefficient of cross correlation and the time domain correspondence. *J Electromyogr Kinesiol*. 1999;9(6): 385–9.
22. Lucia A, Hoyos J, Chicharro JL. The slow component of $\dot{V}O_2$ in professional cyclists. *Br J Sports Med*. 2000;34(5):367–74.
23. Petrofsky JS. Frequency and amplitude analysis of the EMG during exercise on the bicycle ergometer. *Eur J Appl Physiol Occup Physiol*. 1979;41(1):1–15.
24. Sanderson DJ. The influence of cadence and power output on the biomechanics of force application during steady-rate cycling in competitive and recreational cyclists. *J Sports Sci*. 1991;9(2): 191–203.
25. Sanderson DJ, Black A. The effect of prolonged cycling on pedal forces. *J Sports Sci*. 2003;21(3):191–9.
26. Sarre G, Lepers R. Neuromuscular function during prolonged pedalling exercise at different cadences. *Acta Physiol Scand*. 2005; 185(4):321–8.
27. Saunders MJ, Evans EM, Arngrimsson SA, Allison JD, Warren GL, Cureton KJ. Muscle activation and the slow component rise in oxygen uptake during cycling. *Med Sci Sports Exerc*. 2000; 32(12):2040–5.
28. St Clair Gibson A, Schabort EJ, Noakes TD. Reduced neuromuscular activity and force generation during prolonged cycling. *Am J Physiol Regul Integr Comp Physiol*. 2001;281(1): R187–96.

Scand J Med Sci Sports 2009: 19: 44–54
Printed in Singapore . All rights reserved
DOI: 10.1111/j.1600-0838.2007.00765.x

SCANDINAVIAN JOURNAL OF
MEDICINE & SCIENCE
IN SPORTS

Influence of different racing positions on mechanical and electromyographic patterns during pedalling

S. Dorel[1], A. Couturier[1], F. Hug[1,2]

[1]National Institute for Sports and Physical Education (INSEP), Laboratory of Biomechanics and Physiology, F-75014, Paris, France, [2]University of Nantes, Nantes Atlantic Universities, Laboratory 'Motricity, Interactions, Performance' (JE 2438), F-44000, Nantes, France

Corresponding author: François Hug, PhD, University of Nantes, UFR STAPS, Laboratory 'Motricity, Interactions, Performance', JE 2438, 25 bis boulevard Guy Mollet, BP 72206, 44322 Nantes cedex 3, France, Tel: +33 2 51 83 72 24, Fax:+33 2 51 83 72 10, E-mail: francois.hug@univ-nantes.fr

Accepted for publication 27 November 2007

The aim of this study was to test the hypothesis that, in comparison with standard postures, aero posture (AP) would modify the coordination of lower limb muscles during pedalling and consequently would influence the pedal force production. Twelve triathletes were asked to pedal at an intensity near the ventilatory threshold (VT+Δ20%) and at an intenisty corresponding to the respiratory compensation point (RCP). For each intensity, subjects were tested under three positions: (1) upright posture (UP), (2) dropped posture (DP), and (3) AP. Gas exchanges, surface electromyography and pedal effective force were continuously recorded. No significant difference was found for the gas-exchange variables among the three positions. Data illustrate a significant increase [*gluteus maximus* (GMax), *vastus medialis* (VM)] and decrease [*rectus femoris* (RF)] in electromyography (EMG) activity level in AP compared with UP at RCP. A significant shift forward of the EMG patterns (i.e. later onset of activation) was observed for RF (at VT+Δ20% and RCP), GMax, VL, and VM (at RCP) in AP compared with UP. These EMG changes are closely related to alteration of force profile in AP (higher downstroke positive peak force, lower upstroke negative peak force, and later occurrence of these peaks along the crank cycle).

Air resistance is the dominant force-resisting motion of cyclists on flat terrain. It depends on different external factors (e.g. ambient air velocity or air density) and biomechanical-anthropometric factors (e.g. drag coefficient and frontal area of rider+bicycle system). In an effort to reduce this force, the cyclist's body positioning has received much attention in the past two decades. From a mechanical point of view, a more crouched upper body position (i.e. areo posture, AP), by decreasing the frontal area, allows a lower wind resistance (Capelli et al., 1993) compared with conventional postures (upright posture, UP or dropped posture, DP) and hence a higher riding speed for a given power ouput. In parallel, some research has focused on the effects of this AP on the ventilatory and metabolic responses during submaximal and/or maximal exercises (Ryschon & Stray-Gundersen, 1991; Origenes et al., 1993; Gnehm et al., 1997; Grappe et al., 1998). Although some authors have failed to detect any significant differences in several cardiorespiratory variables between standard and APs (Origenes et al., 1993; Grappe et al., 1998), others concluded that aero position increases the metabolic cost of cycling (Gnehm et al., 1997). It is surprising that the effects of this cycling position on both mechanical aspects of force production on pedals and lower limb muscles activation pattern have not been investigated.

Surface electromyography (EMG) records have been widely used to study muscle activity and neuromuscular coordination during pedalling (Houtz & Fischer, 1959; Ericson, 1986; Gregor et al., 1991; For review see Hug & Dorel, in press). Other investigators have measured the forces exerted on pedals and/or cranks (Hoes et al., 1968; Sanderson et al., 2000; Sanderson & Black, 2003; Bertucci et al., 2005) and computed their effective component (i.e. effective force, tangential to the crank displacement). In order to maintain a given level of performance, the EMG and mechanical patterns vary in timing and magnitude as pedalling conditions change. Along this line, some studies have demonstrated that the pattern of muscles activation and/or of forces exerted on pedals could be modified by factors such as workload (Ericson, 1986; Jorge & Hull, 1986), pedalling rate (Suzuki et al., 1982; Ericson, 1986), shoe–pedal interface (Ericson, 1986; Cruz & Bankoff, 2001) and saddle height (Houtz & Fischer, 1959; Ericson, 1986). Literature concerning the influence of body

position on mechanical and EMG patterns is less profuse. Two studies have showed that standing and seated postures lead to different patterns (Li & Caldwell, 1998; Duc et al., in press). To the best of our knowledge, only one study has focused on the effects of trunk orientation on the activation pattern of lower limb muscles during pedalling (Savelberg et al., 2003b). The authors reported that trunk angle influences the EMG patterns. However, the tested positions (i.e. 20° forward and backward of the vertical) were not comparable to the standard postures used by competitive cyclists (and especially far from the AP). Furthermore, the pedal force production was not measured.

Thus, we designed the present study to test the hypothesis that, in comparison with standard postures, aero position would modify the coordination of lower limb muscles during pedaling and consequently would influence the mechanical aspects of pedal force production. A population of trained triathletes was tested in three different positions (i.e. aero, upright and dropped posture (DP)). Each subject was tested at an intensity near the ventilatory threshold and at an intenisty corresponding to the respiratory compensation point (RCP) with the ulterior motive of transposing our observations to a time trial event.

Materials and methods

Subjects

Twelve male triathletes whose anthropometrical and physiological characteristics are presented in Table 1 volunteered to participate in this study. The subjects had a 9 ± 5 years of competitive experience. None of them had recent or ancient pathology of lower limb muscles or joints. They were informed of the nature of the study and the possible risk and discomfort associated with the experimental procedures before they gave their written consent to participate. The experimental design of the study was approved by the Ethical Committee of Saint-Germain-en-Laye (acceptance no 06016) and was carried out in accordance with the Declaration of Helsinki. All subjects were instructed to refrain from intense physical activities during the 2 days before testing.

Table 1. Anthropometrical and physiological characteristics of the population of triathletes ($n = 12$)

	Mean ± SD
Age (years)	31.1 ± 8.4
Height (m)	1.81 ± 0.08
Body mass (kg)	72.2 ± 6.8
BMI (kg/m)	22.1 ± 1.7
VO_{2max} (mL/min/kg)	63.5 ± 9.1
$\dot{V}_E$ max (L/min)	181 ± 19
MAP (W)	392 ± 31
MAP (W/kg)	5.5 ± 0.7
VT (% MAP)	56.9 ± 4.6
RCP (% MAP)	83.3 ± 3.9

BMI, body mass index; MAP, maximal aerobic power; VT and RCP, ventilatory threshold and respiratory compensation point (expressed in percentage of MAP).

Exercise protocol

The testing protocol consisted of two sessions conducted in the following order: (1) anthropometric measurements and incremental cycling exercise performed until exhaustion in order to characterize our population in terms of physical and physiological capacities; (2) experimental session consisting of two submaximal cycling exercises, each performed in three different upper body postures.

During the first visit, 2 weeks before the experimental session, each subject performed an incremental cycling exercise (workload increments of 25 W/min; starting at 100 W) during which the usual gas-exchange and ventilatory variables were measured. Throughout this exercise trial, the device (K4B2, Cosmed®, Rome, Italy) computed breath-by-breath data of $\dot{V}_E$, VO_2, VCO_2, and the ventilatory equivalents for O_2 ($\dot{V}_E$ VO_2^{-1}) and CO_2 ($\dot{V}_E$ VCO_2^{-1}). The VT and RCP, respectively, were determined with the method based on the ventilatory equivalents for O_2 and CO_2 (Reinhard et al., 1979). Two independent observers detected VT and RCP following the criteria previously described. If they did not agree, the opinion of a third investigator was included. The first power achieved when the maximal oxygen uptake was reached (VO_{2max}) was referred as the maximal aerobic power. All these variables were determined to further adjust the two constant workloads tested during the experimental session. Finally, after a 15-min recovery period, the subjects were acclimatized to the three upper body positions that will be adopted during the subsequent visit.

During the second session, subjects were asked, after a 10 min warm-up at 100 W, to pedal at two different intensities corresponding to the power associated to: (1) VT plus 20% of the difference between power outputs measured at VT and RCP (VT+Δ20%) and (2) RCP. For each of these two intensities, subjects were tested, in a randomized order, under three body positions (detailed below): (1) the UP, (2) the DP, and (3) the AP (Fig. 1(a)). Each position was tested during 6 min at VT+Δ20% (5 min of active recovery between bouts) and 2 min at RCP (7 min of active recovery between bouts, Fig. 1(b)). The reason for choosing short test periods was to avoid fatigue throughout the session. Subjects were asked to keep the same constant preferred pedalling rate chosen at the end of the warm-up period throughout the session ($\pm$ 2 r.p.m.). Gas exchanges, surface EMG and mechanical variables were continuously recorded during this protocol.

Stationary bicycle and body positions

Subjects exercised on an electronically braked cycle ergometer (Excalibur Sport, Lode®, Groningen, the Netherlands) equipped with standard crank (length = 170 mm) and with their own clipless pedals. During both sessions, vertical and horizontal positions of the saddle, handlebar height and stem length were set to match the two usual positions of the participants: (1) UP, with hands on top of the handlebars, near the stem and elbow angle between 160° and 180°; (2) DP, the traditional racing position with the torso partially to fully bent-over, hands on the drops portion of the handlebars and elbows partially flexed (elbow angle less than 160°). To obtain an AP during the second session clip-on aerobars (Aero II, Profile, Los Angeles, USA) were added on the classical handlebar. Aero-handlebars and stem were adjusted (height and length) to custom fit each subject into his own aerodynamic position with the following restrictions: elbows on the pads of aero-handlebars with elbow angle close to 90° and the

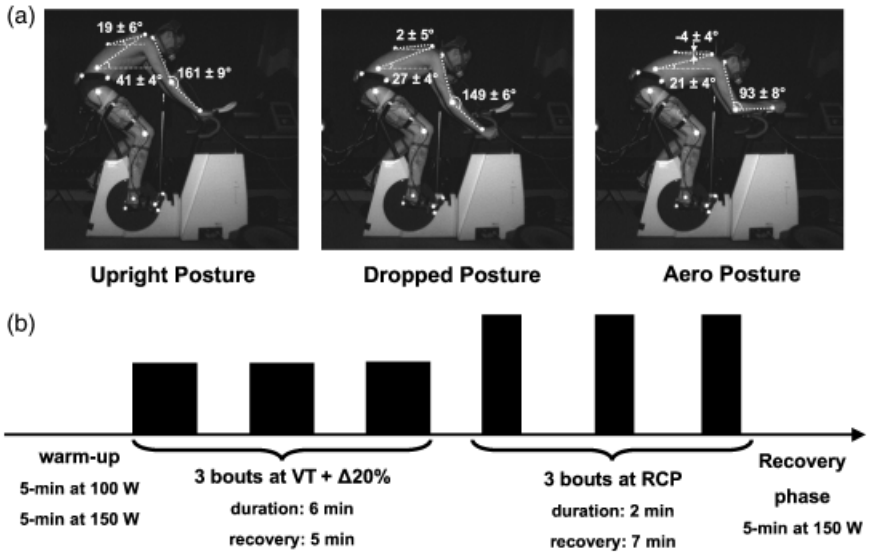

Fig. 1. A/Illustration of the three different positions [i.e. upright, dropped and aero postures (AP)] as defined by the placement of the hands and torso for one subject. Values of angle between (1) the trunk and horizontal (2) the upper part of the torso and horizontal and (3) arm and forearm reported on the photograph are the mean values obtained on the entire population. B/Schematic representation of the protocol.

upper part of the torso (line T10–C7) held parallel to the ground (with 10° tolerance, Fig. 1(a)). All these angles were measured with a goniometer. Video recording was used to check these standardization criterions in each position during the experimental session. Briefly, reflective markers placed on the right side of each subject and video analysis (2D sagittal plane, $f = 250$ Hz) were used to approximate (1) the positions of the trunk (line from iliac crest to C7) and the upper part of the torso (line from T10 to C7) in reference to a horizontal line and (2) the elbow angle (acromion process, olecranon process, and wrist). Figure 1(a) depicts the mean angle values obtained for the group in each position.

Material and data collection

The torque exerted on the left and right cranks was measured by strain gauges located in the crank arms of the cycle ergometer. Before the experiments, a classical calibration procedure (i.e. with known masses) was performed and a zero adjustment was done before each session. Effective force (i.e. the propulsive force applied perpendicularly to the crank arm) was determined by the ratio between torque and the constant length of the crank arm. The crank angle and the angular velocity were calculated (by derivative) based on TTL rectangular pulses delivered each 2° by the cycle ergometer. Additional TTL rectangular pulse permitted to detect the bottom dead center of the right pedal (i.e. BDC: lowest position of the right pedal with crank arm angle = 180°). All these data were digitized at a sampling rate of 2 kHz (USB data acquisition DT9800, Data translation®, Malboro, USA).

Surface EMG activity was continuously recorded for the following 10 muscles of the right lower limb: *gluteus maximus* (GMax), *semimembranosus* (SM), *Biceps femoris* (BF), *vastus medialis* (VM), *rectus femoris* (RF), *vastus lateralis* (VL), *gastrocnemius medialis* (GM) and *lateralis* (GL), *soleus* (SOL) and *tibialis anterior* (TA). A pair of surface Ag/AgCl electrodes (Blue sensor, Ambu®, Ballerup, Denmark) was attached to the skin with a 2 cm interelectrode distance. The electrodes were placed longitudinally with respect to the underlying muscle fibres arrangement and located according to the recommendations by Surface EMG for Non-Invasive Assessment of Muscles (SENIAM) (Hermens et al., 2000). Before electrode application, the skin was shaved and cleaned with alcohol in order to minimize impedance. The wires connected to the electrodes were well secured with adhesive tape to avoid movement-induced artifacts. Raw EMG signals were pre-amplified close to the electrodes (gain 375, bandwidth 8–500 Hz), and digitized at a sampling rate of 1 kHz (ME6000P16, Mega Electronics Ltd®, Kuopio, Finland). BDC TTL rectangular pulses were simultaneously digitized for further synchronization with cycle ergometer data. In order to diminish movement artefacts, a high pass filter (20 Hz) was further applied on the EMG signals (Chart 5.4, AD instruments®, Hasting, UK).

Data processing

All data were analyzed with custom written scripts (Origin 6.1, OriginLab Corporation, Northampton, USA). The BDC TTL rectangular pulses were used to synchronize signals of the right pedal effective force, right crank angle and EMG data. Raw EMG data were root mean squared (RMS) with a time averaging period of 25 ms to produce linear envelope for each muscle activity pattern. Effective force and EMG RMS were then re-sampled in order to obtain one value each 2 degrees of crank displacement. Prior re-sampling, all data were filtered with an anti-aliasing filter which cutoff frequency was dynamically computed according to Shannon Theorem (i.e. 2 degrees TTL pulses half mean frequency). Linear interpolation technique was then used to obtain a mean value of force and EMG RMS each degree of rotation. Finally, these data were respectively averaged over 90 and 45 consecutive pedalling cycles for VT+Δ20% and RCP conditions in order to get a representative effective force profile and an EMG RMS linear envelope for each muscle, each subject and each condition. These values were expressed as a function of the crank arm angle as it rotated from the highest pedal position (0°, top dead center: TDC) to the lowest (180°, bottom dead center, BDC) and back to TDC to complete a 360° crank cycle.

The following mechanical variables were calculated or identified from the effective force profile: the mean values of effective force (F_{cycle}, N), pedalling rate (f_{cycle}, r.p.m.) and power output (P_{cycle}, W) over one complete cycle, the maximal (peak) value of the effective force exerted during the downstroke (F_{max}, N) and minimal value exerted during the upstroke (F_{min}, N) and the arm crank angle corresponding, respectively, to F_{max} ($Angle_{max}$, °) and F_{min} ($Angle_{min}$, °). To quantify the muscle activity pattern, a series of classical variables were calculated from the EMG RMS linear envelope. The overall activity level was identified by the mean EMG

RMS magnitude over one complete cycle (RMS_{cycle}). The EMG timing analysis consisted in determining onset and offset of the burst of muscle activation which was defined as the period of higher activity phase where the signal was above a threshold of 20% of the difference between peak and baseline EMG (Li & Caldwell, 1999). The technique of cross-correlation was also used to measure the relative change in the temporal characteristics of neuromuscular activity (Li & Caldwell, 1998, 1999). Firstly, the cross correlation coefficients of EMG RMS curves between the three body configurations for each muscle were calculated according to the equation proposed by Li and Caldwell (1998) with lag time equal to zero (r_0). Then, the magnitude of a significant time shift between signals obtained in two different body positions was found by assessing the k value (k_{max}) at which the cross correlation coefficient was maximized (r_{max}). The purpose was to estimate the effects of body position on linear envelope patterns of the different muscles by using this more recent and objective approach for comparing signals.

Statistical analysis

All analyses were performed with the statistical package SPPS 11.0 and ORIGIN 6.1 software for Windows. Data were first tested for normality using Kolmogorov–Smirnov test. Because the normality condition was verified, the results are expressed as mean ± standard deviation (± SD). One-way analysis of variance (ANOVA) with repeated measures was employed to test the effect of the three body postures on all the ventilatory, gas-exchange, mechanical and EMG variables at both exercise intensities. When significant F ratios were found, all the means were compared using a Tukey's *post hoc* test. Differences were considered significant when probability (P) of a type I error was $\leq 5\%$.

Results

Ventilatory and gas-exchange variables

No significant difference was found for the ventilatory and gas-exchange variables measured at VT+Δ20% among the three body positions (Table 2). Because no metabolic steady state was achieved during the exercise bouts at RCP, results are not reported for this intensity.

Effective force profile

To achieve the power outputs corresponding to VT+Δ20% and RCP, similar mean effective forces and pedalling rates were maintained among the three body positions (Table 3). Figure 2 depicts the pattern of the mean effective force over the crank cycle for all conditions. F_{min} was significantly lower for UP than for DP and AP at VT+Δ20% and F_{max} was significantly higher for AP than for UP at RCP (Table 3). For sake of clarity, mean values of effective force were calculated for four angular sectors (Fig. 3): Sector 1 represented 330–30°; Sector 2, 30–150°; Sector 3, 150–210° and Sector 4, 210–330°. Sectors 1 and 3 correspond respectively to the top and bottom dead centers; Sectors 2 and 4 correspond respectively to the main propulsive and recovery phases. For AP, effective force at VT+Δ20% was significantly higher in Sector 3 and lower in Sectors 1 and 4 compared with the other positions. In addition to these differences which persist at RCP, effective force for AP was significantly higher in Sector 2 than for UP at RCP (Fig. 3). Furthermore, angles corresponding to minimal ($Angle_{min}$) and maximal ($Angle_{max}$) effective forces were significantly higher for AP than for UP and DP (only for $Angle_{max}$) at RCP (Table 3).

Table 2. Ventilatory and gas-exchange variables (mean ± SD) measured at VT+Δ20% for the three body positions. All the values were averaged during the last 2 min of each bout

	Aero posture (AP)	Dropped posture (DP)	Upright posture (UP)
VO_2 (mL/min)	3458 ± 297	3368 ± 270	3394 ± 234
VE (L/min)	88.7 ± 11.6	86.7 ± 10.9	84.4 ± 9.4
RER	0.94 ± 0.03	0.93 ± 0.04	0.92 ± 0.03
VT (L)	2.83 ± 0.45	2.73 ± 0.41	2.86 ± 0.41
Bf (cycles/min)	32.0 ± 5.7	32.8 ± 6.3	30.2 ± 6.1

VO_2, oxygen uptake; VE, ventilatory flow; RER, respiratory exchange ratio; VT, tidal volume; Bf, breathing frequency.

Muscle activity level

At VT+Δ20%, AP and DP induced significantly higher muscle activity level (RMS_{cycle}) compared with UP for GMax. RMS_{cycle} for SOL was also higher for AP compared with the other positions (Fig. 4). At RCP, these differences persisted only for GMax, while other differences of muscle activation appeared: RMS_{cycle} was significantly higher for AP than for DP and UP for VM, and in AP than for DP for VL. In contrast, UP induced a higher activity level of RF than did any of the other positions.

Muscle activation timing

Muscle activity patterns from the three cycling positions are represented with ensemble linear envelopes (45 or 90 consecutive cycles × 12 subjects per condition and per intensity) of the EMG RMS data (Fig. 5(a) and (b) for VT+Δ20% and RCP, respectively). Figure 6 depicts the mean values of the muscle activation timing variables obtained at VT+Δ20% and RCP. The onset of activation occurred later for RF in AP condition than it did for UP at both VT+Δ20% and RCP. GMax, VL and VM were also recruited later in AP and DP than for UP, only at RCP. The offset of activation of SM occurred later in AP compared with DP. However, no significant difference was found among the three body positions in muscle activation timing for the four leg muscles. All these results were confirmed and emphasized by the cross-correlation analysis (Table 4). The k_{max} values demonstrate a significant pattern shift (i) among the three conditions for GMax, RF and VL,

Table 3. Mechanical variables (mean ± SD) measured at VT+Δ20% and RCP for the three body positions

	VT+Δ20%				RCP			
	AP	DP	UP		AP	DP	UP	
P_{cycle} (W)	**238.2** (22.9)	**238.0** (22.6)	**238.2** (22.8)	NS	**318.6** (27.6)	**318.0** (28.1)	**318.5** (27.7)	NS
f_{cycle} (rpm)	**89.2** (8.1)	**89.6** (10.2)	**89.6** (9.3)	NS	**90.3** (8.9)	**90.3** (9.1)	**90.2** (9.6)	NS
F_{cycle} (N)	**75.9** (11.7)	**75.8** (12.8)	**75.8** (12.8)	NS	**100.1** (14.1)	**99.9** (13.7)	**100.4** (14.6)	NS
F_{max} (N)	**324.8** (31.8)	**317.0** (33.9)	**320.0** (44.3)	NS	**386.9** (45.2)	**380.4** (44.5)	**375.4** (41.0)	*
$Angle_{max}$ (°)	**95.7** (7.3)	**94.0** (6.0)	**92.7** (4.6)	NS	**95.8** (5.5)	**90.8** (5.7)	**90.3** (5.6)	# and *
F_{min} (N)	**−70.0** (26.1)	**−65.6** (27.2)	**−63.9** (26.6)	# **	**−53.2** (31.7)	**−52.6** (29.6)	**−49.1** (30.4)	NS
$Angle_{min}$ (°)	**268.0** (20.6)	**267.7** (22.9)	**265.2** (23.2)	NS	**284.5** (25.3)	**275.8** (25.0)	**271.4** (25.6)	**

AP, aero posture; DP, dropped posture; UP, upright posture.

P_{cycle}, f_{cycle}, and F_{cycle}: mean values of power output, pedalling rate and right pedal effective force calculated over one complete cycle; F_{max} and F_{min}: maximal and minimal value of the effective force exerted during the cycle; $Angle_{max}$ and $Angle_{min}$: respective arm crank angle corresponding to F_{max} and F_{min}.

#Significant difference between AP and DP ($P<0.05$).

*Significant difference between AP and UP ($P<0.05$).

**Significant difference between AP and UP ($P<0.01$).

(ii) between UP and the other conditions for VM, (iii) between AP and DP for SM and BF and AP and UP for SM. The maximal values of cross correlation coefficients (r_{max}) indicate a very high degree of similarity in the EMG activation patterns among the three conditions for all muscles (r_{max}: 0.960–0.997, Table 4).

Discussion

The present investigation is the first to focus simultaneously on both the mechanical aspects of pedal force production and lower limb muscle activation patterns in response to changes in upper body position. Despite the stability of both ventilatory and gas-exchange variables, the results of this study demonstrate significant alterations in pedal effective force and in the level and timing of activation of some lower limb muscles when the upper body configuration is changed, especially from the upright to the AP.

Methodological and general considerations

In addition to randomization, 5-min submaximal exercise at 150 W was performed just before and after the experimental protocol in order to verify the repeatability of the lower limb muscles activation patterns. These results have been previously published (Dorel et al., in press) and show a very good repeatability of the EMG patterns.

The two exercise intensities were chosen in order to reproduce typical training intensities (i.e. VT+Δ20%; corresponding to 238.1 ± 22.8 W) and specific intensities maintained during competitive time trial events (i.e. RCP: corresponding to 318.4 ± 27.8 W). Moreover, VT+Δ20% intensity ensured that a true metabolic steady state was achieved allowing the comparison of ventilatory and gas-exchange variables among the different body configurations. Unlike Gnehm et al. (1997), the present investigation failed to show significant modifications in oxygen consumption or other ventilatory/gas-exchange variables among the three body positions. These results are consistent with the majority of previous studies which also reported no significant posture effect despite some tendencies towards higher metabolic cost and ventilatory flow in the AP (Origenes et al., 1993). Overall, these results confirm the difficulty of demonstrating a true inconvenience in term of metabolic cost in the AP, especially in well-trained cyclists. Indeed, the triathletes serving as subjects in the present work were accustomed to using the three tested positions during training and competition. Moreover, it can be argued that the criteria selected to standardize the positions, and especially the aero position, were voluntarily chosen to not induce larger modifications than those that are common on the field. The question remains to be answered whether a more extremely aerodynamic position used by elite time-trial cyclists (i.e. with a greater torso inclination) and reported in previous studies (Gnehm et al., 1997) would induce greater

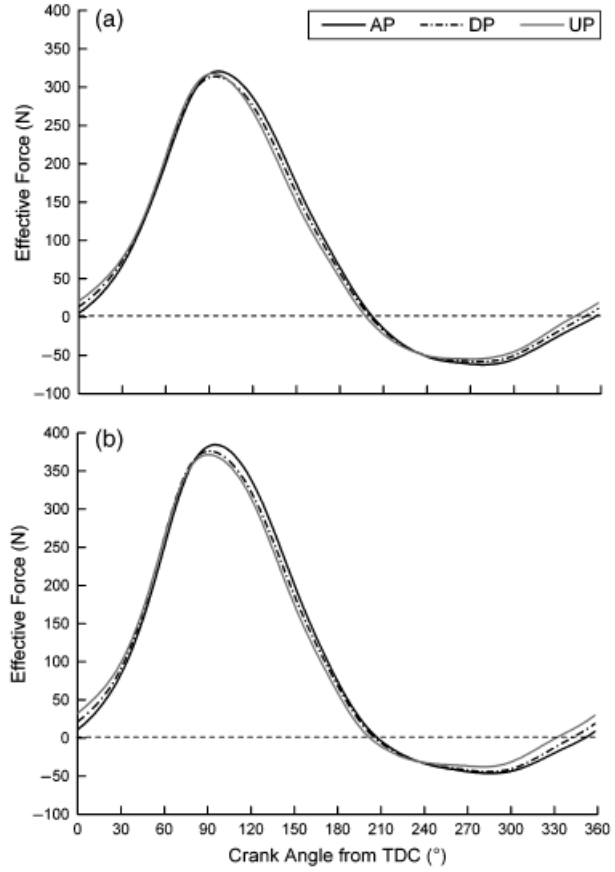

Fig. 2. Mean profile of the effective pedal force measured during the exercises at VT+Δ20% (a) and respiratory compensation point (RCP) (b) in the three upper body positions for the entire population. AP, aero posture; DP, dropped posture; UP, upright posture. Note the higher peak value of force produced during the second part of the downstroke phase and the lower value during the last part of the upstroke and the beginning of the downstroke for AP compared with UP.

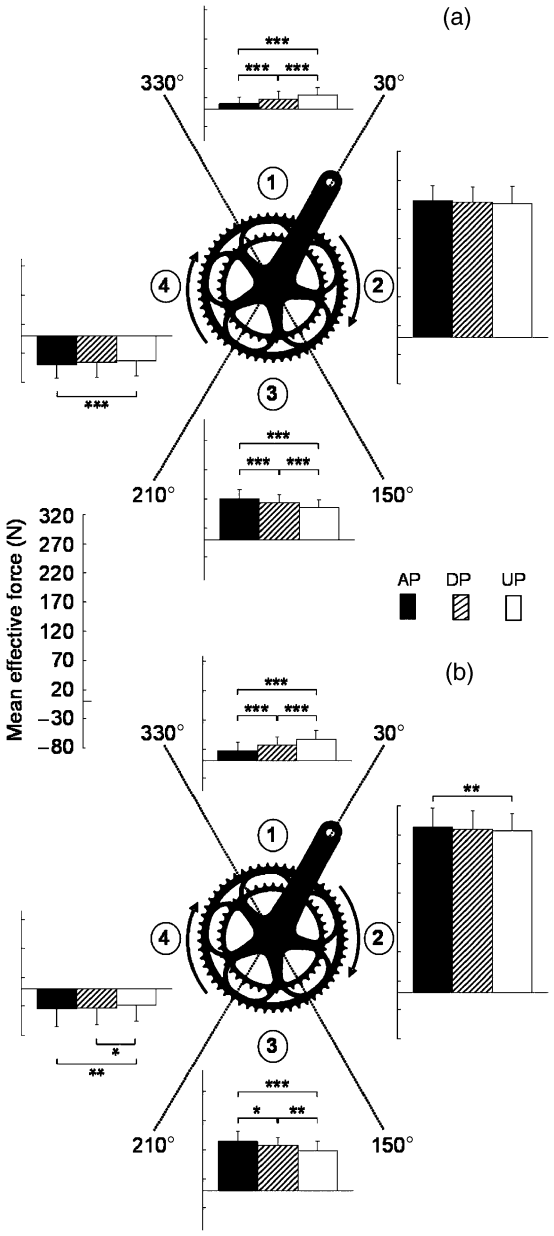

Fig. 3. Mean values of effective force calculated for four angular sectors as a function of crank position over the complete cycle in the three body configurations [(a) at VT+Δ20% and (b) at respiratory compensation point (RCP)]. Sector 1, 330–30°; Sector 2, 30–150°; Sector 3, 150–210° and Sector 4, 210–330°. AP, aero posture; DP, dropped posture; UP, upright posture. $***P<0.001$, $**P<0.01$, $*P<0.05$ significant difference between two conditions.

alterations in ventilatory response as well as in mechanical and neuromuscular responses.

The results concerning the influence of body position on force and EMG variables do not noticeably differ among the two intensities conditions. In a great majority, the significant changes or tendencies observed at VT+Δ20% are respectively amplified or begin significant at RCP. As a consequence, considering these similarities and the purpose of the study, the influence of exercise intensity will not be extensively detailed afterward so that the following discussion will focus on the results obtained at RCP.

Effective force

As expected, mean power output, pedalling rate and hence mean pedal effective force were kept constant among the three conditions for the two exercise intensities (Table 3), allowing the comparison of mechanical and EMG variables in respect to the body positions. Whereas several studies have reported changes in the torque profile in response to alterations of pedalling rate, power output, surface grade, and/or the occurrence of fatigue (Patterson & Moreno, 1990; Li & Caldwell, 1998; Sanderson et al., 2000; Sanderson & Black, 2003; Bertucci et al., 2005), few of them focused on the effects of different body configurations (Brown et al., 1996; Li & Caldwell,

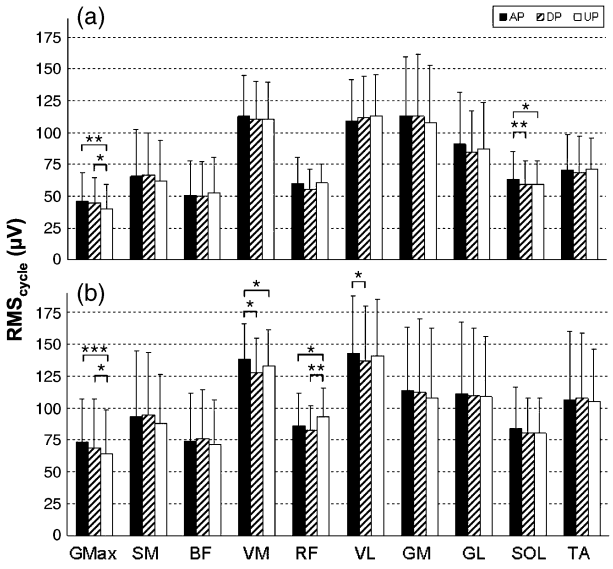

Fig. 4. Mean values of the root mean squared (RMS) magnitude for the complete cycle (RMS_{cycle}, i.e. 0 to 360°) for the three body positions (AP, aero posture; DP, dropped posture; UP, upright posture) at both constant submaximal power outputs [VT+Δ20% and respiratory compensation point ($RCP_{]}$] for 10 lower limb muscles implied in pedalling. GMax, *gluteus maximus*; SM, *semimembranosus*, BF, *Biceps femoris*; VM, *vastus medialis*; RF, *rectus femoris*; VL, *vastus lateralis*; GM, *gastrocnemius medialis*; GL, *gastrocnemius lateralis*; SOL, *soleus* and TA, *tibialis anterior*.

1998). Moreover, they concerned extreme postural adjustments such as standing vs seated (Li & Caldwell, 1998) or recumbent vs traditional posture (Brown et al., 1996). Our results clearly demonstrate that AP, compared with DP and to a large extent to UP, leads to an increase in the magnitude of the negative effective force during the upstroke (Sector 4 and F_{min} more negative) and a decrease of the slight positive force produced just before and after TDC (Sector 1) (Figs 2 and 3). In order to counterbalance these larger counterproductive regions for AP (i.e. mean effective force at RCP in Sector 4 and 1 amounts -8.6% and -3.2% of F_{cycle} for AP and UP, respectively), a greater force would be required during the downstroke for AP (i.e. mean effective force in Sectors 2 and 3 amounted 108.6% and 103.2% of F_{cycle} for AP and UP, respectively). In this line, a significantly higher F_{max} of 3.1% was observed for AP compared with UP at RCP. These results are the first to confirm the pioneering observations of Broker (2002) on cyclists and triathletes. Indeed, this author also reported effective force profiles in AP that are similar to those observed in the present study (i.e. with greater peak-to-peak oscillations). As argued by several authors, the lower hip angle towards more flexion (from almost $-20°$ from UP to AP) alters the mean working length of muscles crossing this articulation (RF, BF, and GMax) which could be responsible for the modification in the amount of force produced by these muscles (Gnehm et al., 1997; Ashe et al., 2003) and finally could change the force profile. It is noteworthy that these force profile adaptations in AP position could have not been detected by measuring only net crank torque (Bertucci et al., 2005). The direct measurement of each pedal effective force allowed a further analysis of the interactions among the specific changes in body configuration, these kinetics parameters and finally the activation patterns of the corresponding lower limb muscles.

EMG patterns

Comparing the EMG changes observed in the present study to those reported on more drastic body orientation manipulations (Brown et al., 1996; Savelberg et al., 2003a) or on differences between standing *vs*. seated positions (Li & Caldwell, 1998; Duc et al., in pres), it becomes clear that the effects of the aero position are less important. However, it is noteworthy that significant modifications of EMG patterns reported in our study seem to be directly linked to changes of the effective force pattern. The absence of change in both the intensity and the timing of the EMG activity of muscles crossing the ankle joint (GM, GL, TA, SOL) confirmed the relative stability of EMG pattern of these muscles in different body postures already reported in the literature: seated vs standing (Duc et al., in press), flexed forward vs upright (Savelberg et al., 2003a). Only one study has focused on the effects of trunk inclination on the activation pattern of lower limb muscles (Savelberg et al., 2003a). Although the body configurations tested in this later study are far away from ecological conditions (i.e. racing conditions), it is interesting to note that our results are consistent with these authors (Savelberg et al., 2003a) who reported a higher activation for GMax and a lower activation for RF in a flexed forward compared with an extended backward configuration. As a consequence, the decrease of pedal force found in AP during the upstroke and TDC phases could be explained by this lower activation of RF. Although this biarticular muscle both acts as knee extensor and hip flexor, a detailed analysis of RF EMG patterns (Fig. 5(b)) confirms that its activation is affected during the upstroke phase (i.e. while acting as hip flexor). However, it should be kept in mind that the relation between muscle activation and force production is not so simple because the increase of trunk inclination (i.e. flexed forward), by modifying pelvis orientation, has been showed to induce alteration of RF and GMax muscle lengths (Savelberg et al., 2003a). Then, it could be hypothesized that in aero position disadvantage due to more marked stretching of GMax (which induces passive resistance) and more

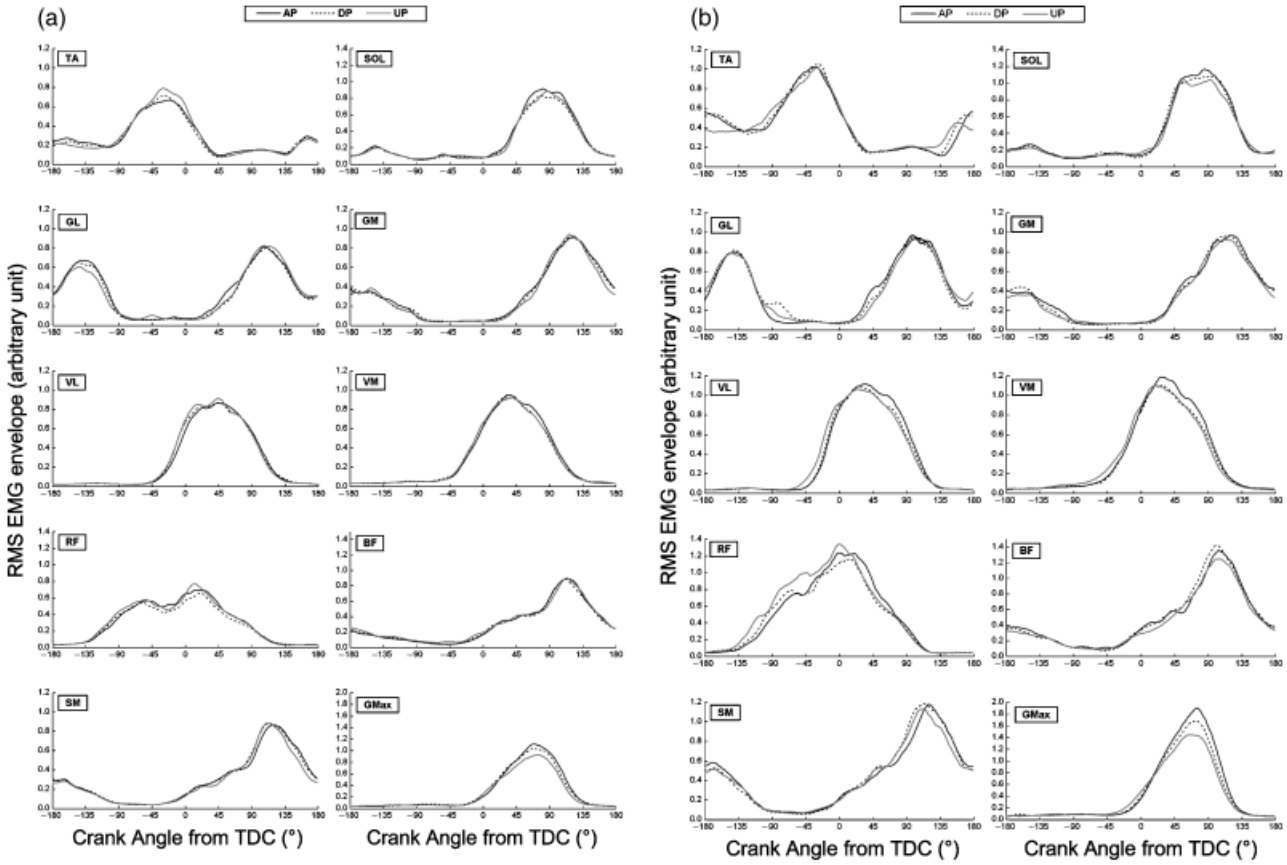

Fig. 5. Ensemble curves of electromyography (EMG) root mean squared (RMS) linear envelope for 10 lower limb muscles for all body positions [A/at VT+Δ20% and B/at respiratory compensation point (RCP)]. AP, aero posture; DP, dropped posture; UP, upright posture. For sake of clarity, all the curves on one panel use same arbitrary unit on vertical axes (AP and DP tests are normalized to maximal EMG obtained during UP). TDC, top dead centre (0°); BDC, bottom dead centre (180°).

marked shortening of RF (which affects its ability to generate force) partly explain the decrease of pedal force during the upstroke and TDC phases.

Considering that the knee joint kinematics is not notably affected by upper body position in seated position (Li & Caldwell, 1998; Savelberg et al., 2003a), the greater effective force found for AP during the downstroke phase could partly be explained by the higher activation of VM (in AP compared with other conditions) and VL (in AP compared with DP). Moreover, even if it is more difficult to conclude on the mechanical advantage/disadvantage of modification of GMax muscle length in AP condition, it is reasonable to think that the significant increase of GMax activity (+13.6% from UP to AP) also contributes to the increase of effective force during the propulsive phase (i.e. during downstroke). Then, because hip flexors was reported to only contribute to 4% of the total positive work (Ericson, 1986), it could be surmized that the subjects spontaneously adopted a compensatory strategy with these monoarticular hip and knee extensors rather than an increase of RF activity in AP condition. To confirm this assumption, it could have been interesting to record other hip flexor muscles as the Psoas major. However, this deep muscle is difficult to record using surface EMG.

Another variable of interest in examining the EMG patterns is the muscles' activation timing. As done in previous studies (Li & Caldwell, 1998; Dorel et al., in press), both onset/offset of EMG bursts and cross-correlation coefficients were used to give an objective estimation of similarities and temporal characteristics of muscle activity patterns. Despite similar patterns among the three riding positions, timing analysis showed: a phase shift (i.e. later activation) of EMG activity for the hip extensor (GMax), flexor (RF) and two knee extensors (VL and VM) from upright to drop and AP (Table 4, Fig. 6). The discrepancy in the values of shift crank angle observed between the two methods can be explained by methodological considerations (Li & Caldwell, 1998; Dorel et al., in press). In fact, the shift reported using ON-OFF method only concerned the onset of the burst (except for VL) whereas the phase shift obtained from the cross correlation method took the entire EMG profile into account. Overall, it is noteworthy that this result could also

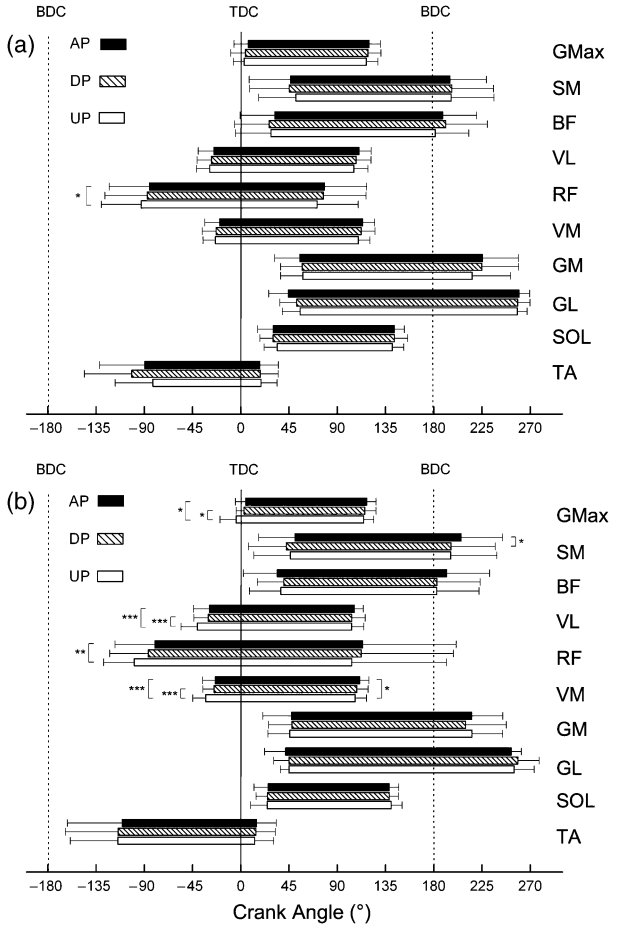

Fig. 6. Mean onset, offset and duration of higher electromyography (EMG) activity phase indicated by bars for the 10 muscles, displayed as a function of crank position. Only the main burst is represented when two bursts were observed for some muscles and some subjects. A/at VT+Δ20% and B/ at respiratory compensation point (RCP). TDC, top dead centre (0°); BDC, bottom dead centre (180°). ***$P<0.001$, **$P<0.01$, *$P<0.05$ significant difference between two conditions.

Table 4. Coefficient of cross correlation and shift angle for the EMG RMS linear envelopes of each muscle for aero vs dropped positions (AP vs DP), for dropped vs upright positions (DP vs UP) and for aero vs upright positions (AP vs UP) at VT+Δ20% (A) and RCP (B)

	AP vs DP			DP vs UP			AP vs UP		
	r_0	r_{max}	k_{max} (deg.)	r_0	r_{max}	k_{max} (deg.)	r_0	r_{max}	k_{max} (deg.)
(A)									
GMax	0.990	0.996	**2.4***	0.990	0.995	**1.5***	0.987	0.995	**3.8***
SM	0.980	0.993	**3.2***	0.987	0.992	0.8	0.981	0.990	**3.7***
BF	0.980	0.993	2.1	0.984	0.985	−1.4	0.973	0.981	0.9
VM	0.990	0.996	**2.3***	0.992	0.996	0.5	0.989	0.996	**3.2***
RF	0.977	0.982	1.6	0.977	0.989	**2.3***	0.969	0.983	**3.8***
VL	0.990	0.997	**2.7***	0.992	0.998	**1.6***	0.989	0.997	**4.1***
GM	0.986	0.996	0.0	0.988	0.992	1.8	0.982	0.988	2.2
GL	0.975	0.984	0.0	0.987	0.990	0.5	0.965	0.972	0.7
SOL	0.982	0.994	0.0	0.989	0.995	−1.0	0.983	0.992	−0.6
TA	0.968	0.987	0.2	0.969	0.979	−1.9	0.949	0.972	−1.7
(B)									
GMax	0.989	0.996	**2.6***	0.984	0.993	**2.4***	0.974	0.990	**5.2***
SM	0.978	0.988	**3.3***	0.986	0.989	1.3	0.967	0.982	**5.0***
BF	0.983	0.993	**3.6***	0.979	0.988	−0.9	0.968	0.982	2.3
VM	0.992	0.996	1.5	0.988	0.995	**3.8***	0.983	0.993	**5.7***
RF	0.979	0.988	**4.4***	0.975	0.985	**4.9***	0.949	0.977	**9.7***
VL	0.993	0.997	**2.1***	0.988	0.995	**4.3***	0.979	0.993	**6.4***
GM	0.981	0.990	1.3	0.987	0.991	1.8	0.971	0.986	**3.6***
GL	0.956	0.963	1.6	0.969	0.976	−0.4	0.943	0.960	1.6
SOL	0.989	0.994	1.0	0.982	0.989	−0.9	0.979	0.988	1.0
TA	0.972	0.986	−0.4	0.972	0.984	1.8	0.945	0.978	1.1

Values are cross correlation coefficients (r_0) with no shift angle ($k=0$), and maximal value of cross correlation coefficients (r_{max}) obtained with a shift angle $k=k_{max}$. Only the shift angle values with asterisk (and in bold) are considered as significant according to the method (95% of confidence interval) proposed by Li and Clawell (1999). Positive *k*-value corresponds to a backward shift in crank angle and indicates EMG activity of the second condition cited is shifted *k* degree(s) earlier in the crank cycle. GMax, *gluteus maximus*; SM, *semimembranosus*; BF, *Biceps femoris*; VM, *vastus medialis*; RF, *rectus femoris*; VL, *vastus lateralis*; GM, *gastrocnemius medialis*; GL, *gastrocnemius lateralis*; SOL, *soleus*; TA, *tibialis anterior*.

explain the differences observed in effective force distribution along the crank cycle (Figs 2 and 3) and is completely consistent with the shift of the $Angle_{max}$ corresponding to a later application of the maximal effective force during the downstroke phase (i.e. 5.5° from UP to AP; Table 3). Finally, the later burst offset observed for SM in AP compared with UP (Fig. 6) was confirmed by the phase shift of 5° obtained by the cross correlation method. This result could be induced by the fact that, as argued by Van Ingen Schenau et al. (1992), hamstring activity might be employed to transfer the power produced by monoarticular muscles (GMax, VM, VL). As a consequence, these muscles could be activated later in the way similar to the monoarticular muscles. It this case, it remains unclear why BF activity seems not to be affected in the same way. However, in line with hypotheses of Ericson (1988) according to which SM acts more as knee flexor than as hip extensor, it is also possible that the shift of SM allows subjects to generate a higher propulsive force in the BDC phase (i.e. Sector 3, Fig. 3).

Conclusion

This study shows that riding in AP induces significant alteration of both intensity and timing of EMG activity of lower limb muscles crossing hip (GMax, RF) and knee joints (VM, VL, and to a lower extent SM) whereas muscles crossing the ankle joint were unaffected. The EMG activity modifications (increased activity for GMax, VL, VM, and decreased activity for RF) and the shift forward reported when the upper body configuration is changed (especially from UP to AP) is strongly related to the changes of pedal effective force profile: i.e. higher downstroke

peak positive force, lower upstroke peak negative force and later occurrences of these values along the crank cycle. Further investigations are needed to evidence the necessity or not of training in this specific AP and to clarify evolution of these adaptations during an exhausting exercise such a time trial event.

Perspectives

It is obvious that the benefits of reducing air drag in AP (and to a lesser extent in DP) on the field (Capelli et al., 1993), far outweigh the disadvantage of a slightly increased activity of some lower limb muscles. Nevertheless, this higher activity in AP seems not to be negligible in the course of a time trial event since it would induce greater neuromuscular fatigue. Thus, it questions on the pertinence to perform a specific training program to improve mechanical patterns for cyclists or triathletes using an aero-position in competition. Along this line, Lucia et al. (2000) suggested that professional cyclists who show best performance in time trials may have a greater ability to pull the pedal up slightly, resulting in less work by the knee and hip extensors. Although we focused essentially on the differences between AP and UP, our results also showed significant higher activation of knee and hip extensors and lower activation of hip flexors in DP compared with UP (at RCP). The fact that cyclists naturally adopt UP as an alternative to AP (during a time trial) or DP (during a race) when air drag is less important (e.g. climbing) could therefore be an interesting strategy for optimizing the EMG pattern in order to pull the pedal better during the upstroke and hence delay fatigue in hip and knee extensor muscles.

Key words: body position, aero position, dropped position, upright position, electromyography, torque, cycling, triathlon.

Acknowledgements

This study was funded in part by ''La fondation d'entreprise de la Française Des Jeux'' and the French Ministry of Sport (contract no 06-046). The authors are grateful for the subjects for having accepted to participate in this study. They also thank Olivier NICOLLE and Benjamin MAZE for their help in preparing the experimental protocol.

References

Ashe MC, Scroop GC, Frisken PI, Amery CA, Wilkins MA, Khan KM. Body position affects performance in untrained cyclists. Br J Sports Med. 2003: 37: 441–444.

Bertucci W, Grappe F, Girard A, Betik A, Rouillon JD. Effects on the crank torque profile when changing pedalling cadence in level ground and uphill road cycling. J Biomech 2005: 38: 1003–1010.

Broker JP Cycling biomechanics: road and moutain. In: Burke ED, ed. High-tech cycling. Human Kinetics, Stanningley, 2002: 134–135.

Brown DA, Kautz SA, Dairaghi CA. Muscle activity patterns altered during pedaling at different body orientations. J Biomech 1996: 29: 1349–1356.

Capelli C, Rosa G, Butti F, Ferretti G, Veicsteinas A, di Prampero PE. Energy cost and efficiency of riding aerodynamic bicycles. Eur J Appl Physiol Occup Physiol 1993: 67: 144–149.

Cruz CF, Bankoff AD. Electromyography in cycling: difference between clipless pedal and toe clip pedal. Electromyogr Clin Neurophysiol 2001: 41: 247–252.

Dorel S, Couturier A, Hug F (in press) Intra-session repeatability of lower limb muscles activation pattern during pedaling. J Electromyogr Kinesiol.

Duc S, Bertucci W, Pernin JN, Grappe F (in press) Muscular activity during uphill cycling: effect of slope, posture, hand grip position and constrained bicycle lateral sways. J Electromyogr Kinesiol.

Ericson M. On the biomechanics of cycling. A study of joint and muscle load during exercise on the bicycle ergometer. Scand. J Rehabil Med 1986: 16: 1–43.

Ericson MO. Muscular function during ergometer cycling. Scand J Rehabil Med 1988: 20: 35–41.

Gnehm P, Reichenbach S, Altpeter E, Widmer H, Hoppeler H. Influence of different racing positions on metabolic cost in elite cyclists. Med Sci Sports Exerc 1997: 29: 818–823.

Grappe F, Candau R, Busso T, Rouillon JD. Effect of cycling position on ventilatory and metabolic variables. Int J Sports Med 1998: 19: 336–341.

Gregor RJ, Broker JP, Ryan MM. The biomechanics of cycling. Exerc Sport Sci Rev 1991: 19: 127–169.

Hermens HJ, Freriks B, Disselhorst-Klug C, Rau G. Development of recommendations for SEMG sensors and sensor placement procedures. J Electromyogr Kinesiol 2000: 10: 361–374.

Hoes MJ, Binkhorst RA, Smeekes-Kuyl AE, Vissers AC. Measurement of forces exerted on pedal and crank during work on a bicycle ergometer atdifferent loads. Int Zeitschrift Angewandte Physiol, Einschliesslich Arbeitsphysiol 1968: 26: 33–42.

Houtz SJ, Fischer FJ. An analysis of muscle action and joint excursion during exercise on a stationary bicycle. J Bone Jt Surg 1959: 41-A: 123–131.

Hug F, Dorel S (in press) An electromyographic analysis of pedaling: a review. J Electromyogr Kinesiol.

Jorge M, Hull ML. Analysis of EMG measurements during bicycle pedalling. J Biomech 1986: 19: 683–694.

Li L, Caldwell GE. Muscle coordination in cycling: effect of surface incline and posture. J Appl Physiol 1998: 85: 927–934.

Li L, Caldwell GE. Coefficient of cross correlation and the time domain correspondence. J Electromyogr Kinesiol 1999: 9: 385–389.

Lucia A, Joyos H, Chicharro JL. Physiological response to professional road cycling: climbers vs. time trialists. Int Jo Sports Med 2000: 21: 505–512.

Origenes MMt, Blank SE, Schoene RB. Exercise ventilatory response to upright and aero-posture cycling. Med Sci Sports Exerc 1993: 25: 608–612.

Patterson RP, Moreno MI. Bicycle pedalling forces as a function of

pedalling rate and power output. Med Sci Sports Exerc 1990: 22: 512–516.
Reinhard U, Muller PH, Schmulling RM. Determination of anaerobic threshold by the ventilation equivalent in normal individuals. Respirat Int Rev Thoracic Diseases 1979: 38: 36–42.
Ryschon TW, Stray-Gundersen J. The effect of body position on the energy cost of cycling. Med Sci Sports Exerc 1991: 23: 949–953.
Sanderson DJ, Black A. The effect of prolonged cycling on pedal forces. J Sports Sci 2003: 21: 191–199.
Sanderson DJ, Hennig EM, Black AH. The influence of cadence and power output on force application and in-shoe pressure distribution during cycling by competitive and recreational cyclists. Jo Sports Sci 2000: 18: 173–181.
Savelberg H, Van de Port I, Willems P. Body configuration in cycling affects muscle recruitment and movement pattern. J Appl Biomech 2003a: 19: 310–324.
Savelberg HHCM, Van de Port IGL, Willems PJB. Body configuration in cycling affects muscle recruitment and movement pattern. J Appl Biomech 2003b: 19: 310–324.
Suzuki S, Watanabe S, Homma S. EMG activity and kinematics of human cycling movements at different constant velocities. Brain Res 1982: 240: 245–258.
Van Ingen Schenau GJ, Boos PJ, de Groot G, Snackers RJ, Van Woensel WW. The constrained control of force and position in multi-joint movements. Neuroscience 1992: 46: 197–207.

Available online at www.sciencedirect.com
SCIENCE DIRECT®
Respiratory Physiology & Neurobiology 150 (2006) 75–81
RESPIRATORY PHYSIOLOGY & NEUROBIOLOGY
www.elsevier.com/locate/resphysiol

Short communication

Optimized analysis of surface electromyograms of the scalenes during quiet breathing in humans

François Hug [a,b], Mathieu Raux [a,b], Maura Prella [a,b], Capucine Morelot-Panzini [a,b], Christian Straus [a,c], Thomas Similowski [a,b,*]

[a] *UPRES EA 2397, Université Pierre et Marie Curie Paris VI, Paris, France*
[b] *Laboratoire de Physiopathologie Respiratoire, Service de Pneumologie et de Réanimation, Groupe Hospitalier Pitié Salpêtrière, 47-83 Boulevard de l'Hôpital, 75651 Paris Cedex 13, France*
[c] *Service Central d'Explorations Fonctionnelles Respiratoires, Groupe Hospitalier Pitié Salpêtrière, Assistance Publique, Hôpitaux de Paris, Paris, France*

Accepted 6 April 2005

Abstract

Studying the inspiratory recruitment of the scalenes is clinically relevant, but the interpretation of surface electromyographic (EMG) recordings is difficult. The aim of this study was to optimize an averaging method to analyze the surface EMG activity of the scalenes. Ten healthy subjects were studied. Nasal flow and surface EMG of the right scalene were recorded during 15 min epochs of quiet breathing. In four subjects, needle scalene EMG was also recorded. The flow signal was used to trigger the ensemble averaging of the ventilatory wave forms from 80 consecutive breaths. In eight cases, this evidenced a phasic inspiratory activation of the scalenes and permitted the determination of the electromechanical inspiratory delay (134 ± 55 ms) and post-inspiratory activity (811 ± 233 ms). When simultaneously available, surface and intramuscular recordings provided identical results. An averaging method triggered from a respiratory flow signal can identify and characterize a low phasic inspiratory activity of the scalenes within a noisy surface signal.

Keywords: Respiratory muscle; Scalene; Root mean square; Electromechanical delay; Post-inspiratory activity

1. Introduction

During quiet breathing in humans, the diaphragm is the main agonist of inspiration, but other inspiratory muscles are also activated. So, a phasic inspiratory activity can be detected in the scalenes (Raper et al., 1966) during quiet inspiration in normal humans, but this activity is low in magnitude, inconstant among

* Corresponding author. Tel.: +33 1 42 17 67 61; fax: +33 1 42 17 67 08.
E-mail address: thomas.similowski@psl.ap-hop-paris.fr (T. Similowski).

1569-9048/$ – see front matter © 2005 Elsevier B.V. All rights reserved.
doi:10.1016/j.resp.2005.04.008

subjects, and variable over time in a given subject. The scalenes are recruited early in response to acute respiratory loading (Raper et al., 1966). Chronic respiratory diseases placing the diaphragm at mechanical disadvantage are often associated with a permanent phasic inspiratory activity of the scalenes (De Troyer et al., 1994), long known as the "respiratory pulse" (Magendie, 1816). Yet, an increased activity of inspiratory neck muscles (including the scalenes) is associated with respiratory discomfort, both during experimental loading in healthy subjects (Ward et al., 1988) and during quiet breathing in disease (Similowski et al., 2000). All in all, it seems reasonable to consider that an increased inspiratory activity of the scalenes can be both a sign that the respiratory system is loaded and a source of dyspnea. Studying this activity is thus clinically relevant.

The electromyographic activity of the scalenes can be studied using intramuscular or surface electrodes. Intramuscular electrodes provide high quality signals, but they sample a limited number of motor units and their invasive nature limit their use in clinical practice. Surface electrodes placed over anatomical landmarks of the scalenes give a more global picture of muscle function and are easy to use for prolonged or repeated studies. However, the scalenes have a low level of phasic activity during unloaded breathing and exhibit a strong tonic activity because their primary function is to contribute to the stability of the head. This determines a low signal-to-noise ratio. Under loading conditions sufficient to activate the sternomastoid muscles, cross-talk is likely to occur and influence surface EMG signals. These factors make the interpretation of surface recordings difficult in terms of the scalene inspiratory activity. This is all the more so in the clinical field where the lack of cooperation from the patients and the frequent occurrence of interferences from a variety of sources concur to worsen the signal-to-noise ratio. This probably explains the scarcity of information on the function of the scalene muscles in clinical situations.

Signal averaging is an efficient way to improve the signal-to-noise ratio. This does apply to electromyography in general. Although this method is frequently used in EMG studies, few authors have applied it to respiratory muscles. Bruce et al. (1977) described an averaging method for reducing the electrocardiogram (ECG) and noise artefacts on diaphragmatic EMG. In this study, an average wave form corresponding to one respiratory cycle was produced by ensemble averaging of the wave forms from several consecutive breaths. However, the authors reported difficulties to reliably detect the beginning of an inspiration from the EMG signal and acknowledged this as a limitation to their approach. In particular, Bruce et al. (1977) were not able to determine the relationship between the myoelectrical activity of the diaphragm and its mechanical activity namely the beginning of inspiration.

This obstacle can theoretically bypassed by triggering the EMG averaging from a respiratory mechanical signal. This was performed in the present study, conducted in healthy humans during quiet breathing (hence with a presumably low level of scalene inspiratory activity), with the objective of providing an optimized tool for the study of the function of the scalenes in clinical settings.

2. Methods

2.1. Subjects and experimental protocol

After completion of the French legal procedure for biomedical research in human volunteers, 10 healthy subjects participated in the study (five men, five women; aged 32.9 ± 6.4 years; height 171 ± 9 cm; weight 68.3 ± 18.7 kg). The body mass index (BMI) of the subjects was 19.8 ± 0.9 (range: 18.6–21.2) for women and 26.2 ± 4.3 (range: 20.7–31.5) for men. The subjects were informed in detail of the purpose of the study and methods used, and gave written consent.

Recordings were gathered during a 15 min epoch of quiet nose breathing through an air tight nasal mask (Comfort classic, Respironics, USA), with the subjects sitting in a comfortable chair and prealably instructed not to move or talk. Two subjects were studied on two separate occasions.

2.2. Measurements

2.2.1. Ventilatory flow

Ventilatory flow was qualitatively estimated from the measurement of mask pressure, using a differential pressure transducer (DP 45-14, range: ± 4 cm H_2O, Validyne, Nothridge, CA, USA).

2.2.2. Surface EMG recordings

A pair of skin-taped silver cup electrodes aimed at recording a putative scalene phasic inspiratory activity was placed in the posterior triangle of the neck at the level of the cricoid cartilage with an inter-electrode distance of 1 cm. Inter-electrode impedance was kept below 2000 Ω by careful skin shaving and abrasion with an ether-saturated pad. The wires connected to the electrodes were carefully secured with tape to avoid artifacts from upper limb movements. The common electrode was placed at the level of the *manubrium* sternum.

2.2.3. Intramuscular EMG recordings

In four subjects, a concentric needle electrode (Oxford medical instruments, London, England) was implanted into the right scalene muscle, 1–2 cm above the clavicle, just behind the clavicular fibers of the sternomastoid according to the method described by De Troyer et al. (1994). None of the subjects reported significant discomfort attributable to the needle.

2.3. Signal processing

All signals were fed to a Nihon Kohden Neuropack electromyograph (Nihon Kohden, Tokyo, Japan), with a 10 kHz sampling rate and were filtered (between 40 and 500 Hz and between 40 and 3 kHz for surface and intramuscular measurements, respectively). Then, they were stored on an apple Macintosh computer for subsequent analysis (PowerLab, AD Instruments, Hastings, UK). The root mean square (RMS), an index of global EMG activity, was numerically calculated using fixed windows (duration = 1 ms).

For each subject, an ensemble averaging of 80 successive breaths was first performed after splitting the continuous RMS and flow signals in as many epochs starting 1 s before the beginning of the mechanical inspiration determined from the flow signal and ceasing 1 s after its end (Chart 5.2, AD Instruments, Hastings, UK). This treatment made it possible to identify a phasic activity within the continuous signal, if any. In such instance, the mean myoelectrical inspiratory activity (i.e. mean RMS value during inspiration) was calculated, and an electromechanical inspiratory delay corresponding to the time between the onset of myoelectrical activity and the beginning of inspiration was measured.

In a second step, the procedure was repeated using the flow signal to detect the end of the mechanical inspiration rather than its start. The continuous signal was split into epochs starting one second before the end of the mechanical inspiration and ending 2 s after its start. This was performed to assess the post-inspiratory activity (PIA), and in order to take into account the breath-to-breath variability of ventilatory timing.

Fig. 1 depicts the successive steps of the averaging method.

3. Results

In 8 out of the 10 subjects, the flow triggered averaging of the continuous RMS signal recorded by the surface electrodes unmistakably evidenced a phasic inspiratory activity. In these subjects, the electromechanical delay between the onset of the myoelectrical activity and the beginning of actual inspiration determined from the flow signal was 134 ± 55 ms (mean ± S.D.). A post-inspiratory activity was consistently visible, lasting 811 ± 233 ms after the end of inspiration.

Fig. 2 depicts an example of the results obtained in the four subjects where both needle and surface EMG measurements were made. In three subjects (JM, TS, LC), the averaging process identifies a clear phasic inspiratory activity within the surface signal. Applying this process to the intramuscular recordings shows that the surface activity is matched to the intramuscular one, with comparable electromechanical inspiratory delay and post-inspiratory activity (Table 1). In the fourth subject (AD), processing the surface signal as described failed to evidence a clear phasic inspiratory

Table 1
Electromechanical delay and post-inspiratory activity values calculated in the three subjects where both needle and surface EMG measurements were detected

	JM	TS	LC
Needle EMID (ms)	235	53	115
Surface EMID (ms)	199	93	110
Needle PIA (ms)	1050	980	1024
Surface PIA (ms)	735	815	1035

EMID, electromechanical inspiratory delay; PIA, post-inspiratory activity.

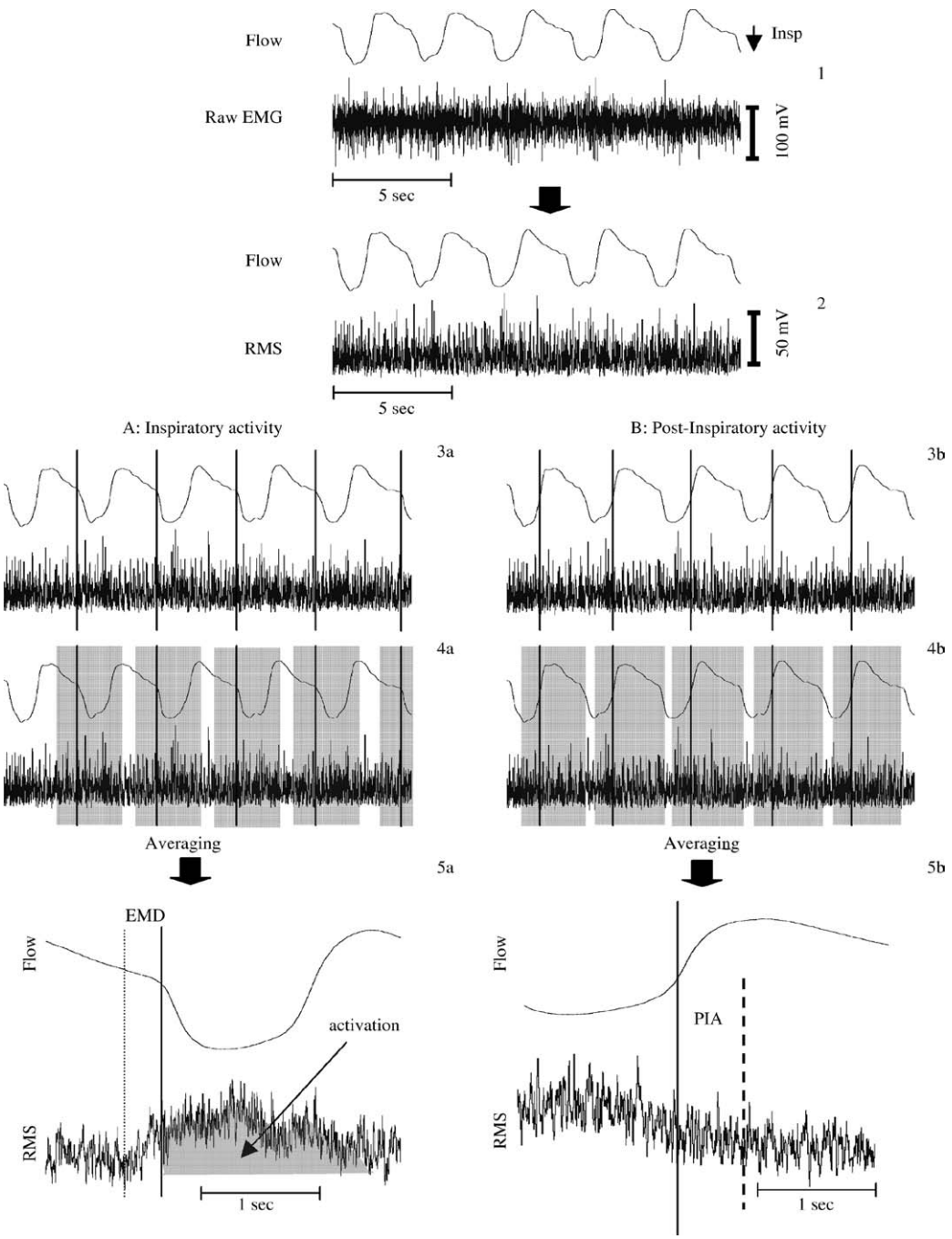

Fig. 1. The step-by-step averaging technique. Five consecutive cycles of the raw surface EMG and flow signals are depicted (1). The root mean square was calculated using fixed windows (duration = 1 s) (2). Then, the flow signal was used to detect the beginning (3a) and the end (3b) of each inspiration phase. An ensemble averaging of 80 successive breaths was performed after splitting the continuous RMS and flow signals in as many epochs starting 1 s before the markers and ceasing 1 s after inspiration (4a) or 2 s after the end of inspiration (4b). The averaging results show the mean inspiratory activity, the electromechanical inspiratory delay (5a) and the post–inspiratory activity (5b). EMID, electromechanical inspiratory delay; PIA, post-inspiratory activity; RMS, root mean square; Insp, inspiration.

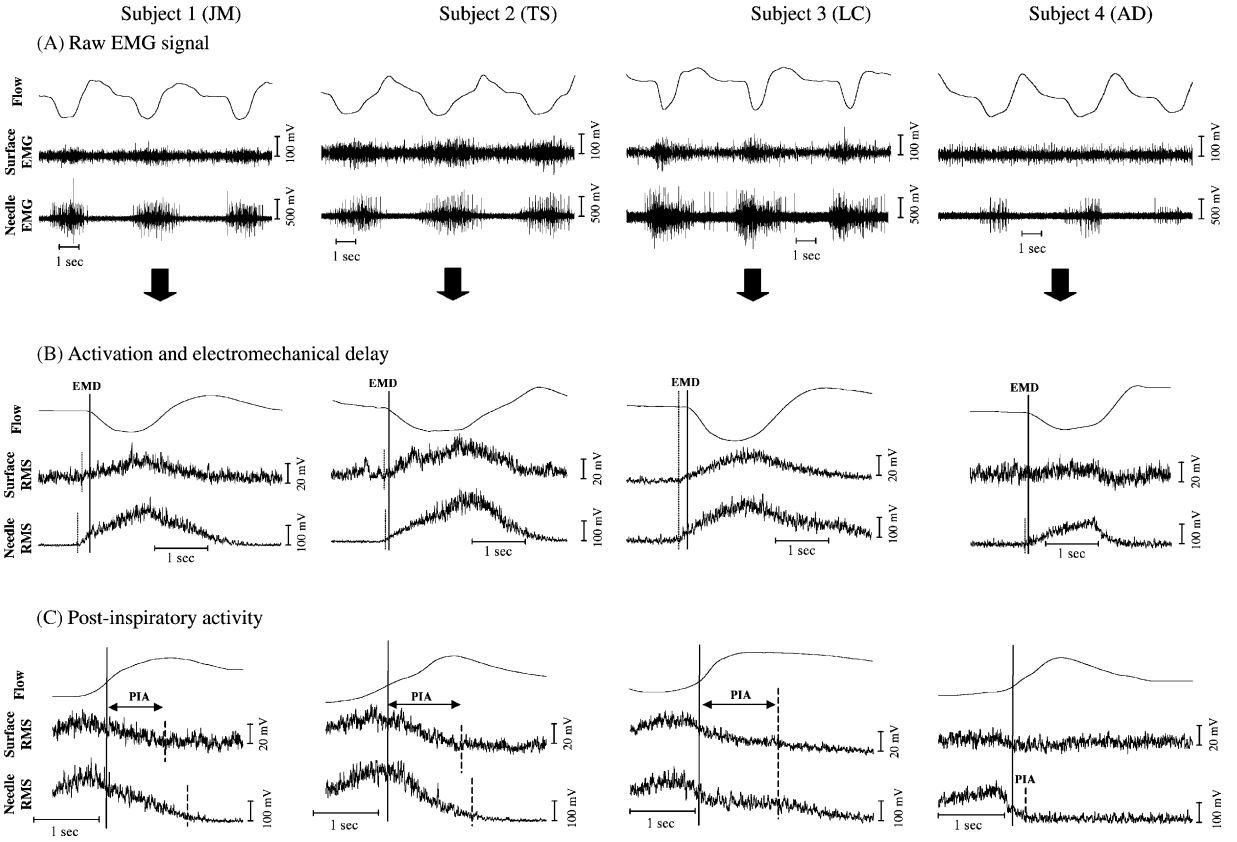

Fig. 2. Example of the results obtained, with the averaging method, in the four subjects where both needle and surface EMG measurements of the scalene were made. Three consecutive cycles of the raw flow, needle and surface EMG signals are depicted for each subject (A). The averaging technique permitted an easy detection of the scalene inspiratory activity and the electromechanical delay in three subjects (JM, TS, LC) (B). A post-inspiratory activity was also determined in these three subjects (C). Despite a weak needle EMG activity in the fourth subject (AD), the surface recording failed to show a clear phasic inspiratory activity. EMD, electromechanical inspiratory delay; PIA, post-inspiratory activity; RMS, root mean square.

activity in spite of the presence of a weak such activity on the intramuscular recording.

Two subjects (AD and TS) were studied twice at a several weeks interval. In both cases, the second experiment confirmed the results of the first. Of note, the pattern of the phasic activity picked up by the surface electrodes was similar in shape on the two occasions.

4. Discussion

This study shows that triggering a surface EMG averaging from a mechanical respiratory signal is a simple way to detect and characterize the phasic inspiratory activity of the scalene. This approach gives access, seemingly for the first time, to a non-invasive measure of the corresponding electromechanical inspiratory delay and post-inspiratory activity.

4.1. Source of the averaged inspiratory activity

The source of the inspiratory activity that was isolated by the processing of the surface recordings in our subjects is most likely the scalene muscle. The electrodes were positioned above the anatomical landmark of the upper insertion of the scalene, above its division in anterior, middle and posterior scalenes. This alone would not exclude cross-talk, mostly from the sternomastoid. However, the presence of an inspiratory activity of the sternomastoid during quiet breathing in healthy humans is highly unlikely (Magendie, 1816;

Raper et al., 1966; De Troyer et al., 1994). Most importantly, the concordance of the intramuscular and surface recordings in those of the subjects so tested attests the origin of the surface signal in the scalene. Of note, we were unable to extract a reliable inspiratory signal in two of our subjects, although one of them exhibited a low intensity phasic activity of the scalene according to the intramuscular recording (see bottom trace in the rightmost lower panel of Fig. 2). Note that these two subjects were not those with the highest body mass index within the study population. Available data in the literature suggest that there is a considerable degree of interindividual variability regarding the activation of the scalenes during quiet breathing. Our results are compatible with this notion. The observation in subject AD suggests that, although the flow triggered averaging method that we used is efficient in extracting an inspiratory activity of the scalene from a noisy surface signal, it may not be sensitive enough in all cases. Of note, our subjects were studied sitting: the expected changes in the tonic and phasic activity of the scalenes in the supine posture could influence the performance of our technique. We have tested this in two subjects studied first sitting and then supine (data not shown). We indeed observed an important deterioration in the signal to noise ratio, principally due to a reduction in the intensity of the phasic activity, but this was not sufficient for the averaging approach to fail. The sensitivity issue is however not likely to be a problem during loaded breathing.

4.2. Comparison with available data

Other investigators (Bruce et al., 1977; Duiverman et al., 2004) used averaging techniques for analyzing the EMG activity of respiratory muscles. In the study by Bruce et al. (1977), this approach was applied to esophageal recordings of the diaphragmatic electromyogram, a hallmark of which is a high signal-to-noise ratio (in addition to the semi-invasive nature of the method). Therefore this study was not designed to address the issue that we raised, namely the possibility to characterize an inspiratory muscle EMG activity non-invasively from a noisy signal. Bruce et al. (1977) identified the onset of inspiration as the beginning of the EMG activity. Therefore, they could not use their method to measure the electromechanical inspiratory delay or the post-inspiratory EMG activity. Duiverman et al. (2004) also used an averaging technique to improve the detection of a scalene inspiratory activity. Using a chest band signal to define the beginning of inspiration these researchers failed to detect a phasic activity of the scalenes during both quiet breathing and during a moderately loaded breathing. This discrepancy with our results and with the literature (Raper et al., 1966; De Troyer et al., 1994) could lie in several particularities of the experimental approach used by Duiverman et al. (2004) (i.e. the application of an ECG removal technique prior to the EMG processing, the type of signal used to detect the beginning of inspiration, the number of breaths averaged, movements of the head).

4.3. Electromechanical inspiratory delay and post-inspiratory activity

Our method gives access to an easy measure of the delay that separates the beginning of the scalene myoelectric activity and the actual inspiration (electromechanical inspiratory delay, EMID) that does not require a particularly high signal to noise ratio. The average EMID that we found in the scalene is of the same order of magnitude that the electromechanical delay found in locomotor muscles during minimally loaded non-isometric contractions (Li and Baum, 2004), which lends some physiological plausibility to our results. Of note, the EMID as defined here does not correspond to the electromechanical delay of a muscle activation in the classical sense of the term, namely the time that elapses between the onset of the myoelectrical activity and the onset of myofribrillar shortening. Rather, it corresponds to the delay between the onset of the myoelectrical activity and the beginning of the action it is engaged in, inspiration in our case. There is seemingly no previous report of the scalene EMID during quiet breathing. Indeed, Raper et al. (1966) reported that the myoelectrical activity of the scalenes started after, not before, the onset of a quiet inspiration. The apparent discrepancy between this observation and ours may be due to the fact that Raper et al. (1966) relied on a raw signal to detect the beginning of the EMG activity and thus may have been unable to detect the actual onset of the scalene EMG. Our method also gives access to a measure of the post-inspiratory activity of the scalenes. This does not seem to have been reported before from surface recordings, and a fortiori quantified.

4.4. Perspective

We have developed the present technique with the aim of studying the function of the scalene muscles in humans non-invasively, in settings where it is known that the signal-to-noise ratio is a major issue. The intensive care unit is typically one of such settings. The clinical relevance of studying inspiratory neck muscles in patients receiving ventilatory assistance is probably important. For example, Chao et al. (1997) observed that the uncoupling of inspiratory neck muscle contractions from onset of machine breaths was accurate in identifying cases of ventilator-patient asynchrony. Brochard et al. (1989) observed a relationship between the occurrence of diaphragmatic fatigue and the recruitment of inspiratory neck muscle, and concluded that the clinical monitoring of sternomastoid activity could be useful in optimizing ventilator settings to prevent fatigue. In both these studies, the assessment of inspiratory muscle activity was clinical. Our method should be much more sensitive, giving access to an early diagnosis of patient-ventilator asynchrony, and to a quantitative approach through the measurement of the electromechanical inspiratory delay. However, specific studies are required to precisely delineate the physiological meaning and clinical value of these indexes. The influence of sternomastoid recruitment on the results of our method to assess the activity of the scalenes will also have to be determined.

Acknowledgments

This study was funded in part by a “Contrat de recherche triennal “Legs Poix” de la Chancellerie de l’Université de Paris” and by Association pour le Développement et l’Organisation de la Recherche En Pneumologie (ADOREP), Paris, France. François HUG was supported by a scholarship of the Fédération ANTADIR, Paris, France. Mathieu RAUX was supported in part by a scholarship of the Comité National Contre les Maladies Respiratoires, Paris, France and in part by a scholarship of the Fédération ANTADIR, Paris, France. The authors are grateful to Pr André De Troyer for teaching them the technique for intramuscular scalene recordings. They are also grateful to Pr Jean-Philippe Derenne and Pr Marc Zelter for their input.

References

Brochard, L., Harf, A., Lorino, H., Lemaire, F., 1989. Inspiratory pressure support prevents diaphragmatic fatigue during weaning from mechanical ventilation. Am. Rev. Respir. Dis. 139, 513–521.

Bruce, E.N., Goldman, M.D., Mead, J., 1977. A digital computer technique for analyzing respiratory muscle EMG’s. J. Appl. Physiol. 43, 551–556.

Chao, D.C., Scheinhorn, D.J., Stearn-Hassenpflug, M., 1997. Patient-ventilator trigger asynchrony in prolonged mechanical ventilation. Chest 112, 1592–1599.

De Troyer, A., Peche, R., Yernault, J.C., Estenne, M., 1994. Neck muscle activity in patients with severe chronic obstructive pulmonary disease. Am. J. Respir. Crit. Care. Med. 150, 41–47.

Duiverman, M.L., van Eykern, L.A., Vennik, P.W., Koeter, G.H., Maarsingh, E.J., Wijkstra, P.J., 2004. Reproducibility and responsiveness of a noninvasive EMG technique of the respiratory muscles in COPD patients and in healthy subjects. J. Appl. Physiol. 96, 1723–1729.

Li, L., Baum, B.S., 2004. Electromechanical delay estimated by using electromyography during cycling at different pedaling frequencies. J. Electromyogr. Kinesiol. 14, 647–652.

Magendie, F., 1816. Traité de Physiologie. Paris.

Raper, A.J., Thompson Jr., W.T., Shapiro, W., Patterson Jr., J.L., 1966. Scalene and sternomastoid muscle function. J. Appl. Physiol. 21, 497–502.

Similowski, T., Attali, V., Bensimon, G., Salachas, F., Mehiri, S., Arnulf, I., Lecomblez, L., Zelter, M., Meininger, V., Derenne, J.P., 2000. Diaphragmatic dysfunction and dyspnoea in amyotrophic lateral sclerosis. Eur. Respir. J. 15, 332–337.

Ward, M.E., Eidelman, D., Stubbing, D.G., Bellemare, F., Macklem, P.T., 1988. Respiratory sensation and pattern of respiratory muscle activation during diaphragm fatigue. J. Appl. Physiol. 65, 2181–2189.

Respiratory Physiology & Neurobiology 164 (2008) 441–448

Contents lists available at ScienceDirect

Respiratory Physiology & Neurobiology

journal homepage: www.elsevier.com/locate/resphysiol

Scalene muscle activity during progressive inspiratory loading under pressure support ventilation in normal humans

Linda Chiti[a,b], Giuseppina Biondi[a,b], Capucine Morelot-Panzini[a,b], Mathieu Raux[a], Thomas Similowski[a,b,1], François Hug[a,c,*,1]

[a] Université Paris 6 Pierre et Marie Curie, EA 2397, Paris, F-75013 France
[b] Assistance Publique - Hôpitaux de Paris, Groupe Hospitalier Pitié-Salpêtrière, Service de Pneumologie et Réanimation, Paris, F-75013 France
[c] Université de Nantes, Nantes Atlantique Universités, EA 4334, Nantes, F-44000 France

ARTICLE INFO

Article history:
Accepted 25 September 2008

Keywords:
Sternomastoid
Electromyography
Dyspnea
Asynchrony

ABSTRACT

We hypothesized that (1) in healthy humans subjected to intermittent positive pressure non-invasive ventilation, changes in the ventilator trigger sensitivity would be associated with increased scalene activity, (2) if properly processed – through inspiratory phase-locked averaging – surface electromyograms (EMG) of the scalenes would reliably detect and quantify this, (3) there would be a correlation between dyspnea and scalene EMG. Surface and intramuscular EMG activity of scalene muscles were measured in 10 subjects. They breathed quietly through a face mask for 10 min and then were connected to a mechanical ventilator. Recordings were performed during three 15-min epochs where the subjects breathed against an increasingly negative pressure trigger (−5%, −10% and −15% of maximal inspiratory pressure). With increasing values of the inspiratory trigger, inspiratory efforts, dyspnea and the scalene activity increased significantly. The scalene EMG activity level was correlated with the esophageal pressure time product and with dyspnea intensity. Inspiration-adjusted surface EMG averaging could be useful to detect small increases of the scalene muscles activity during mechanical ventilation.

1. Introduction

Quiet inspiration in healthy humans is mainly driven by the diaphragm, but it also involves the parasternal intercostals and the scalene muscles (Beau and Maissiat, 1843; Raper et al., 1966; De Troyer and Estenne, 1984; Gandevia et al., 1996; Hug et al., 2006; Saboisky et al., 2007). The scalene are recruited during inspiratory maneuvers, either static (Hudson et al., 2007) or dynamic (Raper et al., 1966; Katagiri et al., 2003; Hudson et al., 2007). Their tidal activity can increase in chronic diseases placing the diaphragm at mechanical disadvantage (chronic obstructive pulmonary disease (COPD) or kyphoscoliosis (De Troyer et al., 1994; Estenne et al., 1998)). Indeed patients with these conditions often exhibit palpable scalene inspiratory activity event when they are in stable condition. When breathing is acutely shifted to high lung volumes, the activity of the scalenes increases (Raper et al., 1966; Hudson et al., 2007). During spontaneous breathing trials in mechanically ventilated patients, irrespective of the underlying disease, palpable scalene muscle recruitment in inspiration can be a sign of respiratory distress (Pardee et al., 1984). In mechanically ventilated patients, the uncoupling of inspiratory neck muscle contractions from onset of machine breaths identifies certain forms of patient–ventilator asynchrony (Chao et al., 1997). Inspiratory neck muscle contractions can provide a useful clinical monitoring tool for the optimization of ventilator settings (Brochard et al., 1989). Inspiratory neck muscles are recruited progressively and intensely during incremental exercise in patients with chronic obstructive pulmonary disease (Yan et al., 1997). They are also recruited in critically ill patients failing a spontaneous breathing trial during mechanical ventilator weaning (Parthasarathy et al., 2007). Of note, there seems to be a relationship between the acute activation of inspiratory neck muscles and dyspnea, as pointed at as early as the beginning of the XIXth century (Magendie, 1816). The intensity of inspiratory neck muscle recruitment is associated with the intensity of dyspnea in healthy subjects submitted to experimental inspiratory loading, during either fatiguing protocols (Ward et al., 1988) or non-fatiguing ones (Bradley et al., 1986). The presence of a clinically visible inspiratory activation of inspiratory neck muscle is statistically associated with dyspnea in patients suffering from amyotrophic lateral sclerosis (Similowski et al., 2000).

* Corresponding author at: Laboratoire «Motricité, Interactions, Performance» (EA 4334), Université de Nantes – UFR STAPS, 25 bis boulevard Guy Mollet, 44300 Nantes, France. Tel.: +33 2 51 83 72 24; fax: +33 2 51 83 72 10.
E-mail addresses: thomas.similowski@psl.ap-hop-paris.fr (T. Similowski), francois.hug@univ-nantes.fr (F. Hug).
[1] The two senior authors contributed equally to this work.

1569-9048/$ – see front matter © 2008 Elsevier B.V. All rights reserved.
doi:10.1016/j.resp.2008.09.010

The above elements are clear clues to the clinical relevance of studying the inspiratory recruitment of human neck muscles. Quantifying and monitoring their activity is however difficult. A compromise must be found between clinical examination, simple but hardly quantifiable, and intramuscular electromyogramic (EMG) recordings, precise but too invasive and expertise-demanding for clinical applications. Within this frame, we have previously shown that phase-locking the averaging of surface scalene electromyograms to inspiration allowed an optimized detection of the scalene activity during quiet breathing and its quantification (Hug et al., 2006). The scalenes and sternomastoids are known to be recruited sequentially in humans. During progressive inspiratory effort, the activity of the sternomastoid typically starts well after the first half of the effort, whereas that of the scalene is noticeable as early as during the first tenth of the effort (Campbell, 1955; Raper et al., 1966; Hudson et al., 2007).

With these elements in mind, we hypothesized that (1) in healthy humans subjected to intermittent positive pressure non-invasive ventilation, modest increases in inspiratory loading induced by changes in the ventilator trigger sensitivity would be associated with increased scalene activity; (2) the inspiratory pressure-adjusted average surface electromyograms of the scalenes would reliably detect and quantify this increase in activity; (3) this would correlate with the intensity of respiratory discomfort.

2. Methods

2.1. Subjects

This study was part of an experimental program approved by the appropriate review board (*Comité de Protection des Personnes se prêtant à des Recherches Biomédicales Pitié-Salpêtrière*) and devoted to the study of patient–ventilator interactions from a model of normal volunteers receiving non-invasive mechanical ventilation. Ten healthy subjects participated in the study (six men, four women; aged 28.7 ± 2.0 years; height 176 ± 10 cm; weight 68.2 ± 13.8 kg). They were informed in detail of the purpose of the study and methods used, and gave written consent. During the experiments, they were seated in a comfortable chair with the arms and head supported, and had been instructed not to move or talk.

2.2. Measurements

The experimental setup is depicted by Fig. 1.

2.2.1. Pressure

Airway opening pressure was measured within an airtight facial mask (Pmask) (Comfort classic, Respironics, USA), using a linear differential pressure transducer (DP 15–34, range: ± 200 cm H_2O, Validyne, Nothridge, CA, USA). Esophageal (Pes) and gastric (Pga) pressures were measured with two balloon-tipped catheters (thin-walled balloon sealed over a polyethylene catheter with distal side holes, 80 cm length, 1.4 mm internal diameter, Marquat, Boissy-St-Léger, France). The insertion of the catheters through the nose was carried out after topical anaesthesia (lidocain spray 10%). The gastric and esophageal balloons were inflated with, respectively, 1 and 2 mL of air. The catheters were connected to two differential pressure transducers (MP 45, range: ± 100 cm H_2O Validyne, Northridge, CA, USA). Transdiaphragmatic pressure (Pdi) was calculated on-line as the Pga–Pes difference. All the pressure signals were stored on an apple Macintosh computer for subsequent analysis (PowerLab, AD Instruments, Hastings, UK). The contribution of the diaphragm to a given inspiratory effort was assessed by computing the ratio of the corresponding Pga and Pdi swings (ΔPga/ΔPdi), according to Gilbert et al. (1981).

2.2.2. $P_{ET}CO_2$

End-tidal CO_2 was continuously measured through a dedicated port of the face mask using an infrared gas analyzer (IR505, Servomex SA, Saint-Denis La Plaine, France).

2.2.3. Surface EMG recordings

One pair of skin-taped silver cup electrodes 7 mm in diameter (Nihon Kohden, Tokyo, Japan) aimed at recording scalene EMG activity was placed in the posterior triangle of the neck (right side) at the level of the cricoid cartilage, so as to lie over the lower portion of the anterior scalene muscle. It was located during sniff maneuvers through palpation of the neck in the lower third of a line drawn between the middle of the mastoid process and the sternal notch. Another pair of electrodes was placed over the body of the right sternomastoid, 3 cm above the anterior head of this muscle. Within each electrode pair, the inter-electrode distance was 1 cm and impedance was kept below 2 kΩ by careful skin shaving and abrasion with an ether-saturated pad. The wires connected to the electrodes were carefully secured with tape to minimize movement artefacts. The common electrode was placed at the level of the manubrium sternum.

2.2.4. Intramuscular EMG recordings

In six subjects, a fine wire EMG electrodes (Inomed, Tullastraße, Germany) was inserted into the left anterior scalene and sternomastoid muscles at the above-described locations, under real-time ultrasonographic guidance (Hewlett-Packard, Sonos 2000; probe = 5 MHz). The subjects were then asked to perform inspiratory maneuvers and opposed neck rotations to confirm the correct electrode placement.

2.2.5. Dyspnea

The intensity of dyspnea was rated using a visual analogue scale (VAS) constituted of a 100-mm horizontal scale over which the subjects had to place a cursor according to the intensity of their respiratory discomfort, between "none" (left) and "intolerable" (right) in response to the question: "How short of breath are you right now?"

2.3. Protocol

It is summarized by Fig. 1. In brief, the subjects first performed maximal inspiratory static maneuvers (of the Mueller type and from end-expiratory lung volume) in order to determine the maximal inspiratory pressure ($P_{I,max}$) at the airway openings. Then, the balloon-tipped catheters and the EMG electrodes were placed and the subjects breathed quietly through the face mask for 10 min (i.e. Quiet Breathing condition; QB). After which they were connected to a mechanical ventilator (Servo i, Maquet SA, France) with an inspiratory support of +4 cm H_2O to compensate for the resistance of the breathing circuit. Three 15' epochs during which the subjects were confronted with an increasingly negative pressure trigger (approximately −5%, −10% and −15% of the maximal inspiratory pressure) were recorded. They were separated by 15' epochs of quiet breathing after disconnection from the ventilator. At the end of this protocol, the subjects were disconnected from the mechanical ventilator and asked to breath quietly for 15 additional minutes (washout condition, WO). Five of the 10 subjects were studied twice at a several weeks interval.

2.4. EMG processing

All EMG signals were fed to a Nihon Kohden Neuropack electromyograph (Nihon Kohden, Tokyo, Japan), with a 10 kHz sampling rate and were filtered (between 20 and 500 Hz and between 20 and 3 kHz for surface and intramuscular recordings, respectively). They were stored on an apple Macintosh computer for subsequent analysis (PowerLab, AD Instruments, Hastings, UK). Raw EMG data were root mean squared (RMS) with a time averaging period of 2 ms to quantify the activity level of the muscle.

The following procedure was then applied (Hug et al., 2006). For each condition in each subject, inspiratory efforts were identified from the Pmask signal (Chart 5.2, AD instruments, Hastings, UK). The continuous EMG RMS signal was then truncated in as many epochs as there were inspiratory efforts, each epoch starting 1 s before the beginning of the corresponding inspiratory effort and ceasing 2 s after its end and therefore containing the full inspiratory-related EMG activity. In the end, 40–50 consecutive such epochs of EMG, phase-locked to inspiration, were ensemble averaged. This produced a mean EMG RMS trace that was used for subsequent analysis (Fig. 1). Its mean value was used to quantify the intensity of the corresponding phasic inspiratory activity. All values were expressed in percentage of the activity so measured during quiet breathing (RMS%).

2.5. Statistical analysis

Data distributions consistently passed the Shapiro-Wilk normality test (Prism®4.01, Graphpad Software, San Diego, CA, USA). Values are therefore reported as mean ± SD. RMS% values were compared using an analysis of variance for repeated measures (subjects as the random factor, breathing condition as the inter-subject factor) with orthogonal contrasts as the post-hoc test (Statistix®®, Tallahassee, FL, USA). The relationship between the scalene activity (RMS%) and the diaphragmatic contribution to inspiration ($\Delta Pga/\Delta Pdi$), the pressure time product of esophageal pressure (PTPes), ΔPes, $\Delta Pga/\Delta Pes$, the intensity of dyspnea were studied by calculating the Pearson product–moment correlation coefficient. This procedure was applied after correcting the data according to the normalization–renormalization procedure recommended by Poon (1988), to account for the possible distortions induced by pooling intra-subjects and inter-subjects measures (StatEL®, Paris, France). The degree of similarity of averaged RMS linear envelope patterns between intramuscular and surface recordings was assessed for each subject by using the cross-correlation technique. The cross-correlation coefficient (with lag time equal to zero, R_0) was calculated according to the equation proposed by Li and Caldwell (1999) (custom written script, Origin 6.1, OriginLab Corporation, USA) from smoothed (triangular Barlett window width 3001 points) averaged signals. In the five subjects studied twice, the reproducibility of the

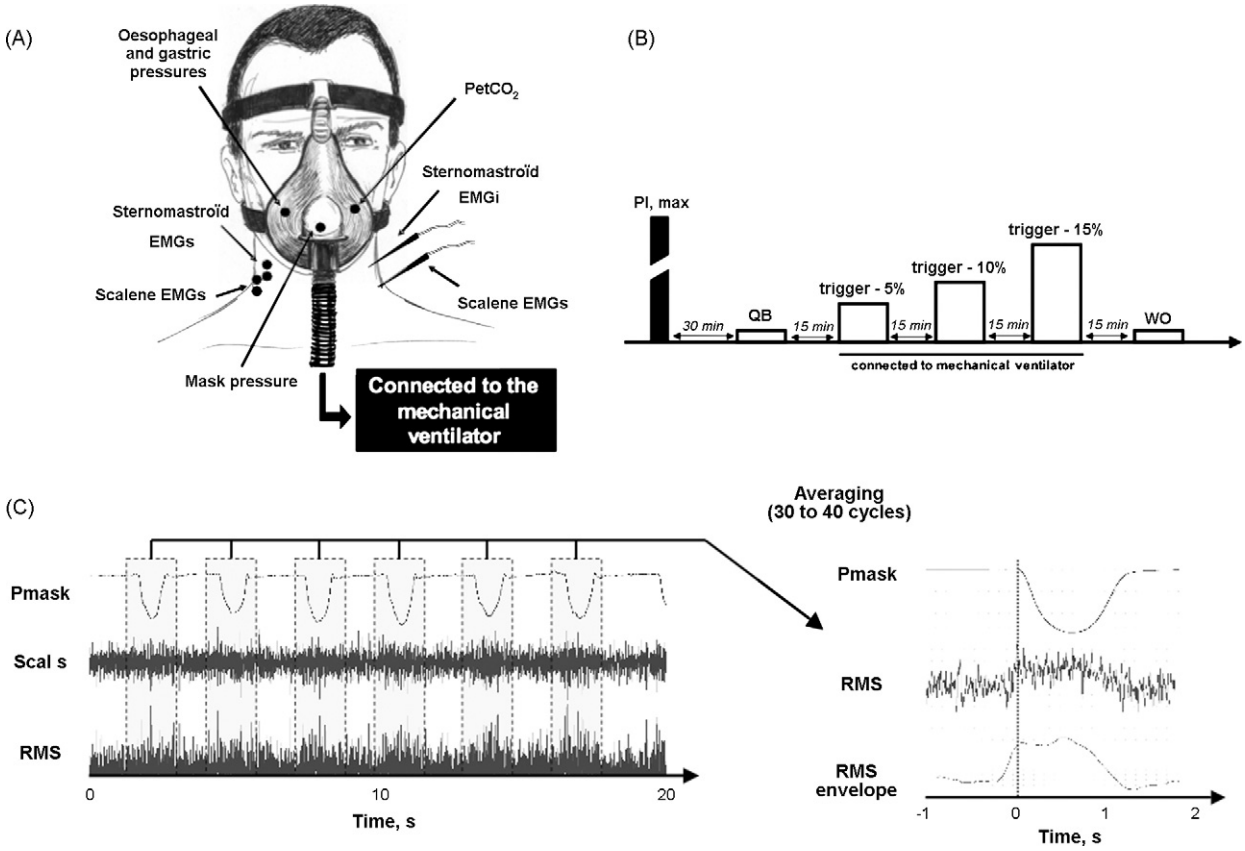

Fig. 1. Experimental setup (panel A), protocol (panel B) and signal processing (panel C). Panel A – airway opening pressure was measured within an airtight facial mask (mask pressure). Esophageal (Pes) and gastric (Pga) pressures were measured with balloon-tipped catheters. End-tidal CO_2 ($P_{ET}CO_2$) was continuously measured through a dedicated port of the face mask. Panel B – P_I,max, maximal inspiratory pressure; QB, quiet breathing; WO, washout. Ventilator triggering levels ("trigger") are expressed in % of P_I,max. Panel C – the step-by-step averaging technique. Six consecutive cycles of the raw surface EMG and mask pressure (Pmask) signals are depicted. The root mean square (RMS) was calculated using fixed windows (duration = 2 ms). Then the mask pressure signal was used to detect the beginning of each inspiration phase. An ensemble averaging of 30–40 successive breaths was performed after splitting the RMS and mask pressure signal in many epochs starting 1 s before the beginning of the inspiration and ceasing 1 s after. The averaged RMS signal was smoothed in order to obtain an EMG RMS envelope.

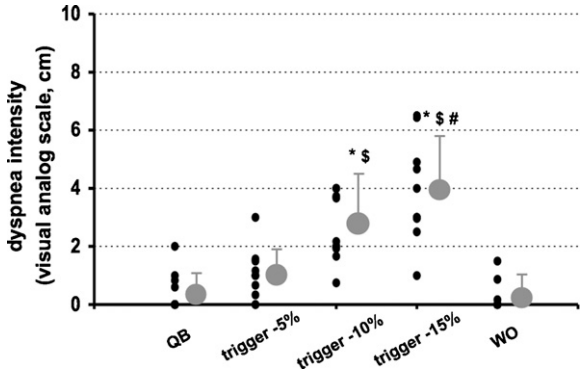

Fig. 2. Dyspnea intensity. Ventilator triggering levels ("trigger") are expressed in % of maximal inspiratory pressure. For each trigger value, the individual data points are presented. The circles beside these values correspond to the average value, with indication of one standard deviation. Overlapping values explain a number of visible data points less than the number of subjects. QB, quiet breathing; WO, washout. (*) Shows significant difference with QB condition. ($) Shows significant difference with Trigger–5% condition. (#) Shows significant difference with Trigger–10% condition.

trigger-related increases in the surface scalene RMS was assessed in terms of the η^2 coefficient of an intraclass correlation analysis (percentage of the total variability that reflects the tendency of two measures within any particular pair to have the same value) (Shrout and Fleiss, 1979). A P value below 0.05 was considered indicative of statistical significance, namely of a less than 5% probability of erroneously rejecting the null hypothesis (type I error).

3. Results

3.1. Dyspnea

Dyspnea increased with the intensity of the inspiratory effort required to trigger the ventilator (Fig. 2).

3.2. Maximal inspiratory pressure and trigger values

$P_{I,max}$ amounted to 98 ± 18 cm H_2O on average for women and 118 ± 6 cm H_2O for men, within the normal range (ATS/ERS statement). In the four women, the trigger value was set to -4.7 ± 0.9 cm

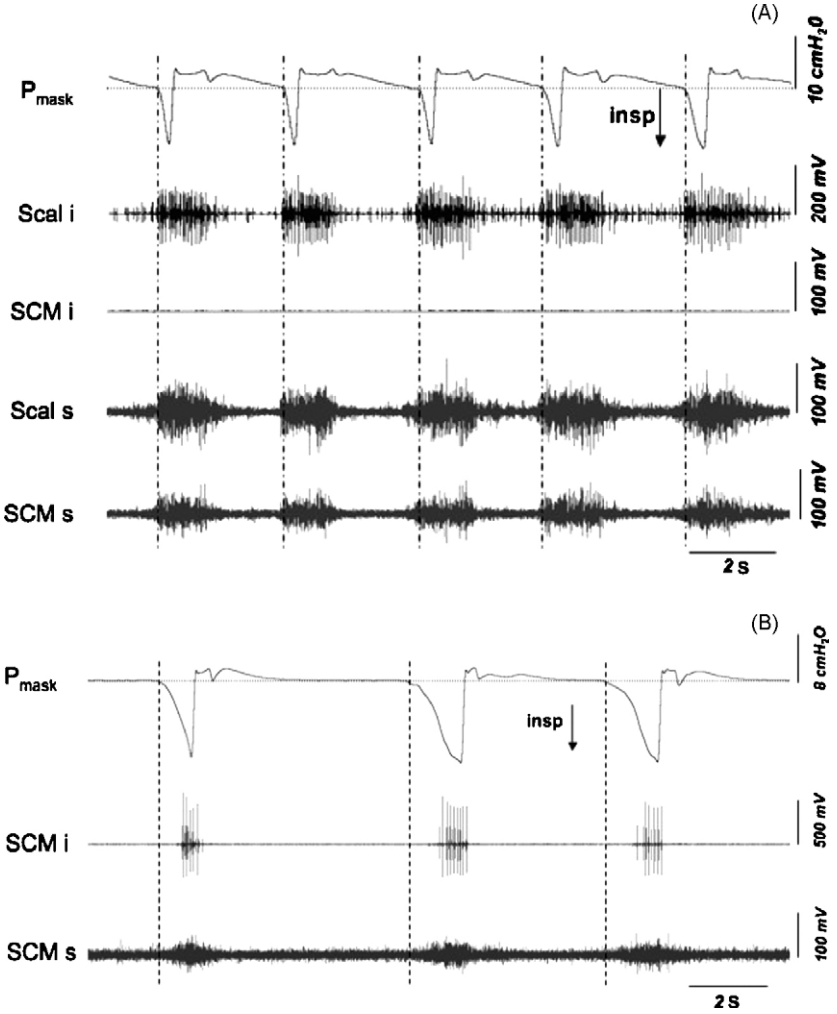

Fig. 3. Sternomastoid EMG activity with a 10% $P_{I,max}$ ventilator triggering value in one subject with silent intramuscular recording (panel A) and one subject exhibiting phasic intramuscular activity (panel B). In the two panels, the top trace represents the evolution of mask pressure over time, with "Insp" standing for "inspiration"; Scal i corresponds to the intramuscular EMG activity of the anterior scalene muscle (fine wire electrode); SCM i corresponds to the intramuscular EMG activity of the sternomastoid muscle (fine wire electrode); Scal s represents the surface EMG activity of the anterior scalene muscle (surface electrodes); SCM S represents the surface EMG activity of the sternomastoid muscle. The vertical dashed lines denote the point chosen to adjust the EMG averaging process on the mask pressure tracing (start of inspiration). Sternomastoid intramuscular electrode was consistently silent (panel A), except in one subject (#6) (panel B). The example in panel A clearly shows that the surface electrodes aimed at recording the sternomastoid pick up a cross-talk signal from other muscles, among which the scalene is probably the most important.

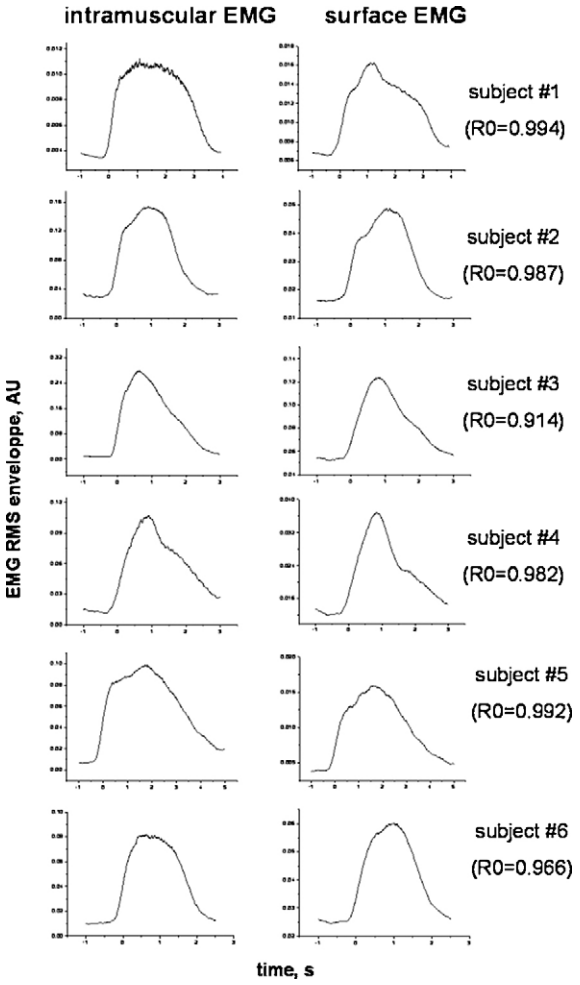

Fig. 4. Comparison of the scalene surface and intramuscular EMG patterns after inspiration-adjusted averaging (ventilator triggering set at 10% of maximal inspiratory pressure) in the six subjects where intramuscular recordings were performed. In all cases, the cross correlation coefficient (R_0) indicates a very high degree of similarity between intramuscular and surface recordings. For the sake of clarity the averaged EMG patterns are smoothed (triangular Barlett window width 3001 points). Of note, the surface EMGs are recorded on the right side, and the intramuscular ones are recorded on the left side.

H_2O; -9.5 ± 1.9 cm H_2O and -14.2 ± 2.9 cm H_2O for the 5%, 10% and 15% trigger condition, respectively. Because PI,max was very similar among the six men, the trigger values were the same for all of the m (i.e. −6, −12 and −18 cm H_2O for, respectively, the 5%, 10% and 15% trigger condition).

3.3. $P_{ET}CO_2$

No noticeable change in $PETCO_2$ was observed during the course of the study, both on average and on an individual basis

3.4. Intramuscular EMG recordings

Two of the six subjects so studied reported a slight discomfort attributable to the insertion of the needle. In all the conditions, the scalene intramuscular recordings showed a phasic activity during tidal breathing with the exception of one subject (#6) during unloaded breathing (i.e. QB and WO conditions). Conversely, the sternomastoid intramuscular electrode was consistently silent, except in one subject (#6) when the trigger was set to 10% and 15% of PI,max (Fig. 3). Thus, the surface electrodes aimed at recording the sternomastoid picked up a cross-talk signal from the scalene. We, therefore, discarded this signal, and focused the analysis on the activity recorded by the surface electrodes lying over the anatomical landmark of the anterior scalene. Of note, this activity was consistently synchronous with the intramuscular one with the exception of one case during QB (subject #2) where the intramuscular signal disappeared intermittently from the recordings in spite of the persistence of the surface one.

3.5. Surface EMG recordings

The Pmask triggered averaging of the surface EMG signal consistently evidenced a phasic inspiratory activity of the scalene muscle. This was true in all the subjects and all the conditions, with the exception of two cases during unloaded breathing (#6 and #9). The cross correlation analysis indicated a very high degree of shape similarity of the surface and intramuscular EMG patterns ($R_0 = 0.968 \pm 0.037$; ranging from 0.818 to 0.996) (Fig. 4). With increasingly intense inspiratory efforts, the surface scalene RMS increased significantly for the two triggers fixed at −10% and −15% of PI,max, and returned to its initial value during the washout period (Figs. 5 and 6). Of note, the baseline EMG activity increased significantly during the 15% trigger condition, suggestive of an increased tonic activity.

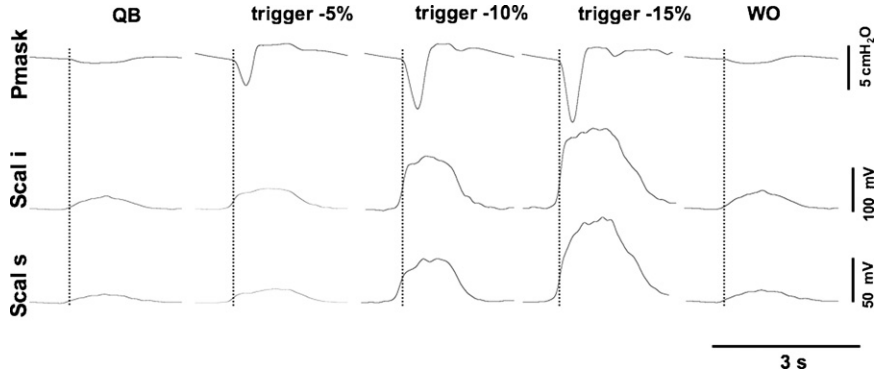

Fig. 5. Example, in one subject, of the inspiration-adjusted average EMGs of the scalene surface and intramuscular recordings. From top to bottom: Pmask, mask pressure; Scal i, intramuscular EMG recording of the anterior scalene (fine wire electrode); Scal s, surface EMG recording of the anterior scalene. For sake of clarity the averaged EMG patterns are smoothed (triangular Barlett window width 3001 points). "QB" stands for "quiet breathing", "WO" for "washout". Ventilator triggering levels ("trigger") are expressed in % of the maximal inspiratory pressure developed by the subjects.

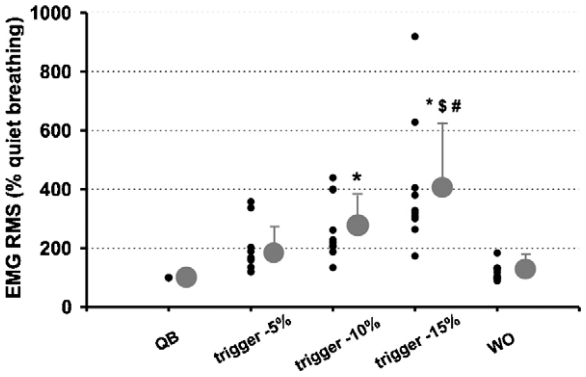

Fig. 6. Surface scalene EMG activity level. The mean RMS value of inspiration adjusted averaged signals is expressed in percentage of the mean activity measured during the first quiet breathing epoch. For each trigger value, the individual data points are presented. Overlapping values explain a number of visible data points less than the number of subjects. The circle beside these values correspond to the average value, with indication of one standard deviation. QB, quiet breathing; WO, washout. Ventilator triggering levels ("trigger") are expressed in % of the maximal inspiratory pressure developed by the subjects. (*) Shows significant difference with QB condition, ($) Shows significant difference with Trig–5% condition. (#) Shows significant difference with Trig–10% condition.

There was no change in the $\Delta Pga/\Delta Pdi$ ratio with increasing values of the ventilator trigger, and no correlation between the RMS and the $\Delta Pga/\Delta Pdi$ ratio. There were however significant correlations between RMS and ΔPes (the more negative ΔPes, the higher the RMS; $R = -0.49$; 95% CI: −0.69 to −0.23, $P < 0.01$), RMS and the $\Delta Pga/\Delta Pes$ ratio ($R = 0.34$; 95% CI: 0.04–0.57, $P > 0.05$), and RMS and the pressure time product of esophageal pressure (PTPes) (the more negative the PTPes, the greater the RMS; $R = -0.56$; 95% CI: −0.63 to −0.31, $P < 0.01$). The strongest correlation was between the RMS and dyspnea intensity ($R = 0.85$; 95% CI: 0.75–0.91).

3.6. Repeated experiments

In the five subjects who could be studied on a second occasion, the repeated experiment showed a fair reproducibility ($\eta^2 = 0.81$) of the trigger-related increases in the surface scalene RMS.

4. Discussion

This study shows that in healthy subjects receiving inspiratory pressure support via a face mask, decreasing the sensitivity of the ventilator trigger in a stepwise manner (namely increasing inspiratory loading) is associated with a progressive increase in the EMG activity level of the scalene muscle. This increase correlates with the increasing magnitude of the inspiratory effort (as assessed by ΔPes, the $\Delta Pes/\Delta Pga$ ratio, or PTPes). The RMS increase is strongly correlated with an increase in the self-rated intensity of dyspnea, in line with the relationship between respiratory discomfort and inspiratory neck muscle activity (Ward et al., 1988). The contribution of the diaphragm to the inspiratory effort does not vary, in contrast with the changes in task repartition that has been described in response to other types of inspiratory loading (Aliverti et al., 1997). The sternomastoid muscle does not appear to be recruited within the loading range studied.

Of note, the trigger pressures used in our subjects may seems very high in absolute value, in comparison of what is encountered in intensive care patients. In fact, in proportion of maximal inspiratory pressures, they are not that high. This is because critically ill patients placed under mechanical often have greatly reduced inspiratory pressures (median maximal inspiratory pressure of 30 cm H_2O only—with a lower interquartile of 20 cm H_2O—in 79 such patients studied by De Jonghe et al. (2007): a ventilator trigger of −2 cm H_2O can correspond to 10% of the maximal inspiratory pressure). In addition, it must be kept in mind that many patients who have to trigger a ventilator also have to overcome an intrinsic positive end-expiratory pressure due to dynamic hyperinflation that can amount to several cm H_2O (Petrof et al., 1990). As a result, our experimental protocol appears realistic in the perspective of future intensive care applications.

4.1. Sequence of recruitment of inspiratory neck muscles

With one exception, our subjects did not exhibit sternomastoid recruitment in response to the increasing inspiratory loading in spite of a marked increase in the scalene activity. This is consistent with the current knowledge of about the recruitment of inspiratory neck muscles. Hudson et al. (2007) have shown that during both static and dynamic inspiratory efforts, the recruitment of the sternomastoid is delayed until about 20% of the maximal inspiratory pressure has been developed (and at times much later depending on the subjects). This sequence of recruitment that is in line with the greater mechanical advantage of the scalene as compared to the sternomastoid (Legrand et al., 2003) is unaffected by changes in lung volume. In our study, the higher load chosen was of 15% of maximal inspiratory pressure. The absence of sternomastoid activation is therefore not surprising. It also supports the idea, expounded by Hudson et al. (2007), that the recruitment threshold of the scalene and sternomastoid is not sensitive to the type of inspiratory efforts performed. Hudson et al. (2007) asked their subjects to perform either static efforts at constant lung volumes against a closed airway, or dynamic efforts during which lung volume increased from FRC to TLC. They found that this did not markedly change the sequence and timing of the respective scalene and sternomastoid activation. The type of effort performed by our subject was more complex in nature, the first part of inspiration being devoted to reach the ventilator trigger and performed at constant lung volume ("static"), the second part being devoted to the production of tidal volume ("dynamic") with the aid of the ventilator. Yet, as during simpler types of efforts, the threshold of scalene activation appeared to be low, and in any case lower than that of the sternomastoid.

From another point of view, our study also concords with the idea that the nature of the neural command involved in a given inspiratory activity does not modify the scalene-sternomastoid sequence. The scalene muscles are recruited early and the sternomastoid only late in the course of the response to a stimulation of the automatic respiratory command by carbon dioxide (Campbell, 1955). In the study by Hudson et al. (2007), where the scalenes were also recruited early and first, the subjects performed volitional efforts involving the primary motor cortical representation of inspiratory muscles. Our subjects, who were naive to respiratory physiology experiments, were confronted to sustained inspiratory mechanical loading. In this setting, load compensation occurs — attested to by the maintenance of $PETCO_2$ — and involves cortical mechanisms (Raux et al., 2007a,b) that are probably behavioral rather than volitional strictly speaking. Yet, the scalenes were also recruited before the sternomastoid in our subjects. Again this supports the notion that the sequence of the inspiratory activation of the scalene and the sternomastoid is neurally preset and does not depend on the source(s) of the inspiratory command. Of note, it is consistent with the respective mechanical advantage of these muscles (Hudson et al., 2007).

4.2. Significance and usefulness of surface scalene EMG recordings

The electromyographic activity of the scalenes can be studied using intramuscular or surface electrodes. Intramuscular electrodes provide high quality signals, but they sample a limited number of motor units and their invasive nature limit their use in clinical practice. Surface electrodes give a more global picture of muscle function and are easy to use for prolonged or repeated studies, with a reasonable inter-experiment reproducibility (Duiverman et al., 2004) Their use, however, raises the question of signal contamination due to the cross-talk of adjacent muscle groups. Indeed, surface electrodes placed over the anatomical landmark of the scalene muscles will inevitably pick-up sternomastoid activity if it is present, and reciprocally, making the interpretation of the signal difficult. Of note on this, our study confirms that surface recordings are not appropriate to study the recruitment of the sternomastoid, even though they are often used with this purpose (Mananas et al., 2000; Ribeiro et al., 2002; Tassaux et al., 2002; Ratnovsky et al., 2003; Perlovitch et al., 2006). The plastysma could also be a source of signal contamination. Available data however suggest that the inspiratory recruitment threshold of this postural muscle is very high (Fitting et al., 1988) and that its activation occurs in very particular clinical conditions such as tetraplegia (De Troyer et al., 1986) or very severe respiratory distress in ICU patients (personal observations, unpublished). Recruitment of the platysma is thus not likely to have occurred in our subjects. In addition, postural activity of the platysma should also not have been an issue, given the inspiratory-adjusted nature of our EMG averaging approach.

What can we infer from our results regarding the potential usefulness of surface recordings of inspiratory neck muscles in acutely ill patients? In such patients, sternomastoid activation hallmarks the severity of a given clinical condition. In the weaning study of Parthasarathy et al. (2007), sternomastoid activity was noted after the first minute of a spontaneous breathing trial in 8 out of 11 patients who failed this trial. These patients had very low maximal inspiratory pressures (32.7 cm H_2O on average) and at the beginning of the spontaneous breathing trial, their inspiratory effort amounted to 11.3 cmH_2O, namely more than 30% of $P_{I,max}$. At the end of the trial all these patients exhibited sternomastoid activity and their average inspiratory effort amounted to 18.7 cm H_2O, more than half of the available $P_{I,max}$. Conversely, only three of the eight weaning success patients exhibited sternomastoid activity during the trial, in line with a ratio of inspiratory effort to $P_{I,max}$ that was generally well below 30%. These observations are in keeping with the results of Hudson et al. (2007) and they emphasize the notion that sternomastoid activation in respiratory distress probably has a strong negative prognostic value. Although Parthasarathy et al. (2007) did not assess the activity of the scalenes in their patients, it is almost certain that such an activity was present and would have been picked up by surface electrodes, as indicated by our results. All in all, surface recordings are not likely to provide an appropriate answer to the question "are the sternomastoid activated?" This sets a limit to their value as prognostic indicators during respiratory distress, but in practice there is no need of an EMG approach to answer this question. In contrast, identifying the activation of the scalenes can be more difficult, let alone quantifying it. Yet answering the question "are the scalenes activated and how much?" in situations where loading is not sufficient to activate the sternomastoid is putatively important. This is subtended by the correlation that exists between scalene EMG and dyspnea. This correlation was first documented by Ward et al. (1988) during experimental respiratory muscle fatigue protocols involving high level of inspiratory loading. We found a similar correlation in our subjects even though the intensity of loading was much lower than in the study by Ward et al. (1988). This suggests that the relationship between scalene activity and dyspnea is linear and has a low threshold, slight increases above the resting activity being likely to be associated with respiratory discomfort. Of note, we observed this relationship in individuals subjected to intermittent positive pressure ventilation that is known to exert a non-chemical inhibitory influence on respiratory drive (Simon et al., 1991; Leevers et al., 1993; Fauroux et al., 1998). This phenomenon was therefore not of sufficient magnitude to stamp out the effects of scalene recruitment on respiratory sensations. It could have changed the slope of the relationship, but the design of the study was not meant to assess this hypothesis.

In the absence of sternomastoid activation, as in our subjects, the similarity in shape and timing evidenced by cross-correlation analysis of the intramuscular and surface scalene EMG patterns that we observed (Fig. 4) indicates that the averaging method that we used can reliably identify changes in scalene activity over time, from surface recordings.

This result must be seen as a mere proof of concept, and requires corroboration in mechanically ventilated patients receiving noninvasive or invasive ventilation. If such corroboration is obtained in the future, then real time scalene RMS at the bedside could allow clinicians to monitor the neural reactions to small changes in inspiratory loading. This is clinically relevant, because identifying an increase in scalene activity could then alert clinicians to subtle or impending respiratory discomfort. This would be the case even in the absence of actual patient–ventilatory asynchrony (Chao et al., 1997), and would have the advantage of occurring far earlier than inspiratory loading induced sternomastoid recruitment. This would be particularly important in mechanically ventilated patients who, for whatever reasons, are not capable of full communication with their caregivers (e.g. intubated and partially sedated patients). Real time scalene RMS could then become an adjunct to the current methods used to adjust mechanical ventilation to the demands of the patients. Of note, the evaluation the activity of extradiaphragmatic inspiratory muscles of the neck or of the chest wall must be seen as complementary of the evaluation of the activity of the diaphragm, as it is used for example using esophageal EMG probes during neurally adjusted ventilatory assistance.

Acknowledgments

The authors thank the volunteers who accepted to participate in this study and Dr Antoine Couturier (National Institute for Sports, INSEP, Paris, France) for its technical assistance (custom written script for calculation of the cross correlation coefficients).

Grants: This study was funded in part by a "Contrat de recherche triennal "Legs Poix" de la Chancellerie de l'Université de Paris" and by Association pour le Développement et l'Organisation de la Recherche En Pneumologie (ADOREP), Paris, France. Linda Chiti was supported by a scholarship of the Centre d'Assistance Respiratoire à Domicile d'Ile-de-France (CARDIF), Fontenay-aux-Roses, France. François Hug was supported in part by a scholarship of the Fédération ANTADIR, Paris, France. Mathieu Raux was supported in part by a scholarship of the Comité National Contre les Maladies Respiratoires, Paris, France and in part by a shcolarship of the Fédération ANTADIR, Paris, France.

Conflicts of interest: This study did not involve any commercial or financial conflict of interest. Two of the authors (TS, MR) are listed as inventors on patent WO/2008/006963 "Device for detecting the improper adjustment of a ventilatory support machine used on a mammal", that describes various neurophyisological approaches (EEG and EMG) to detect and quantify the neural reactions induced by "ventilator fighting".

References

Aliverti, A., Cala, S.J., Duranti, R., Ferrigno, G., Kenyon, C.M., Pedotti, A., Scano, G., Sliwinski, P., Macklem, P.T., Yan, S., 1997. Human respiratory muscle actions and control during exercise. J. Appl. Physiol. 83, 1256–1269.

Beau, J.H.S., Maissiat, J.H., 1843. Recherches sur le mécanisme des mouvements respiratoires (deuxième article). Archives Générales de Médecine, 265–295.

Bradley, T.D., Chartrand, D.A., Fitting, J.W., Killian, K.J., Grassino, A., 1986. The relation of inspiratory effort sensation to fatiguing patterns of the diaphragm. Am. Rev. Respir. Dis. 134, 1119–1124.

Brochard, L., Harf, A., Lorino, H., Lemaire, F., 1989. Inspiratory pressure support prevents diaphragmatic fatigue during weaning from mechanical ventilation. Am. Rev. Respir. Dis. 139, 513–521.

Campbell, E.J., 1955. The role of the scalene and sternomastoid muscles in breathing in normal subjects; an electromyographic study. J. Anat. 89, 378–386.

Chao, D.C., Scheinhorn, D.J., Stearn-Hassenpflug, M., 1997. Patient-ventilator trigger asynchrony in prolonged mechanical ventilation. Chest 112, 1592–1599.

De Jonghe, B., Bastuji-Garin, S., Durand, M.C., Malissin, I., Rodrigues, P., Cerf, F., Outin, H., Sharshar, T., 2007. Respiratory weakness is associated with limb weakness and delayed weaning in critical illness. Crit. Care Med. 35, 2007–2015.

De Troyer, A., Estenne, M., 1984. Coordination between rib cage muscles and diaphragm during quiet breathing in humans. J. Appl. Physiol. 57, 899–906.

De Troyer, A., Estenne, M., Wincken, W., 1986. Rib cage motion and muscle use in high tetraplegics. Am. Rev. Respir. Dis. 133, 1115–1119.

De Troyer, A., Peche, R., Yernault, J.C., Estenne, M., 1994. Neck muscle activity in patients with severe chronic obstructive pulmonary disease. Am. J. Respir. Crit. Care Med. 150, 41–47.

Duiverman, M.L., van Eykern, L.A., Vennik, P.W., Koëter, G.H., Maarsingh, E.J., Wijkstra, P.J., 2004. Reproducibility and responsiveness of a noninvasive EMG technique of the respiratory muscles in COPD patients and in healthy subjects. J. Appl. Physiol 96, 1723–1729.

Estenne, M., Derom, E., De Troyer, A., 1998. Neck and abdominal muscle activity in patients with severe thoracic scoliosis. Am. J. Respir. Crit. Care Med. 158, 452–457.

Fauroux, B., Isabey, D., Desmarais, G., Brochard, L., Harf, A., Lofaso, F., 1998. Nonchemical influence of inspiratory pressure support on inspiratory activity in humans. J. Appl. Physiol. 85, 2169–2175.

Fitting, J.W., Bradley, T.D., Easton, P.A., Lincoln, M.J., Goldman, M.D., Grassino, A., 1988. Dissociation between diaphragmatic and rib cage muscle fatigue. J. Appl. Physiol. 64, 959–965.

Gandevia, S.C., Leeper, J.B., McKenzie, D.K., De Troyer, A., 1996. Discharge frequencies of parasternal intercostal and scalene motor units during breathing in normal and COPD subjects. Am. J. Respir. Crit. Care Med. 153, 622–628.

Gilbert, R., Auchincloss Jr., J.H., Peppi, D., 1981. Relationship of rib cage and abdomen motion to diaphragm function during quiet breathing. Chest 80, 607–612.

Hudson, A.L., Gandevia, S.C., Butler, J.E., 2007. The effect of lung volume on the co-ordinated recruitment of scalene and sternomastoid muscles in humans. J. Physiol. 584, 261–270.

Hug, F., Raux, M., Prella, M., Morelot-Panzini, C., Straus, C., Similowski, T., 2006. Optimized analysis of surface electromyograms of the scalenes during quiet breathing in humans. Respir. Physiol. Neurobiol. 150, 75–81.

Katagiri, M., Abe, T., Yokoba, M., Dobashi, Y., Tomita, T., Easton, P.A., 2003. Neck and abdominal muscle activity during a sniff. Respir. Med. 97, 1027–1035.

Leevers, A.M., Simon, P.M., Xi, L., Dempsey, J.A., 1993. Apnoea following normocapnic mechanical ventilation in awake mammals: a demonstration of control system inertia. J. Physiol. 472, 749–768.

Legrand, A., Schneider, E., Gevenois, P.A., De Troyer, A., 2003. Respiratory effects of the scalene and sternomastoid muscles in humans. J. Appl. Physiol. 94, 1467–1472.

Li, L., Caldwell, G.E., 1999. Coefficient of cross correlation and the time domain correspondence. J. Electromyogr. Kinesiol. 9, 385–389.

Magendie F., 1817. Précis élémentaire de Physiologie, Tome Second. Méquignon-Marvis, Paris, France, pp. 372–476.

Mananas, M.A., Jane, R., Fiz, J.A., Morera, J., Caminal, P., 2000. Study of myographic signals from sternomastoid muscle in patients with chronic obstructive pulmonary disease. IEEE Trans Biomed. Eng. 47, 674–681.

Pardee, N.E., Winterbauer, R.H., Allen, J.D., 1984. Bedside evaluation of respiratory distress. Chest 85, 203–206.

Parthasarathy, S., Jubran, A., Laghi, F., Tobin, M.J., 2007. Sternomastoid, rib cage, and expiratory muscle activity during weaning failure. J. Appl. Physiol. 103, 140–147.

Perlovitch, R., Gefen, A., Elad, D., Ratnovsky, A., Kramer, M.R., Halpern, P., 2006. Inspiratory muscles experience fatigue faster than the calf muscles during treadmill marching. Respir. Physiol. Neurobiol..

Petrof, B.J., Legaré, M., Goldberg, P., Milic-Emili, J., Gottfried, S.B., 1990. Continuous positive airway pressure reduces work of breathing and dyspnea during weaning from mechanical ventilation in severe chronic obstructive pulmonary disease. Am. Rev. Respir. Dis. 141, 281–289.

Poon, C.S., 1988. Analysis of linear and mildly nonlinear relationships using pooled subject data. J. Appl. Physiol. 64, 854–859.

Raper, A.J., Thompson Jr., W.T., Shapiro, W., Patterson Jr., J.L., 1966. Scalene and sternomastoid muscle function. J. Appl. Physiol. 21, 497–502.

Ratnovsky, A., Zaretsky, U., Shiner, R.J., Elad, D., 2003. Integrated approach for in vivo evaluation of respiratory muscles mechanics. J. Biomech. 36, 1771–1784.

Raux, M., Ray, P., Prella, M., Duguet, A., Demoule, A., Similowski, T., 2007a. Cerebral cortex activation during experimentally induced ventilator fighting in normal humans receiving noninvasive mechanical ventilation. Anesthesiology 107, 746–755.

Raux, M., Straus, C., Redolfi, S., Morelot-Panzini, C., Couturier, A., Hug, F., Similowski, T., 2007b. Electroencephalographic evidence for pre-motor cortex activation during inspiratory loading in humans. J Physiol 578, 569–578.

Ribeiro, E.C., Marchiori, S.C., Silva, A.M., 2002. Electromyographic analysis of trapezius and sternocleidomastoideus muscles during nasal and oral inspiration in nasal- and mouth-breathing children. J. Electromyogr. Kinesiol. 12, 305–316.

Saboisky, J.P., Gorman, R.B., De Troyer, A., Gandevia, S.C., Butler, J.E., 2007. Differential activation among five human inspiratory motoneuron pools during tidal breathing. J. Appl. Physiol. 102, 772–780.

Shrout, P.E., Fleiss, J.L., 1979. Intraclass correlations: uses in assessing rater reliability. Psychol. Bull. 2, 420–428.

Similowski, T., Attali, V., Bensimon, G., Salachas, F., Mehiri, S., Arnulf, I., Lacomblez, L., Zelter, M., Meininger, V., Derenne, J.P., 2000. Diaphragmatic dysfunction and dyspnoea in amyotrophic lateral sclerosis. Eur. Respir. J. 15, 332–337.

Simon, P.M., Skatrud, J.B., Badr, M.S., Griffin, D.M., Iber, C., Dempsey, J.A., 1991. Role of airway mechanoreceptors in the inhibition of inspiration during mechanical ventilation in humans. Am. Rev. Respir. Dis. 144, 1033–1041.

Tassaux, D., Dalmas, E., Gratadour, P., Jolliet, P., 2002. Patient-ventilator interactions during partial ventilatory support: a preliminary study comparing the effects of adaptive support ventilation with synchronized intermittent mandatory ventilation plus inspiratory pressure support. Crit. Care Med. 30, 801–807.

Ward, M.E., Eidelman, D., Stubbing, D.G., Bellemare, F., Macklem, P.T., 1988. Respiratory sensation and pattern of respiratory muscle activation during diaphragm fatigue. J. Appl. Physiol. 65, 2181–2189.

Yan, S., Kaminski, D., Sliwinski, P., 1997. Inspiratory muscle mechanics of patients with chronic obstructive pulmonary disease during incremental exercise. Am. J. Respir. Crit. Care Med. 156, 807–813.

Journal of Strength and Conditioning Research, 2006, 20(3), 704–708

Technical Note

A Comparison of Visual and Mathematical Detection of the Electromyographic Threshold During Incremental Pedaling Exercise: A Pilot Study

François Hug,[1,2] David Laplaud,[2] Alejandro Lucia,[3] and Laurent Grelot[2]

[1]Laboratory of Motricity, Interactions, Performance, University of Nantes, Nantes Universities, Nantes, France; [2]Department of Sport Physiology, UPRES EA 3285, Faculty of Sport Sciences, University of Mediterranean, Marseille, France; [3]European University of Madrid, Madrid, Spain.

Abstract. Hug, F., D. Laplaud, A. Lucia, and L. Grelot. A comparison of visual and mathematical detection of the electromyographic threshold during incremental pedaling exercise: A pilot study. *J. Strength Cond. Res. 20(3):704–708. 2006.*—During exhaustive incremental pedaling exercises, root mean square or amplitude of integrated electromyographic values exhibits a nonlinear increase, i.e., the so-called electromyographic threshold (EMG_{Th}). As proposed by various authors, this EMG_{Th} could be used as a complementary indicator of the aerobic–anaerobic transition in physiological evaluations. However, most of these studies used visual detection for the EMG_{Th} and to date no previous study has shown the reliability of this type of EMG_{Th} detection. We aimed to compare a visual and a mathematical method for EMG_{Th} detection in each of 8 lower limb muscles during incremental cycling exercise. Our results showed an overestimation in the number of cases in which EMG_{Th} was detected when using visual inspection ($n = 45$) compared with the mathematical method ($n = 32$). However, no significant differences were observed between the 2 methods concerning the power output at which EMG_{Th} occurred. These results suggest that EMG_{Th} should be mathematically detected. In this context, coaches can easily perform such measurements in order to evaluate the impact of their training programs on the neuromuscular adaptations of their athletes. For example, an automatic mathematical detection of EMG_{Th} could be performed during a pedaling exercise in order to detect neuromuscular fatigue. Furthermore, this index could be used during test or training sessions performed either in a lab or in ecological situations. Moreover, the use of EMG_{Th} to predict ventilatory threshold occurrence could be an interesting tool for trainers who cannot use the very expensive devices needed to analyze respiratory gas exchanges.

Key Words. root mean square, cycling, signal analysis, mathematical, visual, muscle recruitment

Introduction

Exercise on a cycle ergometer is commonly used in sports medicine for physical and physiological evaluation. Ordinarily, the estimation of muscle metabolism is based on measurements of heart rate, lactate production, $\dot{V}O_2$, and the determination of the 2 ventilatory thresholds characterized by nonlinear increases in minute ventilation. However, a pivotal variable, i.e., global electromyographic (EMG) activity (root mean square [RMS]), is less used.

For many years, surface EMG has been used as a noninvasive method to quantify the level of activation of working skeletal muscles. During exhaustive incremental exercises, although some authors found a linear relationship between the RMS of EMG or the amplitude of integrated EMG (iEMG), on the one hand, and workload level, on the other (2, 20, 21), a nonlinear increase of RMS or iEMG values has been considered a typical pattern (1, 5, 7, 9, 14, 17, 22). This breakpoint, the so-called EMG threshold (EMG_{Th}), has been linked to overrecruitment of new motor units, particularly of those made up of Type II fibers, to maintain the required energy supply for contraction (15). Moreover, various studies have showed a correlation between the occurrence of the first ventilatory threshold (VT_1) and the EMG_{Th} (12–14, 17, 22) or the second ventilatory threshold (VT_2) (4, 6, 7, 12, 13). Therefore, other investigators have demonstrated the between-days reproducibility of the EMG_{Th} occurrence (11, 13). For all these reasons, and as proposed by several authors (10, 13, 14, 17), the EMG_{Th} could be a new noninvasive estimation of the metabolic response to incremental exercise.

However, most of these studies used visual detection of the EMG_{Th}. Also, surface EMG remains a method less used than ventilatory threshold assessment in exercise physiology. Even if simple visual inspection has proven to be valid for VT_1 and VT_2 detection (19), to date no previous study has shown the accuracy and/or reliability of EMG_{Th} visual detection.

The aim of this study was to compare a visual and a mathematical method of EMG_{Th} detection in each of 8 lower limb muscles during an incremental leg-pedaling exercise.

Methods

Experimental Approach to the Problem

In order to compare visual and mathematical detection of the EMG_{Th}, we analyzed RMS response of 8 lower limb muscles to an incremental pedaling exercise. For each muscle and each subject, 2 independent observers visually detected the EMG_{Th}. The results given by each observer were compared using the kappa coefficient. The EMG_{Th} was also mathematically detected.

First, we compared the number of times EMG_{Th} was detected by using the 2 different methods (quantitative analyses); in a second step, we compared these 2 methods in term of power output at which the EMG_{Th} occurred (qualitative analyses).

Subjects

Six healthy men (age = 27 ± 1 years; height = 180 ± 10 cm; body mass = 78 ± 9 kg), volunteered for the study

and gave informed consent. Subjects were not engaged in regular athletic activities, but they performed 3 ± 1 hours of recreational activities (football, climbing, basketball, swimming, and rugby) per week. The experiment was conducted in accordance with the code of ethics of the World Medical Association (Declaration of Helsinki) and approved by the local ethic committee (Consultative Committee for the Protection of the People in Biomedical Research).

Study Protocol

Each subject performed an incremental cycling test until exhaustion on an electrically braked cycle-ergometer (Excalibur Sport, Lode, The Netherlands). The progressive exercise consisted of a 3-minute constant level warm-up (at 100 W) after which power output was increased by 25 $W \cdot min^{-1}$. Subjects wore cycling shoes with clipless pedals and maintained pedal cadence within the 75–85 $rev \cdot min^{-1}$ range. The test ended upon volitional exhaustion of the subjects or when cadence could not be maintained at a minimum of 75 $rev \cdot min^{-1}$.

EMG Recording and Analysis

EMG activity was continuously recorded from the following 8 muscles of the right lower limb: vastus lateralis, rectus femoris, vastus medialis, semimembranosus, biceps femoris, gastrocnemius lateralis, gastrocnemius medianus, and tibialis anterior. A pair of surface electrodes (Universal Ag/AgCl electrodes; Contrôle Graphique Medical, Brie-Comte-Robert, France) was attached to the skin with a 2-cm interelectrode distance. The electrodes were placed longitudinally with respect to the underlying muscle fiber arrangement and located according to the recommendations of Surface EMG for the Non-Invasive Assessment of Muscles (8). Prior to electrode application, the skin was shaved and cleaned with alcohol in order to minimize impedance. The wires connected to the electrodes were well secured with tape to avoid movement-induced artifacts.

Raw EMG signals were preamplified (gain 375) close to the electrodes, and band pass was filtered between 8 and 500 Hz, amplified (ME3000P8; Mega Electronics Ltd., Kuopio, Finland), and analog-to-digital converted at a sampling rate of 10 kHz. The RMS was averaged every 5 crank revolutions (corresponding to about 3 seconds at 85 rpm) throughout the test.

Visual and Mathematical Determination of EMG_{Th}

EMG_{Th} was first determined mathematically (EMG_{Th} Math) using a computer algorithm (Centro de Datos; UCM, Madrid, Spain) that models RMS response to gradual exercise using simple linear regression (14). With this method, a single linear regression is fitted to all data points. A brute force method is then used to fit 2 lines to the data points. The program calculates regression lines for all possible divisions of the data into 2 contiguous groups, and the pair of lines yielding the least pooled residual sum of squares is chosen as representing the best fit. Figure 1a shows an example of the aforementioned mathematical determination of EMG_{Th} in 1 of the subjects' muscles.

Two independent observers (who were unaware of the results of the mathematical method) visually detected the EMG_{Th} as the breakpoint occurring in absolute and relative RMS values throughout the incremental test. An individual example of the aforementioned visual detection of EMG_{Th} is depicted in Figure 1a,b.

Statistical Analyses

Statistical analyses were performed using the statistical package SPSS for Windows (version 10.1; SPSS, Chicago, IL). Results were expressed as mean ± *SD*.

The interobserver variation of EMG_{Th} determination was assessed using the kappa coefficient. Interobserver agreement was classified as follows: poor, κ = 0–0.20; fair, κ = 0.21–0.40; moderate, κ = 0.41–0.60; good, κ = 0.61–0.80; and excellent, κ = 0.81–1.00.

Intraclass correlation coefficient (ICC) was determined as the criterion of concordance between the 2 methods. The ICC was defined as the ratio of the intraclass variance and the total variance. Good reliability occurred when the ICC ranged from 0.8 to 1.

Further analysis of the reliability of visual and mathematical EMG_{Th} detection methods was accomplished by applying the procedures suggested by Bland and Altman (3). For this analysis, the mean difference (bias) and *SD* of the differences between the mean values of EMG_{Th} (in W) obtained using mathematical and visual determination were calculated. The data were shown graphically, comparing the difference between the 2 methods against their average value in W. The mean difference (bias) was indicated in the graph.

We also applied the statistical procedure described by Passing and Bablok (18) for testing the equality of measurements from the 2 methods. After testing for a linear relationship between the results of the 2 methods, confidence limits are given for the slope beta and the intercept alpha. These are used to determine whether there is only a chance difference between beta and 1 and between alpha and 0.

RESULTS

The 2 observers visually detected the same EMG_{Th}, and the kappa coefficient was 0.88, showing an excellent concordance between the 2 observers for the power output of each EMG_{Th}. Table 1 shows the number of subjects with an EMG_{Th} visually and mathematically detected during the incremental test. Visual detection overestimated the number of cases of actual EMG_{Th} occurrence, i.e., there were totals of 45 and 32 for visual and mathematical detection, respectively. ICC values showed a good concordance between the 2 methods concerning the power output at which the EMG_{Th} occurred. An individual example of both visual and mathematical detection of EMG_{Th} is depicted in Figure 1a. Figure 1b depicts 1 case in which EMG_{Th} was visually but not mathematically detected.

The Passing and Bablok regression and the Bland and Altman procedure (Figure 2) confirm the ICC results, showing a good concordance of the 2 methods regarding determination of the power output at which EMG_{Th} occurs.

DISCUSSION

This is the first study to compare, in 8 lower limb muscles, visual and mathematical detection methods for the EMG_{Th}. Our results showed an overestimation of the number of EMG_{Th} cases using visual detection. However, no significant difference existed between the 2 methods (i.e., visual vs. mathematical) concerning the power output at which the EMG_{Th} occurred.

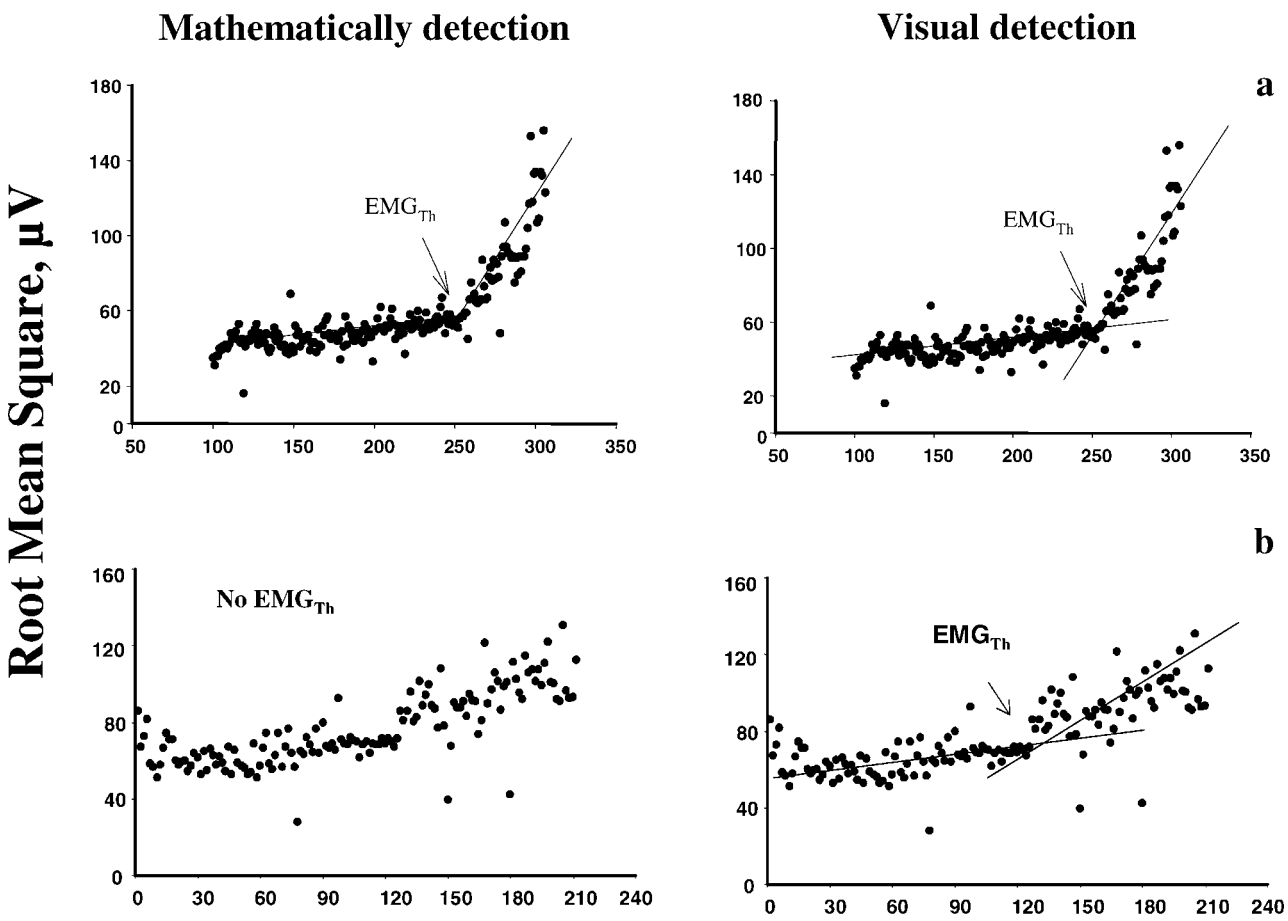

FIGURE 1. Individual examples of the mathematical and visual determination of electromyographic threshold (EMG_{Th}) on the vastus lateralis muscle. (a) EMG threshold mathematically and visually detected. (b) EMG threshold only visually detected.

TABLE 1. Detection of EMG_{Th}.*

	Number of subjects showing				Power (W)		
	EMG_{Th} Vis	EMG_{Th} Math	Both EMG_{Th} Vis and EMG_{Th} Math	No EMG_{Th} Vis and no EMG_{Th} Math	EMG_{Th} Vis	EMG_{Th} Math	ICC
VL	6	6	6	0	250 ± 42	254 ± 33	0.88
RF	6	4	4	0	225 ± 35	225 ± 35	0.91
VM	6	5	5	0	240 ± 33	240 ± 42	0.94
SM	4	2	2	2	275 ± 0	250 ± 35	
BF	6	5	5	0	235 ± 42	260 ± 72	0.87
GL	6	4	4	0	231 ± 43	237 ± 33	0.67
GM	5	2	2	1	250 ± 70	275 ± 70	
TA	6	4	4	0	256 ± 43	244 ± 43	0.83
All muscles	45 (93.7%)	32 (66.7%)	32 (66.7%)	3 (6.2%)	241 ± 38	248 ± 43	0.86

* Data are shown as mean ± *SD*. EMG_{Th} = electromyographic threshold; Vis = visually determined; Math = mathematically determined; ICC = intraclass correlation coefficient; VL = vastus lateralis; RF = rectus femoris; VM = vastus medialis; SM = semimembranosus; BF = biceps femoris; GL = gastrocnemius lateralis; GM = gastrocnemius medianus; TA = tibialis anterior.

Our results show that visual determination of EMG_{Th} occurrence is a subjective method; it could be influenced by the experience and skill of the examiners. To avoid this, some authors have used various mathematical models to determine EMG_{Th}, comparing slopes that have been calculated using the EMG-intensity relationship (7, 16). The problem of such a determination is that the subject must perform various constant-load exercises. In contrast, one of the advantages of our mathematical method is that it can be applied during a single incremental pedaling exercise. Moreover, this mathematical method has been shown to be reproducible and reliable for EMG_{Th} determination (11, 13).

However, interference of EMG signals with movement

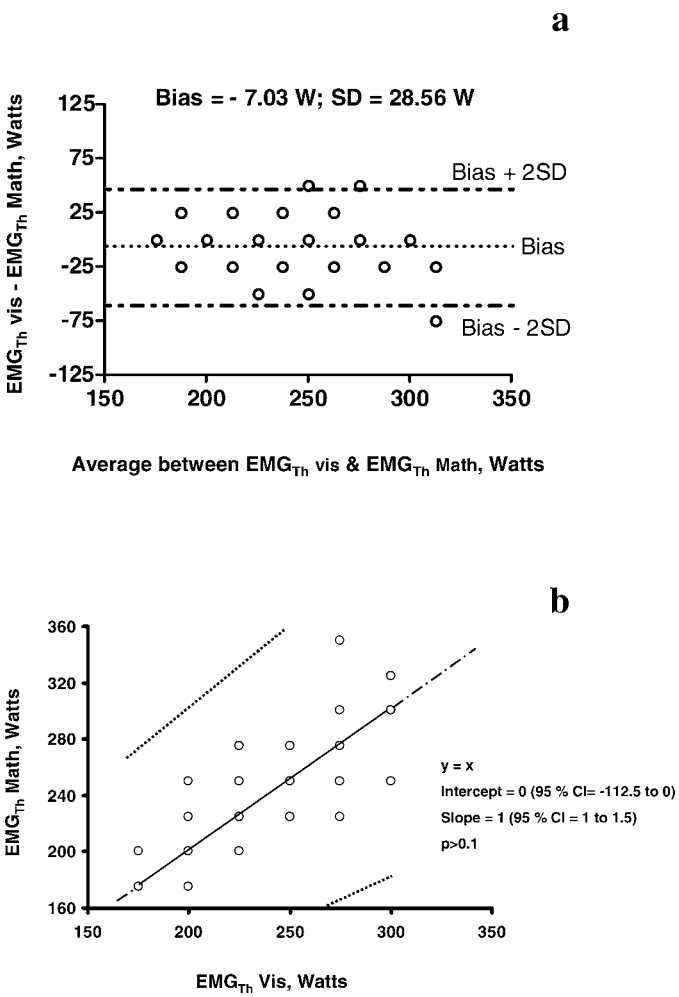

FIGURE 2. (a) Graphic analysis of the power output data (in W) corresponding to the electromyographic threshold (EMG_{Th}) as visually and mathematically detected. Data for all muscles are shown. Only the data points from the 32 EMG_{Th} that were both visually and mathematically detected are shown in this figure. Several values are identical; that is why there are only 21 visible values on the diagram. (b) Passing and Bablok regression. We found no significant deviation from linearity ($p > 0.1$).

artifacts may occur. For this reason, any completely automated method for identification of EMG_{Th} needs to recognize and reject traces in which the EMG_{Th} is confused by artifacts. Currently, no method exists with the complex pattern recognition skill required to perform this task. Until this is achieved, it is necessary to visually check each trace against the computer-derived values to ensure that the EMG_{Th} is meaningful.

PRACTICAL APPLICATIONS

To conclude, we showed that mathematical detection of EMG_{Th} is a more objective method to detect the nonlinear increase of RMS or iEMG values during an incremental exercise. The other advantages of this mathematical method are the reduced time required to perform analysis, and a lower requirement for investigator experience, because the only requirement of the investigator is to ensure that movement artifacts or other interferences do not affect EMG_{Th} detection. In this context, coaches can easily perform such measurements in order to evaluate the impact of their training programs on the neuromuscular adaptations of their athletes. For example, an automatic mathematical detection of EMG_{Th} could be performed during a pedaling exercise in order to detect neuromuscular fatigue. Furthermore, this index could be used during test or training sessions performed either in a lab or in an ecological situation. Moreover, the use of EMG_{Th} to predict VT occurrence could be an interesting tool for trainers who cannot use the very expensive devices needed to analyze respiratory gas exchanges.

Also, the results of previous studies using only visual detection of EMG_{Th} should be reconsidered.

REFERENCES

1. AIRAKSINEN, O., A. REMES, P.J. KOLARI, T. SIHVONEN, O. HANNINEN, AND I. PENTTILA. Real-time evaluation of anaerobic threshold with rms-EMG of working and nonworking muscles during incremental bicycle ergometer test. *Acupunct. Electrother. Res.* 17:259–271. 1992.
2. BIGLAND-RITCHIE, B., AND J.J. WOODS. Integrated EMG and oxygen uptake during dynamic contractions of human muscles. *J. Appl. Physiol.* 36:475–479. 1974.
3. BLAND, J., AND D. ALTMAN. Statistical methods for assessing agreement between two methods of clinical measurement. *Lancet.* 8:307–310. 1986.
4. BUNC, V., P. HOFMANN, H. LEITNER, AND G. GAISL. Verification of the heart rate threshold. *Eur. J. Appl. Physiol. Occup. Physiol.* 70:263–269. 1995.
5. CHWALBINSKA-MONETA, J., H. KACIUBA-USCILKO, H. KRYSZTOFIAK, A. ZIEMBA, K. KRZEMINSKI, B. KRUK, AND K. NAZAR. Relationship between EMG blood lactate and plasma catecholamine thresholds during graded exercise in men. *J. Physiol. Pharmacol.* 49:433–441. 1998.
6. HANON, C., C. THEPAUT-MATHIEU, C. HAUSSWIRTH, AND J. LE CHEVALLIER. Electromyogram as an indicator of neuromuscular fatigue during incremental exercise. *Eur. J. Appl. Physiol. Occup. Physiol.* 78:315–323. 1998.
7. HELAL, J. N., C. Y. GUEZENNEC, AND F. GOUBEL. The aerobic-anaerobic transition: Re-examination of the threshold concept including an electromyographic approach. *Eur. J. Appl. Physiol. Occup. Physiol.* 56:643–649. 1987.
8. HERMENS, H., B. FRERIKS, C. DISSELHORST-KLUG, AND G. RAU. Development of recommendations for SEMG sensors and sensor placement procedures. *J. Electromyogr. Kinesiol.* 10:361–374. 2000.
9. HUG, F., M. FAUCHER, N. KIPSON, AND Y. JAMMES. EMG signs of neuromuscular fatigue related to the ventilatory threshold during cycling exercise. *Clin. Physiol. Funct. Imaging* 23:208–214. 2003.
10. HUG, F., M. FAUCHER, T. MARQUESTE, C. GUILLOT, N. KIPSON, AND Y. JAMMES. Electromyographic signs of neuromuscular fatigue are concomitant with further increase in ventilation during static handgrip. *Clin. Physiol. Funct. Imaging* 24:25–32. 2004.
11. HUG, F., D. LAPLAUD, A. LUCIA, AND L. GRELOT. EMG threshold determination in eight lower limb muscles during a cycling exercise: A pilot study. *Int. J. Sports Med.* 27:456–462. 2006.
12. HUG, F., D. LAPLAUD, B. SAVIN, AND L. GRÉLOT. Occurence of electromyographic and ventilatory thresholds in professional road cyclists. *Eur. J. Appl. Physiol.* 90:643–646. 2003.
13. LUCIA, A., O. SANCHEZ, A. CARVAJAL, AND J.L. CHICHARRO. Analysis of the aerobic-anaerobic transition in elite cyclists during incremental exercise with the use of electromyography. *Br. J. Sports Med.* 33:178–185. 1999.
14. LUCIA, A., A.F. VAQUERO, M. PEREZ, O. SANCHEZ, V. SANCHEZ, M.A. GOMEZ, AND J.L. CHICHARRO. Electromyographic response to exercise in cardiac transplant patients: A new method for anaerobic threshold determination? *Chest* 111:1571–1576. 1997.

15. MORITANI, T., AND H.A. DEVRIES. Reexamination of the relationship between the surface integrated electromyogram (IEMG) and force of isometric contraction. *Am. J. Phys. Med.* 57:263–277. 1978.
16. MORITANI, T., T. TAKAISHI, AND T. MATSUMOTO. Determination of maximal power output at neuromuscular fatigue threshold. *J. Appl. Physiol.* 74:1729–1734. 1993.
17. NAGATA, A., M. MURO, T. MORITANI, AND T. YOSHIDA. Anaerobic threshold determination by blood lactate and myoelectric signals. *Jpn. J. Physiol.* 31:585–597. 1981.
18. PASSING, H., AND W. BABLOK. A new biometrical procedure for testing the equality of measurements from two different analytical methods. Application of linear regression procedures for method comparison studies in clinical chemistry, Part I. *J. Clin. Chem. Biochem.* 21:709–720. 1983.
19. SANTOS, E.L., AND A. GIANNELLA-NETO. Comparison of computerized methods for detecting the ventilatory thresholds. *Eur. J. Appl. Physiol.* 93:315–324. 2004.
20. TAYLOR, A.D., AND R. BRONKS. Electromyographic correlates of the transition from aerobic to anaerobic metabolism in treadmill running. *Eur. J. Appl. Physiol. Occup. Physiol.* 69:508–515. 1994.
21. TAYLOR, A.D., AND R. BRONKS. Reproducibility and validity of the quadriceps muscle integrated electromyogram threshold during incremental cycle ergometry. *Eur. J. Appl. Physiol. Occup. Physiol.* 70:252–257. 1995.
22. VIITASALO, J.T., P. LUHTANEN, P. RAHKILA, AND H. RUSKO. Electromyographic activity related to aerobic and anaerobic threshold in ergometer bicycling. *Acta Physiol. Scand.* 124:287–293. 1985.

Acknowledgments

This work was supported by ASO (Société du Tour de France). The authors gratefully acknowledge Dr. Will G. Hopkins (University of Otago, New Zealand) for his statistical advice during corrections of this manuscript.

Address correspondence to François Hug, PhD, francois_hug@hotmail.com.

EMG Threshold Determination in Eight Lower Limb Muscles During Cycling Exercise: A Pilot Study

F. Hug[1,2,3]
D. Laplaud[1]
A. Lucia[4]
L. Grelot[1]

Abstract

The first aim of this study was to verify the occurrence of the EMG threshold (EMG_{Th}) in each of eight lower limb muscles (vastus lateralis [VL], vatus medialis [VM], rectus femoris [RF], semimembranosus [SM], biceps femoris [BF], gastrocnemius lateralis [GL] and medialis [GM], and tibialis anterior [TA]) during incremental cycling exercise. The second aim was to investigate the test-retest reproducibility of the EMG_{Th} occurrence. Six sedentary male subjects (27 ± 1 years) performed the same incremental cycling test until exhausted, (workload increments of 25 W/min starting at 100 W) twice. During the tests, the EMG Root Mean Square (RMS) response was studied in the aforementioned muscles. The EMG_{Th} was detected mathematically from the RMS vs. workload relationship. All the subjects showed an EMG_{Th} in the VL muscle, and the response was reliable in both tests (246 ± 33 W and 254 ± 33 W for the first and second test, respectively; coefficient of variation: 9.6%, standard error of measurement: 28.9). However, few of them showed an EMG_{Th} in the other muscles, especially in RF, SM or GM. When present, the EMG_{Th} occurred at 75–80% of the peak power output obtained during the tests. Our results suggest that EMG_{Th} determination can be used as a reliable method for studying neuromuscular adjustments in the VL of untrained individuals, but not in other lower limb muscles.

Key words

Root mean square · cycle-ergometer · neuromuscular fatigue · motor unit

Introduction

Since the 1970s, surface electromyography (EMG) is widely used to quantify the level of activation of working skeletal muscles and to detect the occurrence of neuromuscular fatigue in humans. Numerous reports are available on the EMG response during exhaustive incremental exercise [1,3,11,14,16,23,24,26,31]. Some authors have described a linear relationship between the Root Mean Square (RMS) of EMG or the amplitude of integrated EMG (iEMG), on one hand, and the workload level, on the other [3,29,30]. However, several studies [1,5,16,24,26,31] have reported a non-linear increase of RMS or iEMG values after a certain workload is reached during incremental cycle-ergometer exercise. This breakpoint, the so-called "EMG threshold" (EMG_{Th}), is attributable to an increased recruitment of fast twitch motor units to maintain the required energy supply for contraction [25].

Affiliation
[1] Department of Sport Physiology, UPRES EA 3285, IFR Etienne-Jules Marey, Faculty of Sport Sciences, University of Mediterranean, Marseille, France
[2] Laboratory of Respiratory Physiopathology, UPRES EA 2397, Faculty of Medicine, University Pierre et Marie Curie, Paris, France
[3] Laboratory of Respiratory Physiopathology, UPRES EA 2201, Faculty of Medicine, IFR Jean-Roche, Marseille, France
[4] Exercise Physiology Laboratory, European University of Madrid, Madrid, Spain

Correspondence
F. Hug · UPRES EA 3285, Faculty of Sport Sciences, University of Meditarranean · 163, avenue de Luminy CC 910 · 13288 Marseille cedex 09 · France · E-mail: francois_hug@hotmail.com

Accepted after revision: April 25, 2005

Bibliography
Int J Sports Med 2006; 27: 456–462 © Georg Thieme Verlag KG · Stuttgart · New York ·
DOI 10.1055/s-2005-865787 · Published online August 30, 2005 ·
ISSN 0172-4622

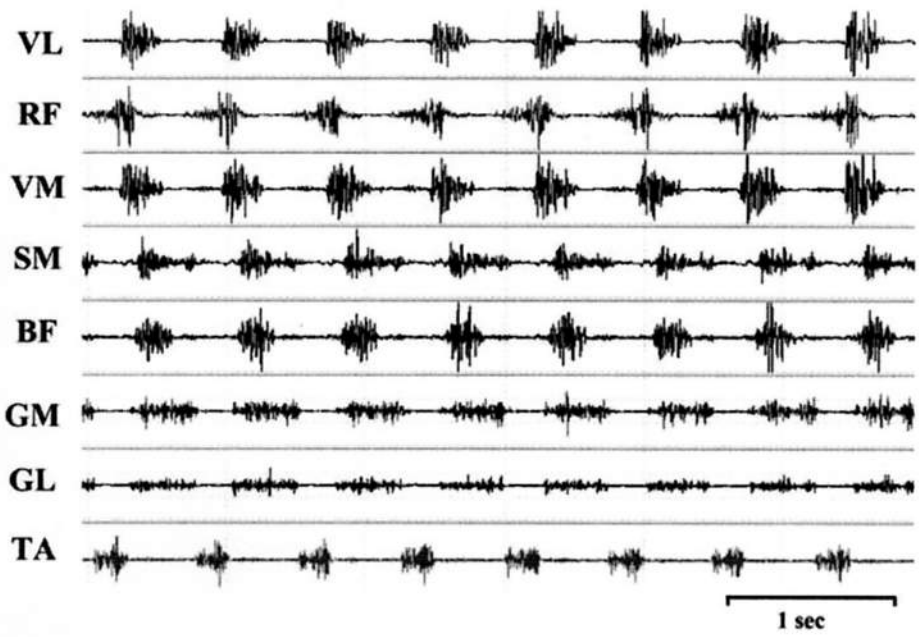

Fig. 1 Individual example of raw EMG signals recorded during the pedalling exercises.

In most cases, the EMG_{Th} has only been determined in one [14,24,26] or few lower limb muscles [1,5,31]. On the other hand, although the between-days reproducibility of EMG measurements has been reported in a single muscle [10] or in various muscles [30], these studies have not focused on the reliability of the EMG_{Th}.

The first aim of this study was to verify the occurrence of the EMG_{Th} in each of eight lower limb muscles during incremental cycling exercise. The second aim was to investigate the test-retest reproducibility of the EMG_{Th} occurrence in the aforementioned muscles.

Methods

Subjects

Six healthy males (age: 27 ± 1 years, height: 180 ± 10 cm, body mass: 78 ± 9 kg), volunteered for the study and gave informed consent. Subjects were not engaged in regular athletic activities, but they performed 3 ± 1 h of recreational activities (football, climbing, basketball, swimming, and/or rugby) per week. None of them were cyclists. The experiment was conducted in accordance with the code of ethics of the World Medical Association (Declaration of Helsinki) and approved by the local ethic committee.

Protocol

Each subject performed the same incremental cycling test, to exhaustion, on two separate occasions. These tests were performed on an electrically-braked cycle-ergometer (Excalibur sport, Lode®, Netherlands). The two tests (i.e. Test 1 and Test 2) were separated by three days during which the subjects refrained from strenuous physical activity. Each test consisted of a 3-min constant level warm up period (at 100 W), after which the power output (PO) was increased by 25 $W \cdot min^{-1}$. Subjects wore cycling shoes with clip-less pedals and maintained pedal cadence within the 75 – 85 $rev \cdot min^{-1}$ range. A cadence monitor was placed in view of the subject during each test and a designated investigator was placed in charge of monitoring the subjects in order to insure that they maintained the required pedalling cadence throughout the duration of the test. The tests were terminated upon volitional exhaustion of the subjects and/or when cadence could not be maintained at a minimum of 75 $rev \cdot min^{-1}$. At the beginning of each experiment, the height of the saddle and handlebars was adjusted to obtain a conventional cycling posture. Considering that muscle activity can be influenced by the position of the subject, as previously described [8], special care was taken to place each subject in the same position on the cycle-ergometer during the two tests.

EMG analysis

During each test, EMG activity was continuously recorded from the following eight muscles of the right lower limb: Vastus lateralis (VL), Rectus femoris (RF), Vastus medialis (VM), Semimembranosus (SM), Biceps femoris (BF), Gastrocnemius lateralis (GL) and medianus (GM) and Tibialis anterior (TA). A pair of surface electrodes (Universal Ag/AgCl electrodes, Contrôle Graphique Medical®, France) was attached to the skin with a 2 cm interelectrode distance. The electrodes were placed longitudinally with respect to the underlying muscle fibre arrangement and located according to the recommendations by SENIAM (Surface EMG for Non-Invasive Assessment of Muscles) [12]. Prior to electrode application, the skin was shaved and cleaned with alcohol in order to minimize impedance. The wires connected to the electrodes were well secured with tape to avoid movement-induced artefacts.

Raw EMG signals were pre-amplified (gain 375) close to the electrodes, band pass filtered between 8 and 500 Hz, amplified (ME3000P8 by Mega Electronics Ltd®, Finland), and analog-to-digital converted at a sampling rate of 10 kHz (Fig. 1). The Root Mean Square (RMS) was averaged every five crank revolutions (corresponding to about 3 s at 85 rpm) throughout the test.

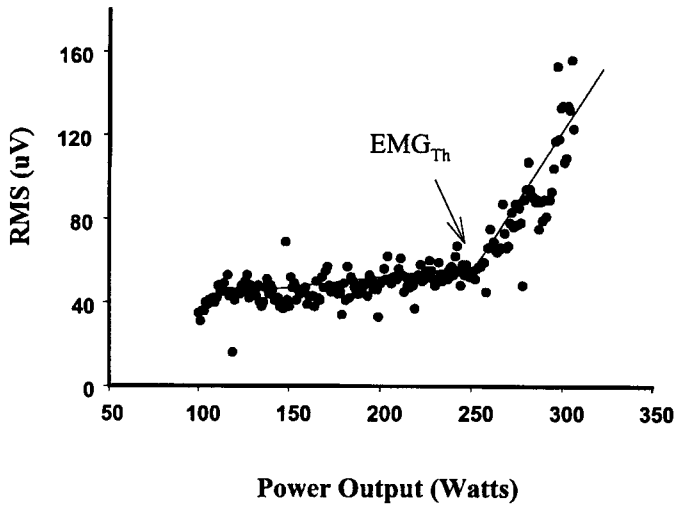

Fig. 2 Example of the mathematical determination of EMG_{Th} in one (Rectus femoris) of subjects' muscles.

Determination of EMG_{Th}

We used a computer algorithm (Centro de Datos, UCM, Madrid) that models RMS response to gradual exercise using simple linear regression [24]. With this method, a single linear regression is fitted to all data points. The program calculates regression lines for all possible divisions of the data into two contiguous groups, and the pair of lines yielding the least pooled residual sum of squares is chosen as representing the best fit. Fig. **2** shows an example of the aforementioned mathematical determination of EMG_{Th} in one of subjects' muscles.

Statistical analysis

All statistics were performed using the statistical package SPSS for windows (version 10.1). Results were expressed as mean ± Standard Deviation (SD). For all statistical comparisons outlined below, the level of significance was set at 0.05. Possible differences in EMG_{Th} values between repeated tests were assessed with a Wilcoxon's test. The same test was used to compare the peak power output (PPO) and mean pedalling cadence in Tests 1 and 2.

We determined the standard error of measurement (SEM, defined as the square root of mean square error within trials) and coefficient of variation (CV, i.e. standard deviation/mean, in %) for the EMG_{Th} values obtained in Tests 1 and 2.

Further analysis of EMG_{Th} reliability was accomplished by applying the procedures suggested by Bland and Altman [4]. For this analysis, the mean difference (bias) and SD of the differences between the mean values of EMG_{Th} (in W), obtained in Test 1 and Test 2, were calculated. The data were shown graphically comparing the difference between the two tests against their average value in W. The mean difference (bias) was indicated in the graphs (Figs. **4** and **5**).

Results

There was no significant difference between Test 1 and Test 2 in the PPO reached by the subjects (300 ± 32 W vs. 300 ± 32 W, respectively) or in their mean pedalling rate (80 ± 4 rpm vs. 82 ± 3 rpm, respectively).

The EMG_{Th} did not occur in all the subjects' muscles and tests. When present, the EMG_{Th} corresponded on average to 77 ± 14% and 79 ± 8% of the PPO attained in Tests 1 and 2, respectively. For each muscle and test, the percentage of subjects showing an EMG_{Th} is shown in Table **1**. The only muscle in which we found the EMG_{Th} to occur in 100% of the subjects (in both tests) was the VL muscle. Furthermore, the response of this muscle was reliable between trials (Table **1**). The EMG_{Th} of the VL muscle is depicted for each subject and each test in Fig. **3**.

Table 1 Comparison of the EMG threshold (EMG_{Th}) between Test 1 and Test 2

	Number of subjects showing EMG_{Th}		*EMG_{Th} in Test 1 (W)*	*EMG_{Th} in Test 2 (W)*	*n*	*p*	*CV (%)*	*SEM*
	Test 1	*Test 2*						
VL	6 (100%)	6 (100%)	246 ± 33	254 ± 33	6	NS	9.6	28.9
RF	2 (33%)	4 (66%)	237 ± 53	250 ± 35	2			
VM	5 (83%)	5 (83%)	237 ± 43	231 ± 42	4	NS	5.8	8.8
SM	3 (50%)	2 (33%)	233 ± 52	275 ± 0	1			
BF	3 (50%)	5 (83%)	242 ± 63	258 ± 52	3	NS	5.4	14.4
GL	5 (83%)	4 (66%)	231 ± 55	237 ± 32	4	NS	11.9	8.8
GM	3 (50%)	2 (33%)	275 ± 52	275 ± 70	1			
TA	5 (83%)	4 (66%)	244 ± 66	244 ± 43	4	NS	7.6	25.0
Mean ± SD for all muscles			243 ± 14	253 ± 16				
CV (%) for all muscles			5.8	6.3				

Data are shown as mean ± SD. VL, vastus lateralis; RF, rectus femoris; VM, vastus medialis; SM, Semimembranosus; BF, Biceps femoris; GL, Gastrocnemius lateralis; GM, Gastrocnemius medianus; TA, Tibialis anterior; n, number of subjects showing an EMG_{Th} in both tests; NS, no significant difference; CV, coefficient of variation; SEM, square root of mean square error within trials

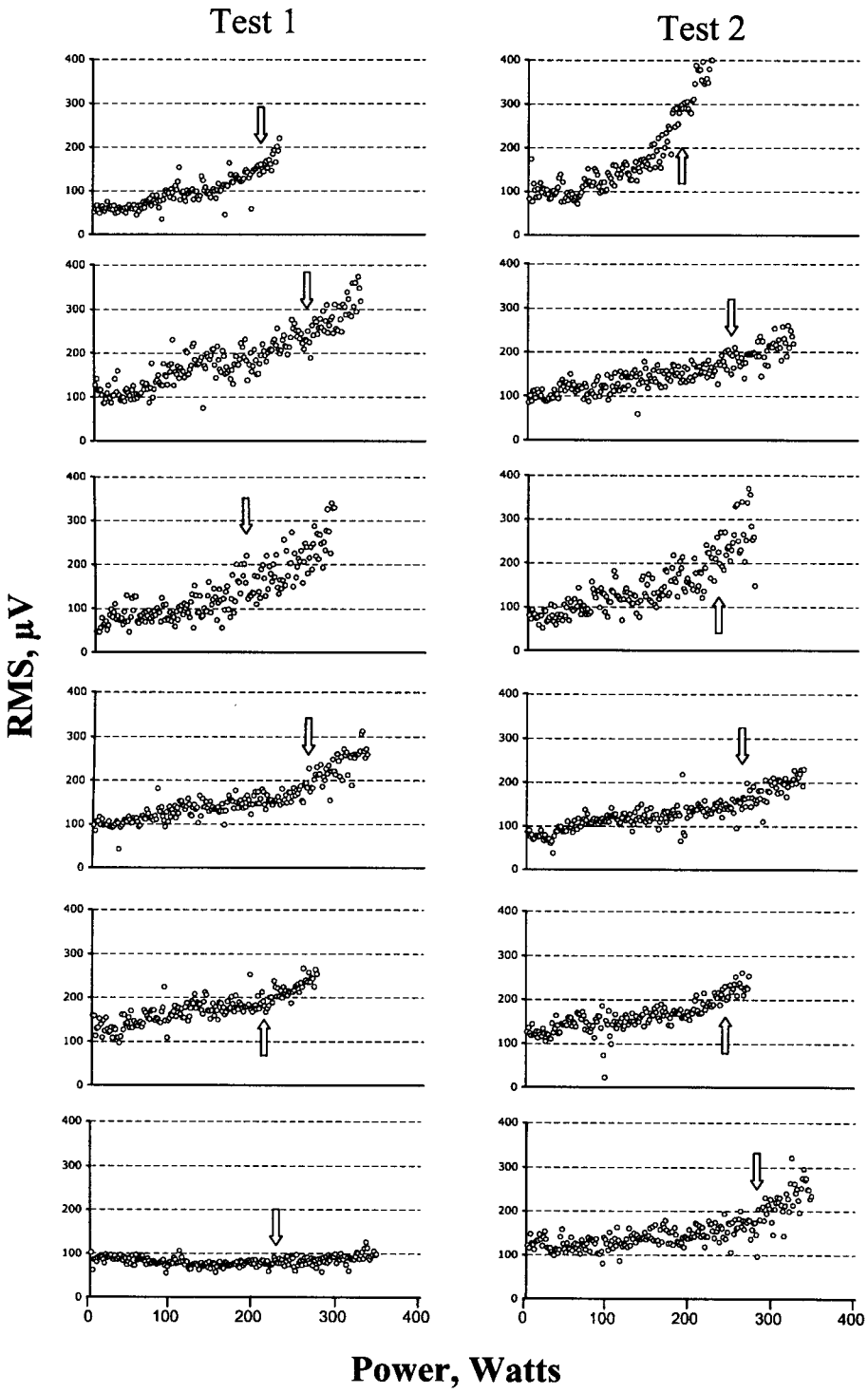

Fig. 3 Vastus lateralis EMG_{Th} of each subject is depicted for test 1 and test 2.

All the muscles taken together, the workload at which the EMG_{Th} occurred did not differ between the two tests (Table 1). For each muscle, we applied the Bland and Altman procedure when we found the EMG_{Th} to occur in both tests for at least 3 subjects (Fig. 4). For all the muscles and subjects, we applied the Bland and Altman procedure when we found the EMG_{Th} to occur in both tests (i.e. 25 values) (Fig. 5).

Discussion

This is the first report to compare, in untrained subjects, the EMG_{Th} occurrence in eight lower limb muscles during incremental cycling exercise. All the subjects showed an EMG_{Th} in the vastus lateralis muscle, and this response was reliable, whereas few of them showed an EMG_{Th} in the RF, SM and GM muscles.

Although surface EMG technique can serve as a useful tool in assessing muscles activation, this method is not without limitations. First, cross talk from adjacent muscles may influence EMG signals. To minimize this phenomenon, we used small bipo-

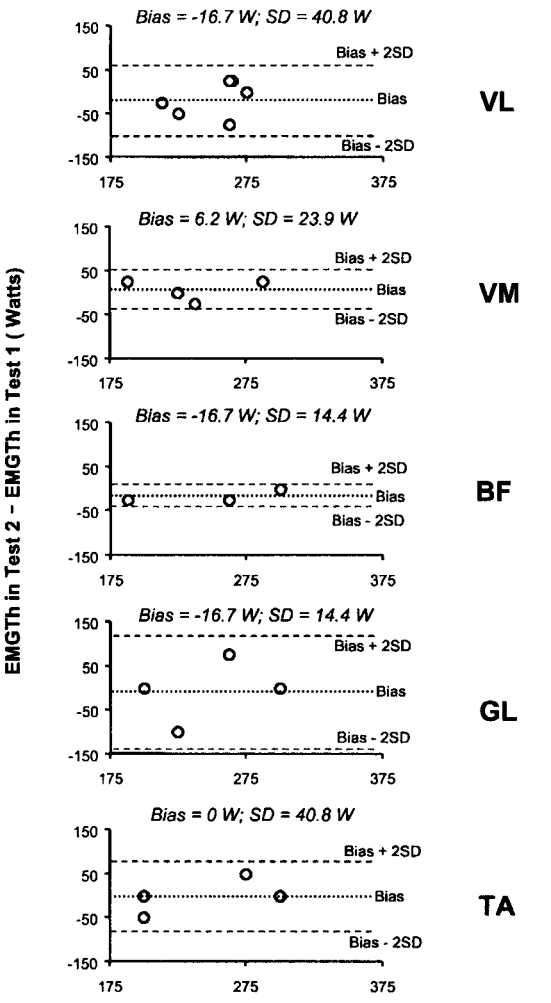

Fig. 4 For each muscle, a graphic analysis of the power output (Watts) data corresponding to the EMG_{Th}, determined during test 1 and 2, is depicted. Because of the few number of subjects showing an EMG_{Th} in RF, SM and GM, only the 5 other muscles are depicted.

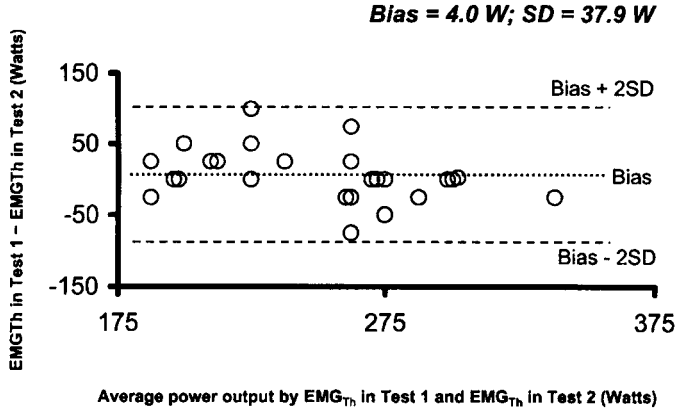

Fig. 5 Graphic analysis of the power output (Watts) data corresponding to the EMG_{Th} determined during test 1 and 2. Data for all muscles are shown. Only the data points from the 25 subjects exhibiting an EMG_{Th} in both Tests 1 and 2 are shown in this figure.

lar electrodes, and special care was taken for the electrode placement. Before each test, the contribution of the eight muscles to the signals recorded by the corresponding electrodes was ascertained by the presence of bursts of EMG activity during tonic contractions. Second, EMG signals can be influenced by movement artefacts. We minimized these influences by using a preamplifier placed near the electrodes for each muscle, and securing the electrode wires well with tape.

On average, the EMG_{Th} of all the muscles was 75 – 80% of the subject's PPO for Tests 1 and Test 2. As this exercise intensity is close to the power output value at which both ventilatory equivalents for oxygen ($VE \cdot \dot{V}O_2^{-1}$) and carbon dioxide ($VE \cdot \dot{V}CO_2^{-1}$) exhibited a systematic increase (i.e. the second ventilatory threshold [VT_2]) in sedentary individuals, our results are in agreement with previous studies which showed the EMG_{Th} to occur near VT_2 [1,11,26]. However, other studies reported a correlation between EMG_{Th} and the power output value at which $VE \cdot \dot{V}O_2^{-1}$ exhibited a systematic increase without a concomitant increase in $VE \cdot \dot{V}CO_2^{-1}$ (i.e. first ventilatory threshold [VT_1]) [14,24,31]. These discrepancies can be due to differences in experimental protocols (pedalling cadence, rate of workload increments, method of EMG_{Th} and VT_1/VT_2 determination [visual or mathematical, etc.]) or in the training status of the subjects (i.e. trained, untrained or diseased subjects). For example, Viitasalo and co-workers [31] used only three workload levels to show the EMG_{Th} occurrence at VT_1 and Lucia and co-workers [24] found that the EMG_{Th} occurred at the VT_1 in cardiac transplant patients.

Simple visual inspection has been shown to be valid for VT_1/VT_2 detection [28]. However, EMG_{Th} is not so commonly used and measured in exercise physiology laboratories as the aforementioned ventilatory thresholds, and to date, no previous study has shown the accuracy and/or reliability of EMG_{Th} visual detection. For this reason, we chose to use a mathematical model as an objective method to detect the EMG_{Th}.

The physiological mechanism behind an abrupt increase in EMG activity above certain exercise intensity (75 – 80% of PPO) is not fully understood. The non-linear increase of RMS can be due to several factors, such as 1) an increase in M-Wave duration, 2) a central motor drive regulation and/or 3) disruptions of excitation-contraction coupling. A lengthening of M-wave duration may partly cause an increase in RMS, independent of any central activation failure [17,18]. In the present study, we did not record M-Wave because it was very difficult to obtain a measurement for the eight muscles simultaneously. However, some studies showed M-Wave alterations to occur only during prolonged exercise (> 2 h) [19,20], as opposed to short-duration exercise [21]. In this line, considering that the mean duration of our progressive exercise test was of only ~ 11 min, we could hypothesize that no M-Wave alteration occurred in our subjects and that the abrupt increase of RMS was most likely due to another mechanism.

Previous studies [1,16,23] showed that EMG_{Th} occurred simultaneously in muscles that are clearly different both in terms of fibre type distribution and in their implication during the pedalling task. Another investigation demonstrated, during a sustained static contraction of the Flexor digitorum, that a concomitant EMG_{Th} and VT_1 persist during complete arterial blood flow interruption [15]. Because these responses persisted in the absence of any blood release of metabolites, neurogenic factors seem to be responsible for both EMG and ventilatory thresholds.

Thus, all these results suggest a central motor drive regulation. The activation of group III and IV muscle afferents, during fatiguing contraction, is suspected to play a key role in adjusting the motor drive to working muscles through a reflex control of the recruitment of motor neurons [2,22]. These muscle afferents detect changes in intramuscular acidosis and potassium outflow from working muscles fibres [6] and are activated after a sufficient accumulation of metabolites has occurred in a fatiguing muscle [7]. In other words, the amount of intramuscular accumulation of metabolites and/or acidosis, that occurs in those muscles more involved in an exercise task, could play a key role in the changes of central motor drive for all the other muscles. In our study, the EMG_{Th} seemed to occur at the same workload level in the eight muscles studied (i.e. very low CV for all muscles taken together in both tests). However, no subject showed an EMG_{Th} in all the recorded muscles, which suggests that other mechanisms could be in the origin of the threshold occurrence.

As workload increases, the accumulation of hydrogen ions, oxygen reactive species and potassium has been shown to impair excitation-contraction coupling [32]. In this case, it is necessary to recruit additional motor units in order to compensate for the deficit in contractility. This phenomenon can explain an abrupt increase in EMG activity. As shown in Table **1**, an EMG_{Th} was determined in 100% of the subjects in the VL muscle. This result confirms previous EMG [27], biopsy [9] and Magnetic Resonance Imaging (MRI) studies [13] showing that this muscle is highly involved during leg pedalling exercise. In contrast, EMG_{Th} was not detectable in the majority of the subjects in GM, SM and RF, all of which are less implicated in the cycling task [8]. These results confirm the local hypothesis of EMG_{Th} occurrence, i.e. accumulation of metabolites in the most active muscles induces additional motor unit recruitment in these same muscles, but less in other muscles.

However, we found inter-individual differences in the muscles showing an EMG_{Th}, which suggests some heterogeneity in the muscle recruitment strategies of our subjects. This result is in accordance with previous work from our laboratory using EMG and MRI, which showed considerable heterogeneity in the muscle recruitment patterns of a homogeneous population of professional road cyclists [13].

Conclusion

In all the subjects, EMG activity of the VL muscle showed a non-linear increase which occurred at about 75 – 80% of PPO. The results of this study suggest that EMG_{Th} determination can be used as a reliable method for studying neuromuscular fatigue during cycling exercise in this specific muscle, but not in other leg muscles. Because this pilot study was conducted in only 6 subjects, and does not report metabolic measurements, more research is necessary to clearly elucidate the mechanism(s) behind the EMG_{Th} and the reasons that explain its occurrence (or lack of occurrence) in different muscles.

Acknowledgements

The authors gratefully acknowledge Dr. Will G Hopkins (University of Otago, New Zealand) for his statistical advice during the correction of this manuscript.

References

[1] Airaksinen O, Remes A, Kolari PJ, Sihvonen T, Hanninen O, Penttila I. Real-time evaluation of anaerobic threshold with rms-EMG of working and nonworking muscles during incremental bicycle ergometer test. Acupunct Electrother Res 1992; 17: 259 – 271
[2] Bigland-Ritchie B, Johansson R, Lippold OC, Smith S, Woods JJ. Changes in motoneurone firing rates during sustained maximal voluntary contractions. J Physiol 1983; 340: 335 – 346
[3] Bigland-Ritchie B, Woods JJ. Integrated EMG and oxygen uptake during dynamic contractions of human muscles. J Appl Physiol 1974; 36: 475 – 479
[4] Bland J, Altman D. Statistical methods for assessing agreement between two methods of clinical measurement. Lancet 1986; 8: 307 – 310
[5] Chwalbinska-Moneta J, Kaciuba-Uscilko H, Krysztofiak H, Ziemba A, Krzeminski K, Kruk B, Nazar K. Relationship between EMG blood lactate, and plasma catecholamine thresholds during graded exercise in men. J Physiol Pharmacol 1998; 49: 433 – 441
[6] Darques JL, Decherchi P, Jammes Y. Mechanisms of fatigue-induced activation of group IV muscle afferents: the roles played by lactic acid and inflammatory mediators. Neurosci Lett 1998; 257: 109 – 112
[7] Darques JL, Jammes Y. Fatigue-induced changes in group IV muscle afferent activity: differences between high- and low-frequency electrically induced fatigues. Brain Res 1997; 750: 147 – 154
[8] Ericson M. On the biomechanics of cycling. A study of joint and muscle load during exercise on the bicycle ergometer. Scan J Rehabil Med 1986; 16: 165 – 172
[9] Essen B. Intramuscular substrate utilization during prolonged exercise. Ann NY Acad Sci 1977; 301: 30 – 44
[10] Gamet D, Duchene J, Garapon-Bar C, Goubel F. Surface electromyogram power spectrum in human quadriceps muscle during incremental exercise. J Appl Physiol 1993; 74: 2704 – 2710
[11] Hanon C, Thepaut-Mathieu C, Hausswirth C, Le Chevallier J. Electromyogram as an indicator of neuromuscular fatigue during incremental exercise. Eur J Appl Physiol 1998; 78: 315 – 323
[12] Hermens H, Freriks B, Disselhorst-Klug C, Rau G. Development of recommendations for sEMG sensors and sensor placement procedures. J Electromyogr Kinesiol 2000; 10: 361 – 374
[13] Hug F, Bendahan D, Le Fur Y, Cozzone PJ, Grélot L. Heterogeneity of muscle recruitment pattern during pedalling in professional road cyclists: a magnetic resonance imaging and electromyography study. Eur J Appl Physiol 2004; 92: 334 – 342
[14] Hug F, Faucher M, Kipson N, Jammes Y. EMG signs of neuromuscular fatigue related to the ventilatory threshold during cycling exercise. Clin Physiol Funct Imaging 2003; 23: 208 – 214
[15] Hug F, Faucher M, Marqueste T, Guillot C, Kipson N, Jammes Y. Electromyographic signs of neuromuscular fatigue are concomitant with further increase in ventilation during static handgrip. Clin Physiol Funct Imaging 2004; 24: 25 – 32
[16] Hug F, Laplaud D, Savin B, Grélot L. Occurrence of electromyographic and ventilatory thresholds in professional road cyclists. Eur J Appl Physiol 2003; 90: 643 – 646
[17] Kadefors R, Kaiser E, Petersen I. Dynamic spectrum analysis of myopotentials and with special reference to muscle fatigue. Electromyography 1968; 8: 39 – 74
[18] Kranz H, William A, Cassel J, Caddy S, Silberstein R. Factors determining the frequency content of the electromyogram. J Appl Physiol 1983; 55: 392 – 399
[19] Lepers R, Hausswirth C, Maffiuletti N, Brisswalter J, van Hoecke J. Evidence of neuromuscular fatigue after prolonged cycling exercise. Med Sci Sports Exerc 2000; 32: 1880 – 1886
[20] Lepers R, Maffiuletti N, Rochette L, Brugniaux J, Millet G. Neuromuscular fatigue during a long-duration cycling exercise. J Appl Physiol 2002; 92: 1487 – 1493

[21] Lepers R, Millet GY, Maffiuletti NA. Effect of cycling cadence on contractile and neural properties of knee extensors. Med Sci Sports Exerc 2001; 33: 1882 – 1888
[22] Lindstrom L, Magnusson R, Petersen I. Muscular fatigue and action potential conduction velocity changes studied with frequency analysis of EMG signals. Electromyography 1970; 10: 341 – 356
[23] Lucia A, Sanchez O, Carvajal A, Chicharro JL. Analysis of the aerobic-anaerobic transition in elite cyclists during incremental exercise with the use of electromyography. Br J Sports Med 1999; 33: 178 – 85
[24] Lucia A, Vaquero AF, Perez M, Sanchez O, Sanchez V, Gomez MA, Chicharro JL. Electromyographic response to exercise in cardiac transplant patients: a new method for anaerobic threshold determination? Chest 1997; 111: 1571 – 1576
[25] Moritani T, Tanaka H, Yoshida T, Ishii C, Shindo M. Relationship between myoelectric signals and blood lactate during incremental forearm exercise. Am J Phys Med 1984; 63: 122 – 132
[26] Nagata A, Muro M, Moritani T, Yoshida T. Anaerobic threshold determination by blood lactate and myoelectric signals. Jpn J Physiol 1981; 31: 585 – 597
[27] Nilsson J, Tesch P, Thorstensson A. Fatigue and EMG of repeated fast voluntary contractions in man. Acta Physiol Scand 1977; 101: 194 – 198
[28] Santos EL, Giannella-Neto A. Comparison of computerized methods for detecting the ventilatory thresholds. Eur J Appl Physiol 2004; 93: 315 – 324
[29] Taylor AD, Bronks R. Electromyographic correlates of the transition from aerobic to anaerobic metabolism in treadmill running. Eur J Appl Physiol 1994; 69: 508 – 515
[30] Taylor AD, Bronks R. Reproducibility and validity of the quadriceps muscle integrated electromyogram threshold during incremental cycle ergometry. Eur J Appl Physiol 1995; 70: 252 – 257
[31] Viitasalo JT, Luhtanen P, Rahkila P, Rusko H. Electromyographic activity related to aerobic and anaerobic threshold in ergometer bicycling. Acta Physiol Scand 1985; 124: 287 – 293
[32] Wolosker H, de Meis L. pH-dependent inhibitory effects of Ca2 +, Mg2 +, and K+ on Ca2 + efflux mediated by sarcoplasmic reticulum ATPase. Am J Physiol 1994; 266: 1376 – 1381

Eur J Appl Physiol (2009) 107:193–201
DOI 10.1007/s00421-009-1114-6

ORIGINAL ARTICLE

Can the electromyographic fatigue threshold be determined from superficial elbow flexor muscles during an isometric single-joint task?

François Hug · Antoine Nordez · Arnaud Guével

Accepted: 8 June 2009 / Published online: 24 June 2009

Abstract The purpose of this study was to compare the electromyographic fatigue threshold (EMG_{FT}) values determined simultaneously from superficial elbow flexor muscles during an isometric single-joint task. Eight subjects performed isometric elbow flexions at randomly ordered percentages of maximal voluntary contraction (20, 30, 40, 50 and 60%). During these bouts, electromyographic (EMG) activity was measured in the anterior head of *Deltoïd*, lateral head of *Triceps brachii*, *Brachioradialis* and both short and long head of *Biceps brachii*. For each subject and each muscle, the EMG amplitude data were plotted as function of time for the five submaximal bouts. The slope coefficient of the EMG amplitude versus time linear relationships were plotted against force level. EMG_{FT} was determined as the *y*-intercept of this relationship and considered as valid only if the following criteria were met: (1) significant positive linear regression ($P < 0.05$) between force and slope coefficient, (2) an adjusted coefficient of determination for force versus slope coefficient relationship greater than 0.85, and (3) a standard error for the EMG_{FT} below 5% of maximal voluntary contraction. The EMG_{FT} could only be determined for one muscle (the long head of *Biceps brachii*) and only in three out of the eight subjects (mean value = 24.9 ± 1.1% of maximal voluntary contraction). The lack of EMG_{FT} in most of the subjects (5/8) could be explained by putative compensations between elbow muscles which were indirectly observed in some subjects. In this way, EMG_{FT} should be studied from a more simple movement i.e., ideally a movement implying mainly one muscle.

Keywords Biceps brachii · Deltoïd · Brachioradialis · Isometric · Root mean square · Accuracy

F. Hug (✉) · A. Nordez · A. Guével
Laboratory «Motricité, Interactions, Performance» (EA 4334), University of Nantes, 25 bis boulevard Guy Mollet, BP 72206, 44322 Nantes Cedex 3, France
e-mail: francois.hug@univ-nantes.fr

Introduction

Muscle fatigue can be defined as "any exercise-induced reduction in the ability to exert muscle force or power, regardless or whether or not the task can be sustained" (Bigland-Ritchie and Woods 1984). The evolution may be fast or slow, depending on the effort performed, and will lead sooner or later to mechanically detectable changes of performance. In this way, prolonged submaximal isometric contraction at constant force level induces a progressive increase in surface electromyographic (EMG) amplitude (Edwards and Lippold 1956; DeVries 1968). While some non-physiological factors contribute to this increase in EMG amplitude [for review, see (Farina et al. 2004)], it can be mainly explained by an enhancement of the central drive as a result of an increase in the number of active motor units and/or a modulation of the discharge rate to compensate for the decrease in the force of contraction that occurs in fatigued muscle fibers (Garland et al. 1994; Garland et al. 1997; Hunter et al. 2003). DeVries (1968) reported a linear relationship between EMG amplitude and time during fatiguing exercises. The slope coefficient of this linear relationship is proportional to the force level. Based on these findings, deVries et al. (1982) proposed a cycle ergometer test to determine the fatigue threshold in quadriceps femoris muscle group. The protocol consisted to determine the rate of rise in integrated EMG amplitude (i.e., integrated EMG slope) as a function of time for pedaling

bouts performed at three or four different power outputs. The integrated EMG slopes obtained were plotted against power output resulting in linear plots which were extrapolated to a zero slope to give an intercept on the power axis. This *y*-intercept, named the EMG fatigue threshold (EMG_{FT}), was defined as the highest power output that can be maintained without an increase in EMG activity level over time (i.e., iEMG slope = 0). The EMG_{FT} has been widely studied using pedaling tests (Matsumoto et al. 1991; Moritani et al. 1993; Pavlat et al. 1993; Pringle and Jones 2002; Graef et al. 2008; Smith et al. 2009) and has been shown to be an interesting tool to assess the fitness level/muscle performance (deVries et al. 1982; Matsumoto et al. 1991; Moritani et al. 1993; Graef et al. 2008; Smith et al. 2009). This method has the advantage that it does not require submaximal exercise bouts to be performed until exhaustion. For this reason, it would be very useful for patients who are not able to tolerate maximal effort, which is known to depress the immune system and to be deleterious in muscle diseases such as myopathy.

In most of these studies, EMG_{FT} was determined from the *Vastus lateralis* muscle (deVries et al. 1982; Matsumoto et al. 1991; Moritani et al. 1993; Graef et al. 2008; Smith et al. 2009) assuming that this muscle is representative of all the muscles implied in pedaling. However, pedaling is a bilateral multi-joint task requiring the usage of numerous muscles [for review, (Hug and Dorel 2009)] and thus, the EMG fatigue characteristics of other muscles could result in different EMG_{FT} values, as demonstrated by Housh et al. (1995). In this way, the high inter-individual variability of EMG patterns reported during pedaling (Hug et al. 2008) could explain the fact that some studies failed to report EMG_{FT} in some subjects (Pringle and Jones 2002). In addition, since pedaling is a dynamic exercise, the intensity (power output) is difficult to control because both mechanical loads (i.e., resistance imposed by the cyclo-ergometer) and movement velocity (i.e., pedaling rate) must be standardized. Taken together, these information suggest that a more simple (single-joint) and standardized task would permit more accurate EMG_{FT} determination. Surprisingly, there are only three recent studies that have determined the EMG_{FT} from an isometric single-joint task (Cardozo and Goncalves 2003; Dias da Silva and Goncalves 2006; Hendrix et al. 2009). Hendrix et al. (2009) compared the EMG_{FT} and critical force (i.e., the isometric force threshold above which fatigue will occur during a sustained muscle action) for isometric actions of the elbow flexors but, as discussed by the authors, their conclusions were limited by the fact that EMG_{FT} was determined only from *Biceps brachii*. In fact, the generation of elbow torque results from the contribution of all of the muscles surrounding this joint. The moment arms (Murray et al. 1995), cross sectional areas and muscle typologies (Johnson et al. 1973) are different among the muscles. This fact alone would imply different muscles' contribution to the total torque (Murray et al. 1995) and thus possible different EMG_{FT}.

Therefore, the purpose of this study was to compare the EMG_{FT} values determined simultaneously from superficial elbow flexor muscles (*Biceps brachii* long head, *Biceps brachii* short head and *Brachoradialis*) during an isometric single-joint task (i.e., elbow flexion). It was hypothesized that EMG_{FT} would be different for each of these superficial flexor muscles.

Methods

Subjects

Eight healthy subjects volunteered to participate in this study (2 women, 6 men; aged 27.0 ± 9.5 years; height 172.0 ± 6.5 cm; weight 64.8 ± 11.0 kg). They were informed of the possible risk and discomfort associated with the experimental procedures before they gave written consent. The experimental design of the study was approved by the local Ethical Committee and was done in accordance with the Declaration of Helsinki.

Measurements

Ergometer

A home made ergometer was used to measure the force produced by the elbow flexors (Fig. 1a). Subjects were seated upright in an adjustable chair with their dominant arm shoulder joint flexed in the sagittal plane so that the upper arm was horizontal and the forearm was vertical and mid-pronated (90° between arm and forearm). The force exerted at the wrist level was measured with a force sensor (ZF200 kg, sensibility: 3 mV/V, Scaime, Annemasse, France), in the sagittal plane. The force signal was sampled at 1 kHz and stored in a computer.

Electromyography

Rudroff et al. (2008) showed that surface EMG measurements provide a more appropriate measure of the change in muscle activity during a fatiguing contraction than intramuscular recordings. In fact, intramuscular recordings, even measured with wire electrodes, sample a limited number of motor units and thus, the signal is not necessarily representative of the global muscle activity, especially for the lowest levels of muscle activity (Chiti et al. 2008). For this reason only the surface EMG activity of superficial elbow flexor muscles was recorded in the

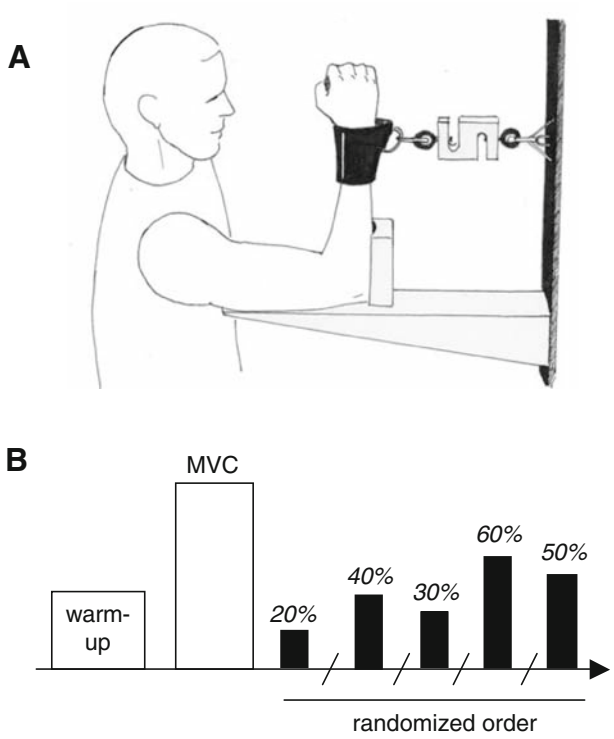

Fig. 1 Experimental setup (**a**) and protocol (**b**). **a** Subjects were seated upright in an adjustable chair with dominant arm shoulder joint flexed in the sagittal plane so that the upper arm was horizontal and the forearm was vertical and mid-pronated (90° between arm and forearm). **b** After a 10 min standardized warm-up, each subject performed three 3 s isometric maximal voluntary contractions (MVC) with the elbow flexors, shoulder flexors and elbow extensors. Following this session, each subject rested 5 min, then performed isometric elbox flexions at randomly ordered percentages of MVC (20, 30, 40, 50 and 60%). Each bout lasted 30 s and was separated by a 10 min recovery period

present study. Since the *Brachialis* lies below the *Biceps brachii*, it is not accessible by surface EMG and was not therefore recorded. Bipolar surface electromyographic (EMG) activity was measured with dry-surface electrodes (Delsys DE 2.1, Delsys Inc, Boston, USA; 1 cm inter-electrode distance) that were placed over the short and long head of *Biceps brachii*, and *Brachioradialis*. Co-activation was also assessed by measuring the EMG activity of the lateral head of *Triceps brachii*. Possible compensation with shoulder flexors was investigated by recording the EMG activity of the anterior head of the *Deltoïd* muscle. The electrodes were placed longitudinally with respect to the underlying muscle fibre arrangement, distal to the motor point. A reference electrode was placed at the level of manubrium sternum. Prior to electrode placement, the skin was shaved and cleaned with alcohol in order to minimize impedance. EMG signals were amplified (×1,000) and digitized (bandwidth of 6–400 Hz) at a sampling rate of 1 kHz (Bagnoli 16, Delsys Inc, Boston, USA), and stored on a computer.

Protocol

After a 10 min standardized warm-up (5 min of rowing at 100 W following by 3 series of 10 dynamic elbow flexions at 4, 6 and 8 kg, 1 min of recovery between each series), each subject performed three 3 s isometric maximal voluntary contractions (MVC) using their elbow flexor muscles. The subjects rested 2 min between trials. The greatest force achieved over a 500 ms interval was taken as the MVC force and used as the reference to normalize the target force for the subsequent submaximal bouts aimed at determining EMG_{FT}. The maximal EMG (RMS_{max}) of the elbow flexor muscles was determined as the maximal average root mean square (RMS) value over a 500 ms interval. Three maximal isometric shoulder flexions with the forearm pronated and three maximal isometric elbow extensions were performed in order to determine the RMS_{max} for the anterior head of *Deltoïd* and lateral head of *Triceps brachii*. Following this session, each subject rested 5 min, then performed isometric elbow flexions at randomly ordered percentages of MVC (i.e., 20, 30, 40, 50 and 60%) (Fig. 1b). Each bout lasted 30 s and was separated by a 10 min recovery period. This exercise duration was chosen to avoid the accumulation of muscle fatigue to a minimal extent and to be sure that all the subjects are able to maintain the require load during all this period (especially for the bouts performed at 50 and 60% of MVC). During each bout, a visual feedback of the force signal has been displayed on a monitor placed in front of the subjects.

EMG_{FT} determination

The data processing was performed using standardized Matlab® scripts (The Mathworks, Natick, USA). For each bout, the interference EMG data obtained for all muscles were root mean squared with a time averaging period of 1.33 s (corresponding to 20 RMS values for each bout) to quantify the activity level. EMG_{FT} was then determined only in *Brachioradialis* and both heads of *Biceps brachii*. As shown in Fig. 2, the rate of rise in RMS as a function of time (slope coefficient of the linear regression) was calculated for each of the five bouts and for each subject. When the slope coefficient was negative (three cases out of 40 for the long head of *Biceps brachii*, 15 cases out of 40 for the short head of *Biceps brachii* and 18 cases out of 40 for the *Brachioradialis*), the bout was not taken into consideration for EMG_{FT} determination. The force levels were then plotted as a function of slope coefficients for the RMS vs. time relationship. The EMG_{FT} was defined as the *y*-intercept of the relationship between force level and slope coefficient (deVries et al. 1982) (Fig. 2). The significance of the linear regression, the adjusted coefficient of determination (R^2) and the standard error for *y*-intercept were then calculated (Origin 8, OriginLab

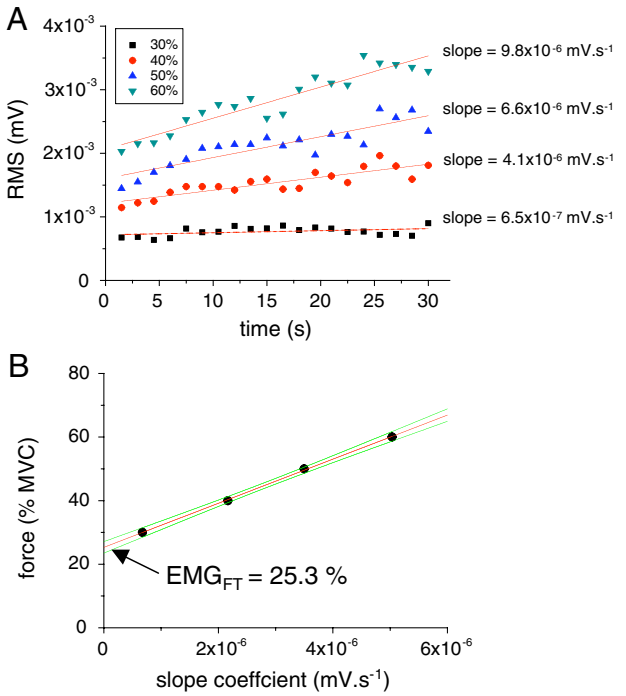

Fig. 2 Method for determining the EMG fatigue threshold (EMG_{FT}). **a** The EMG amplitude (RMS) data are plotted as function of time for the five submaximal bouts (20, 30, 40, 50 and 60% of maximal voluntary contraction (MVC)). **b** The slope coefficients of the RMS versus time relationship obtained are plotted against force level (% of MVC). The EMG_{FT} is determined as the *y*-intercept of this relationship (DeVries et al. 1982). The regression line and its 95% confidence interval are depicted. Note that this individual example corresponds to subject #1. The bout performed at 20% of MVC was not taken into consideration because the slope coefficient was negative (see "Methods" section for more details)

corporation, USA). We chose to report adjusted R^2 because it is a more accurate goodness-of-fit measurement than the R^2 when dealing with small samples. Note that EMG_{FT} was only determined if the following criteria were met: (1) significant positive linear regression ($P < 0.05$) between force and slope coefficient, (2) an adjusted coefficient of determination (R^2) for force versus slope coefficient relationship greater than 0.85, and (3) a standard error for the *y*-intercept (i.e., EMG_{FT}) below 5% of MVC.

Results

Table 1 includes data for each subject, each bout and each elbow flexor muscle. No significant linear relationship was found between force level and slope coefficient in *Brachioradialis* and the short head of *Biceps brachii*. Thus, no EMG_{FT} was determined from these two muscles. EMG_{FT} was determined with a good precision (standard error ranged from 0.42 to 4.6%) in three out of the eight subjects for the long head of *Biceps brachii* (mean value ± SD: 24.9 ± 1.1% of MVC) (Fig. 3). Co-activation of lateral head of *Triceps brachii* was low for all of the exercise bouts (1.9 ± 1.7, 3.4 ± 2.9, 4.2 ± 3.2, 5.3 ± 4.2 and 6.2 ± 4.7% of RMS_{max} for 20, 30, 40, 50 and 60% of MVC, respectively) and no change in EMG activity in this muscle was found during each of the five bouts.

Discussion

This study shows that EMG_{FT} cannot be easily determined from isometric elbow flexions. In fact, EMG_{FT} could only be determined for the long head of *Biceps brachii* in three out of the eight subjects.

Methological considerations

The accuracy of EMG_{FT} mainly depends on the linear fit used to model the force level versus slope coefficient relationships. Because EMG_{FT} could be considered as a valid tool to assess muscle function/fitness level (and to monitor changes in response to training/rehabilitation programs) only if it is determined accurately, we chose to validate the EMG_{FT} determination only for significant positive linear regression between force and slope coefficient resulting in a value of $R^2 > 0.85$ and in a standard error of *y*-intercept (i.e., EMG_{FT}) < 5%. Using these criteria we detected an accurate EMG_{FT} in only one muscle (i.e., long head of *Biceps brachii*) and in only three out of the eight subjects. One study focusing on EMG_{FT} from isometric muscle contractions of the superficial elbow flexors (Hendrix et al. 2009) determined the EMG_{FT} in *Biceps brachii* for all ten subjects. The discrepancy with the present study could be explained by the fact that these authors did not use any criteria for attesting the accuracy of their EMG_{FT} measurement. For instance, using the second criteria (i.e., $R^2 > 0.85$) of the present study, three out of ten EMG_{FT} would not have been determined in the study from Hendrix et al. (2009).

The lack of accurate EMG_{FT} could be explained by various physiological/non-physiological factors known to affect the EMG signal during constant-load exercise (for review, see (Farina et al. 2004)). For instance, motor-unit synchronization or signal cancellation (i.e., superposition of the positive and negative phases of the muscle action potentials) could affect the rise in EMG during the five constant-load exercises. The methodology used in the present study does not allow us to verify this hypothesis.

Possible compensation between muscles

It is well documented that the nervous system has multiple ways of accomplishing a given motor task (Bernstein

Table 1 Data for the long and short head of *Biceps brachii* and *Brachioradialis*, for each subject

S	Force (% MVC)	Long head of *Biceps brachii*			Short head of *Biceps brachii*			*Brachioradialis*		
		Slope (mV s^{-1})	*P*	R^2	Slope (mV s^{-1})	*P*	R^2	Slope (mV s^{-1})	*P*	R^2
1	20	–	*	0.99	–	NS	0.63	–		
	30	6.7×10^{-7}			–			–		
	40	2.2×10^{-6}			1.4×10^{-6}			–		
	50	3.5×10^{-6}			3.3×10^{-6}			1.3×10^{-6}		
	60	5.0×10^{-6}			4.9×10^{-6}			1.3×10^{-6}		
2	20	–	*	0.87	–	NS	−0.71	–		
	30	1.3×10^{-7}			–			–		
	40	1.2×10^{-6}			7.8×10^{-7}			1.2×10^{-9}		
	50	1.5×10^{-6}			1.2×10^{-6}			–		
	60	2.0×10^{-6}			6.0×10^{-7}			5.1×10^{-7}		
3	20	3.0×10^{-7}	NS	0.09	1.2×10^{-6}			2.2×10^{-7}		
	30	1.0×10^{-6}			–			–		
	40	1.0×10^{-6}			–			–		
	50	1.5×10^{-6}			–			–		
	60	2.2×10^{-6}			–			–		
4	20	2.8×10^{-7}	NS	0.32	1.3×10^{-6}	NS	0.76	4.8×10^{-7}	NS	0.36
	30	2.9×10^{-6}			2.0×10^{-6}			2.7×10^{-6}		
	40	1.2×10^{-6}			2.5×10^{-6}			1.2×10^{-6}		
	50	1.0×10^{-6}			–			3.5×10^{-6}		
	60	1.1×10^{-5}			1.3×10^{-5}			3.0×10^{-6}		
5	20	2.0×10^{-7}	*	0.91	1.4×10^{-10}			–		
	30	2.3×10^{-5}			–			–		
	40	1.1×10^{-5}			1.4×10^{-9}			–		
	50	2.2×10^{-5}			–			3.0×10^{-6}		
	60	1.6×10^{-6}			–			1.3×10^{-6}		
6	20	8.2×10^{-7}	NS	0.54	–	NS	0.80	–	NS	−0.57
	30	–			1.3×10^{-5}			3.9×10^{-6}		
	40	1.6×10^{-6}			–			6.3×10^{-8}		
	50	1.2×10^{-5}			2.8×10^{-7}			–		
	60	1.1×10^{-5}			2.5×10^{-8}			1.3×10^{-6}		
7	20	1.0×10^{-6}	NS	0.03	3.9×10^{-7}	NS	0.84	3.4×10^{-7}	NS	0.23
	30	1.8×10^{-6}			1.9×10^{-6}			2.9×10^{-8}		
	40	3.3×10^{-6}			2.0×10^{-6}			2.0×10^{-7}		
	50	5.0×10^{-6}			2.8×10^{-6}			1.9×10^{-7}		
	60	2.0×10^{-6}			–			1.3×10^{-6}		
8	20	2.9×10^{-6}	NS	−0.33	2.9×10^{-6}	NS	−0.30	–		
	30	9.8×10^{-6}			9.2×10^{-6}			–		
	40	1.1×10^{-5}			8.3×10^{-6}			1.3×10^{-6}		
	50	5.6×10^{-6}			7.8×10^{-6}			3.9×10^{-7}		
	60	5.6×10^{-6}			3.5×10^{-6}			–		

Slope corresponds to the slope coefficient of the relationship between EMG and time. En dash indicates negative slope coefficient (not taken into consideration for the EMG_{FT} determination) (asterisk) shows significant linear regression ($P < 0.05$) between force level and slope coefficient. (NS) shows no significant linear regression between force level and slope coefficient (and thus no EMG_{FT}). (R^2) stands for adjusted coefficient of determination. Note that linear regression was not determined with less than three points. *S* subjects

1967). At the muscle level, there are multiple synergists as well as various combinations of agonist/antagonists muscles that can contribute to the same force pattern (van Bolhuis and Gielen 1999). In other words, there are many ways in which a given torque can be exerted at the elbow, because many muscles are capable of substituting

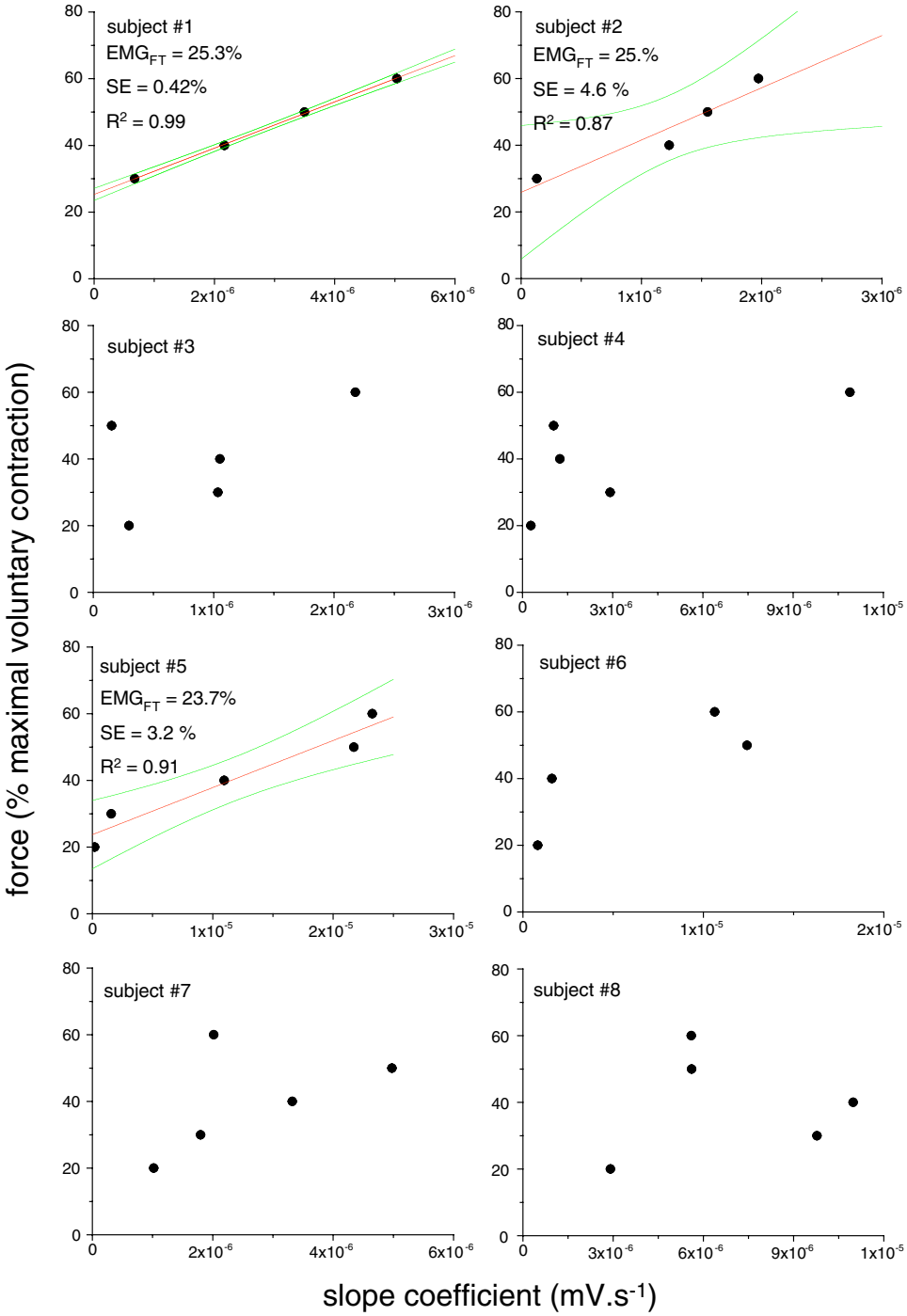

Fig. 3 EMG fatigue threshold determination in the long head of *Biceps brachii*. The relationship between force level and slope coefficient is depicted for the eight subjects. EMG_{FT} has been determined only in three out of eight subjects. The regression line and its 95% confidence interval are depicted for these three subjects. SE corresponds to the standard error of the *y*-intercept (i.e., of the EMG_{FT})

for each other (named here "compensation between muscles").

The lack of EMG_{FT} could be explained by putative co-activation changes with agonist and antagonist muscles between and within each constant-load exercise. In this way, EMG activity of the lateral head of *Triceps brachii* was assessed because the antagonist activity can influence the occurrence of fatigue in agonist muscles (Psek and Cafarelli 1993). However, the level of co-activation was minor (ranged from 1.9 to 6.2% of RMS_{max}) and no change was observed during the five constant-load exercises. Consequently, in this study, coactivation of this antagonist muscle did not interfere with EMG_{FT} determination.

Hunter et al. (2003) showed that the amplitude and rate of increase in EMG activity during fatiguing contraction varied among the elbow flexor muscles. More precisely, these authors reported no significant change in the EMG activity level of the short head of *Biceps brachii* during an

isometric exercise performed until exhaustion. The results of the present study are consistent with this observation showing no significant increase of EMG activity in this muscle (and thus no EMG_{FT}) during the five constant-load exercises performed at 20, 30, 40, 50 and 60%, of MVC. Consequently, EMG_{FT} cannot be determined in this muscle. In the only study which focused on EMG_{FT} from isometric muscle contractions of the superficial elbow flexors (Hendrix et al. 2009), the authors did not specify which head of the *Biceps brachii* was recorded. As they followed the recommendations of SENIAM (surface EMG for non-invasive assessment of muscles) (Hermens et al. 2000) they certainly recorded EMG activity resulting from both the long and short head of *Biceps brachii*. Despite the fact that the three EMG_{FT} values determined in the present study are in agreement with the range of EMG_{FT} that they reported (from 22.2 to 37.8% of MVC), it could be assumed that the localization of the EMG electrodes used by these authors interfered in their EMG_{FT} determination, mainly by overestimating the threshold levels (by adding a responding and a non-responding muscle). As discussed by these authors, other synergic muscles that contribute to elbow flexion (*Brachioradialis* and *Brachialis*) could exhibit different EMG_{FT}. However, since Hunter et al. (2004) reported a similar increase in EMG activity for the long head of *Biceps brachii* and *Brachioradialis* during a fatiguing protocol, the lack of EMG_{FT} in the *Brachioradialis* muscle in the present study is surprising.

While *Brachialis* muscles have been shown to be highly active during sustained isometric exercise, we can also assume that this muscle would exhibit EMG_{FT} or would compense for other elbow flexor muscles between bouts. For instance, EMG_{FT} could not be determined in the long head of *Biceps brachii* for subjects #3 and 7. This is mainly due to one bout (the bout performed at 50% of MVC for subject #3 and that performed at 60% of MVC for subject #7) which exhibited a low EMG rise compared to the bouts performed at lower force levels. Interestingly, if these bouts are not taken into consideration, EMG_{FT} can be determined with a good accuracy (Fig. 4). Since, neither the *Brachioradialis*, nor the short head of *Biceps brachii* showed an increase in EMG during this bout, we can hypothesize that the *Brachialis* muscle is highly activated during this exercise in order to compensate for fatigue. The EMG_{FT} values determined in these two subjects (13.1% of MVC for subject #3 and 14.7% of MVC for subject #7) was much lower than those determined in the other three subjects ($24.9 \pm 1.1\%$) which is highly suggestive that the long head of *Biceps brachii* is more fatigable in these two subjects and thus needed to be compensated for with other muscles during the highest levels of force.

The home made ergometer used in this study was similar to those used in other studies (Rudroff et al. 2007) and

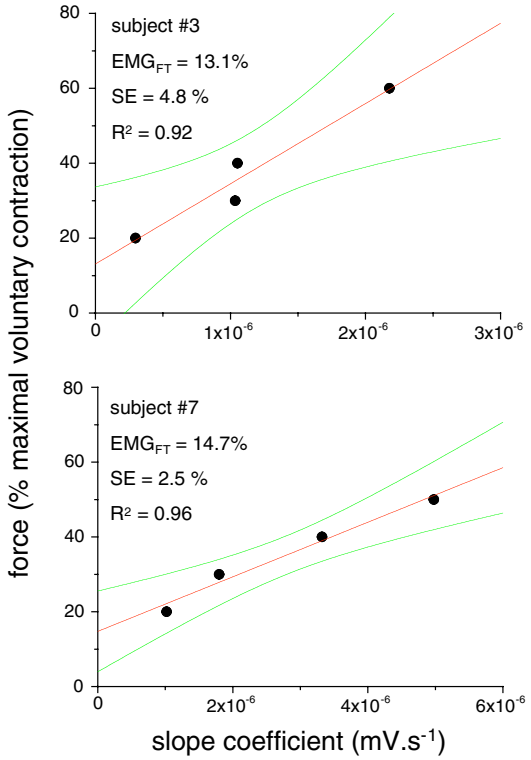

Fig. 4 EMG fatigue threshold determination in the long head of *Biceps brachii* in two subjects (#3 and 7). The EMG_{FT} could not be determined in the long head of *Biceps brachii* for subjects #3 and 7 (see Fig. 3). This is mainly due to one bout (the bout performed at 50% of MVC for subject #3 and that performed at 60% of MVC for subject #7) which exhibited a low EMG rise compared to the bouts performed at lower force levels. This figure shows that, EMG_{FT} can be determined with a good accuracy if these bouts are not taken into consideration. The regression line and its 95% confidence interval are depicted. SE corresponds to the standard error of the *y*-intercept (i.e., of the EMG_{FT})

was used to standardize the single-joint task as much as possible. However, in one subject (#8), the results suggest compensation with a shoulder muscle (anterior head of the *Deltoïd* muscle) during the bouts performed at 50 and 60% of MVC (Fig. 5). While the slope coefficients (i.e., rise in RMS) of the linear relationships between the RMS of the long head of *Biceps brachii* and time increase linearly from 20 to 40% of MVC, a much lower rise of RMS was found at 50 and 60% of MVC. It seems to be compensated for by a higher rise in RMS of the anterior head of the *Deltoïd* muscle. In fact, when the RMS of the long head of *Biceps brachii* and anterior head of the *Deltoïd* were summed and plotted as a function of time for each of the five bouts, a rise in the sum of RMS was linearly linked to the force level and thus EMG_{FT} could be determined with good accuracy (13.5% of MVC; Fig. 5). Note that such compensation was found in only one subject, but we could expect that it may have occured in numerous other studies.

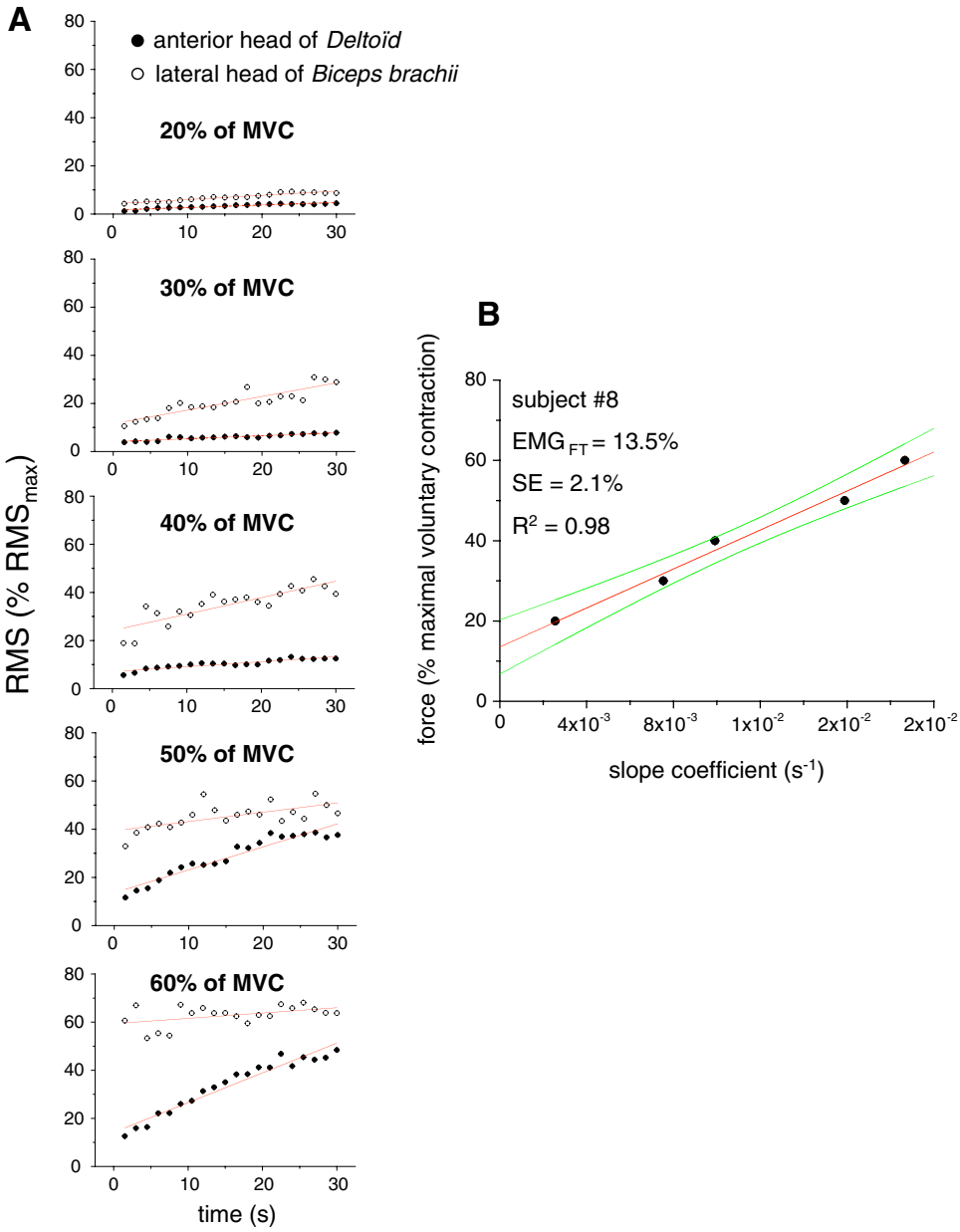

Fig. 5 Illustration of possible compensation with the anterior head of *Deltoïd*. **a** The EMG amplitude (RMS) data are plotted as function of time for the five submaximal bouts (20, 30, 40, 50 and 60% of maximal voluntary contraction (MVC)) and for both the anterior head of *Deltoïd* and the lateral head of *Biceps brachii*. **b** When the RMS of these two muscles were summed and plotted as a function of time for each of the five bouts, a rise in the sum of RMS was linearly linked to the force level and thus EMG_{FT} could be determined with a good accuracy

Conclusion and perspectives

This study shows that EMG_{FT} can be determined only for one superficial elbow flexor muscle (i.e., long head of *Biceps brachii*). The lack of EMG_{FT} in most of the subjects (5 out of 8) could be explained by putative compensations with other muscles which were indirectly observed in two subjects. In this way, the results of the present study suggest that EMG_{FT} cannot be accurately determined from joints like the elbow. Thus, we suggest to study EMG_{FT} from a more simple task during which one main muscle is involved limiting compensation between muscles. For instance, the first dorsal interroseus (FDI) is responsible for about 93% the maximum abduction force of the index and the adductor pollicis (AP) is a major contributor to the adduction force of the thumb (about 80% of the maximum torque) (Chao et al. 1989). In consequence, these two superficial muscles would be used in future studies to test the ability to determine an EMG_{FT} in all subjects.

Acknowledgments The authors are grateful for Benjamin BAGUET and Morgan REMAUD for their technical assitance in this study. They also thank Philippe SARRAZIN for its technical assistance (design of the ergometer) and Jean HUG for drawing Fig. 1.

References

Bernstein N (1967) Coordination and regulation of movements. Pergamon Press, New York

Bigland-Ritchie B, Woods JJ (1984) Changes in muscle contractile properties and neural control during human muscular fatigue. Muscle Nerve 7:691–699. doi:10.1002/mus.880070902

Cardozo AC, Goncalves M (2003) Electromyographic fatigue threshold of erector spinae muscle induced by a muscular endurance test in health men. Electromyogr Clin Neurophysiol 43:377–380

Chao EYS, An KN, Cooner WP, Linscheid RL (1989) Biomechanis of hand. World scientific, Singapore, pp 31–51

Chiti L, Biondi G, Morelot-Panzini C, Raux M, Similowski T, Hug F (2008) Scalene muscle activity during progressive inspiratory loading under pressure support ventilation in normal humans. Respir Physiol Neurobiol 164:441–448. doi:10.1016/j.resp.2008.09.010

DeVries HA (1968) Method for evaluation of muscle fatigue and endurance from electromyographic fatigue curves. Am J Phys Med 47:125–135

deVries HA, Moritani T, Nagata A, Magnussen K (1982) The relation between critical power and neuromuscular fatigue as estimated from electromyographic data. Ergonomics 25:783–791

Dias da Silva SR, Goncalves M (2006) Dynamic and isometric protocols of knee extension: effect of fatigue on the EMG signal. Electromyogr Clin Neurophysiol 46:35–42

Edwards RG, Lippold OC (1956) The relation between force and integrated electrical activity in fatigued muscle. J Physiol 132:677–681

Farina D, Merletti R, Enoka RM (2004) The extraction of neural strategies from the surface EMG. J Appl Physiol 96:1486–1495

Garland SJ, Enoka RM, Serrano LP, Robinson GA (1994) Behavior of motor units in human biceps brachii during a submaximal fatiguing contraction. J Appl Physiol 76:2411–2419

Garland SJ, Griffin L, Ivanova T (1997) Motor unit discharge rate is not associated with muscle relaxation time in sustained submaximal contractions in humans. Neurosci Lett 239:25–28

Graef JL, Smith AE, Kendall KL, Walter AA, Moon JR, Lockwood CM, Beck TW, Cramer JT, Stout JR (2008) The relationships among endurance performance measures as estimated from VO2PEAK, ventilatory threshold, and electromyographic fatigue threshold: a relationship design. Dyn Med 7:15

Hendrix CR, Housh TJ, Johnson GO, Weir JP, Beck TW, Malek MH, Mielke M, Schmidt RJ (2009) A comparison of critical force and electromyographic fatigue threshold for isometric muscle actions of the forearm flexors. Eur J Appl Physiol 105:333–342

Hermens HJ, Freriks B, Disselhorst-Klug C, Rau G (2000) Development of recommendations for SEMG sensors and sensor placement procedures. J Electromyogr Kinesiol 10:361–374

Housh TJ, deVries HA, Johnson GO, Housh DJ, Evans SA, Stout JR, Evetovich TK, Bradway RM (1995) Electromyographic fatigue thresholds of the superficial muscles of the quadriceps femoris. Eur J Appl Physiol Occup Physiol 71:131–136

Hug F, Dorel S (2009) Electromyographic analysis of pedaling: a review. J Electromyogr Kinesiol 19:182–198

Hug F, Drouet JM, Champoux Y, Couturier A, Dorel S (2008) Interindividual variability of electromyographic patterns and pedal force profiles in trained cyclists. Eur J Appl Physiol 104:667–678

Hunter SK, Lepers R, MacGillis CJ, Enoka RM (2003) Activation among the elbow flexor muscles differs when maintaining arm position during a fatiguing contraction. J Appl Physiol 94:2439–2447

Hunter SK, Critchlow A, Shin IS, Enoka RM (2004) Fatigability of the elbow flexor muscles for a sustained submaximal contraction is similar in men and women matched for strength. J Appl Physiol 96:195–202

Johnson MA, Polgar J, Weightman D, Appleton D (1973) Data on the distribution of fibre types in thirty-six human muscles; an autopsy study. J Neurol Sci 18:111–129

Matsumoto T, Ito K, Moritani T (1991) The relationship between anaerobic threshold and electromyographic fatigue threshold in college women. Eur J Appl Physiol Occup Physiol 63:1–5

Moritani T, Takaishi T, Matsumoto T (1993) Determination of maximal power output at neuromuscular fatigue threshold. J Appl Physiol 74:1729–1734

Murray WM, Delp SL, Buchanan TS (1995) Variation of muscle moment arms with elbow and forearm position. J Biomech 28:513–525

Pavlat DJ, Housh TJ, Johnson GO, Schmidt RJ, Eckerson JM (1993) An examination of the electromyographic fatigue threshold test. Eur J Appl Physiol Occup Physiol 67:305–308

Pringle JS, Jones AM (2002) Maximal lactate steady state, critical power and EMG during cycling. Eur J Appl Physiol 88:214–226

Psek JA, Cafarelli E (1993) Behavior of coactive muscles during fatigue. J Appl Physiol 74:170–175

Rudroff T, Christou EA, Poston B, Bojsen-Moller J, Enoka RM (2007) Time to failure of a sustained contraction is predicted by target torque and initial electromyographic bursts in elbow flexor muscles. Muscle Nerve 35:657–666

Rudroff T, Staudenmann D, Enoka RM (2008) Electromyographic measures of muscle activation and changes in muscle architecture of human elbow flexors during fatiguing contractions. J Appl Physiol 104:1720–1726

Smith AE, Moon JR, Kendall KL, Graef JL, Lockwood CM, Walter AA, Beck TW, Cramer JT, Stout JR (2009) The effects of beta-alanine supplementation and high-intensity interval training on neuromuscular fatigue and muscle function. Eur J Appl Physiol 105:357–363

van Bolhuis BM, Gielen CC (1999) A comparison of models explaining muscle activation patterns for isometric contractions. Biol Cybern 81:249–261

ELSEVIER

Ultrasound in Med. & Biol., Vol. 35, No. 5, pp. 878–879, 2009

0301-5629/09/$–see front matter

Letters to the Editor-in-Chief

A NOVEL METHOD FOR MEASURING ELECTROMECHANICAL DELAY ON THE VASTUS MEDIALIS OBLIQUUS AND VASTUS LATERALIS

To the editor: We read with great interest the original contribution by Chen et al. reporting a novel method for measuring electromechanical delay (EMD) of the vastus medialis obliquus (VMO) and vastus lateralis (VL). EMD has been considered to be influenced by several structures and mechanisms such as: (i) the propagation of the action potential and the excitation–contraction coupling processes and (ii) the stretching of the series elastic component (SEC) by the contractile element (Cavanagh and Komi 1979). In this way, EMD has been shown to be modified during a fatiguing task (Paasuke et al. 1999) in response to a training program (Linford et al. 2006) after ligament reconstruction (Kaneko et al. 2002), in case of neuropathies (Granata et al. 2000) or myopathies (Orizio et al. 1997). The original method proposed by Chen et al. could enable researchers/clinicians to perform a better assessment of EMD and could therefore be interesting to follow the alterations in EMD in these situations.

However, in some cases, changes in EMD are very weak (*e.g.*, about 6% [Linford et al. (2006)]; about 15% [Kaneto et al. (2002)]. Despite a higher frame rate than conventional echographic devices, the frame rate (200 Hz) used in the study of Chen et al. induced a temporal resolution of 5 ms, representing about 27% and 20% of the measured delay for VMO and VL, respectively. Therefore, as discussed by the authors, this frame rate limits the accuracy of their measurements and is probably insufficient to accurately monitor changes in EMD, excluding its use in clinical practice or for research purposes.

A solution to this drawback exists. It was reported many times in the literature but is absent in the present paper. Ultrafast echographic devices (frame rate up to 5 kHz) has recently been used to follow the contraction of the muscle (Deffieux et al. 2006, 2008) and earlier to perform elastographic measurements (*e.g.*, Bercoff et al. 2003). The high frame rate of these devices would permit a precise detection of the onset time corresponding to the initial tendon motion and thus would be useful for improving the accuracy of the method reported by Chen et al.

Furthermore, a more complete characterization of the EMD using ultrafast echographic device—including the detection of the onset of muscle and tendon motion—would give more information about the structures and mechanisms (*e.g.*, E-C coupling, aponeurosis, tendon, muscle, tendon stifness, muscle stiffness) implied in the EMD. For instance, it would permit to quantify the delay between: (i) EMG onset and fascicles motion onset, (ii) fascicles motion onset and proximal tendon motion onset and (iii) proximal tendon motion onset and distal tendon motion onset. This original information would provide a better fundamental understanding of the EMD and of muscle force transmission processes.

In conclusion, the main drawback of the method proposed by Chen et al. could easily be overcome using high frame rate echographic devices, not referenced in the paper. It would also help to study more in depth the physiological mechanisms related to the EMD.

Antoine Nordez*
Stefan Catheline†
François Hug*

*University of Nantes, Nantes Atlantique Universités, Laboratoire ''Motricité, Interactions, Performance,'' EA 4334, Nantes, France

†University of Grenoble, LGIT, Grenoble, France

REFERENCES

Bercoff J, Chaffai S, Tanter M, Sandrin L, Catheline S, Fink M. Gennisson JL, Meunier M. In vivo breast tumor detection using transient elastography. Ultrasound Med Biol 2003;29(10): 1387–1396.

Cavanagh PR, Komi PV. Electromechanical delay in human skeletal muscle under concentric and eccentric contractions. Eur J Appl Physiol Occup Physiol 1979;42:159–163.

Chen HY, Liau JJ, Wang CL, Lai HJ, Jan MH. A novel method for measuring electromechanical delay of the vastus medialis obliquus and vastus lateralis. Ultrasound Med Biol, In press.

Deffieux T, Gennisson JL, Nordez A, Tanter M, Fink M. Ultrafast imaging of in vivo muscle contraction using ultrasound. Appl Phys Let 2006;89. 184107–184101-184103.

Deffieux T, Gennisson JL, Tanter M, Fink M. Assessment of the mechanical properties of the muskuloskeletal system using 2-D and 3-D very high frame rate ultrasound. IEEE Trans Ultrason Ferroelectr Freq Control 2008;55:2177–2190.

Granata KP, Ikeda AJ, Abel MF. Electromechanical delay and reflex response in spastic cerebral palsy. Arch Phys Med Rehabil 2000;81: 888–894.

Linford CW, Hopkins JT, Schulthies SS, Freland B, Draper DO, Hunter I. Effects of neuromuscular training on the reaction time and electromechanical delay of the peroneus longus muscle. Arch Phys Med Rehabil 2006;87:395–401.

Orizio C, Esposito F, Paganotti I, Marino L, Rossi B, Veicsteinas A. Electrically-elicited surface mechanomyogram in myotonic dystrophy. Ital J Neurol Sci 1997;18:185–190.

Paasuke M, Ereline J, Gapeyeva H. Neuromuscular fatigue during repeated exhaustive submaximal static contractions of knee extensor muscles in endurance-trained, power-trained and untrained men. Acta Physiol Scand 1999;166:319–326.

doi:10.1016/j.ultrasmedbio.2008.11.005

REPLY

To the Editor-in-Chief: We thank Drs. Nordez, Catheline and Hug for their interest in our article (Chen et al. 2008) and for their constructive comments.

The ultrafast ultrasonic imaging technique was developed by Dr. Deffieux's laboratory. A 128-multichannel fully programmable system is mounted on a conventional ultrasonic probe, and the device give access to radiofrequency images at a few thousand Hertz using a modified imaging sequence that emits a single-plane wave pulse (Deffieux et al. 2006). The cross-correlation technique between two successive images is computed to retrieve a movie of the axial velocity, and then the displacement is computed from time integration of the velocity distribution (Sandrin et al. 2002). This wise design certainly provides a solution to the insufficient frame rate of conventional ultrasonography. Our experimental setup does not mount any extra device to provide a new method to measure the electromechanical delay by conventional ultrasonic probe. We appreciate the helpful suggestion of Dr. Nordez and colleagues.

HAN-YU CHEN*

**Graduate Institute of Physical Therapy, Taipei, Taiwan*

REFERENCES

Chen HY, Liau JJ, Wang CL, Lai HJ, Jan MH. A novel method for measuring electromechanical delay of the vastus medialis obliquus and vastus lateralis. Ultrasound Med Biol 2009;35:14–20.

Deffieux T, Gennisson JL, Nordez A, Tanter M, Fink M. Ultrafast imaging of in vivo muscle contraction using ultrasound. Appl Phys Lett 2006;89:184107–1–184107–3.

Sandrin L, Tanter M, Catheline, Fink M. Shear modulus imaging with 2-D transient elastography. IEEE Trans Ultrason Ferroelectr Freq Control 2002;49:426–435.

doi:10.1016/j.ultrasmedbio.2008.11.007

J Appl Physiol 106: 1970–1975, 2009.
First published April 9, 2009; doi:10.1152/japplphysiol.00221.2009.

Electromechanical delay revisited using very high frame rate ultrasound

Antoine Nordez,[1] Thomas Gallot,[2] Stefan Catheline,[2] Arnaud Guével,[1] Christophe Cornu,[1] and François Hug[1]

[1]*Université de Nantes, Laboratoire "Motricité, Interactions, Performance," Nantes; and* [2]*Université de Grenoble, Laboratoire de Géophysique Interne et Tectonophysique, Centre National de la Recherche Scientifique, Grenoble, France*

Submitted 27 February 2009; accepted in final form 3 April 2009

Nordez A, Gallot T, Catheline S, Guével A, Cornu C, Hug F. Electromechanical delay revisited using very high frame rate ultrasound. *J Appl Physiol* 106: 1970–1975, 2009. First published April 9, 2009; doi:10.1152/japplphysiol.00221.2009.—Electromechanical delay (EMD) represents the time lag between muscle activation and muscle force production and is used to assess muscle function in healthy and pathological subjects. There is no experimental methodology to quantify the actual contribution of each series elastic component structures that together contribute to the EMD. We designed the present study to determine, using very high frame rate ultrasound (4 kHz), the onset of muscle fascicles and tendon motion induced by electrical stimulation. Nine subjects underwent two bouts composed of five electrically evoked contractions with the echographic probe maintained over *1*) the gastrocnemius medialis muscle belly (muscle trials) and *2*) the myotendinous junction of the gastrocnemius medialis muscle (tendon trials). EMD was 11.63 ± 1.51 and 11.67 ± 1.27 ms for muscle trials and tendon trials, respectively. Significant difference ($P < 0.001$) was found between the onset of muscle fascicles motion (6.05 ± 0.64 ms) and the onset of myotendinous junction motion (8.42 ± 1.63 ms). The noninvasive methodology used in the present study enabled us to determine the relative contribution of the passive part of the series elastic component (47.5 ± 6.0% of EMD) and each of the two main structures of this component (aponeurosis and tendon, representing 20.3 ± 10.7% and 27.6 ± 11.4% of EMD, respectively). The relative contributions of the synaptic transmission, the excitation-contraction coupling, and the active part of the series elastic component could not be directly quantified with our results. However, they suggest a minor role of the active part of the series elastic component that needs to be confirmed by further experiments.

muscle; tendon; ultrasonography

ELECTROMECHANICAL DELAY (EMD) represents the time lag between muscle activation and muscle force production (3). It has been shown that EMD is modified during a fatiguing task (32), in response to a training program (14), after ligament reconstruction (19), and in case of neuropathies (13) or myopathies (31). EMD has been considered to be influenced by several structures and mechanisms such as (3) *1*) the propagation of the action potential and the excitation-contraction coupling processes (E-C coupling) and *2*) the muscle force transmission along the series elastic component [SEC; first introduced by Hill (15)]. Experiments have shown significant changes in EMD by experimental manipulation of the tension in the SEC (27, 29, 40). These results are considered by some to provide support for the hypothesis that the time required to stretch the SEC would be the primary determinant of the EMD (29); however, they provide only indirect evidence. In addition, all the structures of the SEC, classically composed of an active part (located in myofibrils) and a passive part (mainly aponeurosis and tendon) (39), could contribute differently to EMD. To date, there is no experimental methodology in humans to quantify the actual contribution of each SEC structure in the EMD.

A more complete characterization of the EMD, including detection of the onset of muscle fascicles and tendon motion, would give more information about the mechanisms and structures (E-C coupling, aponeurosis, tendon, muscle) involved in muscle force transmission efficiency. Real-time motion of muscle fascicles and tendons can be assessed using ultrasonography (for review, see Ref. 9). Since the sampling rates of traditional echographic devices are limited to ~50–100 Hz, the temporal resolution is very limited, and thus these devices cannot be used to study very short events such as EMD (values ranged from ~8 to 80 ms; Ref. 14). A few studies have determined the onset of muscle (34, 38) or tendon (4) motion using high frame rate ultrasound. However, despite a higher sampling rate than conventional echographic devices (200–333 Hz), the temporal resolution remains insufficient. For instance, the frame rate used by Chen et al. (4) induced a temporal resolution of 5 ms, representing ~27% of the measured delay for the vastus medialis muscle. Therefore, these devices cannot be used to accurately determine the onset of tissue motions and to monitor changes in EMD (28). A solution to this drawback exists. The lastest generation of echographic devices gives access to two-dimensional radio frequency (RF) images at a few thousand Hertz (up to 5 kHz) using a modified imaging sequence. In 2006, Deffieux and coworkers published a proof of concept paper demonstrating the feasability of using such very high frame rate ultrasound to track muscle contraction in vivo (7). They recently consolidated these findings showing real-time muscle displacements in response to myoelectrical stimulation (8). However, the latter study was conducted in three subjects and did not focus on the determination of muscle and tendon motion onset.

We designed the present study to determine, using very high frame rate ultrasound, the onset of muscle fascicles and tendon motion evoked by electrical stimulation. The original information gained by this study could contribute to a better understanding of the EMD and muscle force transmission processes.

MATERIALS AND METHODS

Subjects

Nine sedentary healthy men (age: 26.8 ± 5.1 yr; height: 177.8 ± 6.7 cm; weight: 71.7 ± 8.1 kg) volunteered to participate in this study. They were given detailed information about the purpose of the study and methods used and gave written consent. This study was conducted according to the Helsinki Statement (last modified in 2004) and has been approved by the local ethics committee.

Address for reprint requests and other correspondence: F. Hug, Univ. of Nantes, UFR STAPS, Laboratoire "Motricité, Interactions, Performance" (EA 4334), 25 bis boulevard Guy Mollet, BP 72206, 44322 Nantes cedex 3, France (e-mail: francois.hug@univ-nantes.fr).

Instrumentation

Ergometer. A home made ergometer was used to measure the force produced by the plantar flexors (Fig. 1). Subjects were required to lie prone and fully extend their right leg. Their right foot was secured in a rigid cycling shoe fixed on an adjustable system and placed on a force sensor near the metatarsal joint (ZF200kg, sensibility: 3 mV/V, Scaime, Annemasse, France). Rigid cycling shoe was chosen to avoid possible dynamics in coupling between the shoe and the force sensor. The ankle was set at 10° in plantar flexion (0° represents the foot perpendicular to the shank). The force signal was digitized at a sampling rate of 5 kHz (MP36, Biopac) and stored on a computer.

Ultrasonography. A very high frame rate ultrasound device (64 channels, Lecoeur Electronique, Chuelles, France) was piloted by Matlab software (The Mathworks). Raw ultrasonic echoes at a 3.5-MHz central frequency backscattered by tissue heterogeneities were sampled at 40 MHz. These RF images acquired at a 4-kHz rate were stored in a computer. Due to a partial failure of the device, only 40 of the 64 consecutive channels supplied by the medical array were available and used for further analysis. RF images were then segmented into 1.5-mm windows. Then, correlation algorithms between windows of different RF images could give the displacement field consecutive to the contraction (37).

Electromyography. Bipolar surface electromyographic (EMG) signals were recorded from the soleus, gastrocnemius lateralis, and gastrocnemius medialis (GM) muscles. For each muscle, a pair of surface Ag/AgCl electrodes (EL 503, Biopac) was attached to the skin with a 2-cm interelectrode distance. The electrodes were placed longitudinally with respect to the underlying muscle fiber arrangement and located according to the recommendations by SENIAM (surface EMG for noninvasive assessment of muscles). For the GM muscle, electrodes were placed ~1 cm distally of the stimulation electrodes (see below). Reference electrodes were placed over the lateral and medial malleolus. Before electrode application, the skin was shaved and cleaned with alcohol to minimize impedance. EMG signals were amplified (×1,000) and digitized (bandwidth of 0–2,000 Hz) at a sampling rate of 5 kHz (MP36, Biopac), and data were stored on a computer.

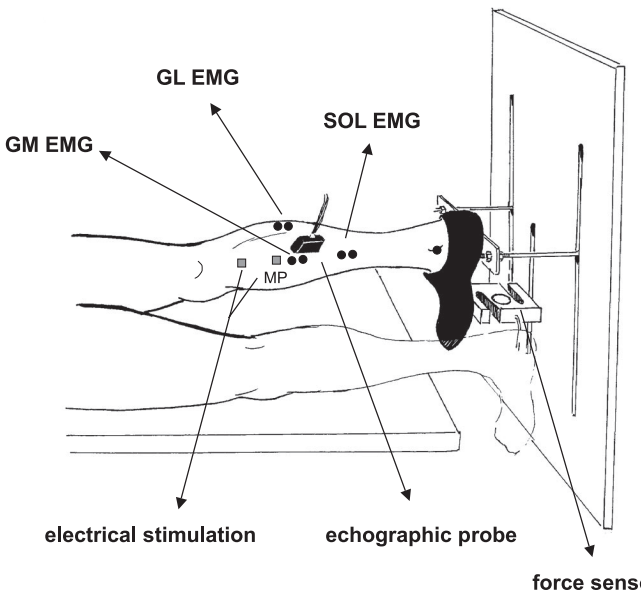

Fig. 1. Experimental setup. Percutaneous electrical stimulation was delivered on the motor point (MP). Force and electromyographic (EMG) activity of the gastrocnemius lateralis (GL), gastrocnemius medialis (GM), and soleus (SOL) muscles were recorded. Each subject underwent two bouts composed of five electrically evoked contractions with the echographic probe maintained over *1*) the GM muscle belly (as depicted in the figure) and *2*) the myotendinous junction of the GM muscle.

Electrical stimulation. Contraction of the GM muscle was elicited by means of percutaneous electrical stimulation. Electrical stimulation was used because it can activate only a target muscle (21, 22, 27). A constant current stimulator (Digitimer DS7A, Digitimer, Letchworth Garden City, UK) delivered single electrical pulses (pulse duration = 200 μs) through two electrodes (2 × 1.5 cm, Compex, Annecy-le-vieux, France) placed on the motor point and proximal portion of GM muscle (27). To find the motor point, the electrode was moved to obtain the strongest twitch with the lowest electrical stimulation. To determine the stimulation intensity, the output current was incrementally increased (incremental step = 1 mA, from 400 V) until a maximum tolerable current output that did not elicit M wave on the two other muscles of the triceps surae (i.e., soleus and gastrocnemius lateralis) was achieved (mean maximum current ouput used: 125 ± 11 mA).

Synchronization. Muscle stimulations were started using a trigger delivered by the ultrafast echographic device with a 50.00-ms delay to have a sufficient baseline to dectect the onset of tissue motion. A preliminary experiment was performed to check that the beginning of the echographic acquisition occurred excactly 50.00 ms before the onset of muscle stimulation. The trigger of the stimulation, force, and GM EMG signals were recorded using the same device (MP36, Biopac), discarding possible desynchronization between them. No detectable delay was found between the trigger of the stimulation and the stimulation artifact recorded by the GM electrodes.

Protocol

For each subject, two bouts (named muscle trials and tendon trials) composed of five electrically evoked contractions with a 3-min rest between each were performed. During the muscle trials, the echographic probe was maintained parallel to the bone, 1 cm medial to the EMG electrodes of the GM muscle. During the tendon trials, the echographic probe was maintained on the previously localized myotendinous junction of the GM muscle as described in many studies (27). These two bouts were performed in a randomized order.

Processing

The data processing was performed using standardized Matlab scripts (The Mathworks) and is depicted in Fig. 2. Ultrasonic raw data (i.e., RF signals) were processed as described by Deffieux et al. (7, 8). First, these raw data were used to create echographic images with a submilimetric resolution by applying a conventional beam formation, i.e., applying a time-delay operation to compensate for the travel time differences. These echographic images were used to determine the region of interest (ROI) for each contraction (i.e., between the two aponeurosis for the GM muscle for muscle trials and on the GM myotendinous junction for tendon trials; see Fig. 2). Then, a processing similar to Doppler was used to measure the tissue motion: the echographic images are segmented into 1.5-mm windows. Using one-dimensional cross correlation of windows of consecutive echographic images, the displacements along the ultrasound beam axis (i.e., *y*-axis in Fig. 2) were estimated. Thus the tissue motion between the two consecutive images (i.e., particle velocity) was measured with a micrometric precision (30).

Then, absolute particle velocities were averaged using previously determined ROI, and these averaged signals were used to detect the onset of motion (Fig. 2). Briefly, the derivative of each of these averaged signals was computed. Then, the onset of motion was defined as the first point with a negative derivative in the reverse direction of time (10). Visual inspection was performed to check the onset detection for each signal. The same method was used to automatically detect the onset of the force production (Fig. 2). We defined the EMD as the time lag between the onset of the electrical stimulation and the onset of force production. We also determined the

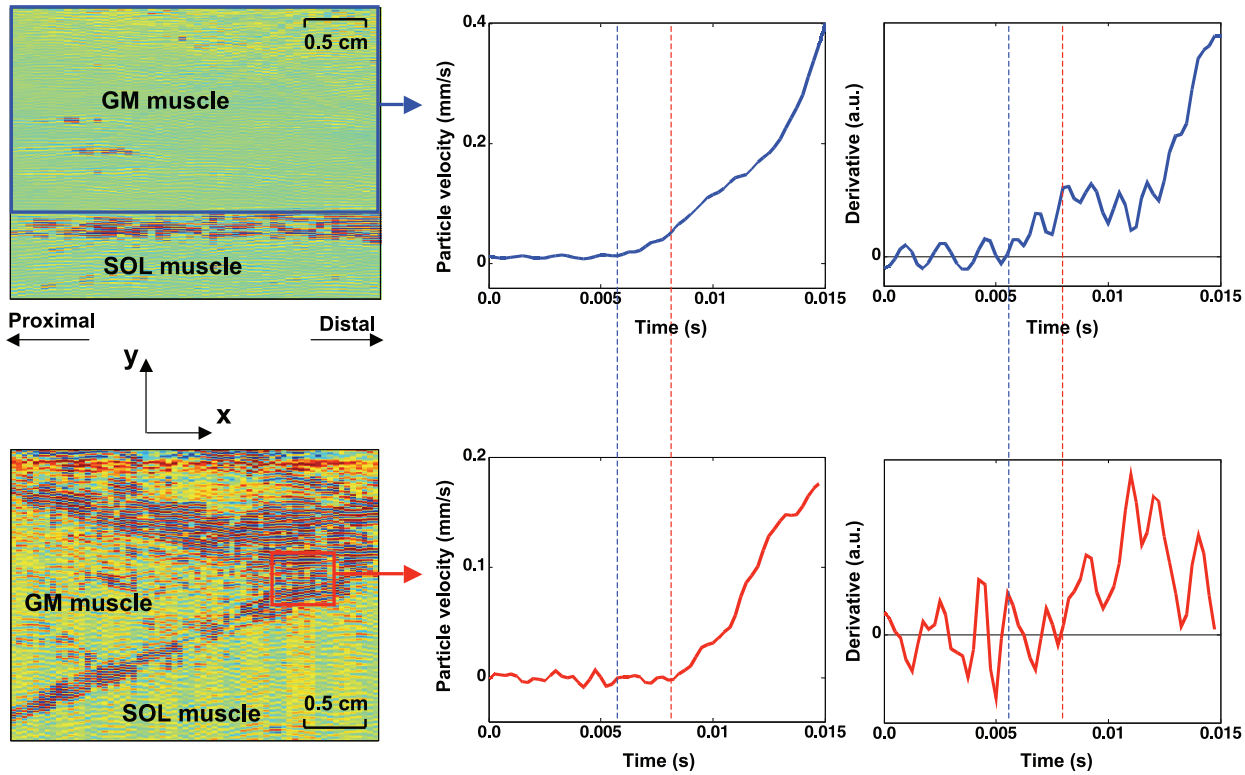

Fig. 2. Determination of the onset of muscle fascicles and tendon motion. Typical examples of the determination of tissue motion onset for muscle trials with the echographic probe placed on the muscle (*top* graphs) and for tendon trials with the probe placed on the musculo-tendinous junction (*bottom* graphs). The *left* graphs represent the echographic images obtained after the beam formation of raw radio frequency signals. The *middle* graphs represent the particle velocity obtained using the cross-correlation algorithm averaged on the regions of interest (blue and red squares for muscle and myotendinous junction, respectively). The *right* graphs represent the derivative of the particle velocity. The onset was automatically detected as the first point with a negative derivative in the reverse direction of time (vertical lines). Note that all displacements were calculated in the ultrasound beam axis (*y*-axis in this figure).

delay between the onset of electrical stimulation and the onset of muscle fasciscles motion (Dm, for muscle trials) and between the onset of electrical stimulation and the onset of tendon motion (Dt, for tendon trials).

Statistical Analysis

Data distributions consistently passed the Shapiro-Wilk normality test (Prism 4.01, Graphpad Software, San Diego, CA). Values are therefore reported as means ± SD. To determine the repeatability of all our measurements, the standard error in measurement (SE) and the coefficient of variation (CV) were calculated for the five repeats within each bout. Finally, the Dm (EMD values of muscle trials) and Dt (EMD values of tendon trials) were compared using analysis of variance for repeated measures with orthogonal contrasts as the post hoc test (Statistix, Tallahassee, FL). Statistical significance was established at $P < 0.05$.

RESULTS

Due to a partial failure of the ultrasound device, two trials of two subjects for the tendon trials were not considered for analysis. The SE and CV values calculated for the five electrically evoked contractions of the muscle trials were 0.66 ms and 11.6%, respectively, for Dm and 0.54 ms and 5.0%, respectively, for the EMD. For the tendon trials, SE and CV were 0.88 ms and 10.5%, respectively, for Dt and 0.71 ms and 6.3%, respectively, for the EMD. Averaged results across the five contractions for each of the nine subjects are provided in Table 1. Statistical analysis showed significant differences ($P < 0.001$) between Dm (6.05 ± 0.64 ms) and Dt (8.42 ± 1.63 ms), between Dm and EMD (11.63 ± 1.51 ms) for muscle trials, and between Dt and EMD (11.67 ± 1.27 ms) for tendon trials. No significant difference was found between the EMD measured in muscle trials and tendon trials.

DISCUSSION

In the present study, very high frame rate (4 kHz) ultrasound was used to analyze the EMD in the GM muscle. The high temporal resolution (i.e., ± 0.125 ms) offered by this technique allowed us to determine in vivo, for the first time, the delay between electrical stimulation and the onset of muscle fascicles and tendon motion. Since these delays are repeatable, they can be used for a more complete characterization of the EMD and thus can give more information about the relative contribution of structures and mechanisms involved in EMD.

Methodological Considerations

Raw RF signals were used to calculate displacements (i.e., tissue velocity) with micrometric precision (30), but only in the ultrasound beam axis (i.e., *y*-axis in Fig. 2). Fortunately, since muscle tissues can be considered as an incompressible material (12), muscle volume remains constant during contraction (20), and thus the longitudinal displacements of the muscle are directly linked to the perpendicular ones measured in the present study (8). In addition, the myotendinous junction dis-

Table 1. *Onset times for muscle trials and tendon trials*

Muscle trials	EMD, ms	Dm, ms	Dm, %EMD
Subject 1	13.08±0.54	7.00±0.87	53.6±7.0
Subject 2	9.08±0.36	5.30±0.27	58.4±3.8
Subject 3	10.40±0.20	6.00±0.50	57.7±5.4
Subject 4	11.32±0.54	5.25±0.68	46.6±7.6
Subject 5	12.96±0.36	6.25±0.31	48.3±2.7
Subject 6	11.96±0.68	6.34±0.45	53.2±5.0
Subject 7	12.15±1.10	6.94±1.84	58.2±19.1
Subject 8	13.56±0.45	5.60±0.28	41.4±3.5
Subject 9	10.20±0.78	5.80±0.89	56.7±6.0
Mean	11.63	6.05	52.5
SD	1.51	0.64	5.9
Tendon trials	**EMD, ms**	**Dt, ms**	**Dt, %EMD**
Subject 1	13.80±0.86	11.16±1.37	80.7±5.3
Subject 2	9.64±0.51	7.9±0.89	82.1±10.0
Subject 3	11.24±0.38	6.45±0.41	57.4±4.4
Subject 4	11.12±0.36	8.75±0.92	78.9±10.6
Subject 5	11.68±0.69	7.24±0.71	62.4±9.6
Subject 6	11.72±0.78	9.35±0.65	81.5±5.9
Subject 7	12.27±0.81	10.5±1.09	85.8±10.0
Subject 8	12.96±0.98	7.35±0.60	56.9±6.1
Subject 9	10.35±0.82	7.12±0.18	69.2±2.7
Mean	11.65	8.42	71.8
SD	1.27	1.63	15.4

Values are means ± SD. Onset times for muscle trials (echographic probe maintained over the muscle belly) and tendon trials (echographic proble maintained over the myotenndineous junction). EMD, electromechanical delay; Dm, onset of muscle fascicles motion; Dt, onset of myotendinous junction motion.

placements always have a component in the ultrasound beam axis as shown in *movie 1* (see supplemental material available online at the *Journal of Applied Physiology* website) and as depicted by Maganaris and Paul (23). Consequently, the latencies of muscle/myotendinous junction thickening measured in the present study and longitudinal displacement are synchronized (18). As demonstrated by Muraoka et al. (27), the ankle joint angle used in the present study (i.e., 10° in plantar flexion) induced a residual tendon strain at rest (tendon is not slack), highly suggesting that the onset of myotendinous junction is directly linked to tendon elongation. However, our method does not permit exclusion of "rigid body motion" of the whole structure from the calculated displacements.

In accordance with various works studying the EMD (17, 27), we chose to use electrical muscle stimulation to evoke muscle contraction because it permits the activation of only a target muscle (4, 22, 27), as displayed in the present study by the absence of M wave on gastrocnemius lateralis and soleus muscles (see METHODS). In addition, it enabled us to better standardize the contraction and thus induce low variability between the trials (17), as demonstrated by the good repeatability of our results. The EMD values determined in the present study (11.63 ± 1.51 and 11.65 ± 1.27 ms for muscle and tendon trials, respectively) are in agreement with the relatively large range of values (7.90–18.77 ms) reported by other studies that used electrical stimulation of GM muscle (14, 17, 25, 27). This relatively large range of EMD values could be partially explained by the methodology used to determine the onset of force production. Most of the previous studies used an arbitrary threshold to determine the onset of force production (14, 17, 25, 27). Since a high threshold may result in a greater delay, this threshold value is an important factor that affects EMD (6). To minimize this artificial delay linked to an arbitrary threshold, we chose to use, for all signals, a method based on the derivative (10) (Fig. 2). Pilot experiments have shown that this detection method is more precise than using an arbitrary threshold value. The high range of values reported in literature focusing on EMD could also be explained by the site of stimulation (nerve vs. muscle) and the reference used for the EMD calculation. Although some studies determined the reference as the onset of the stimulation artifact (4, 27) (i.e., EMD calculated as the time lag between this reference and the onset of force production), others determined the reference as the onset of the M wave (14, 17, 40). The action potentials propagate along the muscle fibers at ~4 m/s (physiological range between 3 and 5 m/s) (26). In our study, the distance between the motor point and the myotendinous junction was ~10 cm, inducing a total propagation time of the action potentials of ~25 ms. Therefore, it can reasonably be assumed that the onset of myotendinous junction displacements observed in our study (i.e., 8.42 ± 1.63 ms) is due to the onset of the force produced by the first recruited motor units (near the motor point) rather than by muscle fibers localized under the EMG electrodes. Consequently, it seems more appropriate to consider the EMD as the time lag between the onset of the stimulation artifact and the onset of force production, as done in the present study.

Physiological Significance

The onset of muscle contraction has been extensively studied in isolated frog muscles in response to electrical stimulation (5, 11, 16, 35, 36). The time interval that elapses between the instant of application of an electrical stimulus to the muscle fiber and the instant at which contraction starts is termed the "latent period" (35). However, as early observed by Rauh (1922; cited by Ref. 35), a minute precontractile elongation of the muscle occurs during the second phase of this latent period. This phenomenon, called latency relaxation, causes the tension to fall before it begins to rise (i.e., before the contraction). Interestingly, focusing on the initial mechanomyographic signals in response to myoelectrical stimulation, some human studies (2, 18, 33) reported an initial negative wave and interpreted it as the transverse latency relaxation. Barry (2) showed that this negative wave is more visible when the probe is placed over the motor point. This phenomenon is in accordance with the initial negative particle velocity of the muscle fascicles that we found in some proximal channels of the echographic probe as shown in Fig. 3. Since we determined the onset of fascicle motion from absolute particle velocity averaged on ROI (and thus independently of the particle velocity sign; Fig. 3), Dm should correspond to the onset of the latency relaxation rather than to the latent period.

Our original results show that the onset of muscle fascicles motion (Dm) is reached at 6.05 ± 0.64 ms after the myoelectrical stimulation, representing ~52.5 ± 5.9% of the EMD (Table 1; Fig. 4). Certainly due to the lack of accurate technique to detect the onset of muscle fascicle motions in vivo, very few studies have been conducted in humans. Using surface mechanomyography, an indirect measurement, Hufshmidt (18) reported a time lag between the onset of myoelectrical stimulation and the onset of muscle motion (named electro-mechanic

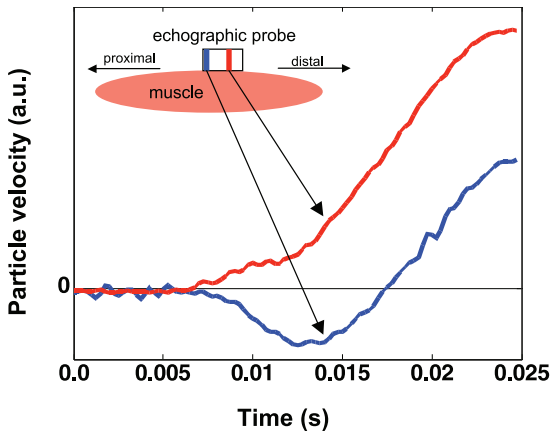

Fig. 3. Spatial changes in particle velocity. A typical example of spatial changes in particle velocity obtained during the muscle trials with the probe placed on the muscle belly for the most proximal (in blue) and the most distal (in red) channels. Because no spatial difference in the onset of fascicle motion (determined from the absolute signals) was found, onset of fascicle motion was determined from the averaged absolute signal (see Fig. 2). The initial negative particle velocity of the muscle fascicles that we found in some proximal channels (in blue) of the echographic probe could be explained by the latency relaxation phenomenon as mentioned in DISCUSSION.

latency) close to the Dm value reported in the present study. In a proof of concept article, Deffieux et al. (8) recently used very high frame rate ultrasound to measure Dm in the biceps brachialis muscle. Despite the fact that this study was conducted in only three subjects, the Dm values obtained were similar to values reported in the present work (i.e., ~7.1 ms). Considering the mechanisms and structures classically cited in literature (3, 4), Dm could be mainly attributed to the synaptic transmission, propagation of the action potential, E-C coupling, and force transmission along the active part of the SEC (located in myofibrils). Assuming a muscle fiber conduction velocity of 4 m/s (26), the propagation of the action potential along the distance corresponding to the 3-cm echographic probe would be ~7 ms. Since no spatial difference in Dm was found (Fig. 3), it can be assumed that the onset of motion for all muscle fascicles is due to the first recruited muscle fibers. Consequently, the propagation of the action potential should not affect the Dm and the EMD, contrary to what is suggested in various papers (14, 17, 27). Thus the Dm could be mainly attributed to the synaptic transmission, the E-C coupling, and the force transmission along the active part of the SEC. To date, to our knowledge, these different contributions to the EMD cannot be separated in vivo. Assuming a relative high velocity of muscle force transmission in the muscle (~30 m/s), as suggested by Morimoto and Takemori (24), we could hypothesize that the force transmission via the active part of the SEC does not represent the major part of Dm, emphasizing the probable important contributions of the synaptic transmission and the E-C coupling. Dm would then be interpreted as an index of these physiological processes, as suggested by some studies (18, 33).

Since the remaining 47.5 ± 6.0% of the EMD could be mainly attributed to the muscle force propagation along the passive part of the SEC (i.e., aponeurosis and tendon) (Fig. 4), our original results confirm previous indirect observations suggesting that a large part of the EMD is due to the stretch of the SEC (27, 29, 40). In addition, the onset of myotendinous junction motion determined in the present study indicates that the delay due to the muscle force transmission along the aponeurosis (Dt-Dm = 2.37 ± 1.30 ms) and tendon (EMD-Dt = 3.22 ± 1.41 ms) represents 20.3 ± 10.7% and 27.6 ± 11.4% of the EMD, respectively. Interestingly, these results highlight an intersubject variability of muscle force transmission velocity along tendon and aponeurosis that could be linked to intersubject variability of tendon and aponeurosis mechanical properties (1). Note that the the delay attributed to the muscle force transmission along the tendon might be slightly affected by dynamic in the couplings between *1*) the shoe and the force sensor and *2*) the foot and the shoe. As mentioned in METHODS, rigid cycling shoe has been used to avoid possible dynamics in the coupling between the shoe and the force sensor (checked by preexperiments).

In conclusion, the noninvasive methodology used in the present study enabled us to isolate the contribution of the passive component of the SEC (47.5 ± 6.0% of the total EMD) and each of the two main structures of this component (20.3 ± 10.7% for aponeurosis and 27.6 ± 11.4% for tendon). The relative contributions of the synaptic transmission, the E-C coupling, and the active part of the SEC cannot be directly quantified with our results. However, they suggest a minor role

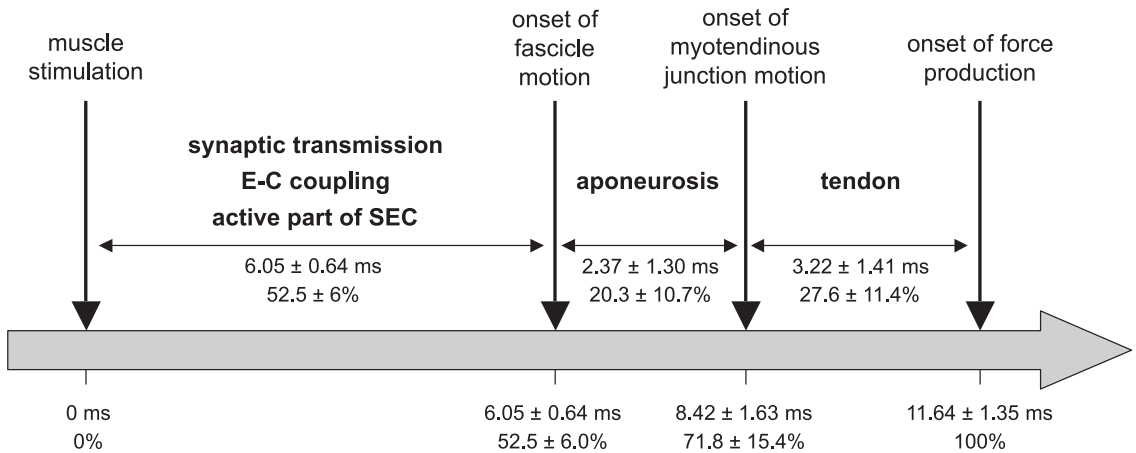

Fig. 4. Schematic representation of the time lag between the muscle stimulation and onset of fascicles motion, musculo-tendinous junction motion, and external force [electromechanical delay (EMD)].

of the active part of the SEC that needs to be confirmed by further experiments. Moreover, our results highlight an intersubject variability of muscle force transmission velocity along tendon and aponeurosis that could be linked to intersubject variability in mechanical properties of these structures.

ACKNOWLEDGMENTS

The authors thank the volunteers who accepted to participate in this study, Philippe Sarazin for technical assistance (design of the ergometer), Lilian Lacourpaille for help during the preexperimental protocol, Julie Morere for English editing, and Jean Hug for drawing Fig. 1. The authors also thank the research mission of the National Institute for Sports (INSEP, Paris, France) for lending them the electrostimulation device.

GRANTS

This study was supported by grants from the "Association Française contre les Myopathies" (contract no. 14084).

REFERENCES

1. **Abellaneda S, Guissard N, Duchateau J.** The relative lengthening of the myotendinous structures in the medial gastrocnemius during passive stretching differs among individuals. *J Appl Physiol* 106: 169–177, 2009.
2. **Barry DT.** Vibrations and sounds from evoked muscle twitches. *Electromyogr Clin Neurophysiol* 32: 35–40, 1992.
3. **Cavanagh PR, Komi PV.** Electromechanical delay in human skeletal muscle under concentric and eccentric contractions. *Eur J Appl Physiol Occup Physiol* 42: 159–163, 1979.
4. **Chen HY, Liau JJ, Wang CL, Lai HJ, Jan MH.** A novel method for measuring electromechanical delay of the vastus medialis obliquus and vastus lateralis. *Ultrasound Med Biol* 35: 14–20, 2009.
5. **Close RI.** Activation delays in frog twitch muscle fibres. *J Physiol* 313: 81–100, 1981.
6. **Conforto S, Mathieu P, Schmid M, Bibbo D, Florestal JR, D'Alessio T.** How much can we trust the electromechanical delay estimated by using electromyography? *Conf Proc IEEE Eng Med Biol Soc* 1: 1256–1259, 2006.
7. **Deffieux T, Gennisson JL, Nordez A, Tanter M, Fink M.** Ultrafast imaging of in vivo muscle contraction using ultrasound. *Appl Phys Lett* 89: 184107–184111, 2006.
8. **Deffieux T, Gennisson JL, Tanter M, Fink M.** Assessment of the mechanical properties of the musculoskeletal system using 2-D and 3-D very high frame rate ultrasound. *IEEE Trans Ultrasonics Ferroelectrics Freq Cont* 55: 2177–2190, 2008.
9. **Finni T.** Structural and functional features of human muscle-tendon unit. *Scand J Med Sci Sports* 16: 147–158, 2006.
10. **Fortier S, Basset FA, Mbourou GA, Favérial J, Teasdale N.** Sarting block performance in sprinters: a statistical method for identifying discriminative parameters of the performance and an analysis of the effect of providing feedback over a 6-week period. *J Sports Sci Med* 4: 134–144, 2005.
11. **Foulks JG, Perry FA.** The time course of early changes in the rate of tension development in electrically-stimulated frog toe muscle: effects of muscle length, temperature and twitch-potentiators. *J Physiol* 185: 355–381, 1966.
12. **Fung YC.** *Biomechanics: Mechanical Properties of Living. Tissues*. New York: Springer-Verlag, 1993.
13. **Granata KP, Ikeda AJ, Abel MF.** Electromechanical delay and reflex response in spastic cerebral palsy. *Arch Phys Med Rehabil* 81: 888–894, 2000.
14. **Grosset JF, Piscione J, Lambertz D, Perot C.** Paired changes in electromechanical delay and musculo-tendinous stiffness after endurance or plyometric training. *Eur J Appl Physiol* 105: 131–139, 2009.
15. **Hill AV.** The heat of shortening and the dynamic constants of muscle. *Proc Royal Soc London Series B Containing Papers of a Biological Character* 126: 136–195, 1938.
16. **Hill AV.** The onset of contraction. *Proc Royal Soc London Series B Containing Papers of a Biological Character* 136: 242–254, 1949.
17. **Hopkins JT, Feland JB, Hunter I.** A comparison of voluntary and involuntary measures of electromechanical delay. *Int J Neurosci* 117: 597–604, 2007.
18. **Hufschmidt A.** Acoustic phenomena in the latent period of skeletal muscle: a simple method for in-vivo measurement of the electro-mechanic latency (EML). *Pflügers Arch* 404: 162–165, 1985.
19. **Kaneko F, Onari K, Kawaguchi K, Tsukisaka K, Roy SH.** Electromechanical delay after ACL reconstruction: an innovative method for investigating central and peripheral contributions. *J Orthop Sports Phys Ther* 32: 158–165, 2002.
20. **Kardel T.** Niels Stensen's geometrical theory of muscle contraction (1667): a reappraisal. *J Biomech* 23: 953–965, 1990.
21. **Li L, Landin D, Grodesky J, Myers J.** The function of gastrocnemius as a knee flexor at selected knee and ankle angles. *J Electromyogr Kinesiol* 12: 385–390, 2002.
22. **Maganaris CN, Paul JP.** In vivo human tendon mechanical properties. *J Physiol* 521: 307–313, 1999.
23. **Maganaris CN, Paul JP.** Tensile properties of the in vivo human gastrocnemius tendon. *J Biomech* 35: 1639–1646, 2002.
24. **Morimoto S, Takemori S.** Initial mechanomyographical signals from twitching fibres of human skeletal muscle. *Acta Physiol (Oxford)* 191: 319–327, 2007.
25. **Moritani T, Berry MJ, Bacharach DW, Nakamura E.** Gas exchange parameters, muscle blood flow and electromechanical properties of the plantar flexors. *Eur J Appl Physiol Occup Physiol* 56: 30–37, 1987.
26. **Moritani T, Stegeman D, Merletti R.** Basic physiology and biophysics of EMG signal generation. In: *Electromyography Physiology Engineering and Noninvasive Applications*. New York: Wiley, 2004 p.1–20.
27. **Muraoka T, Muramatsu T, Fukunaga T, Kanehisa H.** Influence of tendon slack on electromechanical delay in the human medial gastrocnemius in vivo. *J Appl Physiol* 96: 540–544, 2004.
28. **Nordez A, Catheline S, Hug F.** A novel method for measuring electromechanical delay of the vastus medialis obliquus and vastus lateralis. *Ultrasound Med Biol* 35: 878, 2009.
29. **Norman RW, Komi PV.** Electromechanical delay in skeletal muscle under normal movement conditions. *Acta Physiol Scand* 106: 241–248, 1979.
30. **Ophir J, Cespedes I, Ponnekanti H, Yazdi Y, Li X.** Elastography: a quantitative method for imaging the elasticity of biological tissues. *Ultrason Imaging* 13: 111–134, 1991.
31. **Orizio C, Esposito F, Paganotti I, Marino L, Rossi B, Veicsteinas A.** Electrically-elicited surface mechanomyogram in myotonic dystrophy. *Ital J Neurol Sci* 18: 185–190, 1997.
32. **Paasuke M, Ereline J, Gapeyeva H.** Neuromuscular fatigue during repeated exhaustive submaximal static contractions of knee extensor muscles in endurance-trained, power-trained and untrained men. *Acta Physiol Scand* 166: 319–326, 1999.
33. **Petitjean M, Maton B, Fourment A.** Summation of elementary phonomyograms during isometric twitches in humans. *Eur J Appl Physiol Occup Physiol* 77: 527–535, 1998.
34. **Pulkovski N, Schenk P, Maffiuletti NA, Mannion AF.** Tissue Doppler imaging for detecting onset of muscle activity. *Muscle Nerve* 37: 638–649, 2008.
35. **Sandow A.** Excitation-contraction coupling in muscular response. *Yale J Biol Med* 25: 176–201, 1952.
36. **Sandow A.** Excitation-contraction coupling in skeletal muscle. *Pharmacol Rev* 17: 265–320, 1965.
37. **Sandrin L, Tanter M, Catheline S, Fink M.** Shear modulus imaging with 2-D transient elastography. *IEEE Trans Ultrason Ferroelectrics Freq Cont* 49: 426–435, 2002.
38. **Witte RS, Kim K, JMB, O'Donnell M.** Effect of fatigue on muscle elasticity in the human forearm using ultrasound strain imaging. In: *EMBS Annual International Conference. New-York City, USA: Procceding of the 28th IEEE*. New York: IEEE, 2006.
39. **Zajac FE.** Muscle and tendon: properties, models, scaling, and application to biomechanics and motor control. *Crit Rev Biomed Eng* 17: 359–411, 1989.
40. **Zhou S, Lawson DL, Morrison WE, Fairweather I.** Electromechanical delay in isometric muscle contractions evoked by voluntary, reflex and electrical stimulation. *Eur J Appl Physiol Occup Physiol* 70: 138–145, 1995.